The geology of the farms Josefsdal, Dunbar and part of Diepgezet in the Barberton greenstone belt

Isabelle Anne Paris

A thesis submitted to the Faculty of Science, University of the Witwatersrand, Johannesburg, in fulfilment of the requirements for the degree of Doctor of Philosophy

Johannesburg 1984

Abstract

This thesis is an integrated analysis of structural, sedimentological, petrographical and metasomatic aspects of an area located in the south-eastern part of the 3.3 - 3.5 Ga Archaean Barberton greenstone belt.

It is based on detailed mapping, detailed measured stratigraphic and structural sections and microscope analysis of thin sections. A 1 : 10000 geological map of the area is derived from the field observations.

Discovery of previously unrecognised structural and metasomatic events renders the existing stratigraphy of the belt outmoded. A new stratigraphy is derived for this part of the belt. Based on the internal analysis of vertical facies sequences within tectonic slices, previously thought to represent continuous stratigraphic sequences, and structurally restored cross sections, the original stratigraphy thickness of the belt in this area is estimated to have been about 3000 metres.

The lowermost part of the stratigraphy is represented by the upper part of the Onverwacht Group which comprises successively a discontinuous layer of serpentinite, a layer of pillowed and massive lavas and a volcaniclastic layer. The sedimentary rocks are totally silicified while the underlying mafic to ultramafic rocks are mostly silicified. A shallow and a deep water environment can be recognised within rocks of the Onverwacht Group which is interpreted as Archaean oceanic crust.

The Onverwacht Group is conformably overlain by the Lower Group which comprises ferruginous sediments, chert-arenites and conglomerates deposited as a submarine fan. It is unconformably overlain by an Upper Group of conglomerates and quartz-arenites interpreted as an alluvial sequence.

Seventy five per cent of the stratigraphy is affected by metasomatism which is interpreted as related to subaerial and subaqueous hydrothermal activity.

Four phases of deformation of which the first two involved thrusting have been recognised in the study area. D1 affects only the lower part of the stratigraphy, by repeating thin stratigraphic units above well defined thrust-décollement planes and with recumbent folding. D2 has imposed the main structural trend on the area, which is the result of an imbricated thrust fan. Using two major décollement zones, a minimum of 75% shortening across the sedimentary basin has been estimated.

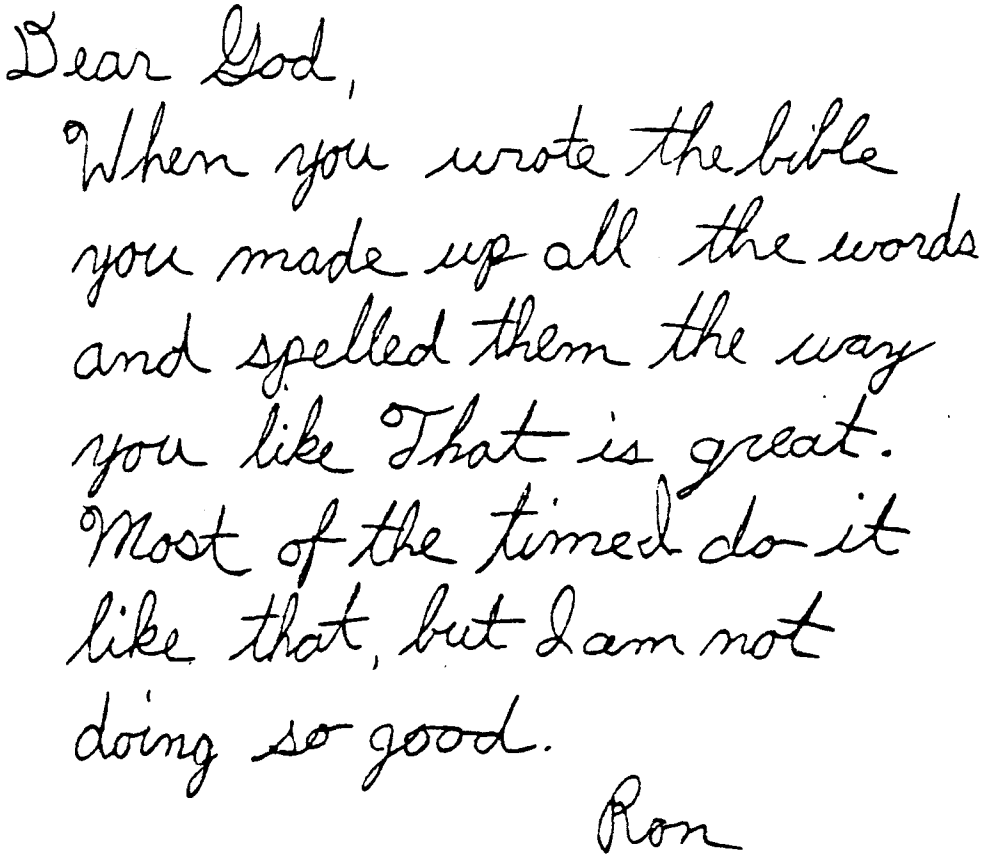
The Barberton greenstone belt is interpreted as an Archaean sequence emplaced by obduction during D2 probably related to collision tectonics.

Declaration

I declare that this dissertation is my own, unaided work. It is being submitted for the degree of Doctor of Philosophy in the University of the Witwatersrand, Johannesburg. It has not been submitted before for any degree or examination in any other University.

---------- 4 day of May , 1984

To Nicole Roos



from: "Children's letters to God", compiled by Marshall and Stuard Hamp (1967).

Preface

This research was funded by Elf-Aquitaine (France), and was carried out under the supervision of Dr I.G Stanistreet of the Geology Department, University of the Witwatersrand whose help is gratefully acknowledged.

I am very thankful to Dr M.J. de Wit; Mr S. Lamb and Mr M.J. W Callow for numerous helpful discussions in the field. I wish to thank Mr A.B. Caddle; Prof. R.G. Cawthorn; Dr E.G. Charleworth; Mr B. Cairncross; Dr. P. Horrocks; Dr G.N. Philipps and Dr J.R. Vearncombe for critically reading early drafts of this manuscript. I am very grateful to Sally and Paul Abbot and Fiona and Eric Sutton for their wonderful hospitality during my field seasons and Anglo American Corporation, limited for access to their grounds. I am indebted to Ms M.R. Jeffrey for undertaking the drawing of the map and some of the diagrams and to Miss R. Abela and Mrs K. Rakitzis from the Computer Centre, University of the Witwatersrand for drafting and editing this manuscript. Thanks to the technical staff of the geology department for assistance in sample preparation and with photographic material.

TABLE OF CONTENTS

1.0 INTRODUCTION 1
1.1 LOCATION OF THE STUDY AREA 1
1.2 GEOLOGICAL REVIEW OF THE BARBERTON GREENSTONE BELT 2
1.2.1 Stratigraphic Review of the Barberton greenstone belt . . 4
1.2.2 Geochronology 15
1.2.3 Structural Geology 15
1.2.4 Metasomatism 19
1.3 AIMS AND METHODS OF THE STUDY 20

2.0 THE ONVERWACHT GROUP: META-IGNEOUS ROCKS 22
2.1 INTRODUCTION 22
2.2 THE KROMBERG FORMATION 22
2.2.1 The mafic and ultramafic rocks 23
2.2.2 The siliceous igneous rocks 30
2.2.3 The "flaser banded rocks" 40
2.3 THE ZWARTKOPPIE FORMATION 41
2.4 CONCLUSIONS 45

3.0 THE ONVERWACHT GROUP: META-SEDIMENTARY ROCKS . . . 46
3.1 INTRODUCTION 46
3.2 THE CHERTS 47
3.2.1 The Black Mudstone Facies 47
3.2.2 The speckled grey mudstone facies 48
3.2.3 The Interbedded Mudstone/Siltstone/Sandstone Facies . . . 51
3.2.4 Angular clast bearing facies 52
3.2.5 The spheroid bearing facies 56
3.2.6 Study of vertical sequences 68
3.2.7 Paleoenvironmental interpretation 69
3.3 THE "AGGLOMERATES" 73
3.4 CONCLUSIONS 78

4.0 POST-ONVERWACHT SEDIMENTARY ROCKS 79
4.1 INTRODUCTION 79
4.2 METHOD OF APPROACH 80
4.3 DESCRIPTION OF THE LITHOF- ES 81

4.3.1 Facies F1 (jaspilite, ferruginous chert, shale and tuff) . . 82
4.3.2 Facies F2 (ferruginous and tuffaceous siltstone, ferruginous 89
4.3.3 Facies F3 (chert-arenite and c-conglomerate) 93
4.3.4 Facies F4, Super mature quartz-arenite 100
4.3.5 Facies 5 (Immature quartz-arenite, pebbly immature Quartz arenite and Q-conglomerate) F5 102
4.4 CONSTRUCTION OF THE FACIES SEQUENCE 105
4.5 DEVELOPMENT OF A PROPOSED STRATIGRAPHY 108
4.6 PALEOENVIRONMENTAL INTERPRETATION 112
4.6.1 The Lower Group 113
4.6.2 The Upper Group 114

5.0 METASOMATISM AND CHEMICAL REPLACEMENT 117
5.1 INTRODUCTION 117
5.2 SILICA METASOMATISM 117
5.2.1 Silica replacement 119
5.2.2 Silica-filled fractures 124
5.2.3 Interpretation 131
5.3 THE IRON METASOMATISM 132
5.4 THE CARBONATE METASOMATISM 137
5.5 SUMMARY AND DISCUSSION 138

6.0 STRUCTURAL GEOLOGY 140
6.1 INTRODUCTION 140
6.2 THE FIRST PHASE OF DEFORMATION: D1 141
6.2.1 Simbubule: locality A, figure 6.3 146
6.2.2 The border post area: Locality B in figure 6.3 147
6.2.3 The Manzima Valley: Locality C in figure 6.3 147
6.2.4 D1 and metasomatism 151
6.2.5 D1 in the rest of the study area and summary 157
6.3 SECOND PHASE OF DEFORMATION: D2 160
6.3.1 The T-Junction area 164
6.3.2 The Xecacatu Ridge 172
6.3.3 D2 elsewhere in the study area and summary 177
6.4 THIRD PHASE OF DEFORMATION: D3 182
6.5 THE LAST PHASE OF DEFORMATION: D4 183
6.6 SUMMARY OF THE POLYPHASE DEFORMATION 186
6.7 THRUST EMPLACEMENT: A KINEMATIC DISCUSSION 188
6.7.1 The first period of thrusting (D1) 193

6.7.2 The second period of deformation (D2) 195

7.0 SUMMARY, CORRELATIONS AND TECTONIC IMPLICATIONS . 204
7.1 INTRODUCTION 204
7.2 PROPOSED MODIFIED STRATIGRAPHY FOR THE SOUTHERN PART OF THE BARBERTON GREENSTONE BELT 205
7.2.1 Problems of defining the boundaries between the groups 207
7.3 POSSIBLE CORRELATION OF THE DEFORMATION PHASE WITH OTHER PARTS OF THE BELT 209
7.4 GEOTECTONIC IMPLICATIONS FOR THE BARBERTON GREENSTONE BELT 212
7.4.1 Summary of existing models for the formation of Archaean Greenstone Belts 212
7.4.2 Possible Evolutionary model for the Barberton Greenstone belt 214

8.0 LIST OF REFERENCES 234

List of appendices

Appendix 1: Measured section in Kromberg cherts on the Western slope of Simbubule (Josefsdal Farm) 220

Appendix 2: Measured section in Kromberg chert (Josefsdal Farm) 221

Appendix 3 : Measured sections in Kromberg chert (Josefsdal Farm) 222

Appendix 4 : Measured section in Kromberg chert (Dunbar Farm) 223

Appendix 5 : Measured section in Kromberg chert (Dunbar Farm) 224

Appendix 6 : Measured section in Kromberg chert (Josefsdal Farm) 225

Appendix 7 : Measured section in Zwartkoppie chert (Josefsdal Farm) 226

Appendix 8 : Measured sections in the Josefsdal block 226

Appendix 9 : Measured section in the Xecacatu block 227

Appendix 10: Measured section in the Xecacatu block 229

Appendix 11: Measured section in the Emlembe block 230

Appendix 12: Measured section in the Diepgezet block 231

Appendix 13: Measured section in the Josefsdal block 232

Appendix 14: Measured section in the Simbubule block 233

List of tables

Table 1.1 Summary of main lithologies in the Onverwacht Group ... 9

Table 4.1 List of lithofacies and sublithofacies recognised in the post-Onverwacht sedimentary rocks 83

Table 6.1 List of abbreviations and symbols 142

Table 6.2 Résumé of the deformational events in the study area . 143

Table 7.1 Proposed stratigraphy for the southern part of the belt 206

Table 7.2 Summary of the polyphase deformation as recognised in different parts of the belt and possible deformation .. 211

List of Figures

Figure 1.1. Geological map of the Barberton area indicating the areas mapped by previous and contemporary workers . . 5

Figure 1.2 Classification of the Barberton Sequence. (modified after SACS, 1980). 6

Figure 2.1. Measured section in the Kromberg Formation showing the two types of pillow lava. 25

Figure 2.2. Type A pillow with ocelli in the centre Msauli Power Station (Kranskop Farm). 26

Figure 2.3. Type B balloon shaped pillow, scale bar = 20cm Msauli Power Station, (Kranskop Farm). 26

Figure 2.4. Pillow breccia associated with type B pillow lava (Msauli Power Station, see Fig. 2.1). 27

Figure 2.5. Locality map of the study area. 27

Figure 2.6. Photomicrograph of massive lava showing spinifex textures. 29

Figure 2.7. Photomicrograph of ocelli bearing lava showing carbonated euhedral and hopper crystals 29

Figure 2.8. Silicified type B pillow lava (Josefsdal Farm) 32

Figure 2.9. Ocelli in silicified type A pillow lava (Josefsdal Farm) 32

Figure 2.10. Photomicrograph of silicified type B pillow lava showing silicified crystals, ... 33

Figure 2.11. Photomicrograph of silicified type A pillow

lava showing silicified skeletal textures in the ocelli. 33

Figure 2.12. Randomly oriented silicified spinifex like textures. 34

Figure 2.13. Chert containing parallel spinifex like textures. 34

Figure 2.14.a. Photomicrograph of chert with spinifex textures. 35

Figure 2.15. Variolitic chert (Diepgezet Farm) 37

Figure 2.16.a. Variolitic chert showing similiarities to variolitic Komatiite. 37

Figure 2.17. Photomicrograph of green homogeneous chert showing silicified crystals, ... 38

Figure 2.18. Photomicrograph of green homogenous chert 38

Figure 2.19. Flaser banded rock (Dunbar Farm) 42

Figure 2.20. Photomicrograph of flaser banded rock 42

Figure 2.21. Photomicrograph of flaser banded rock, ... 43

Figure 3.1. Black mudstone facies with black silica blades. 49

Figure 3.2. Photomicrograph of a siltstone bed within the black mudstone facies with rounded silica blades 49

Figure 3.3. Photomicrograph of the speckled grey mudstone facies 50

Figure 3.4. Photomicrograph of silicified sandstone 53

Figure 3.5. Silicified mudstone/siltstone/sandstone facies showing planar and lenticular bedding (Dunbar Farm). . . 53

Figure 3.6. Interbedded mudstone/siltstone/sandstone facies with convolute and planar lamination (Dunbar Farm). . . 54

Figure 3.7. A sandstone bed within the interbedded mudstone/siltstone/sandstone facies 54

Figure 3.8. Type A ripple drift cross lamination in the interbedded mudstone/siltstone/sandstone facies (Dunbar Farm). 55

Figure 3.9. Type B ripple cross lamination in the interbedded mudstone/siltstone/sandstone facies (Josefsdal Farm). 55

Figure 3.10. Specimen of the angular clast bearing facies (Josefsdal Farm) 57

Figure 3.11. Photomicrograph of the angular clast bearing facies 57

Figure 3.12. Photomicrograph of the angular clast bearing facies showing a pumiceous clast (Josefsdal Farm). . . 58

Figure 3.13. Accretionary spheroids (arrow) mixed with silicified lapilli tuff.(Josefsdal Farm). 58

Figure 3.14. Carbonated lapilli tuff containing fragments up to 3cm in size. (Dunbar Farm). 59

Figure 3.15 Diagram showing the replacement by carbonate of the angular clast bearing facies. 59

Figure 3.16. Carbonated lapilli tuff with large scale trough cross-bedding (Dunbar Farm). 61

Figure 3.17. Photomicrograph of the thin bedded spheroid bearing subfacies. 61

Figure 3.18. Thin bedded spheroid bearing subfacies with graded units (arrow). 62

Figure 3.19. Specimen of the thick bedded spheroid subfacies. 62

Figure 3.20. Photomicrograph of the thick bedded spheroid bearing subfacies 63

Figure 3.21. Photomicrograph of accretionary spheroids 63

Figure 3.22. Photomicrograph of an accretionary spheroid in the thick bedded spheroid bearing subfacies 64

Figure 3.23. Diagram showing the position of carbonate rhombs in the spheroid bearing facies 64

Figure 3.24. Graded units in the thick bedded spheroid bearing subfacies. 66

Figure 3.25. Trough cross-laminae in the thick bedded spheroid bearing subfacies (Dunbar Farm) 66

Figure 3.26a. Complete cycle from the silicified sediment similar to the Bouma sequence (Bouma, 1962). 70

Figure 3.26b. Sedimentary cycles from eleven measured sections in the cherts (see appendixes 1-7) 70

Figure 3.27. Simplified geological map showing the position of the main outcrop of the Hoogenoeg "agglomerates". . . 74

Figure 3.28. The Hooggenoeg "agglomerate" (Facies A) with chert clasts (c) and acid volcanic clasts (a). 76

Figure 3.29. Photomicrograph of the Hooggenoeg agglomerate (Facies A) 76

Figure 3.30. The Hooggenoeg "agglomerate" (Facies B) 77

Figure 3.31. Photomicrograph of the Hooggenoeg "agglomerate" (Facies B) 77

Figure 4.1. Simplified geological map showing the distribution of the post-Onverwacht sedimentary rocks . 84

Figure 4.2. Measured sections in post-Onverwacht sedimentary rocks. 85

Figure 4.3. White chert slabs in the jaspilite subfacies (f1a) resembling a brecciola deposit 86

Figure 4.4. Schematic diagram of graded jaspilite units. 86

Figure 4.5. The ferruginous chert subfacies (f1b). 87

Figure 4.6. "Mud pool" structures in the ferruginous chert subfacies. 87

Figure 4.7. Structures resembling flute casts in the ferruginous shale subfacies (Josefdal Farm). 90

Figure 4.8. Photomicrograph of the ferruginous tuff subfacies (f1d) 90

Figure 4.9. Specimen of the tuffaceous siltstone subfacies (f2b) 91

Figure 4.10. Ferruginous siltstone subfacies (f2c) with a chert pebble embedded into the underlying beds 91

Figure 4.11. Ferruginous chert-arenite subfacies with (f2d) a graded unit 94

Figure 4.12. Ferruginous chert-arenite subfacies (f2d) containing slab shaped clasts (Josefsdal Farm). . . . 94

Figure 4.13. Trough cross-lamination in the ferruginous

chert-arenite subfacies (f2d). (Josefsdal Farm). . . . 95

[illegible] 4.14. Flute casts in the ferruginous chert-arenite subfacies (f2d). (Josefsdal Farm). 95

Figure 4.15. Dewatering pillar structures in the massive chert-arenite subfacies (f3a). 97

Figure 4.16. Pebbly chert-arenite subfacies (f3b) with a cross-bedded unit 97

Figure 4.17. Matrix supported granule C-conglomerate subfacies (f3c). 99

Figure 4.18. The clast supported C-conglomerate subfacies (f3d) with slabs of white chert. 99

Figure 4.19. The supermature quartz-arenite subfacies (f4b) with large scale rough cross-beds. 101

Figure 4.20. The supermature quartz-arenite subfacies (f4a) 101

Figure 4.21. Planar bedded supermature quartz-arenite subfacies (f4b) with dewatering structures. 103

Figure 4.22. Planar bedded supermature quartz-arenite subfacies (f4b) with asymmetric bifurcating ripples. . 103

Figure 4.23. Paleocurrent directions rotated to the horizontal, following the method described by Phillips (1973). 104

Figure 4.24. Immature quartz-arenite subfacies (f5a) with trough cross-bedding. (Diepgezet Farm). 106

Figure 4.25. Desiccation cracks on the bedding plane in the immature quartz-arenite subfacies (f5a). 106

Figure 4.26. Pebbly immature quartz-arenite subfacies

chert-arenite subfacies (f2d). (Josefsdal Farm). . . . 95

Figure 4.14. Flute casts in the ferruginous chert-arenite subfacies (f2d). (Josefsdal Farm). 95

Figure 4.15. Dewatering pillar structures in the massive chert-arenite subfacies (f3a). 97

Figure 4.16. Pebbly chert-arenite subfacies (f3b) with a cross-bedded unit 97

Figure 4.17. Matrix supported granule C-conglomerate subfacies (f3c). 99

Figure 4.18. The clast supported C-conglomerate subfacies (f3d) with slabs of white chert. 99

Figure 4.19. The supermature quartz-arenite subfacies (f4b) with large scale rough cross-beds. 101

Figure 4.20. The supermature quartz-arenite subfacies (f4a) 101

Figure 4.21. Planar bedded supermature quartz-arenite subfacies (f4b) with dewatering structures. 103

Figure 4.22. Planar bedded supermature quartz-arenite subfacies (f4b) with asymmetric bifurcating ripples. . 103

Figure 4.23. Paleocurrent directions rotated to the horizontal, following the method described by Phillips (1973). 104

Figure 4.24. Immature quartz-arenite subfacies (f5a) with trough cross-bedding. (Diepgezet Farm). 106

Figure 4.25. Desiccation cracks on the bedding plane in the immature quartz-arenite subfacies (f5a). 106

Figure 4.26. Pebbly immature quartz-arenite subfacies

(Dunbar Farm). 107

Figure 4.27. Clast supported Q-conglomerate subfacies (f5c) 107

Figure 4.28. Diagram showing the Manzima Valley uncomformity. 110

Figure 5.1. Schematic diagram showing the transition from mafic tosilicified mafic lava. 118

Figure 5.2. Large scale type B replacement 122

Figure 5.3. Banded black and white chert with silica front along and across bedding 123

Figure 5.4. Type B silica replacement in which isolated areas affected by Type A replacement (A) are present. . 123

Figure 5.5. Black silica fractures, parallel (arrow 1) and perpendicular (arrow 2) to bedding in a silicified sediment. 125

Figure 5.6. Network of silica filled veins in silicified sediments. 125

Figure 5.7. Silica cemented breccia in debris flow of the Hooggenoeg Formation. 127

Figure 5.8. Silica cemented breccia in spinifex texture bearing cherts. 127

Figure 5.9. Silica cemented breccias showing the relationships between rounded and angular fragments . . 128

Figure 5.10. Silica cemented breccia with rounded clasts interpreted as hydraulic breccia. 130

Figure 5.11. A sedimentary conglomerate unit in the Onverwacht sedimentary rocks 130

Figure 5.12. Proposed model for the silicification of the upper part of the Onverwacht Group. 133

Figure 5.13. Individual spheroids within silica filled fractures 134

Figure 5.14. a,b Diagrams drawn from thin sections showing the transition from jasper beds to tuffaceous siltstone . . 136

Figure 6.1. Locality map showing the location of the geological maps presented in Chapter 6 144

Figure 6.2. Simplified geological map of the study area showing the D2 tectonic units. 145

Figure 6.3. Simplified geological map showing the repetition of the Onverwacht silicified sedimentary rocks 148

Figure 6.4. View of Simbubule 149

Figure 6.5. Flaser banded rock underlying an Onverwacht chert unit and showing folded and cross cutting quartz veins 150

Figure 6.6. Small scale decollement structure in an Onverwacht chert unit 150

Figure 6.7. Geological map of the Onverwacht cherts in the Manzima Valley 152

Figure 6.8.a Schematic profile of a D1 thrust slice (symbols as in Fig. 6.3). 153

Figure 6.9 Equal area projection of f2 folds, ... 154

Figure 6.10. A small diapir filled with silica cemented breccia within a chert unit (Dunbar Farm). 156

Figure 6.11. Movement along a silica vein in Onverwacht silicified sediments (arrow)(Dunbar Farm). 156

Figure 6.12. Measured section in cherts of the Onverwacht Group 159

Figure 6.13. = Cross section in the Waterfall Synclinorium (location on Fig. 6.2). 161

Figure 6.14. = F2 folds in the Waterfall Synclinorium and adjacent structural units. 161

Figure 6.15. f2 Z fold in the Waterfall Synclinorium. View looking NE. 162

Figure 6.16. Tight, isoclinal f2 syncline in the Waterfall Synclinorium 162

Figure 6.17. Equal area projection of f2 folds axial planes in the Waterfall Synclinorium 163

Figure 6.18. Simplified geological map of the T. junction area 165

Figure 6.19.a. Integrated cross section from the T-junction area (Josefdal Farm) 166

Figure 6.19.b. Photograph showing the features drawn in the cross section of Fig 6.19a and in adjacent areas 166

Figure 6.20. Angular discordance formed by the T-Junction Thrust 167

Figure 6.21. Photomicrograph of pseudo tachylite from the T-Junction thrust width of field = 3,5mm 167

Figure 6.22.a,b,c,d Traverses in the T-Junction area 169

Figure 6.23. Traverse C-D in the T-junction area showing

shallow dipping shear zone (arrow) within unit 6. . . . 170

Figure 6.24. Block diagram showing traverses E - F and E' - F'. 170

Figure 6.25. Simplified geological map of the Xecacatu Ridge 174

Figure 6.26. Upper Group quartz-arenite folded by the Xecacatu Syncline plunging 20° to the NE 175

Figure 6.27. a - c Cross sections along the Xecacatu Ridge 176

Figure 6.28 Cross section showing a klippe of Lower Group material over unit 2, <ON>. 179

Figure 6.29.a = Interpretative cross sections in the ramp of unit 11 Diepgezet Farm 179

Figure 6.29.b = Equal area projection of the f2 folds in the ramp; 179

Figure 6.30. = Diagram showing the refolding of f2 folds by f3 in the Dunbar Valley 184

Figure 6.31. = Photograph of the basin pattern of the folded uncomformity in Manzima Valley. 184

Figure 6.32.a = F3 fold in ferruginous tuff, unit 3 Fig. 6.15. View looking South Josefdal Farm 185

Figure 6.32.b = equal area projection of the f3 fold shown in Fig. 6.32.a 185

Figure 6.33.a,b,c. Cross-sections showing the superposition of the four phase of deformation 189

Figure 6.34 a) diverticulation mechanism (modified after Lemoine, 1973). 191

Figure 6.34 b) formation of an imbricate fan by gravity sliding 191

Figure 6.34 c) gravity spreading (1) mechanism (2) imbricate fan resulting from gravity sliding 191

Figure 6.35. Model for the formation of mud pool structures. 196

Figure 6.36 Simplified geological map showing the interstacking of distal and proximal facies. 199

Figure 6.37 Line restored sections (see Fig. 6.36 for location) 203

Figure 7.1. Simple cartoon showing the proposed palaeoenvironmental evolution of the southern Barberton greenstone belt 219

CHAPTER 1

1.0 INTRODUCTION

1.1 LOCATION OF THE STUDY AREA

The study area is located in the Eastern Transvaal (South Africa), to the immediate west of the border with Swaziland (Fig. 1.1). It occupies an area between 31° 04' and 31° 06'W latitude and 25° 45' and 26° 01'S longitude. The area is divided into three farms, namely Josefsdal 382Ju, Dunbar 383Ju and Diepgezet 388Ju. The topography is very rugged and the altitude varies from 696m to 1851m, with two flat bottomed valleys, 1km wide at the maximum on Dunbar Farm. The area is bounded by the Msauli River to the south, a pine forest to the north, the Swaziland border to the east and the Sigadeni Ridge to the west.

The study area can be approached by road from Badplaas (60km) or Barberton (70km). Both roads are unmacadamised and generally in poor condition. Access to the Dunbar and Manzima Valleys on Dunbar Farm is restricted to four wheel drive vehicles. However, most of the area is easily accessible by foot, footpaths being very abundant throughout the mountain land. The Msauli Mine owns a small private air landing strip which is located 8km south of the study area. Outcrop is generally good except in deep forested gorges and in the Dunbar and Manzima Valleys which are covered by alluvium.

The area has been inhabited since about 1600 by migrant Nguni tribes. White settlements started around 1882 with the start of gold prospecting in the mountain land. Four gold mines are still in operation around Barberton, namely the Sheba, Consort, Fairview and Agnes mines.

Abandoned asbestos and gold prospecting pits and trenches occur throughout the study area. The only mine in production at present is the Msauli asbestos Mine, which started production in 1942, on Diepgezet Farm. The 1982 production was 90,000 tons (Büttner et al., 1983).

1.2 GEOLOGICAL REVIEW OF THE BARBERTON GREENSTONE BELT

The Barberton greenstone belt covers an area of approximately 3300km2 in the Eastern Transvaal (Fig. 1.1). It comprises Archaean granitic and greenstone terranes forming respectively the low and high topographies. The greenstone terranes are predominantly of greenschist facies metamorphic grade.

Numerous books and reviews are available on the geology of the Barberton greenstone belt. Anhaeusser (1971 a,b; 1973; 1978) and Viljoen and Viljoen (1969 a,e; 1970) were the first workers to propose a general coherent model for the belt. Condie (1981) and Tankard et al. (1982) amongst others examined the "Barberton model" together with other Archaean terranes. Finally, Anhaeusser (1983) discussed the early model in the light of the recently available data.

The stratigraphy of the Barberton greenstone belt is briefly outlined below, and will be discussed in more detail in the following section. Fig. 1.2 shows the presently accepted stratigraphy as proposed by Viljoen and Viljoen (1969 a) and followed by the South African Committee for Stratigraphy (SACS, 1980).

The Barberton Sequence comprises three groups. The lowest group, the Onverwacht Group, is subdivided into a lower mafic to ultramafic subgroup and an upper mafic to felsic subgroup, separated by the Middle Marker. The

Onverwacht Group is overlain by the Fig Tree Group which consists of fine grained sedimentary rocks and graywackes. The last group is the Moodies Group which comprises mainly coarse grained sedimentary rocks with some mudstones. The thickness of each group, as they are defined in their respective type areas, is indicated in Fig. 1.2.

The Barberton greenstone belt is a well preserved and well exposed Archaean greenstone belt in which many widely accepted hypotheses on Archaean geology have been developed:

1. The existence of a mobile extrusive peridotitic magma was first demonstrated by Viljoen and Viljoen (1969 b,c) who introduced the rock type komatiite, named after the Komati River.

2. The volcanic cyclicity described by Viljoen and Viljoen (1969 b,d; 1970) has become part of a generalised greenstone belt model (Condie, 1981).

3. Many Archaean tectonic models have relied on the Barberton model in which vertical movement and gravity induced slumping and downfolding are predominant (Anhaeusser, 1975; 1983).

However, in recent detailed studies, several aspects of this "Barberton model" have been criticised:

1. The conformable nature of the stratigraphy of the belt has been questioned by Williams and Furnell (1979), De Wit (1982; 1983), and De Wit et al. (1983).

2. Williams and Furnell (1979) suggested that the Middle Marker, separating the upper from the lower Onverwacht Group, does not represent a major time break indicative of fundamental changes in geodynamic processes as advocated by Viljoen and Viljoen (1969 b,c; 1970).

3. The deformational history of the belt has been shown to be far more complex than postulated in the model developed by Viljoen and Viljoen (1970) (Ramsay, 1963; Philpot, 1979; Fripp et al., 1980; De Wit, 1982; 1983; De Wit et al., 1983; C.M. Barton, 1982).

4. De Wit et al. (1982 a) demonstrated the importance of previously unrecognised metasomatic processes.

1.2.1 STRATIGRAPHIC REVIEW OF THE BARBERTON GREENSTONE BELT

a) The Onverwacht Group

The existence of a thick sequence of lava in the Barberton greenstone belt was first pointed out by Draper (1914) in a section from Barberton to the Komati River. It was later described by Hall (1918) in the southern part of the belt where it is best exposed, and by Visser et al. (1956). The officially accepted sub-divisions of the Onverwacht Group are directly derived from the studies of Viljoen and Viljoen (1969 a-d). They proposed the subdivision of the Onverwacht Group into two subgroups namely, the Tjakastad Subgroup, an essentially metamorphosed ultramafic and mafic, magnesium rich lower unit; and the Geluk Subgroup, an upper unit of metamorphosed mafic and intermediate to acid volcanics with a wide variety of pyroclastics rocks.

Each subgroup is further subdivided into three formations (Fig. 1.2). The two subgroups are separated by a chert band, the Middle Marker, which ranges from a mere parting to a rock unit 9m in thickness and has been traced for 72km. Viljoen and Viljoen (1970) drew attention to repetition of the rock types within the formations, which they interpreted to be due to volcanic cyclicity.

Table 1.1 summarises the main lithologies in the Onverwacht Group. For more petrographic details about the Onverwacht Group the reader is referred to Viljoen and Viljoen (1969 a-d). A brief resume of the type sections of the formations of the Onverwacht Group present in the study area is included below:

The Hooggenoeg Formation type area has been established by Viljoen and Viljoen (1969 d) on the western limb of the Onverwacht Anticline. They suggested that the formation comprises five or more volcanic cycles, each

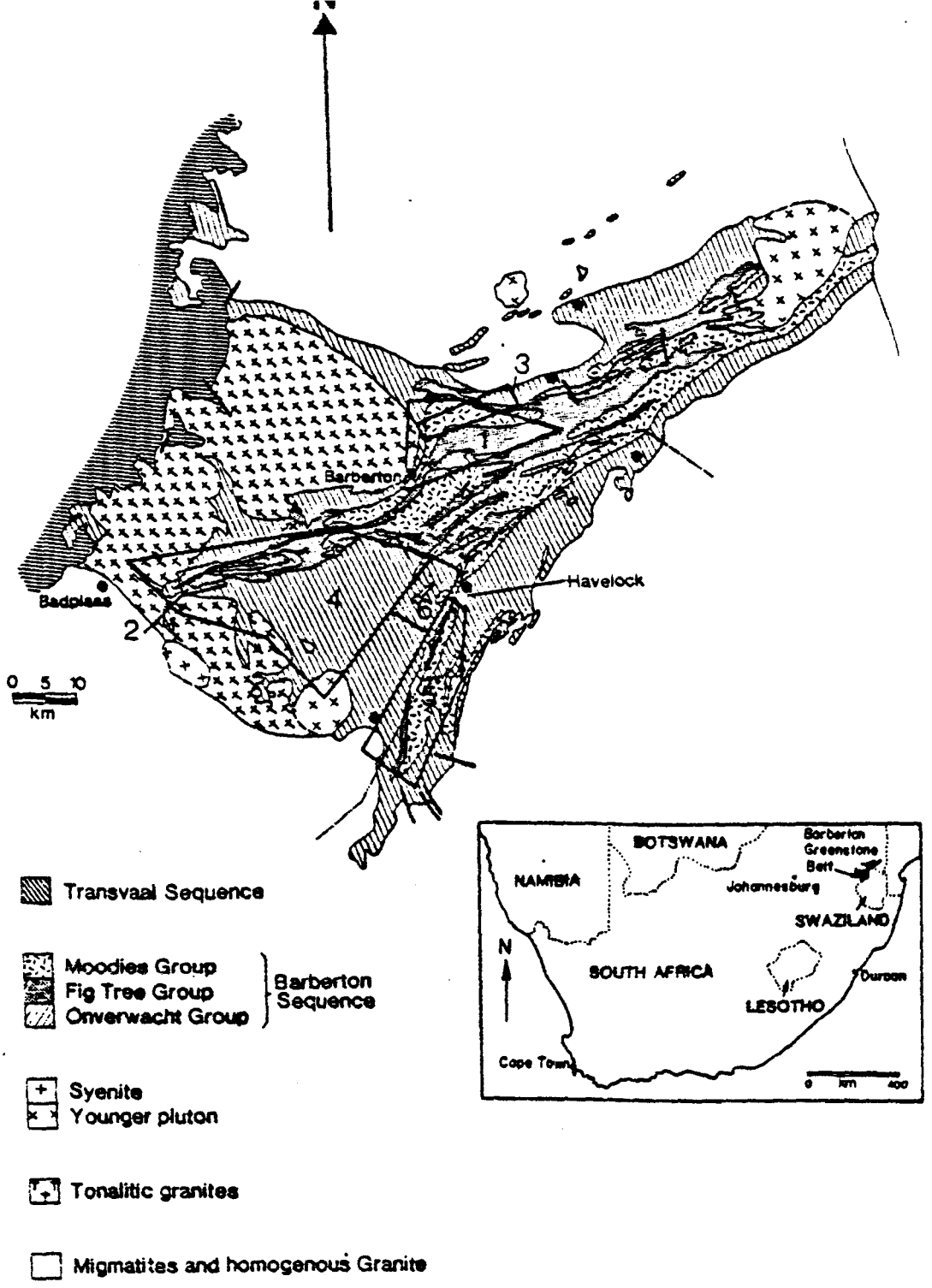


Figure 1.1. Geological map of the Barberton area after SACS, 1980, indicating the areas mapped by previous and contemporary workers.

1) Ramsay (1963), 2) Philpot (1979),

3) Fripp et al. (1980), 4) De Wit (1983),

5) Lamb (1984), 6) This study.

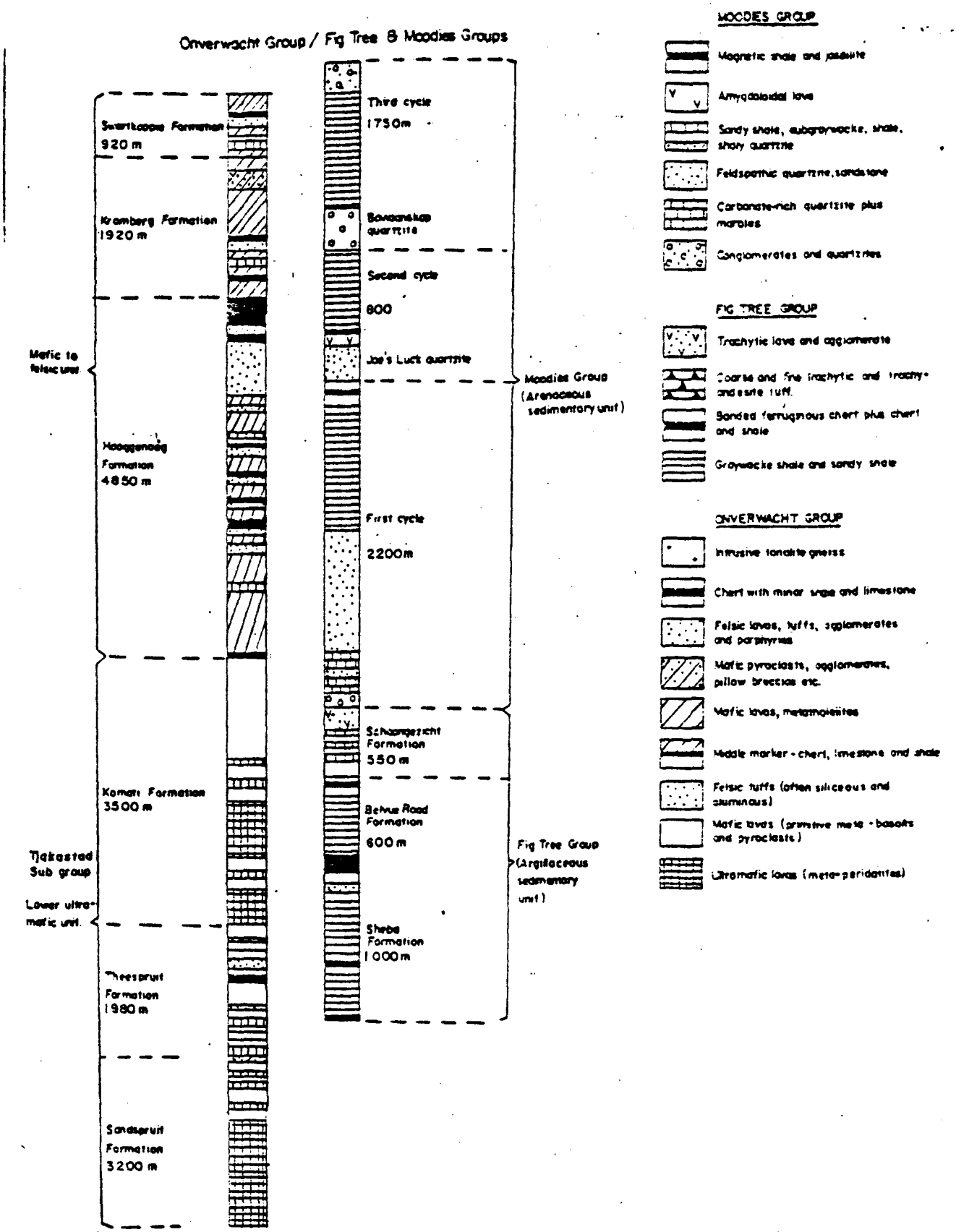


Figure 1.2 Classification of the Barberton Sequence.
(modified after SACS, 1980)

cycle starting with basalts passing upwards into zones of dacitic to rhyodacitic lava capped by black and white chert units. The top of the Hooggenoeg Formation is formed by acid volcanics and cherts. On the eastern limb of the Onverwacht Anticline, the top part of the Hooggenoeg Formation is formed by acid pyroclastic rocks including tuffs and agglomerates in which at least four cycles can be recognised. The cycles consist of coarse rhyodacitic agglomerate grading into tuff and terminated by fine grained tuff. This type of sequence would indicate cycles of violent explosive vulcanicity according to Viljoen and Viljoen (1969 d). However Lowe and Knauth (1977) have re-examined the top part of the Hooggenoeg Formation in the Komati Gorge section and they concluded that, although volcaniclastic, none of these units have an air fall origin. Only the upper sedimentary part of this formation is present in the study area.

The Kromberg Formation type section has been defined in the Komati Gorge by Viljoen and Viljoen (1969 d). They found the rock types to be very similar to the ones forming the Hooggenoeg Formation although the cyclicity is not as striking.

According to Viljoen and Viljoen (1969 d) "the Kromberg Formation is known to be present around the Msauli Mine, east of the Kromberg Fault, no detailed study of the stratigraphy has been made in the area, because of its structural complexity. Van den Berg (1969) mapped part of the formation."

The cherts of the Kromberg Formation were first described by Viljoen and Viljoen (1969 d). Oolitic cherts were first reported in the Kromberg Formation by Van den Berg (1969), Reimer (1975 a,b), and Heinrichs (1980). Van den Berg reported the presence of "micro-bedding" and graded units of oolitic cherts in the Josefsdal area. Lowe and Knauth (1977) studied the cherts of the Kromberg Formation in the type area. They interpreted the grey cherts as silicified detrital sediments with an authigenic cement. These authors (1977) pointed out that most of the Kromberg cherts are in fact silicified detrital sediments.

The Zwartkoppie Formation consists mainly of schists derived from acid intermediate and basaltic rocks, and banded black and white cherts according to Viljoen and Viljoen (1969 d). The Zwartkoppie Formation also contains conformable ultramafic bands and pods often serpentinised and steatized such as the Havelock and Msauli bodies (Viljoen and Viljoen 1969 d). In

their study of the Zwartkoppie Formation, Lowe and Knauth (1977) included ferruginous shales and silicified sediments in the sequence. Other authors (Viljoen and Viljoen, 1969 d; Reimer, 1967; Heinrich, 1980; Eriksson, 1980 a,b) have included these in the Fig Tree Group.

Lowe and Knauth (1977) noted that the Zwartkoppie Formation is similar to sheared complexes associated with thrust faulting in younger sequences and mentioned the possibility of a major structural and stratigraphic discontinuity between the Kromberg Formation and the Zwartkoppie Formation. Their study of the cherts of the Zwartkoppie Formation at several localities throughout the greenstone belt shows that most of the cherts are silicified detrital sediments. They described silicified accretionary spheroids which they interpreted as accretionary lapilli, as well as volcaniclastic sandstones and siltstones within the silicified sedimentary rocks in the Msauli Chert.

Stanistreet et al. (1981) studied the Zwartkoppie Formation at the Msauli Chert locality on Granville Grove Farm and described turbidite sequences containing graded units which include accretionary spheroids.

In the study area, the sedimentary rocks of the Zwartkoppie Formation were not well defined. Viljoen and Viljoen (1969 d), who first described the Zwartkoppie Formation stated that: "Recent mapping in the northern portion of the area depicted in Fig. 2 (Van den Berg, 1969, Heinrichs pers. comm.) has revealed the presence of a relative thickness of argillaceous sediment and banded ferruginous cherts interlayered with felsic pyroclasts and forming part of, or lying apparently conformably above the Kromberg Formation. This assemblage might represent a transitional zone from the Onverwacht Group into the Fig Tree Group. Its position relative to the Zwartkoppie Formation is however unknown so that the question of whether it should be placed in the Fig Tree or in the Onverwacht Group remains unsolved. Heinrich (verbal communication) has also had difficulty in allocating certain sequences containing volcanics and sediments to either Fig Tree or Onverwacht Group". The area they refer to corresponds to the eastern part of the study area, along the Swaziland border.

In this study, the rocks which are overlain by banded iron formation and ferruginous cherts along the eastern side of the Havelock Spruit (Fig. 2.4) and which have similar characteristics to cherts of the underlying

Onverwacht formations have been referred to the Zwartkoppie Formation. The ferruginous black and white banded cherts included in the Zwartkoppie Formation by Viljoen and Viljoen (1969 d) are lithologically identical to those found higher in the stratigraphy elsewhere in the area. They are described below, together with the upper part of the stratigraphy (Chapter 4).

Table 1.1 Summary of Main Lithologies in the Onverwacht Group

Formation	Lithology	Comments
Zwartkoppie	Acid, intermediate, and basic schists; minor pyroclastic rocks: main rock types in centre of belt banded black, white gray and green cherts: sericitic and talc-carbonate schists.	Strongly sheared in south; overlain by Fig Tree Group but relationship to Kromberg Formation not known. Present in the study area.
Kromberg	Basalt with thin intercalations of pillowed basalt; acid lava associated with chert, calc-silicate, and carbonate layers; palagonitic tuff, cross-bedded basic tuff, agglomerate; black, carbonaceous siliceous shaly layers in some chert units.	Best exposed and developed south of the Barberton belt; basaltic flows dominantly massive; some pillow breccia. Present in the study area.

Hooggenoeg	Base marked by thin, persistent chert and carbonate sediment (the Middle Marker); cycles consisting of basalt, andesite, dacite, rhyodacite and banded chert; minor ultramafic units overlie some chert layers; upper part of formation composed of thick zone of acid lava, clastic sediments, and quartz and feldspar porphyries.	Metamorphosed at lower greenschist facies; pillow structures in both basalt and dacite; amygdales, spherulites, and variolites. Upper part present in the study area.
Komati	Alternation of amphibolized, pillowed, and massive basalt and ultramafic rocks serpentinised with olivine kernels. basic rocks: amphibolite composed of variable amounts of tremolite-actinolite, cummingtonite, anthophyllite, talc, chlorite.	Ultrabasic rocks about 30% of formation; spinifex textures and less abundant pillow structures in both basic and ultrabasic rocks. Absent in the study area.
Theespruit	Ultramafic rocks: serpentine, talc-chlorite schist; basic rocks; actinolitic, tremolitic, chloritic, carbonate-bearing schist; acid rocks; sericitic and and pyrophyllitic schist, siliceous schist, intercalations of dark chert, agglomerate.	Formation widely developed throughout Barberton belt; pillow structures preserved but not abundant; formation characterised by acidic rocks interpreted to be tuff. Absent in the study area.

Sandspruit	Ultramafic rocks: serpentinite, antigorite; chlorite schist, tremolite-chlorite schist; basic rocks; amphibolite.	Preserved as large rafts or screens between intrusive tronhjemite-tonalite plutons; ultrabasic rocks constitute - 70% of formation. Absent in the study area.

Modified after Tankard et al. (1982).

The stratigraphic succession in the Onverwacht Group has been questioned by Williams and Furnell (1979). These workers re-investigated part of the type area of the Onverwacht Group and recognised a thick (1000m) sequence of basaltic komatiite in the Hooggenoeg Formation. This unit has a 15km strike length with textural and chemical characteristics identical to the basaltic komatiite of the Komati Formation. Williams and Furnell noted that this unit of basaltic komatiite is reported by Viljoen and Viljoen (1969 d) in a similar position in the Hooggenoeg Formation approximately 5km south east of the area they studied and that basaltic komatiite is also reported by Viljoen and Viljoen (1969 a-d) in the Kromberg Formation.

Williams and Furnell pointed out that the broad scale alteration of komatiite and tholeiite is typical of other greenstone belts and demonstrated that the Middle Marker does not represent a major time break separating two trends in the composition of the rocks (i.e. ultramafic and mafic below the Middle Marker and mafic, intermediate and acid above the Middle Marker). They suggested that the Middle Marker may not represent a major crustal or mantle adjustment as contended by Viljoen and Viljoen (1969 a-d).

Williams and Furnell concluded that there was complex interfingering of basaltic komatiite, dacite, rhyodacite, tholeiite and basaltic andesite in the Hooggenoeg Formation, instead of a repetition of cycles. They envisaged the Hooggenoeg Formation as a complex interplay of overlapping volcanic products of different compositions.

Burke et al. (1976) pointed out that tectonic boundaries, especially thrusts and tectonic slides, concordant to bedding are likely to be present in Archaean sequences. Williams and Furnell (1979) suggested the presence of such discordances (tectonic or stratigraphic) between the Theespruit Formation and the Komati Formation as well as between the Hooggenoeg Formation and the Kromberg Formation and therefore questioned the "layer cake" stratigraphic model of Viljoen and Viljoen (1969 a-d). These findings were disputed by Viljoen and Viljoen (1979)in their discussion of the paper.

De Wit (1982; 1983) and De Wit et al. (1983), suggested that polyphase deformatiom has led to important tectonic repetition within the Onverwacht Group. De Wit et al. (1983), suggested that a deformed unconformity is locally present between the Barberton sequence and an underlying pre-greenstone belt sialic crust.

From their study of the Komati Formation type section, De Wit and Stern (1980), concluded that the Onverwacht Group was very similar to more recent ophiolite complexes, comprising basal ultramafic cumulates, possibly a sheeted dyke complex, a pillowed layer and a sedimentary unit.

b) The Fig Tree Group

The Fig Tree Series was first defined by Van Eeden (1941) as the lower "argillaceous" part of the Moodies Series as defined by Hall (1918). Visser et al. (1956) divided the Fig Tree Series into a lower Zwartkoppie Zone of greenschists, talcose and carbonate rocks followed by six unnamed zones based on distinct lithological units. These units comprised mainly shale, graywacke, conglomerate, chert and banded ironstone.

Viljoen and Viljoen (1969 a), proposed that the Fig Tree Series be regarded as a Group, made up of various Formations. Anhaeusser et al. (1969) regarded the Zwartkoppie succession as the lowermost unit of the Fig Tree Group. They termed it the Zwartkoppie Zone and divided the rest of the Group into middle and upper sequences. However, Viljoen and Viljoen (1969 a) considered the Zwartkoppie succession to be more closely related to the Onverwacht Group and included it within the Onverwacht Group as the Zwartkoppie Formation (Fig. 1.2) This was later followed by SACS (1980).

Field investigations carried out by Reimer (1967) in the Stolzburg and Ulundi Synclines led him to divide the Fig Tree Group into three formations (Fig. 1.2), namely the Schoongezicht Formation, the Belvue Road Formation and the Sheba Formation. This classification has been adopted by SACS (1980).

Various studies of the Fig Tree Group (Reimer 1975 a; Condie et al., 1970; Eriksson 1980 a,b) have shown a conformable relationship between the Onverwacht Group and the Fig Tree Group.

Reimer (1967) subdivided the Fig Tree Group into areas of two different facies. The northern facies, where the type sections have been defined, is characterised by graywackes and shales with lesser amounts of cherts and iron formation. The southern facies consists of cherts, banded ironstones and shales grading upwards into fine and coarser terrigenous clastics and

lenses of conglomerate. Reimer (1967) considered the southern facies to be the equivalent of the Belvue Road Formation. The southern facies has been subdivided by Heinrichs (1980) into three formations: the Schoongezicht Formation, the Mapepe Formation, and the Ngwenya Formation. The study area is situated within the area covered by the southern facies of the Fig Tree Group.

c) The Moodies Group

Kynaston (1906) first proposed the name Moodies Series for the total sedimentary succession within the greenstone belt. The succession was first studied in detail by Hall (1918). The Moodies Series was later subdivided into the Fig Tree Series and the Moodies Series by Visser et al. (1956) (Fig. 1.2) and into the Fig Tree and Moodies Groups by Viljoen and Viljoen (1969 a). Visser et al. (1956) suggested the presence of a major unconformity between the Fig Tree Group and the Moodies Group, while Condie et al. (1970), Anhaeusser (1976) and Eriksson (1977) found the relationships between the two groups to be both conformable and unconformable. Anhaeusser (1969 a; 1976) formally divided the Moodies Group in the Eureka Syncline into three formations: the Baviaanskop Formation, the Joe's Luck Formation, and the Clutha Formation. He considered each formation to represent a cycle of sedimentation (Fig. 1.2). Eriksson (1980 a,b) studied the Moodies Group throughout the belt and proposed a different stratigraphy with correlations throughout the greenstone belt. He subdivided the Moodies Group into five units (MD1, MD2, MD3, MD4, MD5). His correlations are based on a prominent unit of amygdaloidal lava at the base of unit 4 which can be recognised in the Eureka Syncline, the Saddleback Syncline and the Stolzburg Syncline. Correlations in the southern part of the belt were based on conglomeratic units interpreted as marking the base of the Moodies Group. However, Eriksson (1977) noticed the presence of lithologically similar sedimentary rocks in both the Fig Tree Group and the Moodies Group.

1.2.2 GEOCHRONOLOGY

Radiometric age determination on intrusive plutons (Rb/Sr whole rock isochrons) within and surrounding the greenstone belt show that the Barberton Sequence was formed around Ca 3500 to 3200 MA (Barton, 1981 a,b). The Komati Formation has been dated at Ca 3500 MA (Nd/Sm whole rock isochron, Hamilton et al., 1973; Jahn et al., 1982). Barton (1981 a,b) using Rb/Sr biotite-whole rock ages argued that the regional metamorphism occurred at least Ca 3000 MA ago.

Chert bars, carbonates, barites and serpentinites of the Onverwacht group have yielded an age of Ca 3300 MA (De Wit et al., 1982; York et al., 1981), while the Middle Marker was dated at 3355 +/- 70 MA (Hurley et al., 1972). De Wit et al. (1982 a) argued that these ages based on the whole rock K - Ar could represent the early metasomatism.

1.2.3 STRUCTURAL GEOLOGY

Early workers (Hall, 1918; Visser et al., 1956), already emphasised the importance of deformation in the belt. Hall (1918) noticed the presence of tectonic repetition in the Moodies Group.

Visser et al. (1956) described folding and faulting along ENE/WSW axes as well as shear zones within the Onverwacht Group. They related the deformation to granite intrusion. However, they considered that pre-Moodies folds in the Fig Tree Group preceded granite emplacement.

a) The northern part of the belt

The first to document polyphase heterogeneous deformation in the belt was Ramsay (1963). From detailed studies in the northern part of the belt, he distinguished the following three separate phases of deformation: (i) A first phase gave rise to folds with steeply inclined axial planes striking NE/SW. (ii) A second phase resulted in the formation of a sub-vertical

slaty cleavage and schistosity cutting obliquely across these first folds. Large steeply plunging folds were formed during the second phase. (iii) A third phase which deformed the earlier formed cleavage and folds.

Gay (1969) has shown that the amount of strain varied from low strain in the centre of the the belt to high strain in the north and north western parts, most strains being of the flattening type. Anhaeusser (1969 b) has calculated that a 61 to 63% shortening occurred during deformation.

Fripp et al. (1980) studied the major shear zones developed along the northern margin of the belt. They concluded that the base of the belt represented a major, low-angle, south-dipping sole-thrust and postulated a northward motion for the belt.

b) The southern part of the belt

Studies in the southern part of the belt by Viljoen and Viljoen (1969 a) have suggested that most of the deformation in the greenstone belt could be ascribed to the granite emplacement. These authors described the belt as a strongly deformed synclinorial boat shaped remnant, surrounded by granites and with a dominant ENE trend. The synclinoria are formed by tight steeply dipping synclinal folds with poorly developed or sheared out anticlines. While they mention the existence of up to five phases of deformation in the northern part of the belt, Viljoen and Viljoen (1969 a) did not relate it to the southern part nor subdivide the strain history into separate periods. In their opinion, very little evidence existed for lateral compression. They recognised an early phase of regional folding which they attributed to large scale slumping and sagging.

Although Viljoen and Viljoen (1969 a,b; 1970) recognised the presence of vertical schist zones and cleavage development, they related such features to granite emplacement and placed little stratigraphic significance on these zones. This was strongly criticised by Burke et al. (1976).

In accordance with the data and interpretation of Viljoen and Viljoen (1969 a-e; 1970), Anhaeusser (1975) summarised the deformation of the greenstone belt as follows: "

1. The diapiric plutons prized off, stoped, and assimilated greenstone material becoming full of inclusions as the lavas were engulfed.

2. As the granites rose, concomitant downsagging of the adjacent greenstones occurred and the pluton margins developed a pronounced foliation and lineation.

3. Greenstone xenoliths close to the granite contacts became aligned in the foliation directions of the gneisses, parallel to the greenstone belt margins which also developed a strong schistosity parallel to the granite contacts.

4. Differential compression resulted in the development of isoclinal folding, pebble and pillow flattening, and mineral orientation during metamorphism.

5. Various fold styles developed because of competency contrasts existing between the various lithologies.

6. Reactivation of earlier formed planes of weakness produced transcurrent faults, drag and disharmonic folds, and numerous attendant second and higher order faults, fractures and joints.

7. Late stage vertical adjustments produced superimposed small and large scale folds (conjugate, chevron and kink band folds)."

Additionally, the following three features were used to support the view that gravitational influences, as opposed to compressional tectonics, were responsible for the deformation:

1. Very low grades of regional metamorphism;

2. The irregular distribution or absence of all-pervasive, totally penetrative structures (cleavage-schistosity);

3. The preferred tendency for synclines to form and anticlines to be faulted out by high-angled slides.

In the same area as that studied by Viljoen and Viljoen (1969 b), Williams and Furnell (1979) described two possible unconformities within the Onverwacht Group as well as large isoclinal folding in the Theespruit Formation and suggest that more detailed structural studies of the belt were warranted.

Philpot (1979) studied the southwestern part of the belt, around the Sterkspruit complex (Fig 1.1). His work has shown the presence of two phases of folding in the area. The first phase led to the formation of tectonic slices and tectonic repetition. Working on deformed pebbles, he calculated a 4.8/1 strain ratio in the area and estimated a 75% shortening for this part of the belt.

In the southwestern part of the belt De Wit (1982) has clearly demonstrated that an early deformation was present which involved thrusting and internal recumbent folding of allochthonous nappes. These thrust planes are underlain by fuchsite rich tectonites.

De Wit et al. (1983) have shown that tectonic dislocations, and large scale upright folds, have created a complex tectono-stratigraphy in the southern part of the belt. Using structural as well as sedimentological data, they concluded that the tectono-stratigraphy present in the southwestern part of the belt invalidates the existing stratigraphy. Lowe and Nocita (1983) also described the presence of tectonic breaks within the Onverwacht Group, in the same area.

In Swaziland, Barton (1982) studied the Havelock asbestos mine in detail. He concluded that the rock sequences could best be explained if the presence of Alpine style thrusting in the serpentinite body was assumed. Jackson and Robertson (1983), reported four phases of folding in the Onverwacht Group in the Motjane shist belt in Swaziland. The work undertaken in Swaziland (Lamb, 1984) at the same time as this study, has shown the existence of a complex tectono-stratigraphy in which four phases of deformation can be distinguished.

In a recent review, Anhaeusser (1983) concluded that the emplacement of granitic magmas and diapiric plutons were the major causes of the deformation as he felt that evidence for earlier deformation (involving horizontal shortening and thrusting) remained speculative.

In the study area, no detailed structural investigations have been undertaken in the past. Van den Berg (1969) reported the presence of tight synclines with poorly developed anticlines as well as "an important amount of faulting" in the area. Viljoen and Viljoen (1969 d), noted the structural complexity of the area but they did not include it in their studies.

1.2.4 METASOMATISM

In the Barberton greenstone belt, metasomatism is a widespread phenomenon throughout the stratigraphic column.

Silicification of shales and the gradational transition from shales to ironstone have been reported by Visser et al. (1956). Van den Berg (1969), Reimer (1967) and Heinrichs (1980) mentioned the silicification of the Onverwacht sediments.
Viljoen and Viljoen (1969 a,d) reported the presence of carbonate and silica veins within the Onverwacht Group. Condie et al. (1970) suggested that the silica in chert clasts of the Fig Tree and Moodies Groups, in the northern part of the belt, could have been derived from submarine volcanic emanations or "desilication of deeper rocks".
Lowe and Knauth (1978) have shown that many of the cherts in the Onverwacht Group represent silicified volcaniclaustic sediments (see Chapter 3).
De Wit et al. (1982 a) reported the presence of silicified and carbonated igneous and sedimentary rocks throughout the stratigraphic column, and ascribed the metasomatism to hydrothermal systems.

1.3 AIMS AND METHODS OF THE STUDY

This study was prompted by the renewed interest in the geology of the Barberton greenstone belt and the controversy surrounding the Barberton model.

One of the main aims of this study has been to produce a geological map (1 : 10000) of an area hitherto not examined. The area adjoins two other areas, recently and/or currently mapped (Fig 1.1). The map will be used to compile a geological map of the entire southern part of the greenstone belt.

It was realised during the early stages of the project that detailed mapping had to be undertaken and that the effects of deformation and metasomatism had to be understood before any reconstruction of the geological history could be established.

Therefore, this study is an integrated analysis of the deformational, sedimentological, metamorphic and metasomatic features observed in the area. The detailed geological map (1 : 10000) of the area is presented at the back of the volume.

A total of 15 months of field work was conducted over a period of three years, using aerial photographs of an approximate scale of 1 : 13000. Several areas of good exposure have been singled out for more detailed work such as construction of equal area projections of structural data, measured sections, and detailed mapping at a scale of 1 : 5000.

In addition to the mapping, detailed sedimentological sections were measured. These are presented in the appendices. Petrographic studies were carried out by microscope observation of thin sections.

Younging directions mentioned in this study are derived from the following sedimentary structures: graded units, channels and scours, cross-stratification load structures and pillow lavas (Chapter 3, 4). On the main map, younging directions are labelled a, b, or c, according to the degree of confidence: a = very highly confident, b = highly confident, c =

moderately confident. In the diagrams and throughout the thesis, only type a younging directions have been used.

A 10cm wide grid has been marked on the main map for easy reference to geological features mentioned in the text (Chapter 5, 6).

CHAPTER 2

2.0 THE ONVERWACHT GROUP: META-IGNEOUS ROCKS

2.1 INTRODUCTION

As described in Chapter 1, the established stratigraphy of the Onverwacht Group has been questioned by several authors. However, while an alternative stratigraphy will be proposed in Chapter 7, the classic stratigraphy has been followed in this descriptive chapter in order to avoid confusion and for cross reference purposes with earlier work. In the study area, the Onverwacht meta-igneous rocks are developed in the Kromberg Formation and the Zwartkoppie Formation (Van den Berg, 1969; Viljoen and Viljoen, 1969 d; Anhaeusser et al., 1981). In the study area most of the rocks of the Onverwacht Group are extensively weathered. Therefore reference to and comparison with outcrops outside the area has often been necessary.

2.2 THE KROMBERG FORMATION

In the study area the Kromberg Formation outcrops in the valleys and on lower ridges. The various igneous rocks of the Kromberg Formation can be subdivided into four types: mafic and ultramafic rocks; carbonated intru-

sive rocks; siliceous igneous rocks; and the rock type referred to by De Wit (1982) as "flaser banded rock".

2.2.1 THE MAFIC AND ULTRAMAFIC ROCKS

Due to the weathering and to the importance of silicification and carbonation, the mafic and ultramafic rocks are not readily distinguishable in the field and are therefore described together. They have been studied in comparison with established type sections elsewhere in the greenstone belt. The mafic rocks occur as pillow lava and massive lava and the ultramafic rocks are represented pods of serpentinite and pyroxenite.

(a) Pillow lavas

Two types of pillow lava can be distinguished with intermediates between the two types. The measured section within the Kromberg Formation shown in Fig 2.1 is located 2km south of the study area but has nevertheless been studied because it offers the only well exposed outcrop. The pillow characteristics will be described from this section while the microscopic studies and the rock types will be described from outcrops in the study area.

The first pillow type (type A, Fig 2.2) is characterised by irregularly shaped and often poorly defined pillows which fit together well and have no interstitial brecciated material. The edges of the pillows often contain numerous pale green coloured ocelli which coalesce towards the centre of the pillow. These pillows are often elongated and do not have well developed chilled margins, radial cracks or vesicles. In thin sections these pillows (type A) contain chloritised clinopyroxene crystals, augite crystals, and swallow tail shaped plagioclase crystals which have been replaced by sericite and epidote crystals. Unreplaced crystals are rare. The swallow tail shaped crystals are also present in the ocelli.

The second type of pillow (type B, Fig 2.3) is characterised by well defined balloon, bun and bean shapes which can be used, together with other crite-

ria, to indicate younging directions. These pillows have a chilled margin between 2 to 2,5 cm thick and contain rounded or radially elongated vesicles around their edges. In the centre of type B pillows, withdrawal tubes or radial cracks may be present. The interstitial material is formed by pillow breccia material which can comprise much of the rock volume in places (Fig. 2.4). These pillows do not contain any ocelli.

In thin section, the type B pillows show an ophitic texture and clusters of augite crystals. Zeolite crystals fill some of the vesicles. One of the best examples of pillow breccia associated with type B pillows is exposed in the Msauli Power Station measured section (Fig. 2.4). Similar rocks occur on the Dunbar Farm (Fig 2.5 loc. F) from where they are described below. The pillow breccia generally grades along strike into "flaser banded rocks" and underlies silicified sedimentary rocks in units 5 to 10m thick. The breccia contains a fuchsitic and carbonated green matrix and elongated brown carbonated fragments and pillow fragments. The fragments vary in size from 5 to 25cm across. In thin section, the rock is mainly composed of secondary carbonates of several generations. The carbonates occur in tensional veins, in bands and in patches and the groundmass is formed by microcrystalline quartz and sericite.

Similar pillow types have been described by De Wit and Stern (1978) from Chile. They interpreted the type A pillows as intrusive (pseudo pillows). Type A pillows can also be traced into dykes in the Barberton area (De Wit, pers. comm.) and they are thus also interpreted as intrusive units, or pseudo pillows. Type B pillows are interpreted as classic extrusive pillows.

(b) Massive lavas

On the north western part of the Diepgezet Farm (Fig. 2.5 loc. A), one outcrop has been found which displays columnar jointing and spinifex textures similar to those found in the Komati Formation type section area. The rock is fine grained, light green and contains numerous randomly orientated needles, 1 cm long. In thin section, the spinifex textures are formed by amphibole crystals replaced by muscovite and sericite. The groundmass is heavily replaced by carbonates. The rock is mainly composed of carbonates, muscovite and sericite and the above mentioned textures could indicate an original komatiitic composition (Fig. 2.6).

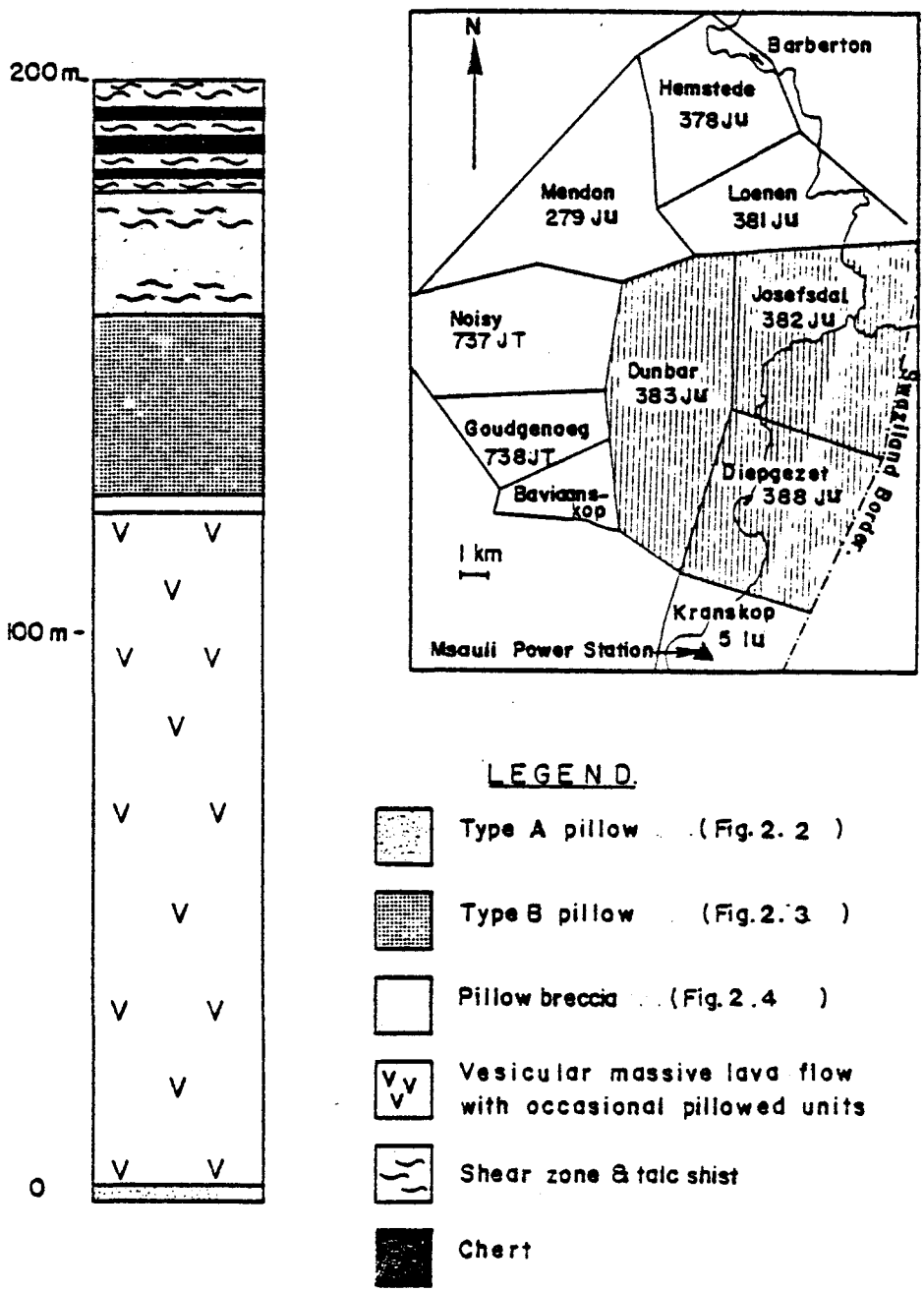


Figure 2.1. Measured section in the Kromberg Formation showing the two types of pillow lava. Msauli Power Station (Kranskop Farm).

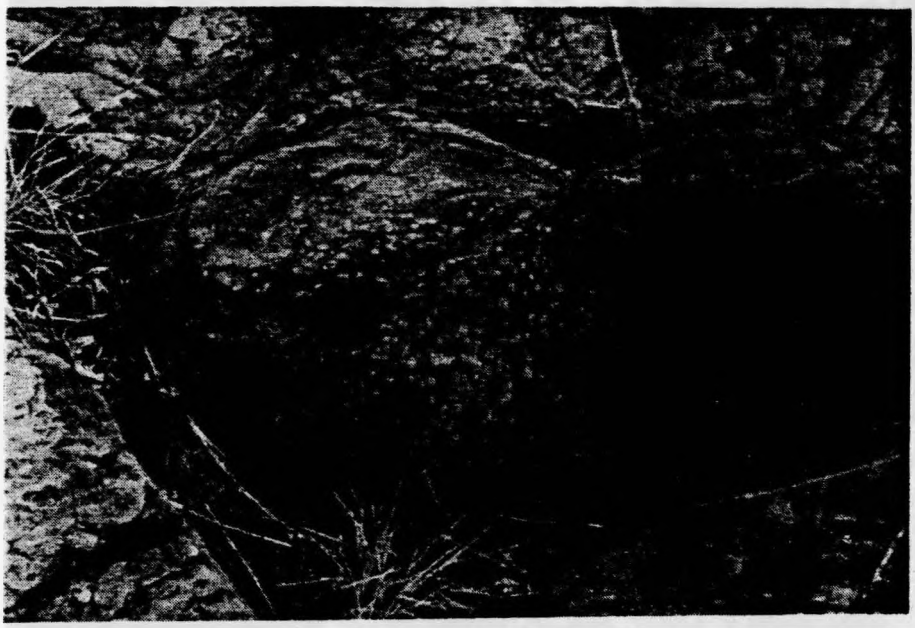


Figure 2.2. Type A pillow with ocelli in the centre Msauli Power Station (Kranskop Farm).



Figure 2.3. Type B balloon shaped pillow, scale bar = 20cm Msauli Power Station, (Kranskop Farm).



Figure 2.4. Pillow breccia associated with type B pillow lava (Msauli Power Station, see Fig. 2.1)

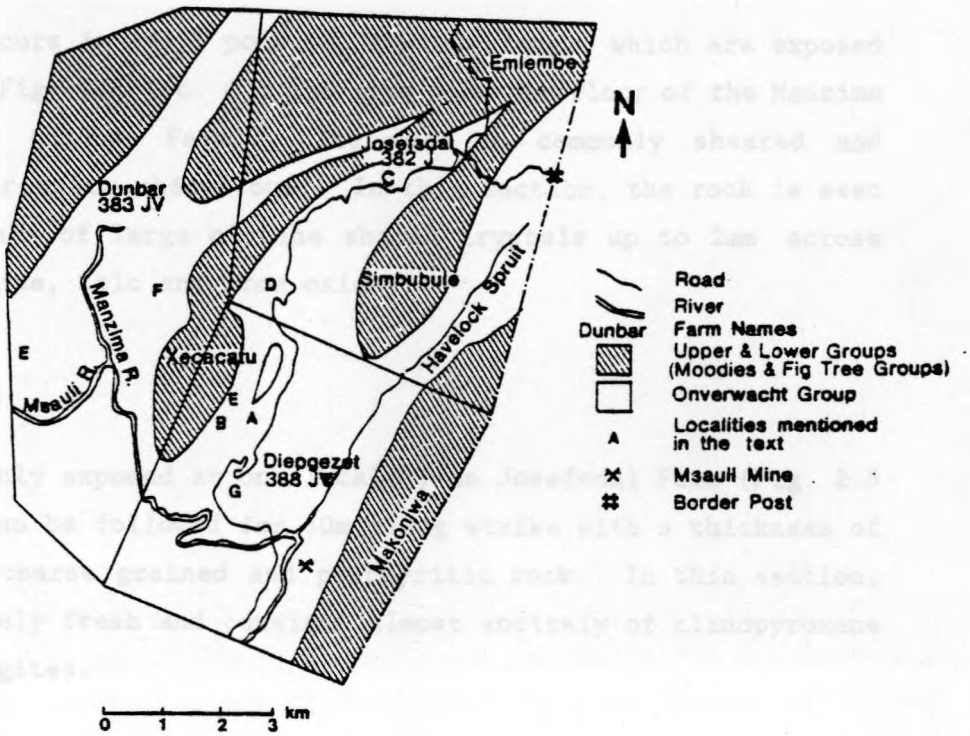


Figure 2.5. Locality map of the study area. A) massive lava with columnar jointing; B) ocelli bearing lava; C) serpentinites; D) pyroxenite; E) carbonated pods; F) volcanic breccia; G) variolitic chert.

On Diepgezet Farm (Fig. 2.5 loc. B), several outcrops have been found of an ocelli bearing lava. The lava is extremely weathered and has a yellow to pink colour due to the leaching of iron. The weathering accentuates the varioles which range in diameter from 1 to 6 cm. In thin section, the rock is composed principally of carbonated ferromagnesian minerals and carbonated hopper and skeletal crystals (Fig. 2.7). The shapes of these crystals are identical to that of supercooled olivine crystals described by Donaldson (1982). No traces of feldspar crystals has been seen in thin section. This suggests an original mafic composition for the rock. Fresher variolitic rocks from the Komati Formation type area also contain hopper and skeletal crystals.

However, in most cases, massive lava has totally weathered into clay in which only occasional pillow shapes indicate that the rock was originally igneous. Thus in the absence of preserved petrographic textures it is not possible to determine whether such lavas were originally mafic or ultramafic.

(c) Serpentinite

The serpentinite occurs in small pods (80 to 100m long), which are exposed on Josefsdal Farm (Fig. 2.4 loc. C), and also form the floor of the Manzima and Dunbar Valleys (Dunbar Farm). The rock is commonly sheared and slickenside structures are ubiquitous. In thin section, the rock is seen to be composed mainly of large olivine shaped crystals up to 2mm across replaced by antigorite, talc and iron oxides.

(d) Pyroxenite

This rock type is only exposed at one locality on Josefsdal Farm (Fig. 2.5 loc. D), where it can be followed for 60m along strike with a thickness of 5m. It is a blue coarse grained and porphyritic rock. In thin section, the rock is relatively fresh and consists almost entirely of clinopyroxene crystals (titano-augite).

(e) Carbonated igneous pods

Only two outcrops of this lithology are present in the study area (Fig. 2.5 loc. E). It occurs in 2m to 4m long pods, which are intrusive into green



Figure 2.6. Photomicrograph of massive lava showing spinifex textures. The crystals are composed of sericite and muscovite. The groundmass is mainly composed of carbonate. Width of field = 3,5 mm. (Diepgezet Farm). Plane polarised light.



Figure 2.7. Photomicrograph of ocelli bearing lava showing carbonated euhedral and hopper crystals believed to be pseudomorphs of olivine crystals. The groundmass is composed of iron oxide. Width of field: 3,5 mm (Diepgezet Farm). Plane polarised light.

cherts and layered in places. On the weathered surface, the rock is yellowish and fine grained with numerous weathered out carbonate rhombs (2mm in size). On a fresh surface, the rock is colour banded with an alternation of bright green and darker bands. The layers are 2mm thick and folded. Carbonate rhombs are present throughout the rock and cross cut the layers. In thin section, only carbonate crystals were noted. They are strongly strained and have replaced the pre-existing mineralogy entirely.

2.2.2 THE SILICEOUS IGNEOUS ROCKS

For reason of convenience, the siliceous igneous rocks will be subdivided into pillowed siliceous igneous rocks and massive siliceous igneous rocks, both types can be seen to disrupt the overlying silicified sedimentary rocks.

(a) The pillowed siliceous igneous rocks

The pillowed siliceous igneous rocks have previously been referred to by Viljoen and Viljoen (1969 d) as felsic with a composition ranging from dacite to rhyodacite and rhyolite. Viljoen and Viljoen (1969 d) mention the frequency of carbonate and silica replacement: "Most specimens examined show signs of carbonate replacement and, in some instances, the rock may contain up to 60% carbonates often preferentially replacing the felspar laths. Silicification is also commonly encountered, the pillow structure in these instances being transected by small veins of quartz and also containing large replacement blebs of quartz".

Although these rocks are generally strongly weathered they often show well developed pillow shapes. They are always rich in iron oxides, and the iron and silica content appears to vary both along and across strike. In the field, the rock is yellow brown to pink and often totally altered to a yellow or white clay, often with liesegang rings produced through weathering. Fresher samples show a fine to medium grained texture. The pillows are mostly type B pillows as illustrated in Fig. 2.8; although in places, the type A pillows are observed (Fig. 2.9). The characteristics of the

pillows may change along strike from type B pillows to a mixed type, i.e. well shaped pillows with vesicles, chilled margin which contain some ocelli. In thin section, the rocks consist of a fine mesh of microcrystalline quartz, sericite and iron oxides in which an ophitic texture can still be recognised. In several thin sections, euhedral crystal shapes, presumably olivine, as well as hopper crystals, and skeletal crystals, all of which have been replaced by microquartz, can be recognised (Fig. 2.10).

The type A pillows are often deformed and always rich in fuchsite, which gives them a bright green colour. The rock is fine grained and the ocelli are light green to white. In thin section, the groundmass is strongly overprinted by carbonate, with small amounts of microcrystalline quartz. The ocelli contain skeletal textures now composed of microquartz in a sericite and microquartz groundmass (Fig. 2.11).

(b) The massive siliceous rocks

These rocks form rather prominent chert layers which are either overlain by silicified sediments or lie in the middle of poorly exposed siliceous pillows. They grade along strike into the pillowed siliceous rocks described above. They can be divided into spinifex textured cherts, variolite bearing cherts and green homogeneous cherts.

The spinifex textured cherts were first recognised by De Wit et al. (1982 a). Similar rocks have also been recorded in the Swaziland part of the greenstone belt (Lamb, pers. comm., 1982). The rock is bright green when fresh and weathers to a yellowish green to pale green colour. It contains long thin blades (1mm wide and 5 to 6 cm long), which are generally parallel to one another and in some outcrops randomly orientated (Fig. 2.12, 2.13). In thin section, the matrix is seen to consist of sericite and microquartz. The blades are composed of microquartz and sericite (Fig. 2.14.a). The texture represented by these blades closely resembles the amphibole spinifex texture present in komatiites of the Komati Formation type section and first reported by Viljoen and Viljoen (1969 c) (see also Viljoen et al., 1983) (Fig. 2.14.b).

The variolite bearing cherts are exposed on Diepgezet Farm (Fig. 2.5, loc. F) as 4 to 7m thick units underlying a silicified sediment.

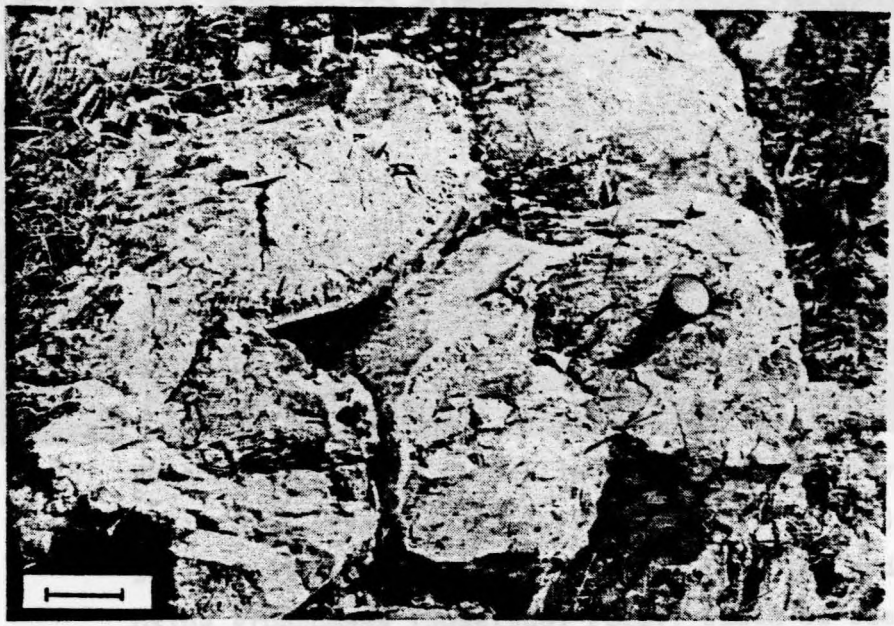


Figure 2.8. Silicified type B pillow lava (Josefsdal Farm)



Figure 2.9. Ocelli in silicified type A pillow lava (Josefsdal Farm)
Scale bar = 10cm



Figure 2.10. Photomicrograph of silicified type B pillow lava showing silicified crystals, interpreted as olivine (O)and silicified hopper crystal (h) in a sericite and iron oxide groundmass (Josefsdal Farm). Width of field = 3,5mm. Plane polarised light.

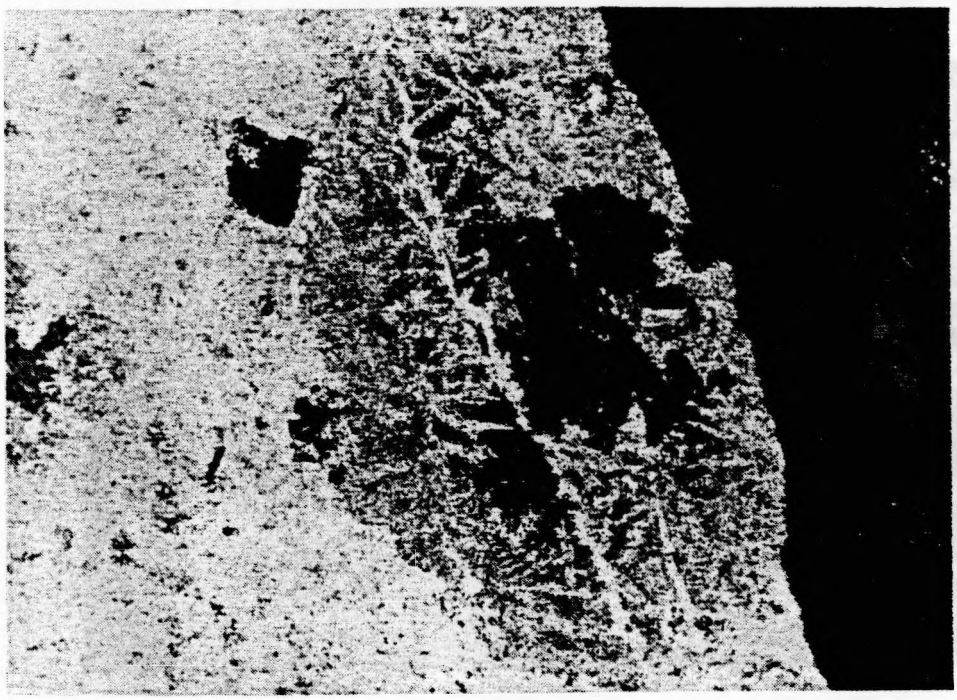


Figure 2.11. Photomicrograph of silicified type A pillow lava showing silicified skeletal textures in the ocelli.
The groundmass is composed of sericite and microquartz.
(Josefsdal Farm) Width of field = 3,5mm.
Plane polarised light.

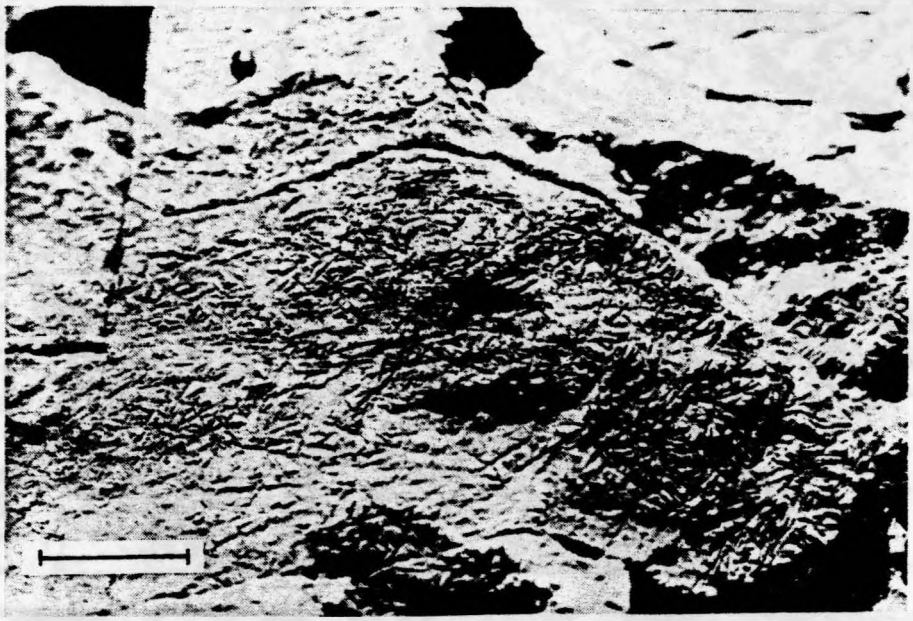


Figure 2.12. Randomly oriented silicified spinifex-like textures. (Josefsdal Farm) Scale bar = 1cm

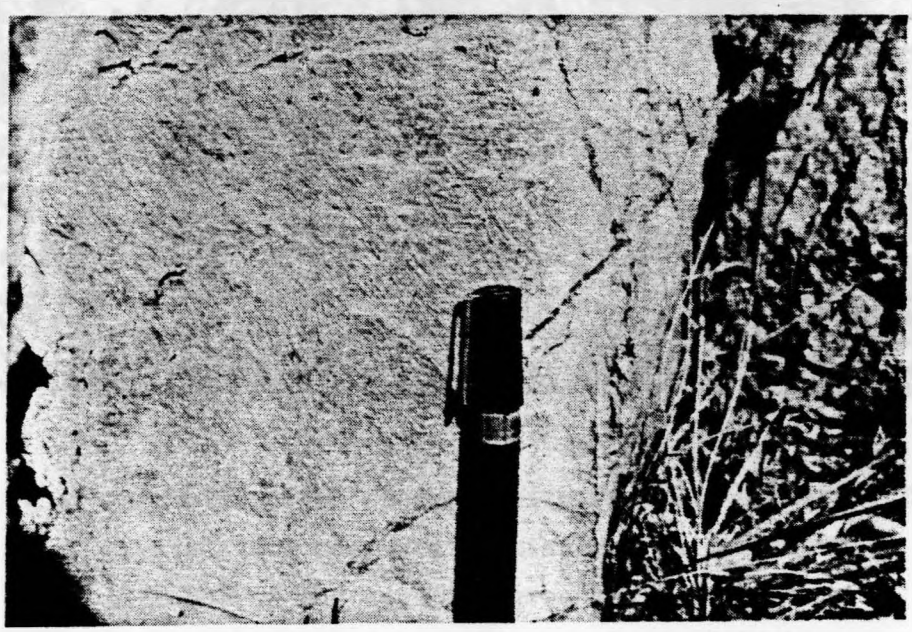


Figure 2.13. Chert containing parallel spinifex-like textures. (Josefsdal Farm)

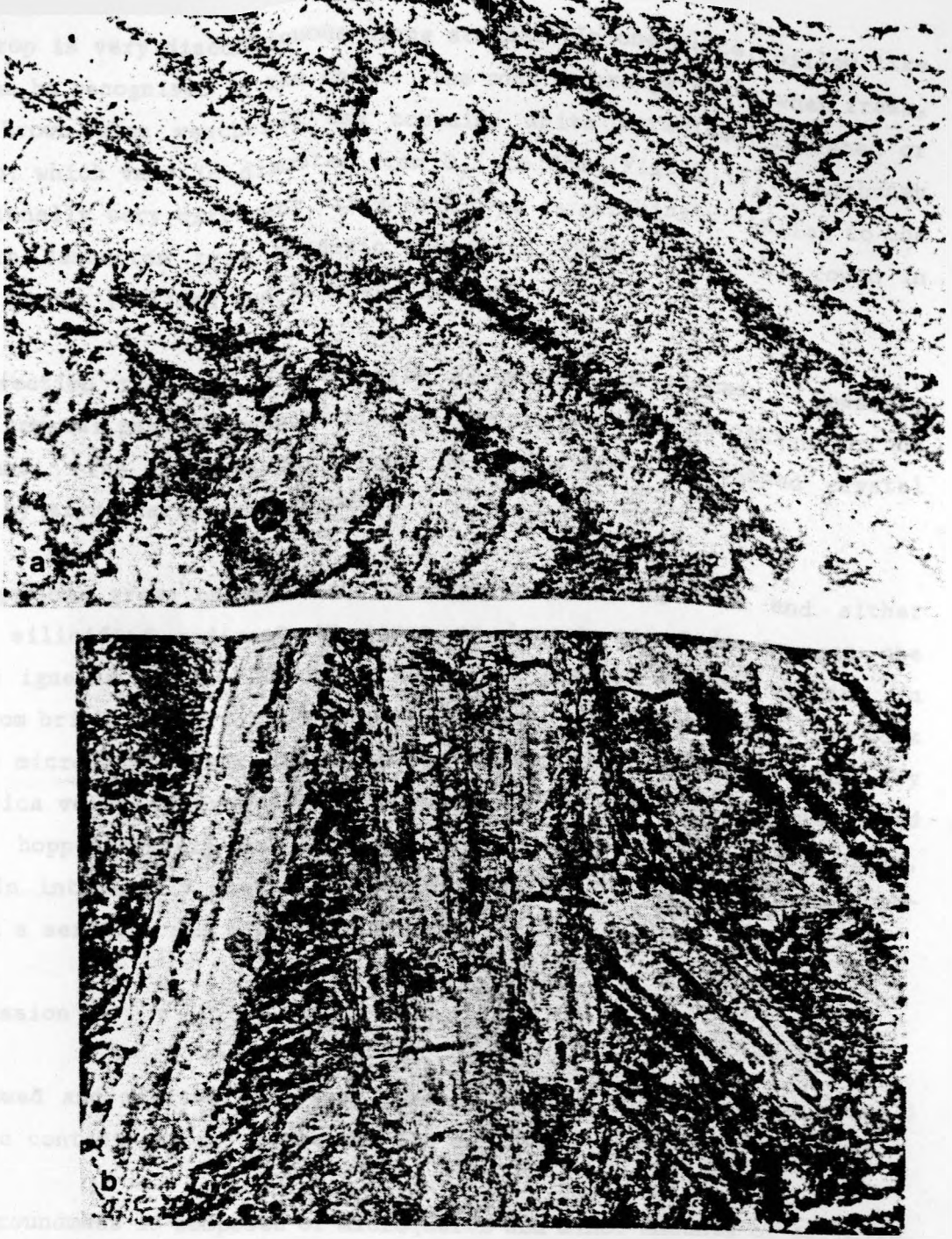


Figure 2.14.a. Photomicrograph of chert with spinifex textures. The long crystals are composed of microquartz and sericite in a microquartz and sericite groundmass.
Width of field: 3,5mm. Plane polarised light.

b. Photomicrograph of spinifex textured komatiite for comparison with 2.14.a. (Komatiite type section, Viljoen and Viljoen, 1969 c).
Width of field: 3,5mm. Plane polarised light.

The outcrop is very discontinuous along strike. In one place, pillow like shapes can be recognised in the chert. The rock is orange-white when fresh, pinkish brown when weathered and contains white varioles, isolated or clustered, which vary in diameter from 0,5 to 8cm (Fig. 2.15). Although compositionally very different, this rock type is strikingly similar to the variolitic Barberton type basaltic komatiite (Fig. 2.16 a,b) found in Spinifex Spruit (Viljoen and Viljoen, 1969 c).

In thin section the rock is strongly carbonated in places. However, euhedral crystal pseudomorphs of microquartz can still be recognised in the ground mass. The varioles are formed by stubby and lath shaped crystal replaced by microquartz and carbonate.

The homogeneous green cherts occur throughout the study area and either underlie silicified sediment or occur as lenses and pods amongst the siliceous igneous rocks. They are very fine grained cherts varying in colour from bright green to pale yellowish green. In thin section, the rock comprises microquartz with minor amounts of sericite, often cross-cut by large silica veins. Microquartz pseudomorphs after euhedral olivine shaped crystals, hoppercrystals and skeletal crystals are present (Fig. 2.17, 2.18). In intensively weathered samples, ophitic textures are still preserved in a sericite and microquartz mesh.

(c) Discussion

The pillowed and massive siliceous igneous rocks described above can all be seen to contain one or several of the following characteristics:

- The groundmass is composed of microquartz and minor amounts of sericite.
- Crystal shapes, including hopper and skeletal crystals and euhedral crystals, are always composed of microquartz.
- Ophitic textures can be recognised.
- The variolite bearing rocks are similar to those found in komatiitic rocks.



Figure 2.15. Variolitic chert (Diepgezet Farm)

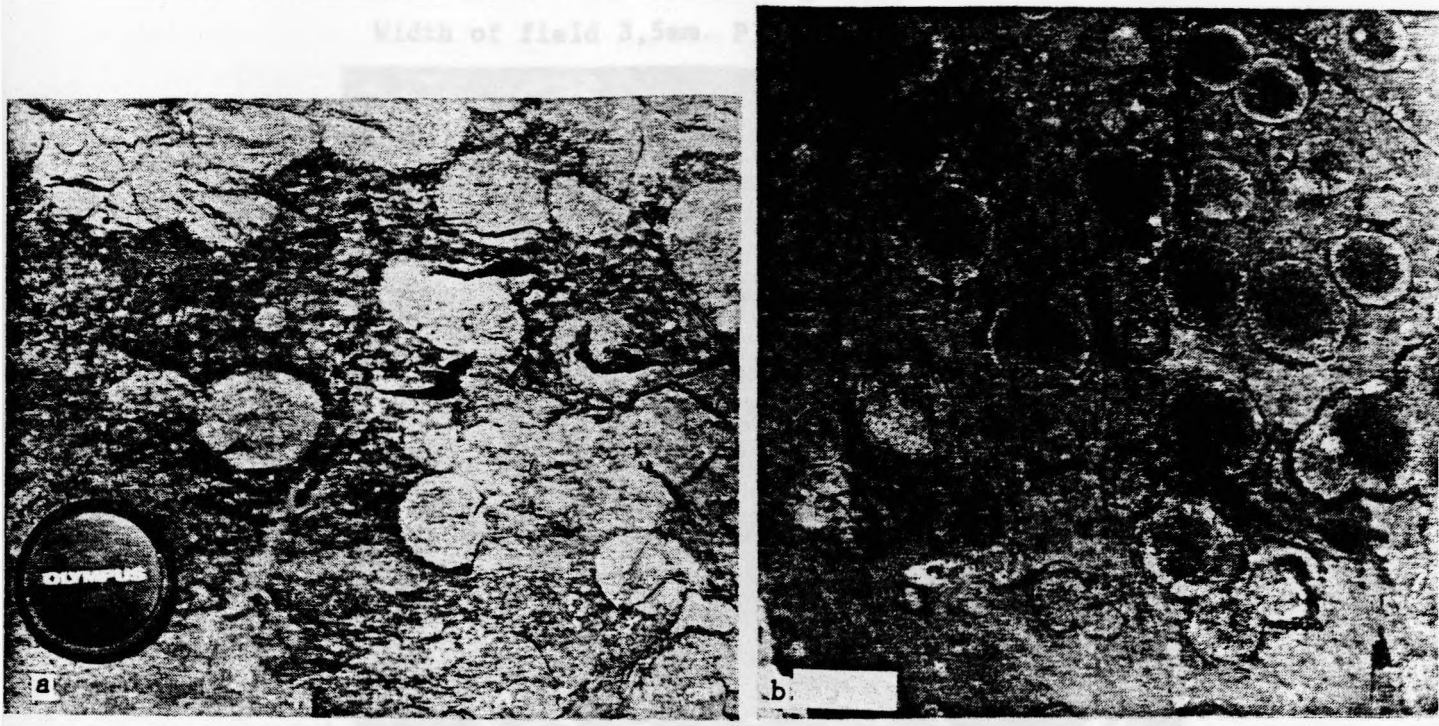


Figure 2.16.a. Variolitic chert showing similiarities to variolitic Komatiite (see Fig. 2.16.b). (Josefsdal Farm).

b. Variolitic Barberton type basaltic komatiite for comparison with Fig. 2.16.a (Komati Formation type section, Viljoen and Viljoen, 1969 c). Scale bar = 5cm



Figure 2.17. Photomicrograph of green homogeneous chert showing silicified crystals, interpreted as olivine (0) in a microquartz and sericite ground mass.
Width of field 3,5mm. Plane polarised light.

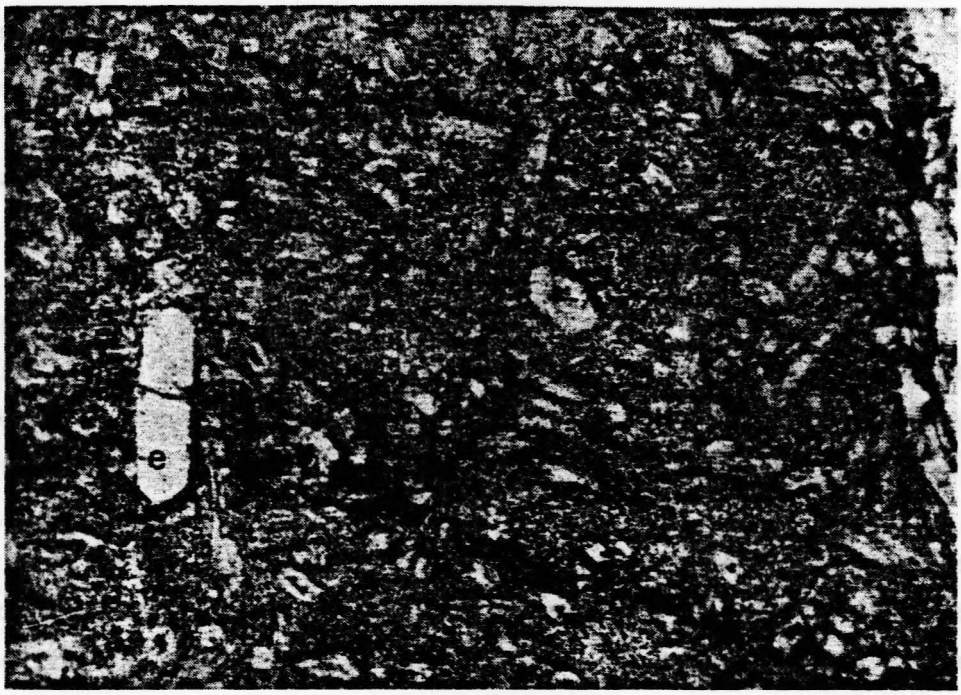


Figure 2.18. Photomicrograph of green homogenous chert showing silicified euhedral (e) and hopper (h) crystals in a microquartz and sericite groundmass.
Width of field = 3,5mm. Plane polarised light.

- Some textures are very similar to amphibole spinifex texture found in komatiitic rocks.

All these characteristics indicate that the present siliceous composition of these rocks is due to a silicification process and does not reflect the original composition. The extent of the silicification varies from the pillowed to the massive lava. The latter have been more completely silicified to the point that they have been previously mapped as sedimentary cherts (Van den Berg, 1969).

The pillowed siliceous rocks have been previously referred to as felsic lavas with a dacitic to rhyodacitic and rhyolitic composition (Viljoen and Viljoen, 1969 d). Several remarks can be made about the above described features which warrant a different interpretation:

1. Hopper crystals are generally found in mafic to ultramafic lava.

2. Olivine crystals indicate a mafic to ultramafic composition. Silicified euhedral, hopper and skeletal crystals have shapes characteristic of olivine crystals. Some of the hopper and skeletal crystals could originally have been plagioclase crystals. However, such plagioclase crystals have only been described in mafic rocks.

3. Spinifex textures have only been described from mafic and ultramafic igneous rocks.

4. The shapes of the pillows are remarkably similar to those found in the komatiitic rocks of the greenstone belt (Komati Formation and Kromberg Formation type sections) and to mafic pillows described elsewhere in the world.

5. Acid pillows, although rare, have been described from Iceland, but they do not compare with the ones described here. Such pillows are podiform, isolated in hyaloclastites, contain flow banding and are strongly brecciated with internal columnar jointing (Furnes et al., 1980).

The above arguments suggest a mafic to ultramafic original composition (possibly komatiitic in some cases) for the siliceous igneous rocks of the Kromberg Formation. Major and trace elements analyses (De Wit et al., 1982

a) of siliceous volcanics in the Kromberg and Hooggenoeg Formations further support this conclusion.

2.2.3 THE "FLASER BANDED ROCKS"

This rock type was first referred to by De Wit (1982) as "flaser banded quartz-carbonate-fuchsite tectonite". Similar rocks have been described from the Kromberg type section (Komati Gorge) and referred to as palagonitic tuffs (Viljoen and Viljoen, 1969 c, plate XLb).

In the study area, these rocks are fairly abundant. They occur in thin lenses (20m long by 1 to 5m thick) both above and beneath silicified sediments (Chapter 3,6) and in thicker units (10 to 50m thick and 500m long) within the silicified volcanics.

The flaser banded rocks are bright to pale green, due to the presence of fuchsite, and are generally banded due to deformed quartz veins which form positive weathering features in the rocks (Fig. 2.19). The silicified sediments which are in contact with the flaser banded rocks are also green.

Petrographic evidence suggests that the grains comprising the rock have undergone deformation, brecciation and recrystallisation (Fig. 2.20). There is a very strong fabric in the matrix and the rock resembles a cataclasite (cf. Bell and Etheridge, 1973). In some specimens, the rock appears to be composed of remnant fold hinges with elongated trailing limbs and a transposed fabric between the fold remnants. Brecciation of the grains and recrystallisation is ubiquitous and numerous quartz veins show fibrous growth which appears to have been rotated and brecciated. Many of the quartz crystals are highly strained and show recrystallisation along the edges of the crystals (Fig. 2.21). Such features are indicative of mylonitic rocks (Bell and Etheridge, 1973; Sibson, 1977).

When they occur in thick units, the flaser banded rocks are carbonated and may grade along strike into green and brown brecciated lava and carbonated

pillow breccia. In thin section, such flaser banded rocks are also strongly brecciated and recrystallised.

A strong fabric is present between the fragments and it often wraps around the fragments. This rock type seems to fit the definitions of mylonite in places and of protomylonite in others (Bell and Etheridge, 1973).

Various terms seem to fit the features seen in the flaser banded rock depending on the outcrop: cataclasite, protomylonite, and mylonite. As all these terms have in common a very strong tectonic connotation, implying intense deformation, the term originally proposed by De Wit (1982) to describe them, tectonite, has been used in this study. The implications of the presence of such rocks will be discussed in Chapter 6.

2.3 THE ZWARTKOPPIE FORMATION

The Zwartkoppie Formation was first considered by Steyn (1965) to be part of the Fig Tree Series (Zwartkoppie Zone) and to rest unconformably on the Onverwacht lavas. Viljoen and Viljoen (1969 d) contended that the apparent unconformity was due to the Manhaar Fault which passes through the Msauli Mine asbestos body and along the Havelock Spruit (Fig. 2.5), and that the Zwartkoppie rocks have more similarities to the Onverwacht Group than to the Fig Tree Group. They therefore included it as the uppermost formation of the Onverwacht Group (Chapter 1). In the southern part of the greenstone belt, the Zwartkoppie Formation occurs to the east of the Stolzburg Syncline (Reimer, 1967) and in a strip along the Swaziland border where it is strongly sheared (Viljoen and Viljoen, 1969 d).

The main igneous rock types described in this formation (Viljoen and Viljoen, 1969 d) comprise:

1. green and grey schists derived from acid and intermediate volcanics as well as basic schists derived from basaltic rocks;



Figure 2.19. Flaser banded rock (Dunbar Farm)



Figure 2.20. Photomicrograph of flaser banded rock showing a folding, brecciation, recrystallisation and the development of shear zones (arrow).
Width of field = 2,4mm. Plane polarised light.



Figure 2.21. Photomicrograph of flaser banded rock, showing undulose extinction of a quartz grain with recrystallisation around the grain. Scale bar = 1mm

2. conformable ultramafic lenses serpentinised and steatized, the major one forming the Havelock and the Msauli bodies. Steyn (1965) regarded the serpentinite lenses as later intrusive pods.

In the study area, the Zwartkoppie igneous rocks are represented by mafic schists, serpentinites and flaser banded rocks. The flaser banded rocks are similar to the ones found in the Kromberg Formation. They vary from cataclasite to mylonite and a description need not be repeated here.

(a) The mafic schist

This rock type is exposed in the lowest part of the Havelock Spruit Valley and in the Msauli Mine where it forms the wall rock of the ore body. On surface, it is too sheared and weathered for descriptive purposes and for an interpretation of its origin to be possible. (b) The serpentinite

Serpentinite occurs in lenses along the Havelock Spruit Valley and across the Makonjwa Ridge at Havelock. Two asbestos bodies are developed in the serpentinite, the Msauli Mine in South Africa and the Havelock Mine in Swaziland.

According to Viljoen and Viljoen (1969 d), the Msauli and Havelock serpentinites occur as conformable lenses within the Zwartkoppie Formation. These authors considered both serpentinites to have formed as a continuous or near continuous differentiated sill. However, recent studies undertaken by Barton (1982) have shown that the Havelock body is more akin to an Alpine type of serpentinite and was emplaced at the cold leading edge of a thrust sheet (see Chapter 6).

Büttner (1983), interpreted the Msauli serpentinite bodies as hydrothermally altered dunitic sills or lava flows formed in an oceanic floor environment. However, he also mentioned that the base of the serpentinite bodies is marked by a shear zone.

The serpentinite is generally strongly sheared both in the hanging wall and in the foot wall. In thin section the serpentinite is seen to have replaced olivine crystals. The rock comprises mainly talc, chlorite and iron oxides. In the Msauli Mine, the serpentinite is affected by carbonation and

silicification (Büttner, 1983). Büttner (1983) recognised α and β type serpentinites within the body and two phases of fibre growth in the asbestos.

2.4 CONCLUSIONS

In the study area, the Onverwacht meta-igneous rock are represented by three main rock types: i) massive and pillowed to ultramafic lava ; ii) intrusive carbonated pod and peridotite ; and iii) serpentinite. The first rock type has been silicified and in places carbonated, to the point that it can resemble a chert. No originally acid lavas have been noted and no evidence for volcanic cyclicity has been found.

CHAPTER 3

3.0 THE ONVERWACHT GROUP: META-SEDIMENTARY ROCKS

3.1 INTRODUCTION

In the study area, the sedimentary rocks of the Onverwacht Group comprise cherts and "agglomerates". The cherts belong to the Kromberg and the Zwartkoppie Formation and occur in layers 0.5m to 25m thick which can be followed along strike for a maximum of 1km and an average of 300m. These cherts are overlain and underlain by silicified igneous rocks (see main map). "Agglomerates" occur in the Hooggenoeg Formation as a 200m thick unit, and in the Kromberg Formation as a 2m thick unit overlying silicified pillow lava. Both cherts and "agglomerates" have their upper and/or lower contacts bounded by thrust faults (Chapter 6). This has prevented a complete stratigraphic sequence from being preserved.

In this study, the sedimentary rocks are discussed as follows, distinct lithofacies, corresponding to mappable units have been distinguished, following the facies definition of Moore (1949): "sedimentary facies is defined as any areally restricted part of a designated stratigraphic unit which exhibits characters significantly different from those of other parts of the unit". As a result, five different facies have been distinguished within the cherts and two within the "agglomerates". Some of these facies only relate to one rock type, while others, which represent distinctive mappable units, comprise several types of lithologies and sedimentary

structures. The primary criteria used in this study for the definition of a facies has been the recognition of lithological and sedimentary structure characteristics of mappable units.

After a description of each chert facies, the vertical arrangement of the facies is discussed by examining several measured sections throughout the study area. This leads to a palaeoenvironmental interpretation. The "agglomerates" are then discussed following a similar procedure.

3.2 THE CHERTS

Lowe and Knauth (1978) have pointed out that many of the Onverwacht cherts are in fact silicified volcaniclastic sediments As the cherts described here represent silicified sedimentary rocks the terms mudstone, siltstone and sandstone are used throughout the descriptive part without the prefix silicified. The five facies recognised in the cherts are: 1) black mudstone facies; 2) speckled grey mudstone facies; 3) interbedded mudstone, siltstone, sandstone facies; 4) spheroid bearing facies; 5) angular clast bearing facies.

3.2.1 THE BLACK MUDSTONE FACIES

This facies occurs in beds ranging from 0,5 to 5m in thickness. The rock is black and homogeneous except for the numerous white silica veins cutting across bedding. Siltstone laminae and beds are commonly found near the base of beds within these facies. In thin section, the rock is composed of microquartz and opaque material and the siltstone laminae contain rounded grains replaced by microquartz and opaque rounded and elongated grains.

In several outcrops near the Swaziland border, black and white silica blades 5 to 8cm long and spindle shaped crystals can be distinguished on the

weathered surface of several beds (Fig 3.1). The blades are composed of microquartz and have rounded edges, an original cement of colloform silica now replaced by microquartz can be seen in between the blades in places (Fig. 3.2.b).

The layer overlying the blades has formed draped over the top of the blades (Fig. 3.1).

The long blades possibly represent eroded silicified gypsum crystals, because they resemble silicified gypsum crystals described in Australian Archaean cherts (Groves et al., 1981; Lowe 1983).

3.2.2 THE SPECKLED GREY MUDSTONE FACIES

This facies is formed by a dull homogeneous grey to blue grey rock which occurs in units 1 to 2m thick. On a fresh cut surface, randomly orientated isolated dark glassy specks with an average size of 1mm by 2mm can be distinguished. In thin section, the specks are composed of microcrystalline quartz and display swallow tail and prismatic shapes. They represent crystal pseudomorphs (Fig. 3.3). The rock is randomly cross-cut by silica veins and is composed of microcrystalline quartz, sericite and opaque material.

Bedding can be seen both in hand specimens and in thin section. The crystals pseudomorphs are generally perpendicular to the bedding and can be seen to cut across laminae. Preserved ghosts of laminae can be seen in some of the pseudomorphs.

As the silicified crystals cross-cut bedding planes, they must be post-depositional. Ghost laminaes visible within the crystals indicate that they have grown within the sediment and cannot represent ash particles. Both the crystals and the sediment have been silicified. The swallow tail shape of some of the crystals indicates that they were probably pseudomorphs after gypsum.



Figure 3.1. Black mudstone facies with black silica blades. Note draping of the top bed over the blades (left top corner) (Josefsdal Farm)

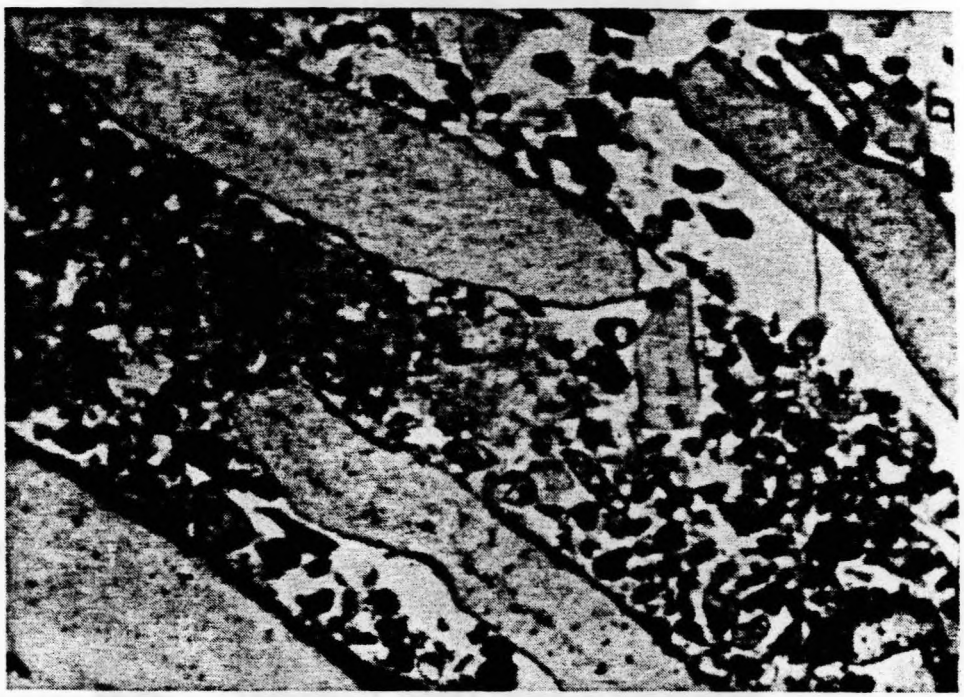


Figure 3.2. Photomicrograph of a siltstone bed within the black mudstone facies with rounded silica blades which are composed of microquartz. The intergranular material contains silt sized grains in a cement composed of microquartz after colloform silica (Josefsdal Farm). Width of field: 3,5mm. Plane polarised light.



Figure 3.3. Photomicrograph of the speckled grey mudstone facies showing swallow tail shaped crystal and euhedral crystals replaced by microquartz (Josefsdal Farm). Width of field 3,5mm. Crossed nicols.

.2.3 THE INTERBEDDED MUDSTONE/SILTSTONE/SANDSTONE FACIES

ı this facies, the rock vary in grain size from silt to sand sized, and ı colour from pale to dark grey. In places mudstone laminae and lenses .5cm by 3cm in size are present. This facies occur as units ranging from to 2m thick. In thin section, the mudstone is similar to that described ı the black mudstone facies. In the silt and sand sized material (Fig. .4), the clasts are subrounded to angular and several types of grains can e distinguished: quartz grains; carbonate grains; pumice grains; grains ɔmposed of sericite, iron oxide and microquartz; and composite grains ɔntaining shards and crystal inclusions replaced by microquartz in a icroquartz, sericite and iron-oxide matrix. The intergranular material etween the grains is composed of microquartz with isolated carbonate hombs. Some of the well rounded composite clasts are similar to the pheroids found in the spheroid bearing facies.

he structures recognised in this facies include: planar lamination and edding, irregular lamination, lenticular bedding, trough cross-lamination, rosive bases, normal size grading and reverse coarse tail grading. The erminology used here is that of McKee and Weir (1963) for the definition f bedding and laminae and Jopling and Walker (1968) for the sedimentary tructures.

lanar lamination and bedding are found in interlaminated and interbedded udstone and siltstone beds up to 3cm thick with an average thickness of ,3cm (Fig. 3.5).

rregular lamination is found in interbedded mudstones and siltstones. long strike, several patterns can be distinguished : wavy parallel, wavy on parallel and discontinuous wavy parallel lamination (Reineck and Singh, 980). Such structures occasionally show convolute lamination (Fig. 3.6).

enticular lamination and bedding occur as lenses of siltstones interbedded ith mudstones. The lenses vary in length from 0,5 to 2cm and in width from to 4cm, and can be isolated or connected (Fig. 3.5).

'rough cross-lamination is found in siltstone and sandstone beds (Fig. 3.7). 'or each individual set of laminae, the maximum thickness is 3cm. The

thickness of the laminae averages 0,2cm and the thickness of a cross-laminated unit varies from 0,6 to 8cm.

In this facies, type A, ripple drift cross-lamination (Jopling and Walker, 1968) is the most frequent, while type B (op. cit.) is found occasionally (Fig. 3.8, 3.9). Some of the cross-laminae are transitional between type A and type B but resemble type A more closely. The laminae have a thickness ranging from 1 to 2mm and a length from 4 to 6cm (Fig. 3.8).

Two types of graded units are found in this facies, within the sandstones.

The first type is a normal distribution grading (Selley, 1982). This type is the most common. The graded beds vary in thickness from 0,2 to 8cm and occur in two forms: (i) coarse sand sized bases grading upward to a fine sand; and (ii) fine sand sized bases grading upward to a silt size material. The normal size graded units frequently have erosional bases and form channels which can be as wide as 15cm with a thickness ranging from 2 to 5cm.

The second type is a reversed coarse tail grading (Selley, 1982). The units are composed of sand and silt beds, and range from 10 to 85cm in thickness. In these units the sand to silt ratio increases from the bottom to the top of the unit.

3.2.4 ANGULAR CLAST BEARING FACIES

This facies is formed by pale to dark green chert clasts in a black silica cement. The rock is clast supported and occurs in units 1,5 to 50m thick. The clasts are angular, and vary in size from 0,1 to 3cm across (Fig. 3.10). In thin section, the cement is composed of microquartz in which colloform silica textures can still be recognised (Fig. 3.11). The clasts are generally very irregular and vesicular and contain crystal shapes replaced by microquartz, set in a microcrystalline quartz, sericite and iron oxide groundmass (Fig. 3.11). Some of the clasts contain needles of sericite, silicified hopper or skeletal crystals or show an ophitic texture. A few clasts have a pumiceous aspect (Fig. 3.12).

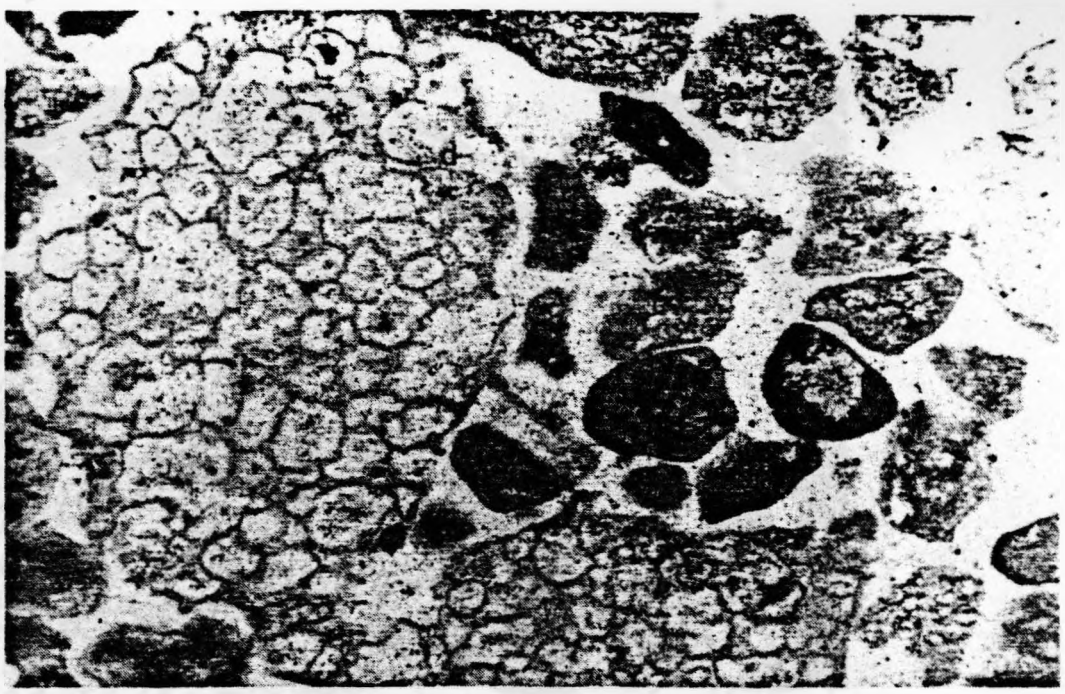


Figure 3.4. Photomicrograph of silicified sandstone, showing rounded, angular and pumiceous (p) grains in a microquartz and sericite matrix. Width of field = 3,5mm. Plane polarised light.

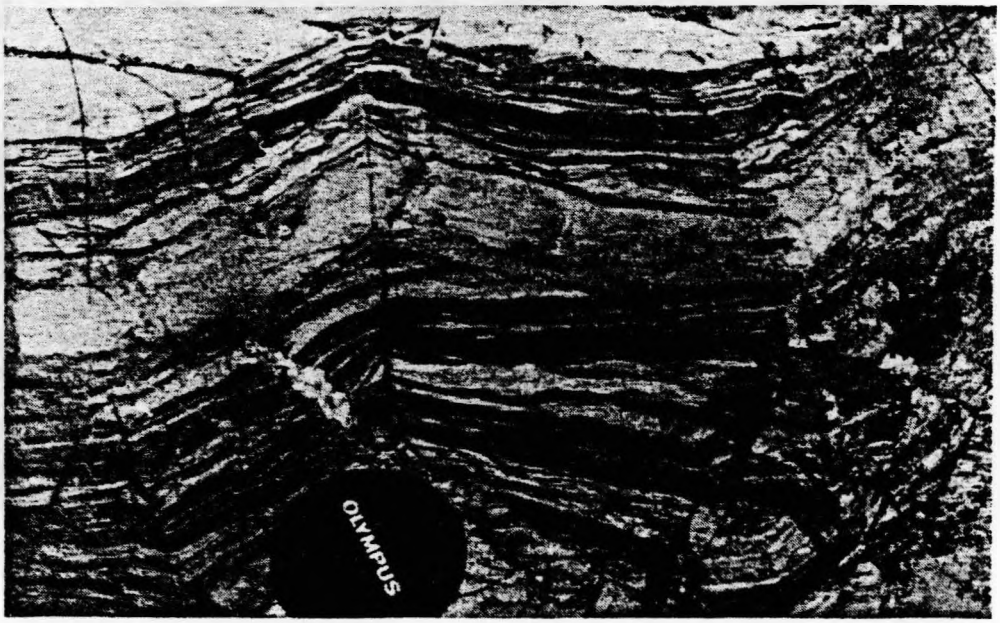


Figure 3.5. Silicified mudstone/siltstone/sandstone facies showing planar and lenticular bedding (Dunbar Farm).



Figure 3.6. Interbedded mudstone/siltstone/sandstone facies with convolute and planar lamination (Dunbar Farm).

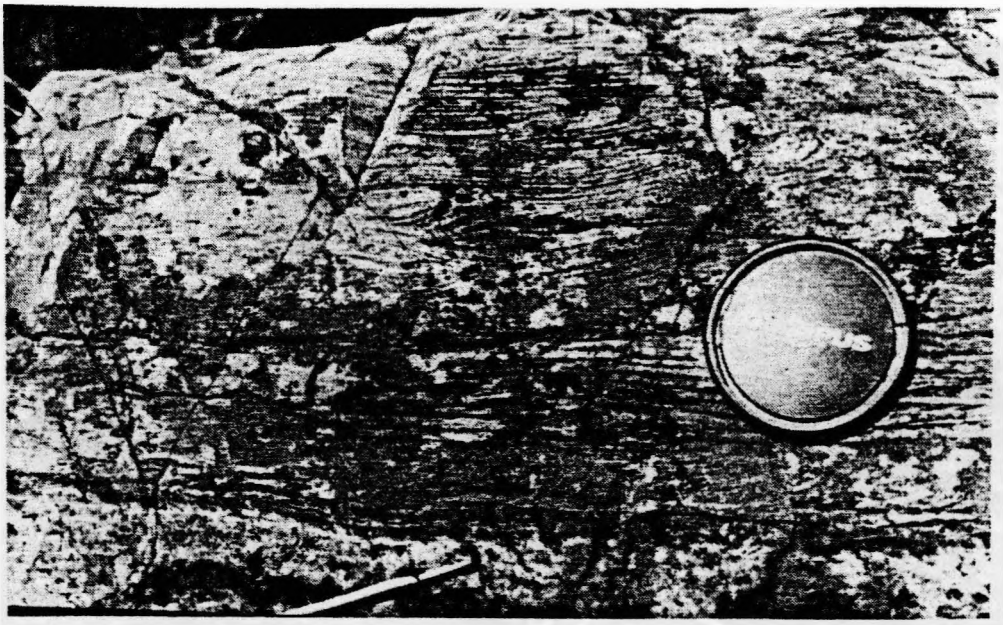


Figure 3.7. A sandstone bed within the interbedded mudstone/siltstone/sandstone facies with trough cross-lamination (Dunbar Farm).

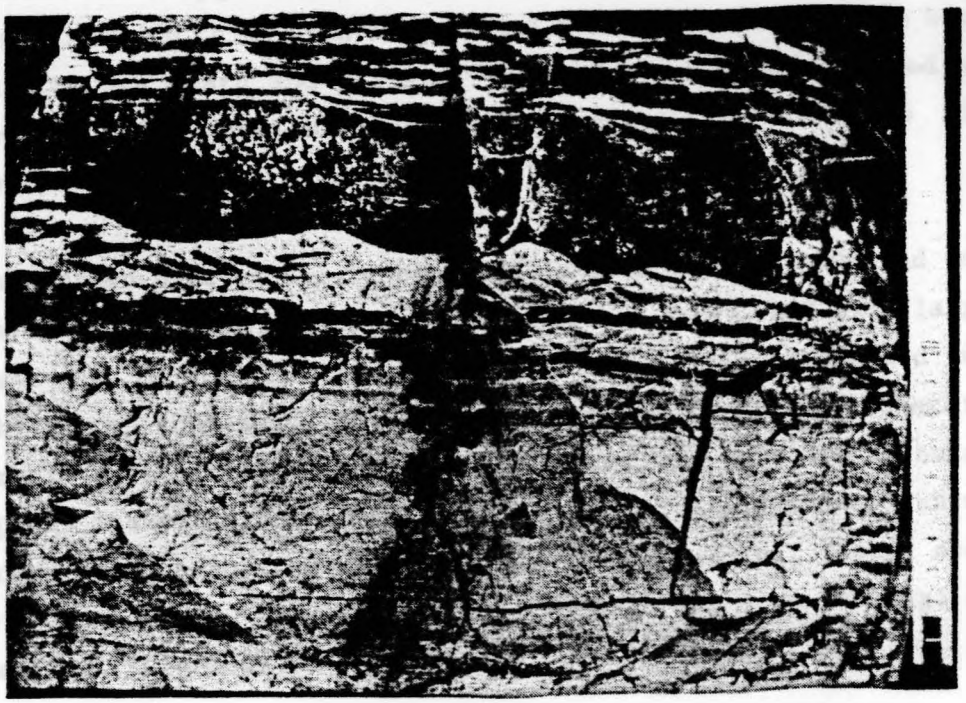


Figure 3.8. Type A ripple drift cross-lamination in the interbedded mudstone/siltstone/sandstone facies (Dunbar Farm).



Figure 3.9. Type B ripple cross-lamination in the interbedded mudstone/siltstone/sandstone facies (Josefsdal Farm).

On the Josefsdal and Diepgezet Farms, the angular clast bearing facies occurs in units 1,5 to 16m thick with fragments 0,5 to 15mm in size. The basal and top contacts are sharp and planar. The units are poorly sorted and occasionally display a normal size grading. Accretionary spheroids (1cm in diameter) can be mixed with the angular clasts (Fig. 3.13).

In the south western part of the Dunbar Farm, a 100m thick carbonated unit contains lenses of chert similar to the one described above, but with larger angular clasts, up to 3cm in diameter (Fig. 3.10). This carbonated unit is bounded by thrust contacts. Microscope observations indicate that the carbonated rocks have similar textures to the chert, and that the carbonate grains overprint the silicified clasts (Fig 3.15). The sedimentary structures present in the carbonated unit include: planar bedding, trough cross bedding (sets 30cm high), channels (40 to 60cm high and 3 to 5m long) and graded units (Fig. 3.14-3.16).

The size of the fragments, their aspect (pumiceous, vesicular, lithic and ophitic fragments) and their internal composition (presence of microquartz shards and crystal pseudomorphs) have led to the conclusion that this facies represents silicified lapilli tuff.

3.2.5 THE SPHEROID BEARING FACIES

The non genetic term spheroid is used here because of the controversy as to the origin of the grains which characterise this facies. A discussion of the origin of the spheroids will be made after the description of the facies. This facies can be sub-divided into two subfacies: the thin bedded spheroid bearing subfacies and the thick bedded spheroid bearing subfacies.

(a) The thin bedded spheroid bearing subfacies

This subfacies is formed by grey to white spheroids in a grey silt size matrix. It occurs in beds 0,5 to 3cm thick which are commonly interbedded with the mudstone/siltstone/sandstone facies. The spheroids range in size from 0,3 to 1mm in diameter and in hand specimen some grains have a darker centre while others seem to be homogeneous.

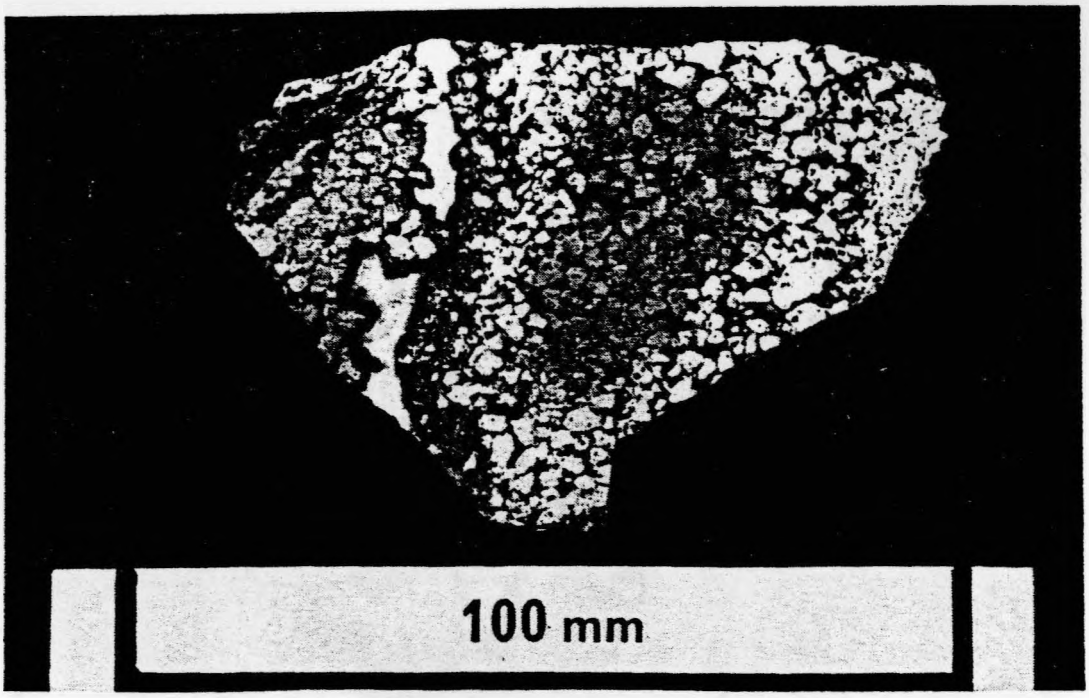


Figure 3.10. Specimen of the angular clast bearing facies (Josefsdal Farm)



Figure 3.11. Photomicrograph of the angular clast bearing facies showing the colloform silica cement (now replaced by microqaurtz) and the presence of crystal pseudomorphs in the clasts. Width of field = 3,5mm. Plane polarised light.

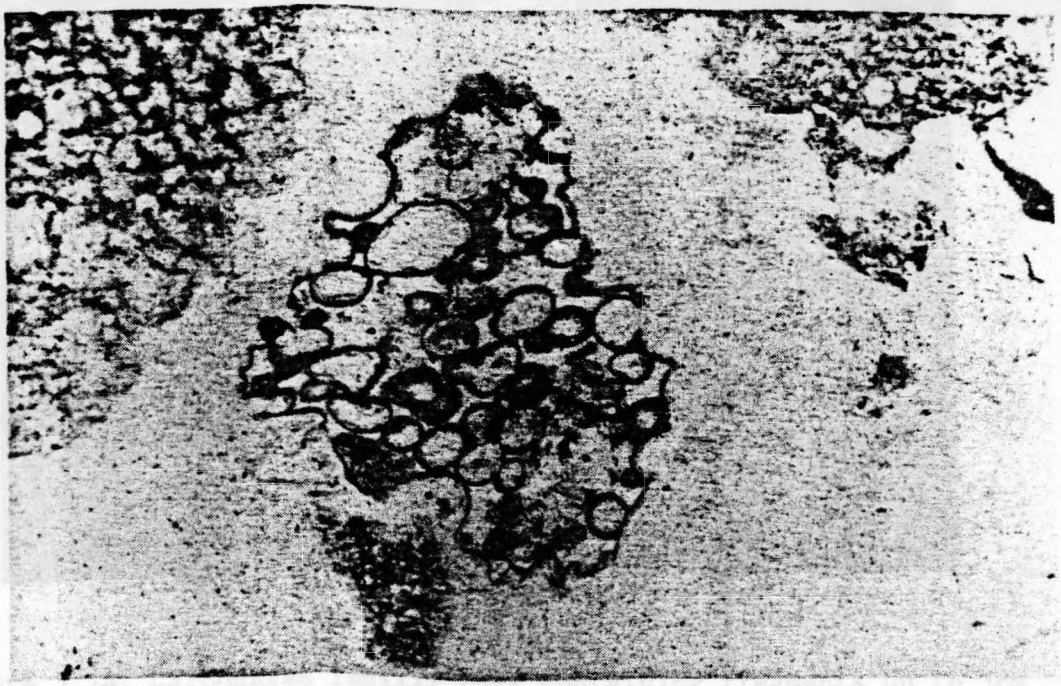


Figure 3.12. Photomicrograph of the angular clast bearing facies showing a pumiceous clast (Josefsdal Farm). Plane polarised light. Width of field = 3,5mm



Figure 3.13. Accretionary spheroids (arrow) mixed with silicified lapilli tuff.(Josefsdal Farm).

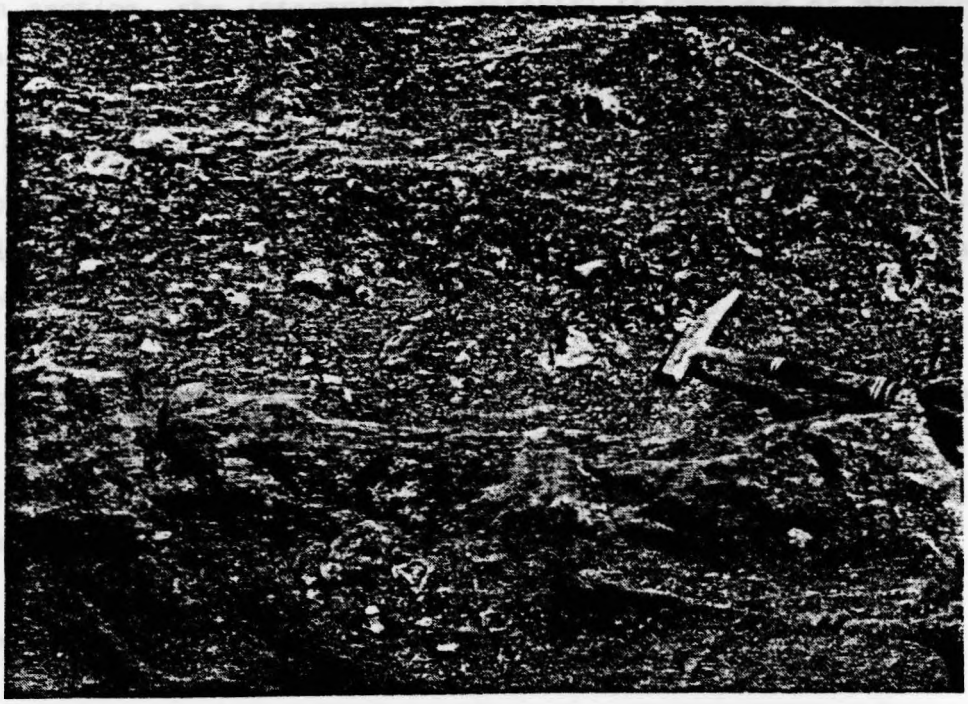


Figure 3.14. Carbonated lapilli tuff containing fragments up to 3cm in size. (Dunbar Farm).

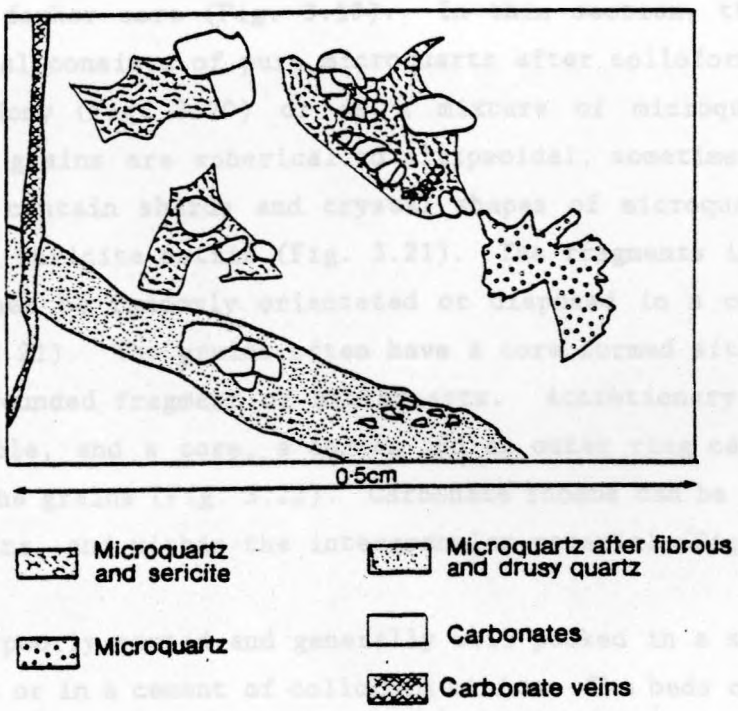


Figure 3.15 Diagram showing the replacement by carbonate of the angular clast bearing facies. Drawn after thin section.

In thin section, the intergranular material is composed of microcrystalline quartz, sericite and iron oxides. The grains are darker than the matrix, and fragmented in place. They consist of a microcrystalline quartz and sericite groundmass in which shards and crystal shapes can be recognised (Fig. 3.17). No accretionary features have been distinguished in the grains of the samples studied, although they may have been destroyed by metasomatic processes.

The rock is moderately well sorted and is grain supported. Most beds show a normal size grading, the base of the bed containing 1mm to 0,6mm large spheroids which pass upward into a silt size sediment (Fig. 3.18). The base of the unit is often loaded into the underlying unit.

(b) The thick bedded spheroid bearing subfacies

This facies occurs in 0,4 to 2m thick units formed by spheroids in a silty matrix or in a grey silica cement. The beds range in thickness from 4 to 120cm. The spheroids are grey to white and vary in size from 0,1 to 1,5cm, with an average size of 0,5cm. In hand specimen, concentric laminae are visible in most grains while some are structureless and/or with a darker core (Fig. 3.19). In thin section, the intergranular material consists of pure microquartz after colloform silica, opal or chalcedony (Fig. 3.20) or is a mixture of microquartz and sericite. The grains are spherical to ellipsoidal, sometimes broken, and frequently contain shards and crystal shapes of microquartz in a microquartz and sericite matrix (Fig. 3.21). The fragments inside the grains can either be randomly orientated or disposed in a concentric pattern (Fig. 3.21). The grains often have a core formed either by an angular or subrounded fragment of microquartz. Accretionary features are often visible, and a core, a cortex and an outer ring can be distinguished in the grains (Fig. 3.22). Carbonate rhombs can be seen both inside the grains, and within the intergranular material (Fig. 3.23).

The grains are poorly sorted and generally well packed in a silicified mudstone matrix or in a cement of colloform silica. The beds often show a normal size grading (Fig. 3.24). The bases of the beds often consist of a scoured surface which eroded into the underlying unit and the upper part of the unit is formed by small spheroids and fine sand sized grains



Figure 3.16. Carbonated lapilli tuff with large scale trough cross-bedding (Dunbar Farm).

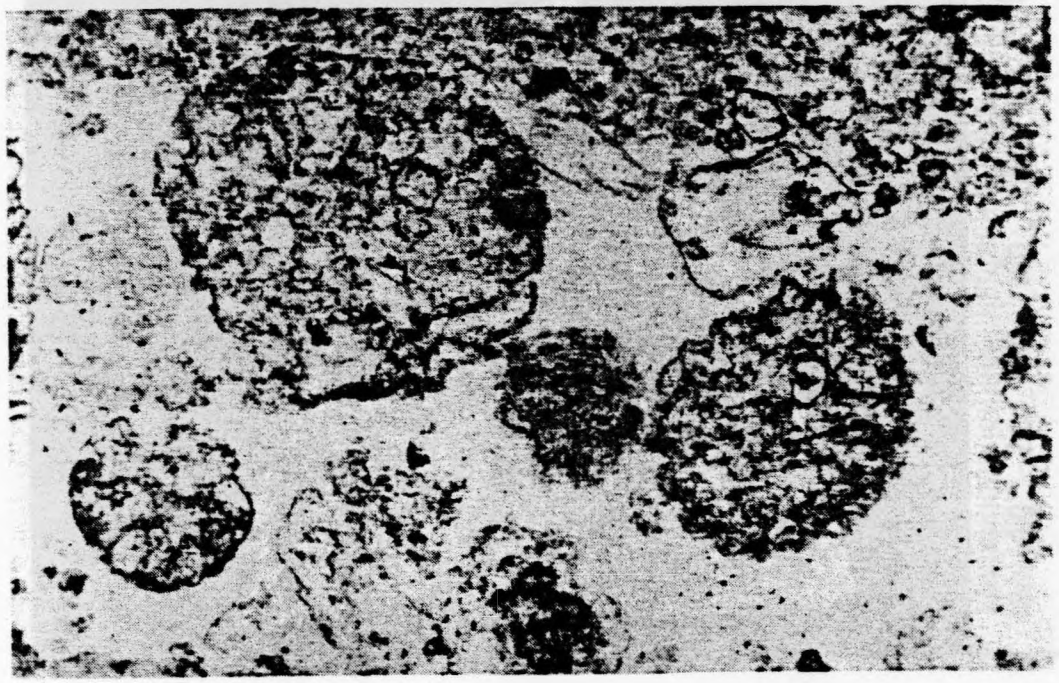


Figure 3.17. Photomicrograph of the thin bedded spheroid bearing subfacies. Width of field = 3,5mm.
Plane polarised light

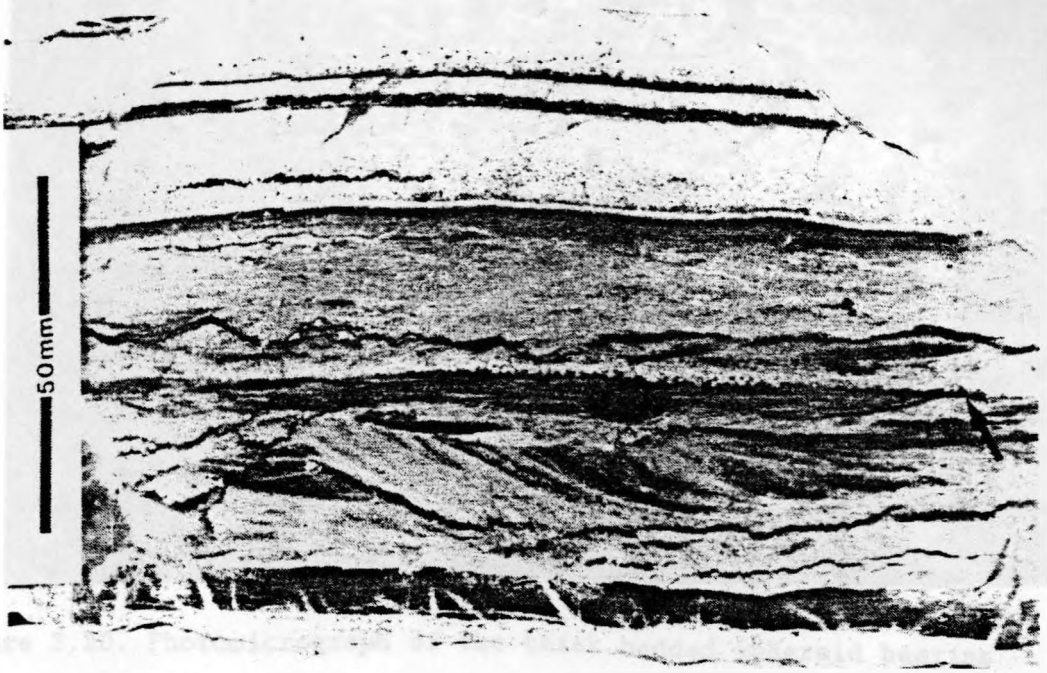


Figure 3.18. Thin bedded spheroid bearing subfacies with graded units (arrow). The base of the sample is formed by the cross-laminated mudstone, siltstone and sandstone facies (Josefsdal Farm).

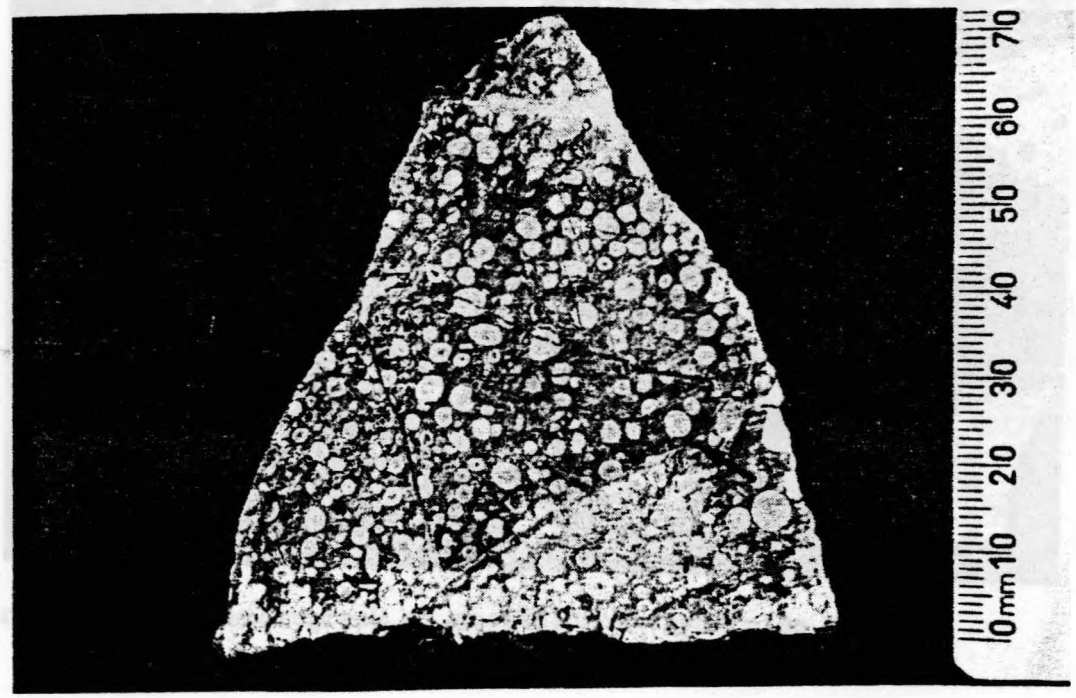


Figure 3.19. Specimen of the thick bedded spheroid subfacies. Accretionary features are visible in some of the grains (arrow) (Josefsdal Farm).

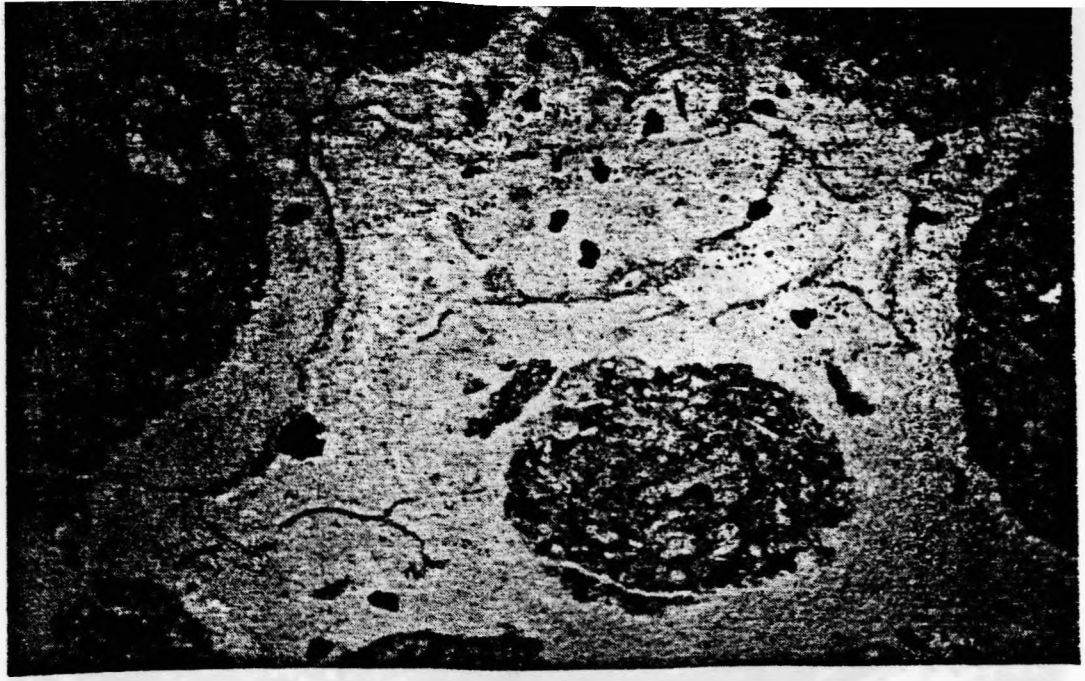


Figure 3.20. Photomicrograph of the thick bedded spheroid bearing subfacies showing the original cement of colloform silica, now replaced by microquartz.
Width of field = 3,5mm. Plane polarised light.

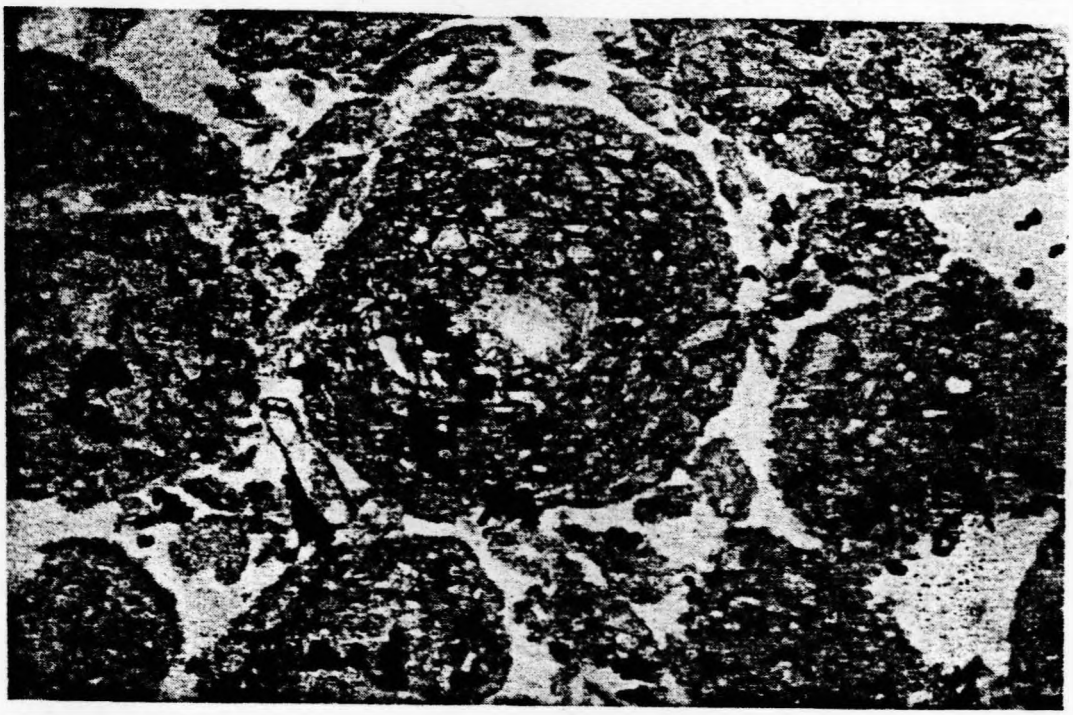


Figure 3.21. Photomicrograph of accretionary spheroids with microquartz replaced
shards disposed in a concentric manner. The core of the central grain is formed by microquartz. The groundmass of the spheroids consists of sericite and microquartz
Width of field = 3,5mm. Plane polarised light.

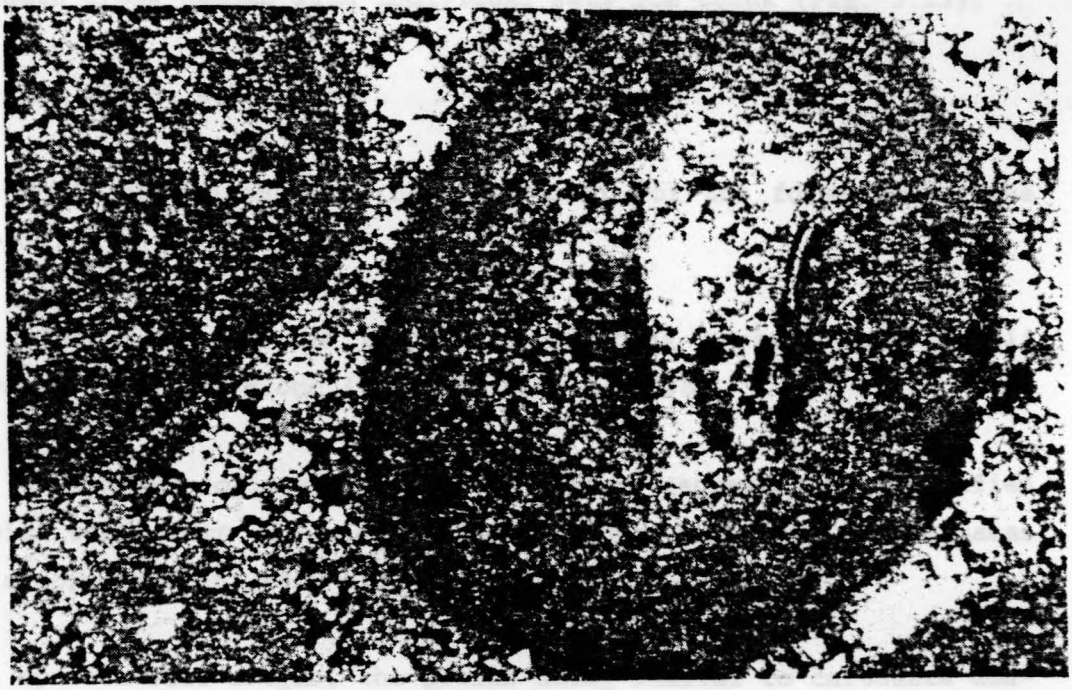


Figure 3.22. Photomicrograph of an accretionary spheroid in the thick bedded spheroid bearing subfacies with microquartz fragments in the centre and a cortex. Width of field = 3,5mm. Plane polarised light.

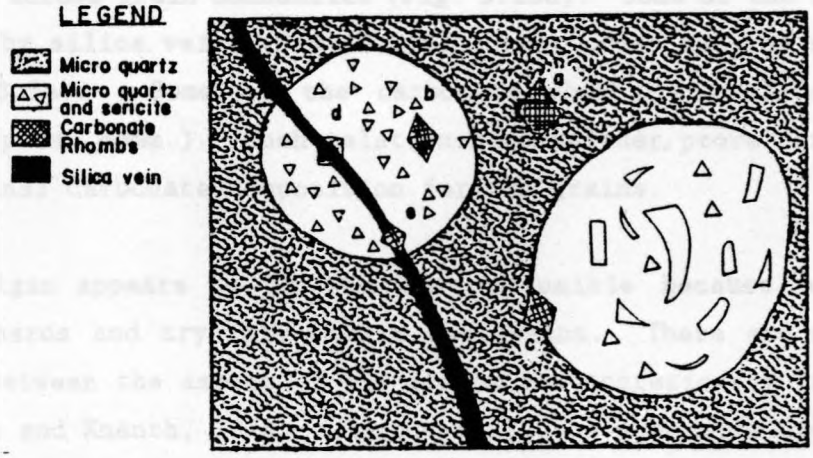


Figure 3.23. Diagram showing the position of carbonate rhombs in the spheroid bearing facies (drawn after thin sections). Width of field = 3,5mm.

(Fig. 3.24). In one chert unit, in the Dunbar Valley, the spheroids are trough cross-bedded with individual sets 5cm thick (Fig. 3.25).

(c) Origin of the spheroids

Three types of origin have been proposed for the formation of the spheroids:

1. A volcanic origin, the grains representing accretionary lapilli formed in an ash cloud (Lowe and Knauth, 1978).

2. A carbonated oolitic origin, the grains representing silicified ooids similar to the ones presently being formed in the Bahamas platform (Reimer, 1975 b).

3. An hydrothermal origin, the grains being similar to carbonate concretions found on the oceanic floors and described by Kimberley (1982), thus the grains would have originally been carbonate (Stanistreet, pers. comm.).

Although carbonate rhombs have been observed in the spheroids, the evidence suggests that carbonate replacement postdated deposition (Fig. 3.23). Carbonate rhombs occur in the matrix, within the grains (Fig. 3.23 a-b), and across grain boundaries (Fig. 3.23c). Some of the rhombs are cross cut by silica veins (Fig. 3.23d), other cross cut the silica veins (Fig. 3.5e). Some of the carbonate rhombs are silicified (Stanistreet, pers. comm.). Such relationships neither prove nor disprove an original carbonate composition for the grains.

A volcanic origin appears to be the most plausible because of the presence of shards and crystals within the grains. There are strong similarities between the aspect of the grains and accretionary lapilli (see also Lowe and Knauth, 1978). Furthermore, the spheroids are commonly mixed with lapilli tuff (angular clast bearing facies, section 3.2.4)

Accretionary lapilli are thought to form during volcanic activity either accompanying explosive interaction of magma and water (Self and Sparks, 1978), or during the eruption of ash clouds (Moore and Peck,



Figure 3.24. Graded units in the thick bedded spheroid bearing subfacies. Note the erosive base of the second graded unit (arrow) (Dunbar Farm)

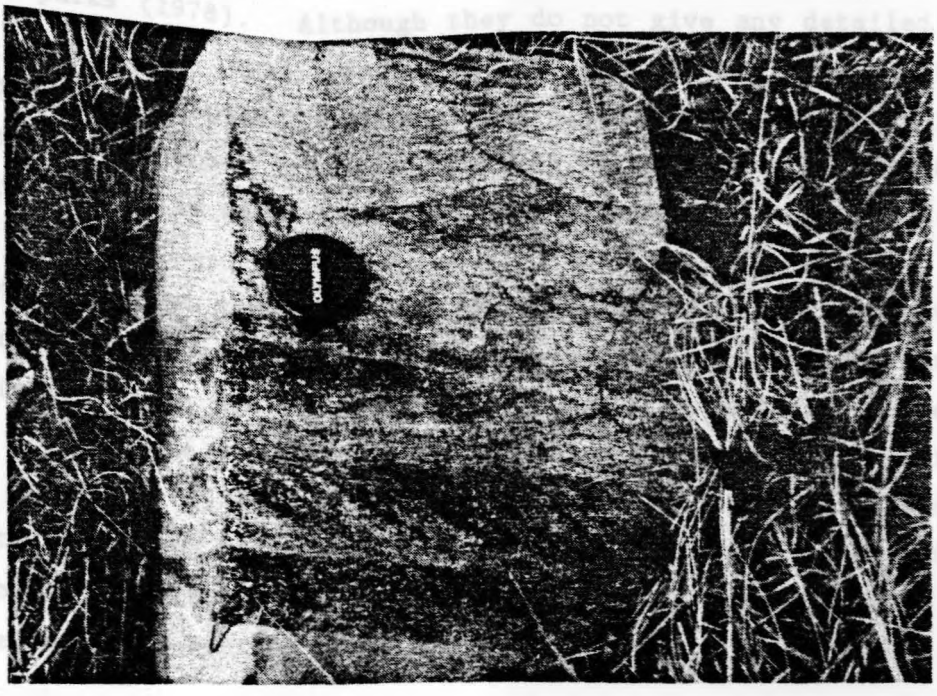


Figure 3.25. Trough cross-laminae in the thick bedded spheroid bearing subfacies (Dunbar Farm)

1962; G.P.L. Walker, 1971). In the latter case, the accretionary lapilli are formed by a process similar to that found in hailstones.

An alternative mode of formation is the accretion on the ground of fresh ash around a nucleus blown by the wind or rolling down the subaerial volcanic slope (Moore and Peck, 1962).

Accretionary lapilli presumed to have been formed by accretion on surface have been described in Australia (Trendall, 1965). However, these accretionary lapilli have characteristics which differ from the ones found in the Barberton greenstone belt. They show an inward increase of grain size, sometimes with up to seven graded units. When no grading is present, the grains are formed by structureless homogeneous tuff.

Modern accretionary lapilli formed in an ash cloud have characteristics similar to those found in Barberton. They are spheroidal, concentrically layered pellets composed of vitric ash and dust with lithic particles. Lapilli formed in this manner are supposedly unable to survive water deposition (Moore and Peck, 1962) although no conclusive evidence has been published and Self and Sparks (1979) dispute this conclusion.

Accretionary lapilli formed by water/magma interaction have been described by Self and Sparks (1978). Although they do not give any detailed description of accretionary lapilli formed in this manner, they point out that they are similar to the ones formed in an ash cloud. Accretionary lapilli formed in this way can occur in sheets covering large areas (up to 140km), and survive deposition in water (Self and Sparks, 1978).

It is thus proposed that the spheroids found in the Barberton greenstone belt represent accretionary lapilli. They were formed during sub aerial volcanic activity, in an ash cloud or more probably in a phreatomagmatic explosion. Some of the spheroids were mixed and deposited with lapilli tuffs. The abundance of current structures in the accretionary lapilli units indicates that they have been reworked after deposition. The thinly bedded spheroid bearing units are interpreted as distal equivalents of the thickly bedded spheroid bearing units.

3.2.6 STUDY OF VERTICAL SEQUENCES

Detailed sedimentological sections have been measured in order to study the vertical distribution of sedimentary structures (Appendices 1-7). Analysis of the measured sections shows that sedimentation took place in cycles which vary from a few centimetres to several metres in thickness. The thinner cycles generally comprise the thin bedded spheroid bearing subfacies while thicker cycles generally comprise the thick bedded spheroid facies. Within each cycle, different units can be recognised with distinct sedimentary structure and grain size. These units are :

A = a graded unit of sandstone or spheroids (such units form part of the (spheroid bearing facies or the sandstone of the interbedded mudstone/siltstone/sandstone facies).
B = a planar laminated unit of sandstone and siltstone (such units are part of the interbedded mudstone/siltstone/sandstone facies).
C = a cross laminated unit of siltstone and mudstone (such units are part of the interbedded mudstone/siltstone/sandstone facies).
D = a mudstone unit occasionally with the siltstone laminae at the base (such units belong to the black mudstone facies or the grey speckled mudstone facies).

The vertical arrangement of the various units is indicated in figure 3.26b. From this table, it appears a complete cycle comprises successively (A), (B), (C) and (D) units (Fig. 3.26a) but most cycles are incomplete. A total of ninety four complete and incomplete cycles is found within the different measured sections (see appendices 1 to 7). The angular clast facies is not represented within these cycles and occurs at the base or at the top of the thin cycles (Appendix 1.3).

In the study area, the cherts rarely have a strike length of more than 50m without being faulted, disrupted by silicified igneous rocks or the sedimentary structures being overprinted by veining and brecciation. However, a set of cycles can be traced for 20m without any thickness variation. Up to 50 complete or incomplete cycles can be seen in single chert units a few metres thick.

3.2.7 PALEOENVIRONMENTAL INTERPRETATION

The sedimentary cycles present in the cherts of the Kromberg and Zwartkoppie Formation bear close resemblance to classic Bouma sequences (Bouma, 1962; Lowe and Knauth, 1977; Stanistreet et al., 1981). A complete cycle contains successively a graded unit of spheroids or sandstone (Bouma interval A), a planar laminated siltstone and/or sandstone unit (Bouma interval B), a siltstone/sandstone cross-laminated unit (Bouma interval C) and a mudstone unit with occasional siltstone lenses and laminae at the base (Bouma intervals D,E) (Fig. 3.26). Two types of cycle can be distinguished: i) thin cycles in which Bouma interval A is formed by thin fine grained sandstone units, or by thin spheroid bearing units. ii) thick cycles in which Bouma interval A is formed by units of coarse sandstone or thick bedded spheroid bearing units (Appendix 1-7).

The cherts show characteristics that are in accord with the following listed criteria for recognition of turbidites, compiled from Reineck and Singh (1982) and Walker (1979):

1. The sedimentary cycles observed in the cherts can be described in terms of Bouma sequences.

2. Bouma sequences may or may not be complete with either the top or bottom part of the sequence missing.

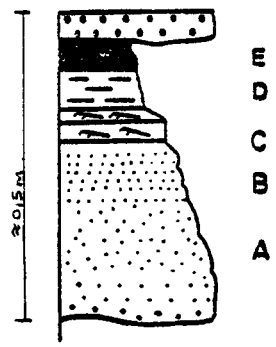
3. Amalgamation of spheroid bearing units is frequent in the thick bedded facies, producing a succession of Bouma intervals A (Fig. 3.24).

4. Thin bedded and thick bedded cycles can be distinguished.

5. The beds do not appear to show any thickness variation laterally.

6. The beds are laterally extensive.

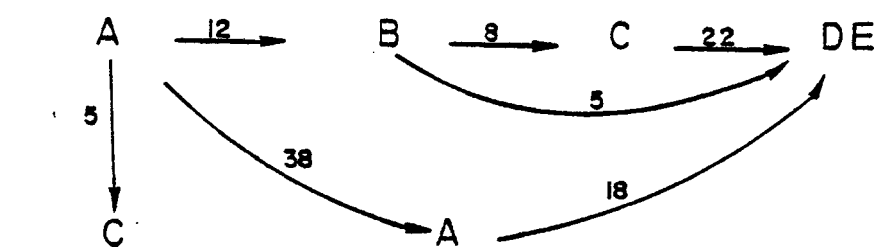
7. The sand sized units have a sharp base and grade upwards into finer siltstones and mudstones (Fig. 3.18).



LEGEND

A = Graded spheroids and/ or sandstones
B = Planar laminated sandstones and / or siltstones
C = Cross laminated siltstones interbedded with mudstones
D = Mudstones interbedded with fine siltstone laminae
E = at the base

a



b

Figure 3.26a. Complete cycle from the silicified sediment similar to the Bouma sequence (Bouma, 1962).

b. Sedimentary cycles from eleven measured sections in the cherts (see appendixes 1-7)

A = graded spheroid and/or graded sandstone unit

B = planar laminated sandstone and/or siltstone unit

C = cross laminated siltstone and/or mudstone unit

D = mudstone unit with planar laminated silstone at the base

8. Erosive bases are abundant at the base of the sand size units (Fig. 3.24).

9. Graded bedding and current ripple cross-laminated beds alternate with hemipelagic beds (Fig. 3.8, 3.9).

10. Typical shallow water features such as wave ripples and large scale (sets higher than 10cm) cross-bedding are absent.

11. Features indicating intermittent subaerial exposure, e.g. mud cracks and rain drop imprints, are completely missing.

In the study area the cherts of the Kromberg and Zwartkoppie Formations which contain the above mentioned cycles are therefore interpreted as proximal and distal turbidity current deposits. Cherts with identical characteristics similar to those of the proximal turbidites described here have been studied by Lowe and Knauth (1977) and Stanistreet et al. (1981). Although all the authors describe current deposited structures and Bouma sequences, they reach totally different conclusions for the depositional environment.

Lowe and Knauth (1977; 1978) interpreted the cherts of the Onverwacht Group as predominantly formed in a shallow water to subaerial environment. They based their interpretation on the following observations: Bouma sequences are rare, silicified gypsum crystals indicate an evaporitic deposits, structures resembling desiccation cracks have been found in one outcrop, the accretionary spheroids represent accretionary lapilli and thus could not survive any current redeposition. However, Self and Sparks (1979), in discussion of Lowe and Knauth (1978) pointed out that accretionary lapilli formed in phreatomagmatic explosions can survive deposition in water.

Stanistreet et al. (1981) interpreted the cherts of the Onverwacht Group as deep water sediments deposited by turbidity currents. Their interpretation is based on the presence of numerous Bouma sequences in the Msauli chert (Zwartkoppie Formation), on evidence of reworking of the accretionary spheroids as indicated by current structures and erosional bases, and on the presence of non vesicular variolitic mafic pillow lava under the chert.

The different interpretations may have arisen from the following questions:

Do accretionary lapilli represent subaerially deposited sediments? If so, can they be reworked? Are Bouma sequences frequent? Are desiccation cracks frequent? Are silicified gypsum crystals indicative of a subaerial environment?

In the study area, these various questions can be answered as follows:

1. Whatever the mode of formation of the accretionary spheroids (see section 3.2.5) they have been reworked by current action as indicated by the erosional bases and the trough cross-laminations present in the accretionary spheroid bearing units.

2. Bouma sequences are abundant although commonly incomplete.

3. No desiccation cracks have been found in the study area, but products of hydraulic brecciation (see Chapter 5) could be mistaken for desiccation cracks and/or mud flakes.

4. Silicified gypsum crystals have been found in the study area, but it is felt that sulphates are not indicative of subaerial environment as they have also been described in deep water environment (Siesser and Rogers, 1976; Criddle, 1974).

Therefore, in the study area, all the features observed in the cherts containing the sedimentary cycles described above are consistent with a turbiditic environment as was proposed by Stanistreet et al. (1981), for the Msauli chert. Turbidity currents can occur in various environment (lakes, delta fronts, continental shelves and mostly in deeper oceanic basins). However, turbidites can only be preserved and recognised if they have not been reworked by other types of current (Walker, 1979). The large lateral extension of the turbidite units can be demonstrated by the abundance of tectonically repeated turbidite units throughout the greenstone belt (see Chapter 6). A hemipelagic environment seems to be the most likely for the preservation of a laterally extensive turbidite sequence. A hemipelagic environment does not have any strict water depth connotation, as hemipelagic sediments are found from depths of 200m (the Nile pro delta, Maldonado and Stanley, 1978) down to 5000m (Mid-oceanic Ridges).

The units of lapilli tuff (angular clast bearing facies) found within the distal turbidite sequences do not show any erosive bases, only occasional grading and no sedimentary structures. This suggests that these lapilli tuffs were deposited by direct air fall on top and beneath the distal turbidites.

On Dunbar Farm, the presence of trough cross-bedding and channels in the carbonated lapilli bearing unit indicates that the fragments have been reworked by current action (section 3.2.4, Fig. 3.16). The scale of the cross-beds (>10cm) and the presence of large fragments suggest a more proximal,shallow water environment. Furthermore, large lapilli do not travel very far away from the vents (Williams and McBirney, 1979). The Dunbar unit is thus interpreted as a proximal unit where lapilli are reworked by high energy shallow water currents while the other thinner and finer grained units represent distal equivalents, directly deposited by air fall, within distal turbidites. Similar lapilli bearing carbonated units associated with poorly sorted accretionary spheroids have also been interpreted as shallow water deposits in the Kromberg fold area, to the south of the present study area (De Wit et al., 1982).

3.3 THE "AGGLOMERATES"

According to Viljoen and Viljoen (1969 d), agglomerates of the Hooggenoeg Formation occur in the southern part of Dunbar Farm (Fig. 3.27), where they can be correlated along strike into the Hooggenoeg Formation type area located in the Komati Gorge. Two facies can be distinguished in the these "agglomerates" (Fig. 3.27).

(a) Facies A

This facies is best exposed along the Msauli River where it is bounded by shear zones (Fig. 3.27 loc. a). It also occurs as a 5m thick sheared unit in the Kromberg Formation, north of Diepgezet Farm. The rock contains angular and rounded clasts of black cherts, banded chert, fuchsitic chert, spheroid bearing cherts and acid volcanics and is very poorly sorted (Fig.

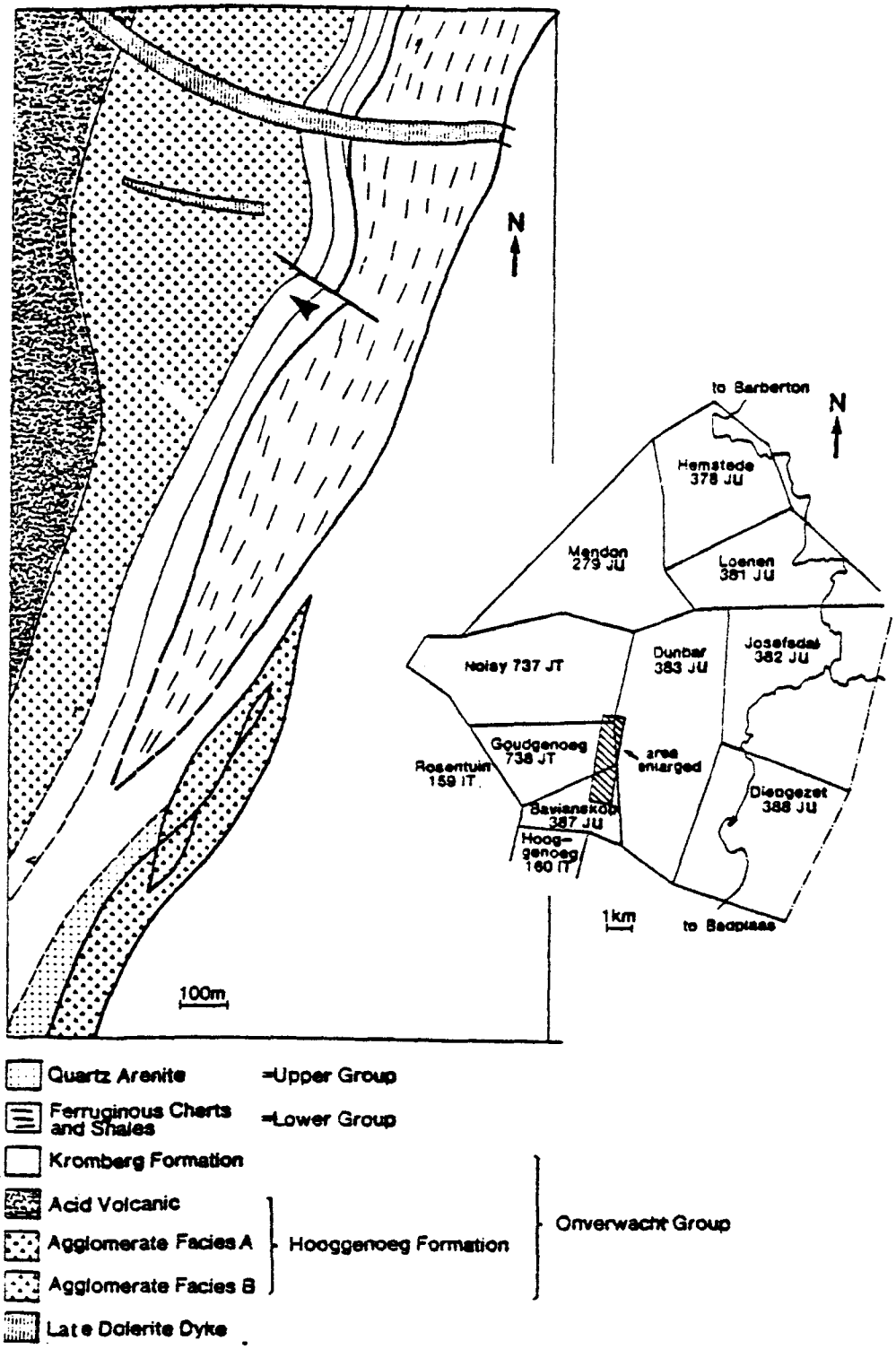


Figure 3.27. Simplified geological map showing the position of the main outcrop of the Hooggenoeg "agglomerates".

3.28). The clasts vary in size from 5 to 15 cm. The rock is generally matrix supported. In thin section, the matrix is composed of microquartz and iron oxides and contains structures resembling devitrified spherulitic textures (Fig. 3.29). The volcanic clasts contain carbonated euhedral or skeletal crystals in a carbonated and silicified matrix.

(b) Facies B

This facies is best exposed on the top of Dunbar Ridge (Fig. 3.27 loc. B.). The rock has the appearance of a medium to fine grained sandstone. It contains lenses of rounded and angular clasts of black chert, banded chert, vein quartz carbonate and acid volcanics (Fig. 3.30). The clasts vary in size from 0,5 to 8 cm. No sedimentary structures nor any bedding planes have been found in this rock type.

In thin section, the matrix is composed of microquartz and carbonate grains. The volcanic clasts contain carbonated euhedral crystals in a microquartz and carbonate groundmass (Fig. 3.31). In some sections, riebeckite crystals are overprinted over the crystals and the groundmass. This facies stratigraphically overlies a zone of flow banded silicic volcanics (Fig 3.26) (De Wit, 1983).

(c) Interpretation

Due to the lack of sorting, absence of sedimentary structures, presence of probable spherulitic textures in the matrix and the mixture of volcanic and detrital clasts, facies A is interpreted as a volcanic mudflow or lahar (Macdonald, 1972). Facies B contains similar clasts to facies A, has a sandy matrix and does not show any sedimentary structures. It is also interpreted as a debris flow type of deposit, possibly a reworked equivalent of facies A. Lahars are indicative of explosive volcanic activity.



Figure 3.28. The Hooggenoeg "agglomerate" (Facies A) with chert clasts (c) and acid volcanic clasts (a). (Dunbar Farm)

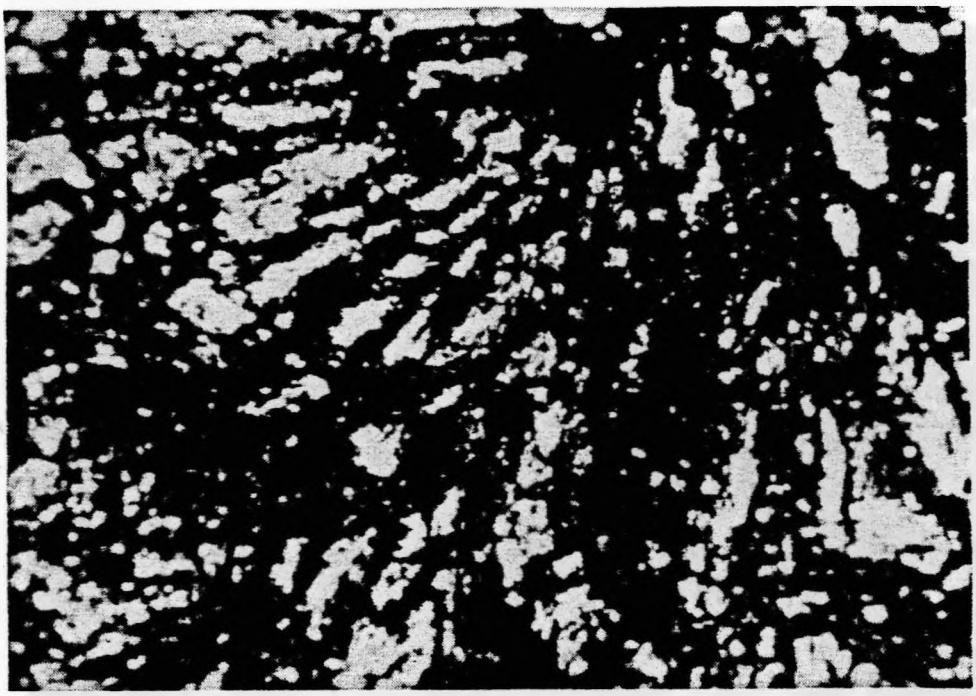


Figure 3.29. Photomicrograph of the Hooggenoeg agglomerate (Facies A) with possible devitrified spherulitic textures marked by iron oxides in the matrix (Baviaanskloof Farm). Width of field = 3,5 mm. Plane polarised light.



Figure 3.30. The Hooggenoeg "agglomerate" (Facies B) with acid volcanic clasts (a) and chert clasts (c) Dunbar Farm.

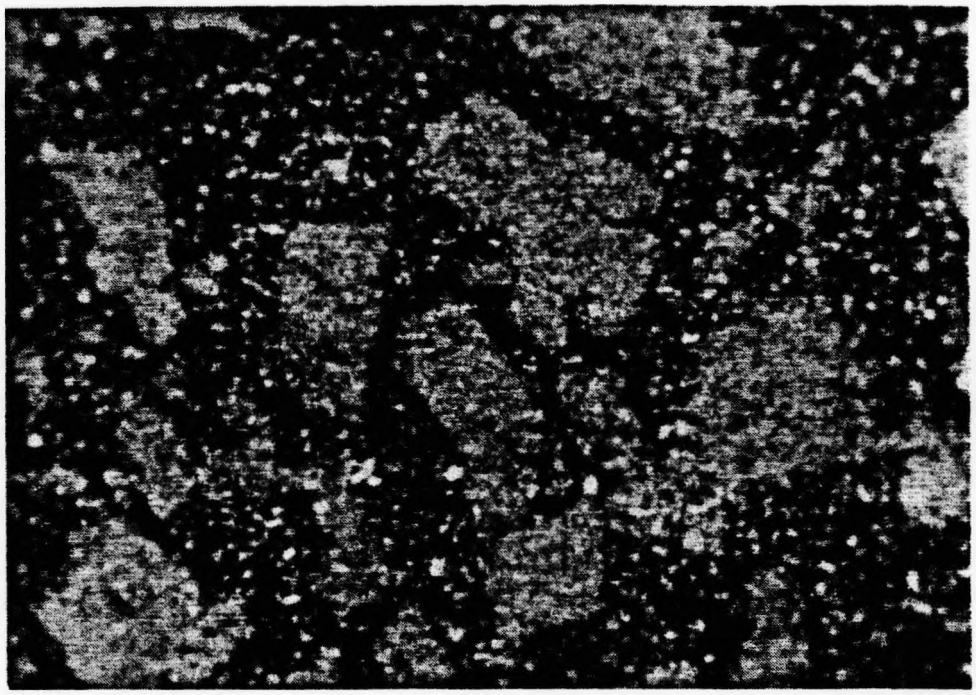


Figure 3.31. Photomicrograph of the Hooggenoeg "agglomerate" (Facies B) showing carbonated euhedral crystals in an acid volcanic clast. The groundmass is composed of microquartz and carbonates. Width of field = 3,5 mm.
Plane polarised light.

3.4 CONCLUSIONS

In the study area, two different environments have been recognised in the sedimentary rocks of the Onverwacht Group:

1. A shallow to subaerial environment in which lahars and lapilli tuffs are deposited.

2. A relatively deeper hemipelagic environment in which turbidite units are preserved. Within the turbidite units, a proximal and a distal facies can be distinguished.

Units of lapilli have also been deposited within the distal turbidites, presumably from direct air fall.

The presence of lahars, lapilli and accretionary lapilli is indicative of subaerial volcanic activity during deposition of the Onverwacht sedimentary rocks.

CHAPTER 4

4.0 POST-ONVERWACHT SEDIMENTARY ROCKS

4.1 INTRODUCTION

The Onverwacht Group is overlain by sedimentary rocks which form successively the Fig Tree Group and the Moodies Group and have been defined as lithostratigraphic units (SACS, 1980). However, in geological maps and in studies prior to SACS definition, the terms Moodies and Fig Tree have been used in terms of mixed lithostratigraphic and chronostratigraphic units, similar lithologies appearing in both units. Conglomerate units have been placed in the Fig Tree Group when interbedded with banded iron formation, while banded iron formation and shales have been placed in the Moodies Group when overlying thick conglomerate units. As the two Groups have been mainly defined and studied in the northern part of the belt (Anhaeusser, 1969 a; Condie et al., 1970; Reimer, 1975 a; Anhaeusser, 1976; Eriksson, 1977; 1980 a,b), it leads to confusion for workers studying the southern part of the belt. For example, no basal conglomerate can be clearly defined in the study area, as is the case in the northern part of the belt (Eriksson, 1977).

Another problem in the southern part of the belt is that different definitions of the Moodies and Fig Tree Groups have been used by the Swaziland Geological Survey. Thus, the same rock unit will appear as part of the

Moodies Group in a South African Survey geological map and as part of the Fig Tree Group in a Swaziland Survey geological map.

Recent mapping (De Wit, 1983; Lamb, 1984) and this study (Chapter 6), have shown that many sedimentary units are bound by tectonic contacts. Thus units cannot be correlated throughout the belt or even in a restricted area unless the tectono-stratigraphy is first recognised. In this study, the terms Moodies and Fig Tree Groups have been avoided in order to prevent confusion with the stratigraphy which has been established in the northern part of the belt and is recognised by SACS (1980). The method followed here is briefly outlined below.

4.2 METHOD OF APPROACH

In the study area, most sedimentary successions are truncated by thrusts (Fig. 4.1). Due to the absence of time markers, correlations from one tectonic unit to another are not necessarily straightforward as two tectonic units could represent lateral correlatives or could represent two different levels in the stratigraphy. For these reasons, it is felt that facies and facies sequences should be studied and recognised before a stratigraphy can be built. The recommendations of Turner and Walker (1973) for the study of Archaean sequences have been followed here. The rocks have been subdivided for descriptive purposes not in terms of successive stratigraphic units but in terms of distinctive facies which may occur or reoccur anywhere in the overall sequence.

The choice of facies subdivision depends on the objective of the study (Walker, 1979; Harms et al., 1982). In this study, the aims are two fold:
i) To establish a stratigraphy;
ii) To make broad palaeoenvironmental interpretations.

Only a few distinctive facies have been distinguished. A facies is defined as a body of rock that differs from vertically and laterally adjacent bodies of rock (Harms et al., 1982). Following Turner and Walker (1973), each facies has been defined in the field on the basis of textures, sedimentary

structures, lithologies, and other features which contribute to the aspect of the rock.

In this way, each facies is described by objective criteria observable in the field and those criteria suggest basic constraints on the interpretation of the facies. No preconceived stratigraphic ideas or complex models are forced upon this analysis (Harms, et al., 1982). The grain sizes in the lithofacies are defined according to the Wentworth scale and the sandstone terminology is after Folk (1974).

After description and basic interpretation of each facies, the sequence in which they occur and the nature of the boundaries between the facies is discussed. This is followed by the construction of vertical sequences and of a stratigraphy. The comparison of the facies sequences with sedimentary models leads to a palaeoenvironmental interpretation (Harms, et al., 1982).

4.3 DESCRIPTION OF THE LITHOFACIES

Within the study area, six main tectonic blocks of Fig Tree and Moodies sedimentary rocks can be distinguished (Fig. 4.1). From east to west, these blocks are informally called: The Diepgezet block, the Simbubule block, the Emlembe block, the Xecacatu block, the Josefsdal block and the Dunbar block (Fig 4.2 and appendices 8 to 13). Within these blocks, five facies can be defined which are numbered from F1 to F5. Some of these facies have been subdivided into subfacies, C in front of a subfacies name indicates a matrix predominantly composed of chert grains, while Q indicates the predominance of quartz grains.

Facies F1, comprises four subfacies, namely, a jaspilite subfacies (f1a); a ferruginous chert subfacies (f1b); a ferruginous shale subfacies (f1c); and a ferruginous tuff subfacies (f1c).
Facies F2, is formed by a ferruginous and tuffaceous siltstone subfacies (f2a); and a ferruginous chert-arenite subfacies (f2b).

Facies F3, contains a massive chert-arenite subfacies (f3a); a pebbly chert-arenite subfacies (f3b); a matrix supported granule C-conglomerate subfacies (f3c); and a clast support C-conglomerate subfacies (f3d).
Facies F4, is characterised by supermature quartz-arenite.
Facies F5, is subdivided into an immature quartz-arenite subfacies (f5a); a pebbly immature quartz-arenite subfacies (f5b); and a Q-conglomerate subfacies (f5c) (Table 4.1).

4.3.1 FACIES F1 (JASPILITE, FERRUGINOUS CHERT, SHALE AND TUFF)

This facies occurs in the Josefsdal, Simbubule and Diepgezet blocks (Figs. 4.1, 4.2). A maximum thickness of 700m has been calculated for this facies, after correction for tectonic thickening. It comprises four subfacies which are interbedded and pass laterally into one another.

a) THE JASPILITE SUBFACIES (f1A)

The jaspilites are oxide facies banded iron formations. The rocks are composed of centimetre thick white and red silica rich layers and ironstone. The red colour is due to iron oxide impurities in the chert. The chert bands are often boudinaged and slab shaped clasts of cherts up to 10cm long can be found within the ironstone, (Fig.4.3). Such clasts can occur in units up to 1m thick which resemble brecciola deposits (Friedman et al., 1982) or the Cow Head breccias of Newfoundland (Kindle and Whittington, 1958). In places, these clasts outline folds and the layers both above and below such folds are undisturbed suggesting a slumping origin. In the Diepgezet block, graded units of angular jasper clasts, 1 to 2 cm in diameter, and chert-arenite can be seen within the ironstone layers (Fig. 4.4).

b) THE FERRUGINOUS CHERT SUBFACIES (f1B)

The ferruginous cherts occur as alternating layers of white and black silica and brown iron-rich layers. The bands vary from a centimetre to a millimetre scale in thickness and are planar laminated (Fig. 4.5). Beds containing slab shaped clasts similar to the ones found in the jaspilite also occur in the ferruginous cherts. In the ferruginous cherts, circular

Table 4.1. List of lithofacies and sublithofacies recognised in the post-Onverwacht sedimentary rocks

Facies F1	Facies F2	Facies F3	Facies F4	Facies F5
Jaspilite subfacies: f1a	ferruginous tuffaceous siltstone subfacies: f2a	massive chert arenite subfacies: f3a	supermature quartz arenite facies	immature quartz arenite subfacies: f5a
ferruginous chert subfacies: f1b	ferruginous chert arenite subfacies: f2b	pebbly chert arenite subfacies: f3b		pebbly immature quartz arenite subfacies: f4c
ferruginous subfacies: f1c		matrix supported granule C-conglomerate subfacies: f3c		Q-conglomerate subfacies: f5c
ferruginous tuff subfacies: f1d		clast supported C-conglomerate subfacies: f3d		

C = Chert grains dominant in the matrix.

Q = Quartz grains dominant in the matrix.

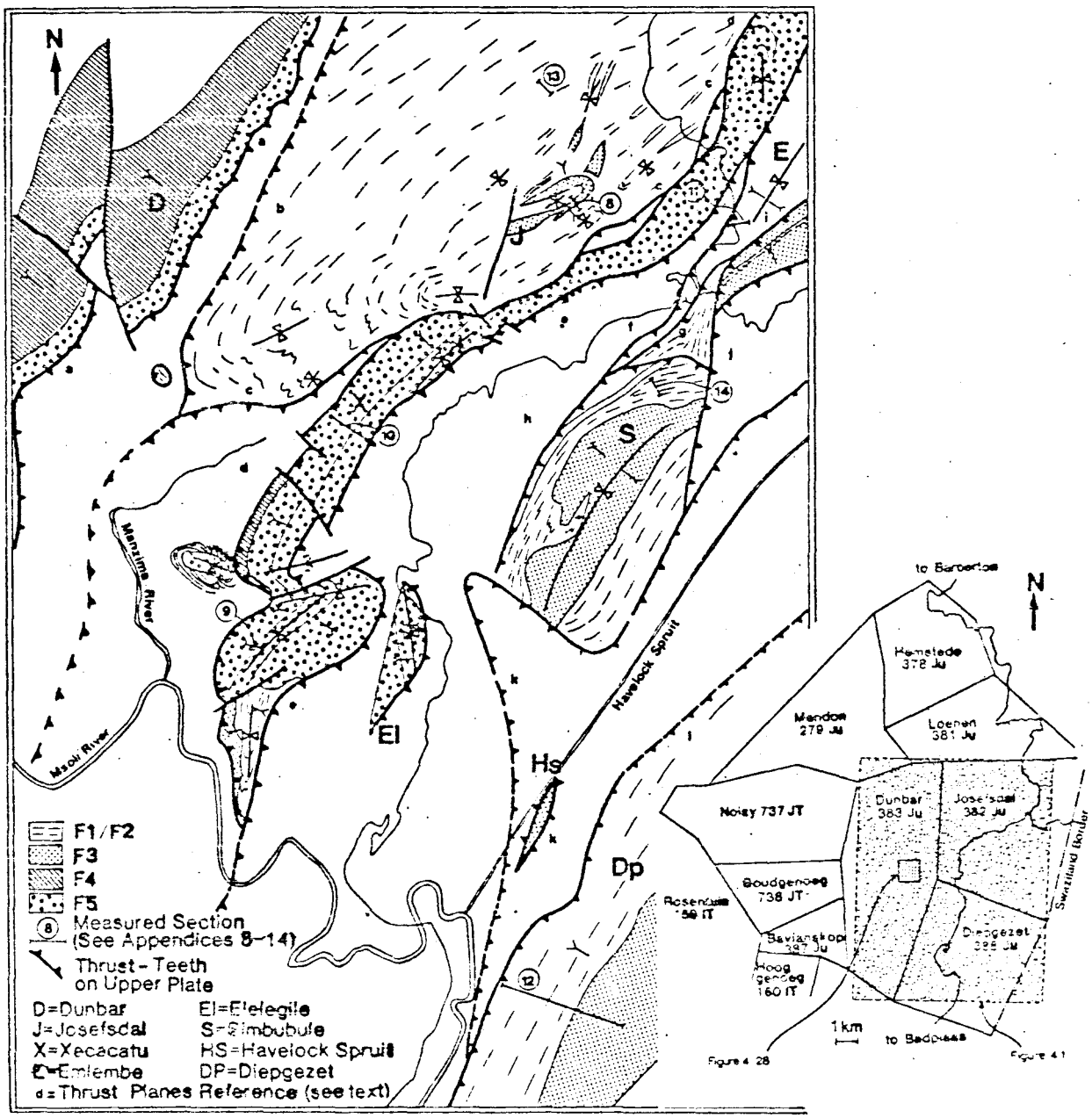


Figure 4.1. Simplified geological map showing the distribution of the post-Onverwacht sedimentary rocks, and the location of the meas used sections (Appendix. 8 - 13, Fig. 4.2).

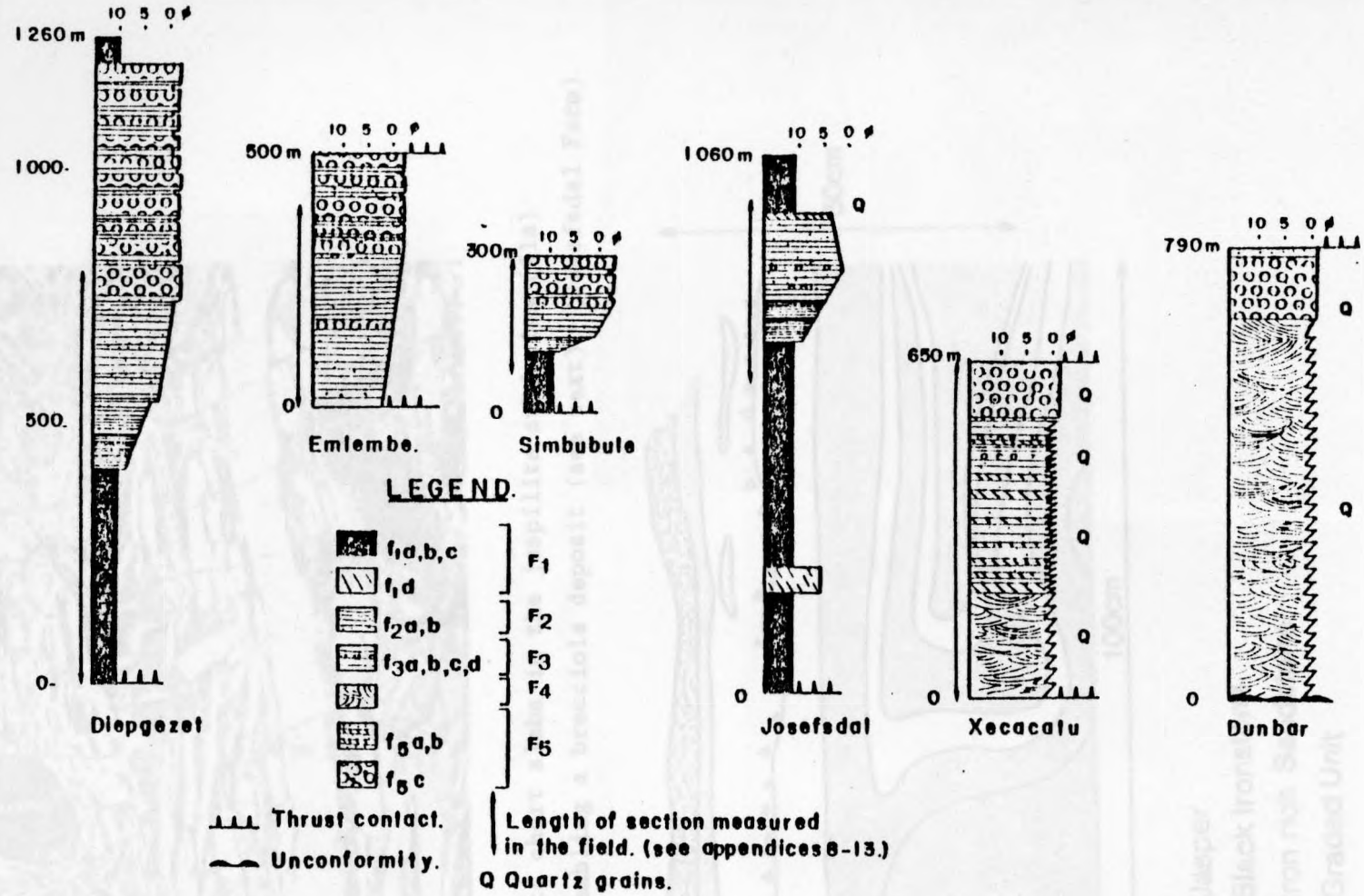


Figure 4.2. Measured sections in post-Onverwacht sedimentary rocks. See Fig. 4.1 for location. Detailed measured sections are presented in appendix 8-13.

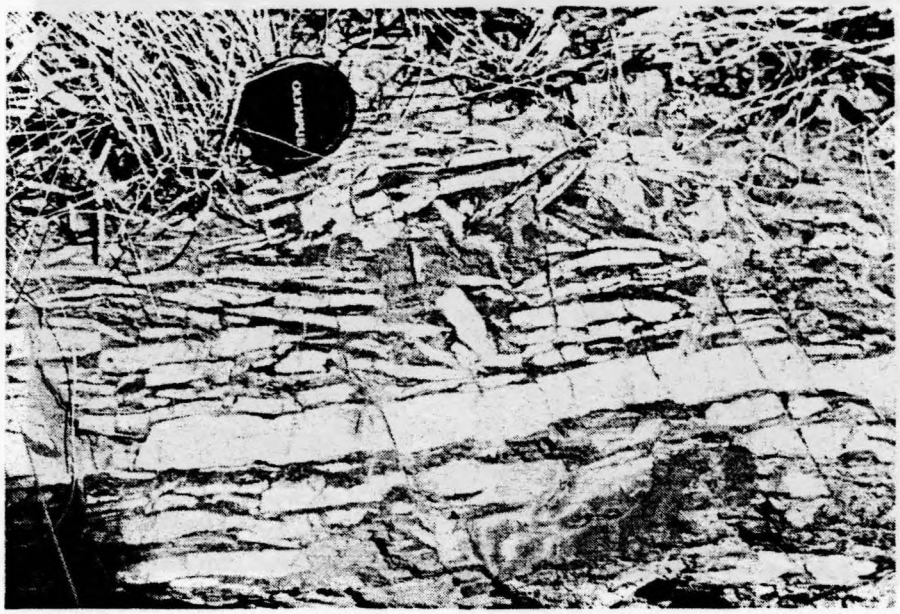


Figure 4.3. White chert slabs in the jaspilite subfacies (f1a) resembling a brecciola deposit (see text). (Josefsdal Farm).

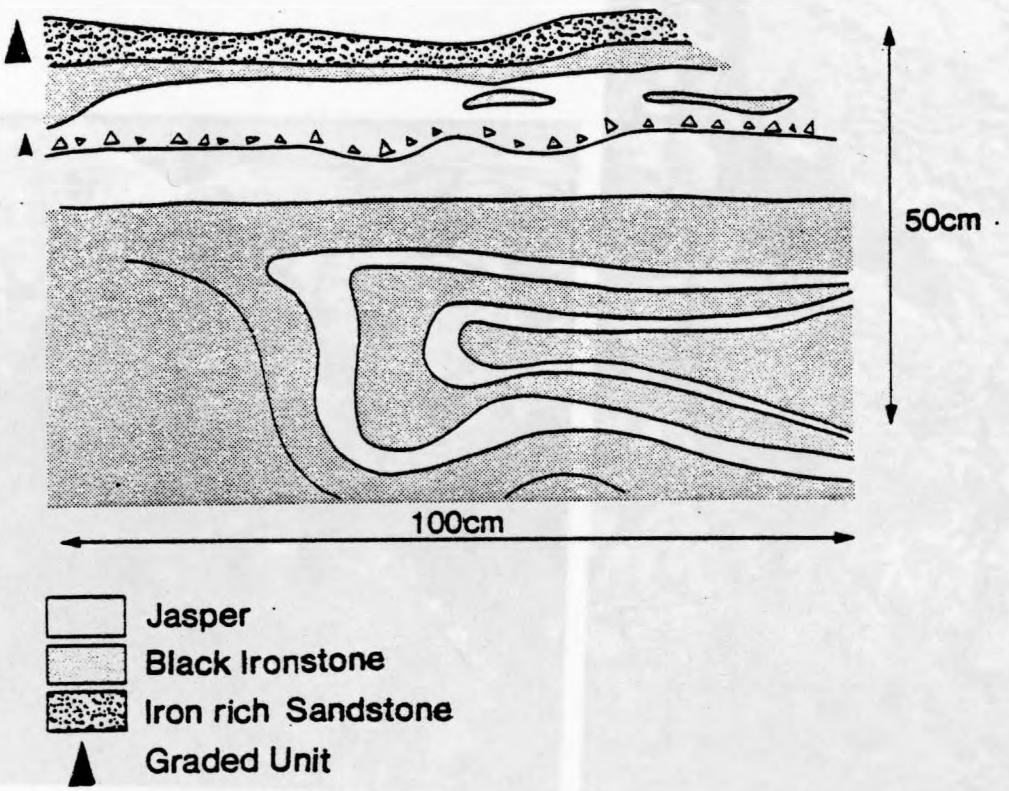


Figure 4.4. Schematic diagram of graded jaspilite units. (Diepgezet Farm).

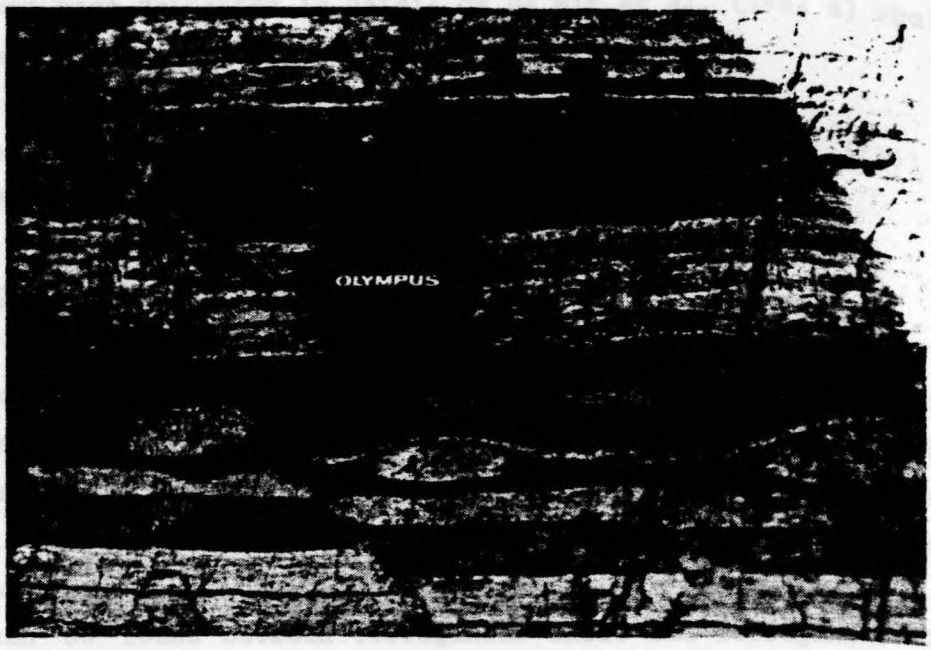


Figure 4.5. The ferruginous chert subfacies (f1b). White bands are composed of silica, dark bands of silica and iron oxides. (Dunbar Farm).





Figure 4.6. "Mud pool" structures in the ferruginous chert subfacies. (a = Granville Grove Farm, scale bar = 5cm, b = Diepgzet Farm).

structures 5 to 10 cm in diameter can often be found (Fig. 4.6). Such structures have been described in detail by De Wit et al. (1982 a) who interpreted the structures as fossil mud pools.

All gradations can be found between true ferruginous cherts (f16) and jaspilites (f1a).

c) THE FERRUGINOUS SHALE SUBFACIES (f1C)

The ferruginous shales are dark brown to red in colour. They are fine grained, micaceous and siliceous, often with a slaty cleavage. The beds are 0.5 to 1mm thick. On the western part of the Josefsdal Farm (Fig. 4.1) slabs of shale show a corrugated surface resembling aligned flute casts with the corresponding mould on the other side of the slab (Fig. 4.7). All gradations can be found between ferruginous shale and ferruginous chert (f1b).

d) THE FERRUGINOUS TUFF SUBFACIES (f1D)

Although this rock type has only been found in the Josefsdal block it is included in F1 because it grades along strike into banded iron formation and ferruginous cherts and is interbedded with the other F1 rock types. The ferruginous tuff occurs in units ranging from 10 to 50m in thickness. In the field, the rock weathers to a pale green to yellow colour and is fine grained. It is exposed as large boulders displaying an onion peel weathering surface.

The rock is composed of fine grained carbonate, sericite and microquartz with isolated fragments. These consist of elongate and angular quartz shards. Some fragments are composed of sericite and microquartz and are surrounded by a halo of iron oxides (Fig. 4.8).

Interpretation of facies 1

The presence of volcaniclastic sediments associated with black cherts, iron formation, iron rich argillites (shales) and cherts is indicative of hemipelagic and pelagic environments (Reading, 1978; Dimroth, 1979; Eriksson, 1980 b). The graded units and the flute casts, although uncommon indicate intermittent current action while the predominance of finely lam-

inated beds suggest that the settling of particles out of suspension was the main depositional process.

The abundance of slab shaped clasts in the jaspilite and ferruginous chert suggests a debris flow type of transport. The resemblance of slab shaped clast bearing units with brecciola deposits and with the Cow Head Conglomerate suggests deposition on an unstable slope. The presence of slump folds further suggests deposition on a slope.

The mud pool structures have been interpreted as indicative of a subaerial environment (De Wit et al., 1982 a). However, similar delicate structures such as mud volcanes can be preserved at any water depth (Gill and Kuenen, 1958; Lucchi, 1970; Reineck and Singh, 1980). Thus it is felt that the presence of mud pool structures alone cannot be used to infer any particular water depth.

F1 is thus seen as representing an hemipelagic environment, with deposition taking place on an unstable slope.

4.3.2 FACIES F2 (FERRUGINOUS AND TUFFACEOUS SILTSTONE, FERRUGINOUS

chert-arenite)

This facies occurs in the Josefsdal, Diepgezet and Simbubule blocks (Fig. 4.1, 4.2). Its maximum thickness is approximately 400m. It comprises two subfacies which are interbedded with one another.

a) THE FERRUGINOUS AND TUFFACEOUS SILTSTONE SUBFACIES (f2A)

The tuffaceous siltstone comprises alternating green and purple beds 1 to 5cm thick (Fig. 4.9). They contain planar lamination and cross-lamination. In thin section, some of the siltstone beds contain quartz shards indicative of a volcaniclastic component. This subfacies differs from the ferruginous

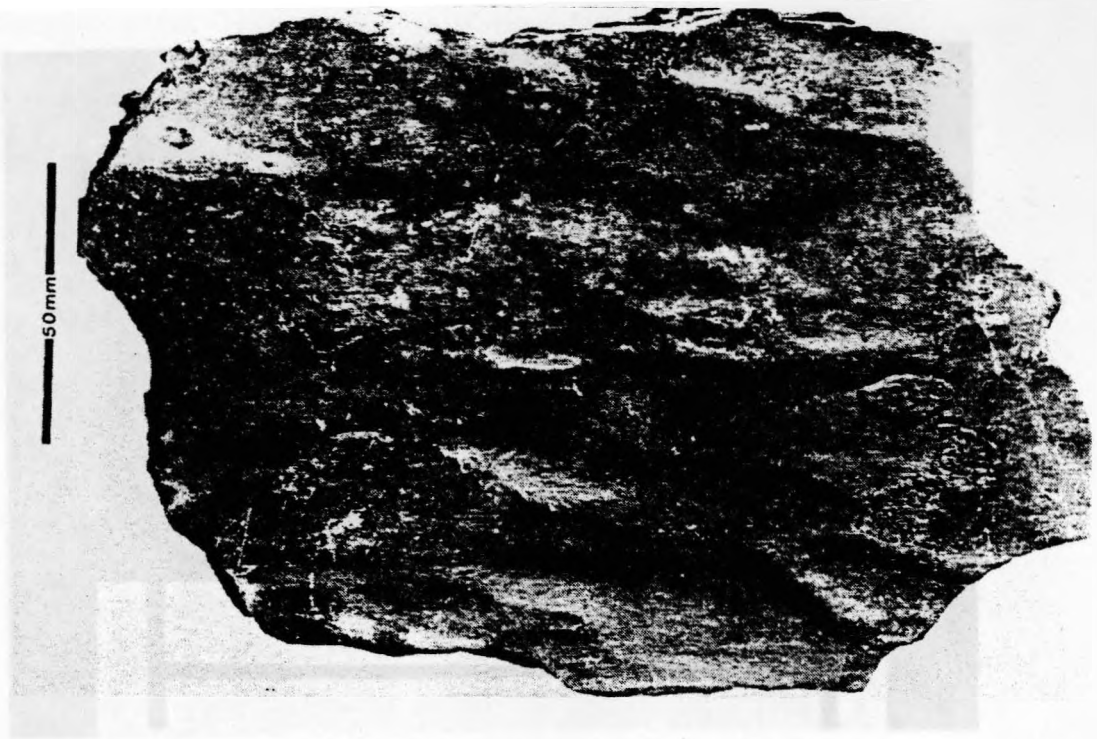


Figure 4.7. Structures resembling flute casts in the ferruginous shale subfacies (Josefdal Farm).

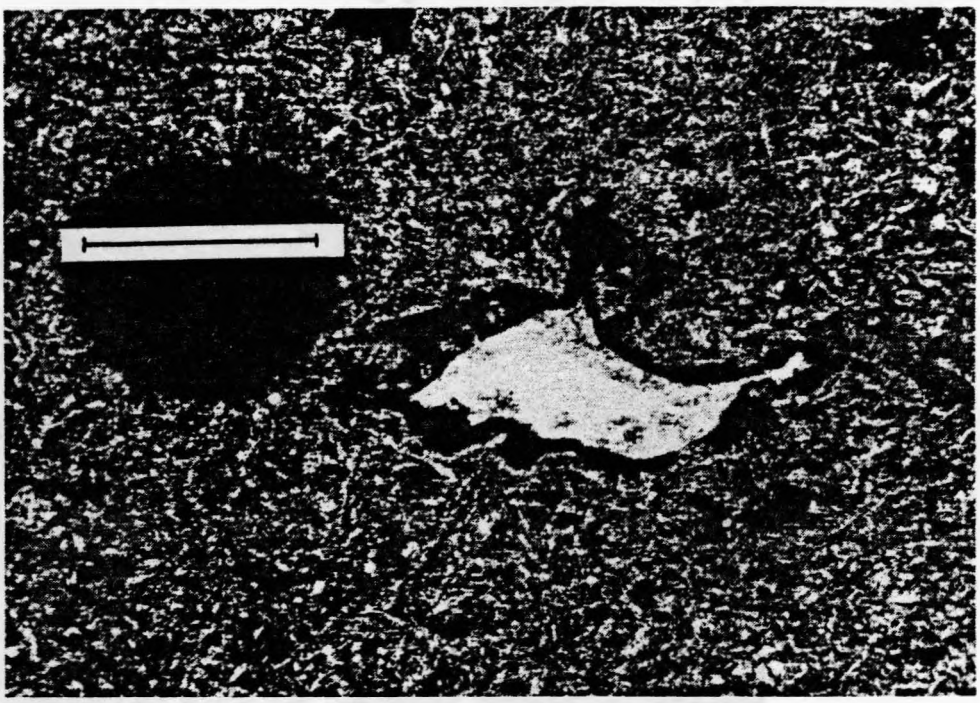


Figure 4.8. Photomicrograph of the ferruginous tuff subfacies (f1d) showing a shard shaped clast composed of microquartz. The matrix comprises sericite, carbonate, iron oxides and microquartz. Scale bar = 1mm. (Josefsdal Farm).

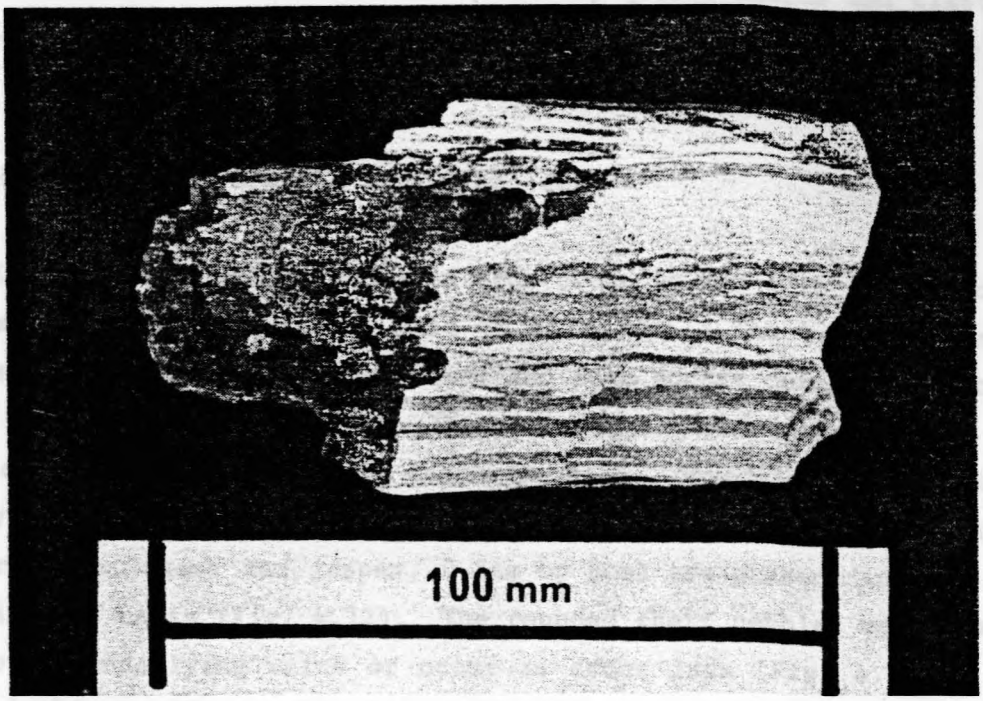


Figure 4.9. Specimen of the tuffaceous siltstone subfacies (f2b) with alternating green (light) and purple (dark) beds. (Josefdal Farm).



Figure 4.10. Ferruginous siltstone subfacies (f2c) with a chert pebble embedded into the underlying beds (arrow) (Josefdal Farm)

tuff (f1d) in that it is coarser grained, well bedded with green and purple beds; it contains cross-laminae and is formed by quartz shards and clastic components.

b) THE FERRUGINOUS CHERT-ARENITE SUBFACIES (f2B)

The ferruginous chert-arenites occur in beds brown to red 1 to 10cm thick. The grain size varies from medium sand to silt size. The beds are frequently graded with sharp erosional bases and form scours cutting into the underlying units (Fig. 4.10, 4.11). The channels have an average size of 15cm by 5cm. Isolated rounded chert pebbles (Onverwacht silicified sedimentary rocks), varying from 1 to 10 cm in diameter, and flat silica slabs (ferruginous chert and jasper, 0,5cm by 8cm) are present in some of the chert-arenite units (Fig. 4.12). The rounded chert pebbles can be embedded into the underlying units or occur as scour lags (Fig. 4.10). In the Simbubule block, (Fig. 4.2 and appendix 13), trough cross-laminae with sets 5cm high are present in the chert-arenite units (Fig. 4.13c). Some sand size chert-arenite beds are draped by ferruginous mudstone laminae (f2a) and can contain mud flakes. In the Josefsdal block, flute casts are preserved on the chert-arenite bedding planes (Fig. 4.14). In the same block a 15m thick unit of F2 has a bright green colour due to the presence of fuchsite in the matrix.

Interpretation of Facies 2

The lithological characteristics of this facies indicate a mixed input of terrigenous, clastic and volcaniclastic detritus. The volcaniclastic material was deposited intermittently with the clastic material. The abundance of iron oxides in this facies could result from volcanic activity. The rounded chert pebbles indicate reworking and the lithology suggest derivation from the Onverwacht sedimentary rocks while the presence of fuchsite in the sandstone matrix (Josefsdal block) suggests that the Onverwacht igneous rocks were also being eroded in the source area. The shape of the jasper and ferruginous chert clasts indicates a small amount of reworking and transport, thus a local derivation.

Flute casts, cross-laminations, mud flakes and the presence of erosive bases and scour lags indicate deposition and erosion by high energy currents. The presence of mud drapes over sandstone beds is indicative of quiescent periods.

These various features can be explained by turbidity currents and this facies is thus interpreted as deposited by turbidity currents.

4.3.3 FACIES F3 (CHERT-ARENITE AND C-CONGLOMERATE)

This facies is exposed in the Diepgezet, Josefsdal,Emlembe and Simbubule blocks (Fig. 4.1). Its maximum thickness is 780m. It comprises four subfacies which are interbedded in an upward coarsening manner (Fig. 4.2). The four lithofacies comprise: massive chert-arenite (f3a); pebbly chert-arenite (f3b); matrix supported granule C-conglomerate (f3c); clast supported C-conglomerate (f3d). The four subfacies of F3 can be partly silicified (chapter 5). An important characteristic common to the four subfacies is the predominance of chert over quartz grains in the matrix. The only exception is found in the Josefsdal block where the massive chert-arenite (f3a), although having similar sedimentary structures, becomes progressively richer in quartz grains to become a quartz-arenite towards the top of the block (Fig. 4.2).

a) THE MASSIVE CHERT-ARENITE SUBFACIES (f3A)

The massive chert-arenite subfacies occurs in units up to 50m thick. Individual beds within the units vary from 20cm to 1m in thickness. They occasionally contain isolated rounded and angular chert clasts up to 4cm in diameter. The chert-arenites vary from fine to coarse sand grade with coarse beds separated by 0,2cm thick fine sand laminae.

Grading is uncommon within individual beds but the units as a whole coarsen upwards. Dewatering structures such as dish structures and pillar structures (Lowe and Lo Piccolo, 1974) occur in the finer sand beds (Fig. 4.15).



Figure 4.11. Ferruginous chert-arenite subfacies with (f2d) a graded unit scouring into the underlying siltstone unit,(arrow) (Josefsdal Farm).

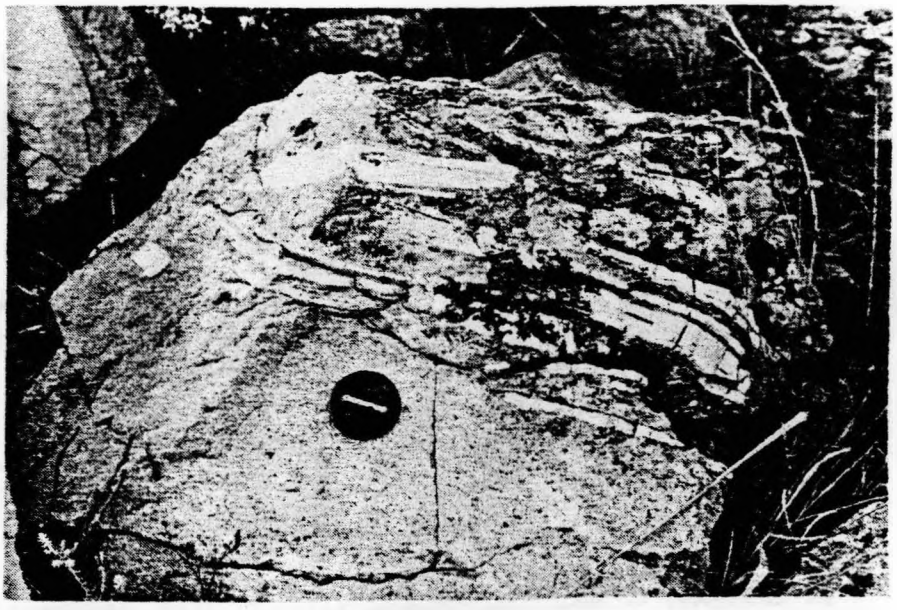


Figure 4.12. Ferruginous chert-arenite subfacies (f2d) containing slab shaped clasts (Josefsdal Farm).



Figure 4.13. Trough cross-lamination in the ferruginous chert-arenite subfacies (f2d). (Josefsdal Farm).

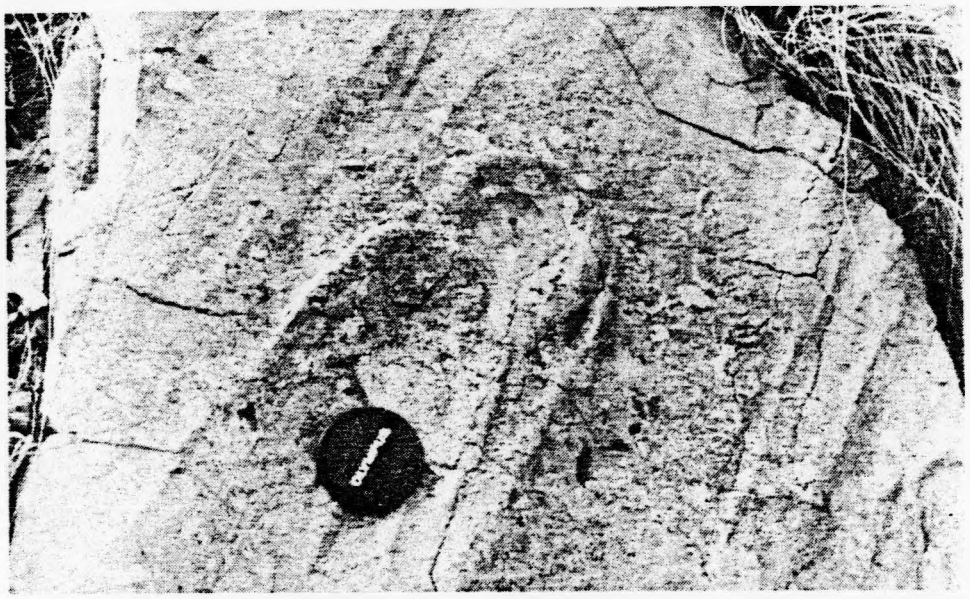


Figure 4.14. Flute casts in the ferruginous chert-arenite subfacies (f2d). (Josefsdal Farm).

Palaeocurrent data can be collected in this subfacies. However, due to the thrusting and subsequent deformation (folding and faulting, see Chapter 5), one cannot quantify the rotation which should be applied to the bedding to return it to a horizontal position. Nine rotated palaeocurrent readings, from less deformed areas in the Emlembe block, are presented in Fig. 4.23 a. They indicate sediment transport to the south and to the north east. However such a small number is not considered to be representative of a palaeocurrent trend.

b) THE PEBBLY CHERT-ARENITE SUBFACIES (f3B)

This lithofacies varies from coarse to medium grained chert-arenite, containing rounded to angular chert pebbles. The pebbles vary in size from 0.5 to 1.5cm. The clast content can vary from one bed to the next, and the beds vary from 10cm to 2m in thickness and contain planar laminae and cross-laminae. The long axes of the pebbles are generally parallel to the laminae (Fig. 4.16). The cross-laminated sets vary from 5 to 15cm in thickness, with an average of 6cm. The beds are commonly well graded, with a pebble rich base and a planar laminated or cross-laminated sand grade top (Fig. 4.16).

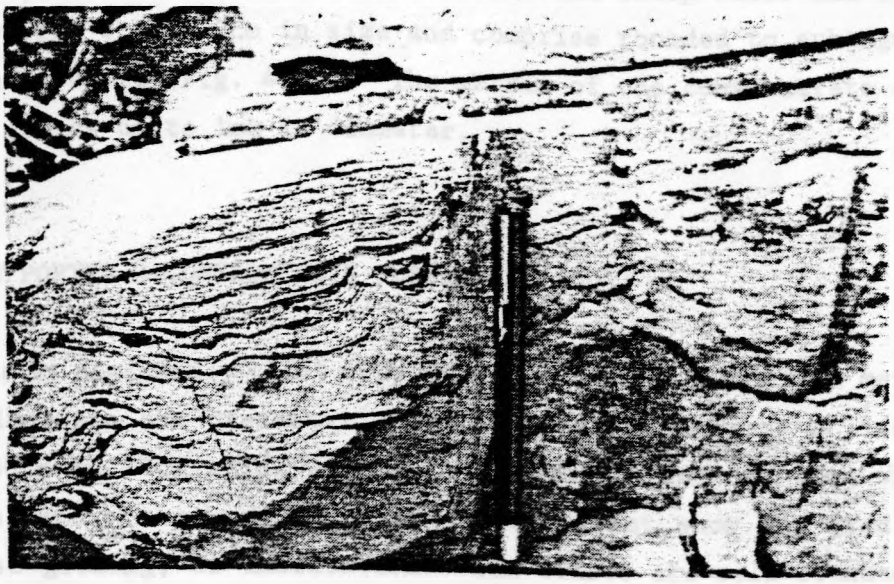


Figure 4.15. Dewatering pillar structures in the massive chert-arenite subfacies (f3a). (Josefsdal Farm).

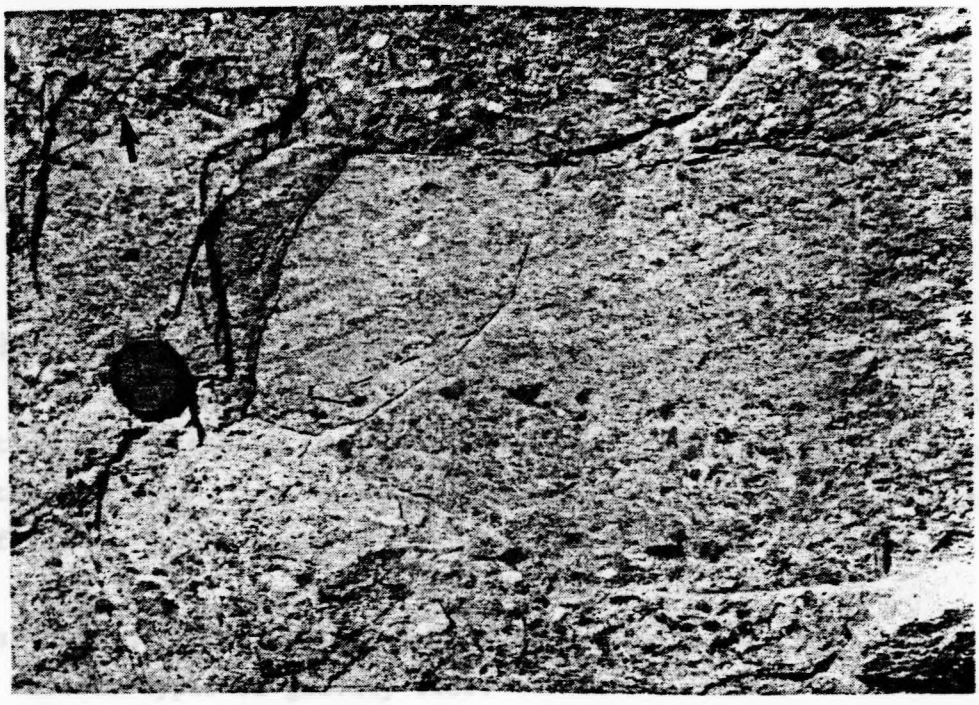


Figure 4.16. Pebbly chert-arenite subfacies (f3b) with a cross-bedded unit (underlined) arrows points to the base of the overlying unit. (Josefsdal Farm).

C) THE MATRIX SUPPORTED GRANULE C-CONGLOMERATE SUBFACIES (f3C)

This lithofacies occurs in units 25cm to 50cm thick. The units are well sorted, with no internal sedimentary structures and sharp bases and tops. The clasts vary from 0,5 to 2cm in size and comprise rounded to subangular massive and banded chert (Fig. 4.17). The matrix of the conglomerate consists of chert grains up to 1mm in diameter.

D) THE CLAST SUPPORTED C-CONGLOMERATE SUBFACIES (f3D)

The conglomerate is dominantly clast supported but locally pockets of matrix supported conglomerate are present. The conglomerate occurs in lenses varying from 80cm to 50cm thick and up to several kilometres long which scour and erode into the underlying units. They do not show any grading, bedding, reverse grading, or imbrication. The clasts are well rounded to angular and vary in size from 2cm to 40cm. They comprise black chert, white chert, banded chert, silicified lapilli tuff, jasper and ferruginous shale. Some of the white chert clasts occur as slabs up to 8cm by 0,5cm in size (Fig. 4.18). The matrix of the conglomerate, although poorly developed, is mostly composed of sand sized chert grains.

Interpretation of facies 3

This facies presents all the characteristics of "resedimented coarse clastics", or "coarse turbidites" as defined by Walker and Mutti (1973) and Walker (1975; 1978; 1979). It contains massive sandstones devoid of interbedded shales and with dewatering structures; which are formed by liquified flow (Lowe, 1979) pebbly sandstones with abundant cross stratification (deposited by turbidity currents); matrix supported granule conglomerates and clast supported conglomerates of type 4 in the classification of Walker (1978, 1979; debris flow deposits).

Facies 3 is thus interpreted as representing coarse grained turbidites deposited by various types of gravity flow.

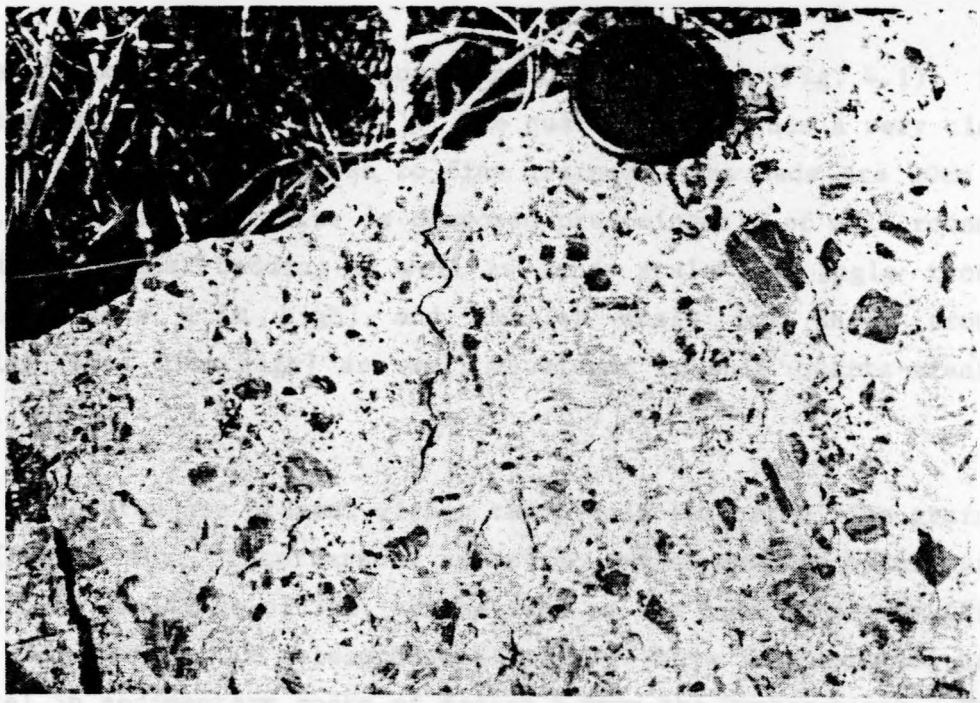


Figure 4.17. Matrix supported granule C-conglomerate subfacies (f3c). (Josefsdal Farm).



Figure 4.18. The clast supported C-conglomerate subfacies (f3d) with slabs of white chert. (Josefsdal Farm).

4.3.4 FACIES F4, SUPER MATURE QUARTZ-ARENITE

This facies is exposed in the Xecacatu and Dunbar blocks (Fig. 4.1). Its maximum thickness is 750m (Fig. 4.2). The quartz-arenite has a very clean aspect and varies from very coarse to fine grained. The beds are 10cm to 50cm thick. The quartz-arenite is composed predominantly of well rounded quartz grains. Planar bedding as well as large scale low angle trough cross-bedding (sets 1,5m high) and smaller scale low angle trough cross-bedding (sets 15cm high) are well developed in this quartz-arenite (Fig. 4.19, 4.20).

Dewatering structures are present within the planar laminated fine grained sandstone (Fig. 4.21). Interference symmetric and asymmetric bifurcating ripples, with an amplitude of 3cm, can be seen on the bedding planes (Fig. 4.22). In this facies, 22 palaeocurrent readings have been rotated back to horizontal in sedimentary rocks of facies 4 from the Dunbar block. They indicate a unimodal current distribution with a large spread, the major current direction being to the south (Fig. 4.23 b).

Interpretation of facies 4

Clean orthoquartzites or quartz-arenite, can form in three ways (Horne and Ferm, 1978): (i) By intense weathering. Such orthoquartzites are restricted to soil zones. (ii) By the erosion of a pure quartz source area. Such deposits are ubiquitous in all depositional environments from fluvial to barrier systems. (iii) The third and most common way in which orthoquartzites accumulate is in environments where the sands have been "cleaned" of material other than quartz due to reworking. These develop at loci of high energy and are frequently interbedded with and laterally equivalent to "dirty" sandstones.

The large scale of the cross-beds (between 15cm and 1.5m high); and the asymmetric and symmetric bifurcating ripples are indicative of environments above wave base, while the palaeocurrent data indicate that a shallow marine or tidal environment is unlikely (Miall, 1977b).



Figure 4.19. The supermature quartz-arenite subfacies (f4b) with large scale rough cross-beds. (Dunbar Farm). Left arrow indicates the bottom of the cross sed, right arrow indicates the top of the set.

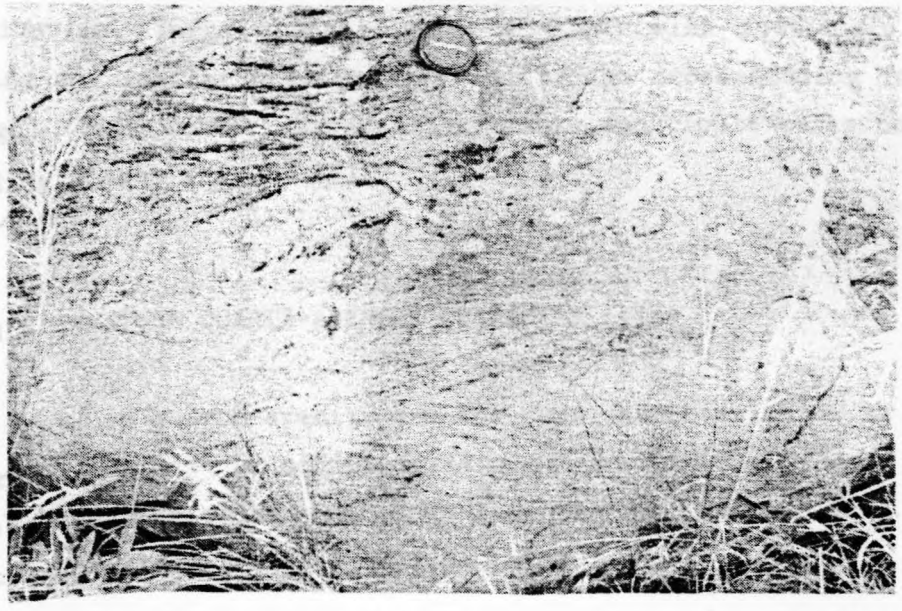


Figure 4.20. The supermature quartz-arenite subfacies (f4a) with medium scale trough cross-bedding (Dunbar Farm).

4.3.5 FACIES 5 (IMMATURE QUARTZ-ARENITE, PEBBLY IMMATURE QUARTZ ARENITE AND Q-CONGLOMERATE) F5

This facies occurs in the Xecacatu and the Dunbar blocks (Fig. 4.1). Its maximum thickness is 350m (Fig. 4.2). It can be subdivided into three subfacies which are interbedded with each other: the immature quartz-arenite subfacies (f5a); the pebbly immature quartz-arenite subfacies (f5b) and the Q-conglomerate subfacies (f5c). In all three subfacies, quartz grains predominate over chert grains. The quartz/chert percentage varies from 75% to 100%, thus both subchert-arenite and quartz-arenite are included in this facies. They have not been distinguished in the facies description because the difference between 75% and 95% quartz grains is not easily made in the field.

a) THE IMMATURE QUARTZ-ARENITE SUBFACIES (f5A)

The immature quartz-arenite subfacies is formed by beds of poorly sorted angular quartz grains and contains iron oxide grains and iron-rich clay laminae which give the rock the appearance of a dirty yellow to orange sandstone. The grain size varies from medium to coarse sand. The beds vary in thickness from 5 to 25cm, they are commonly graded and separated by fine sand laminae. The sedimentary structures found in this facies include planar lamination, large channels (5m by 0.4m) with low angle planar cross-bedding and smaller scale planar and trough cross-bedding (sets 10 to 30cm high) (Fig. 4.24). Desiccation cracks and ripple marks can occur on the bedding planes (Fig. 4.25).

b) THE PEBBLY IMMATURE QUARTZ-ARENITE SUBFACIES (f5B)

The pebbly immature quartz-arenite has the same characteristics as the immature quartz-arenite. In addition, it contains isolated chert clasts, angular to subrounded which vary from 2 to 6cm in diameter (Fig. 4.26). This subfacies occurs in units 5 to 25cm thick.

c) THE Q-CONGLOMERATE SUBFACIES (f5C)

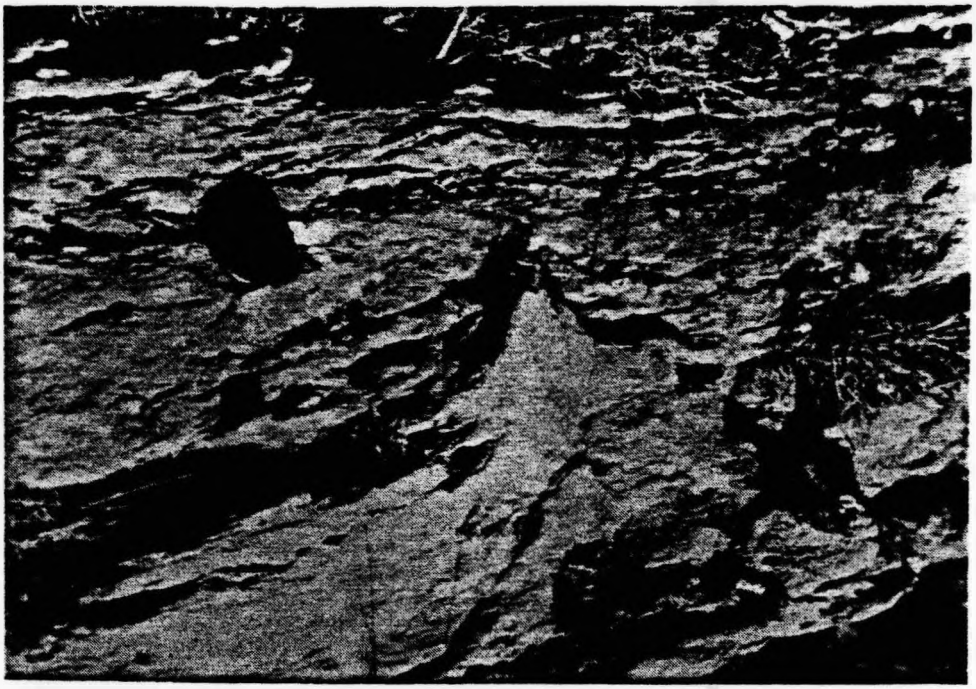


Figure 4.21. Planar bedded supermature quartz-arenite subfacies (f4b) with dewatering structures. (Dunbar Farm)

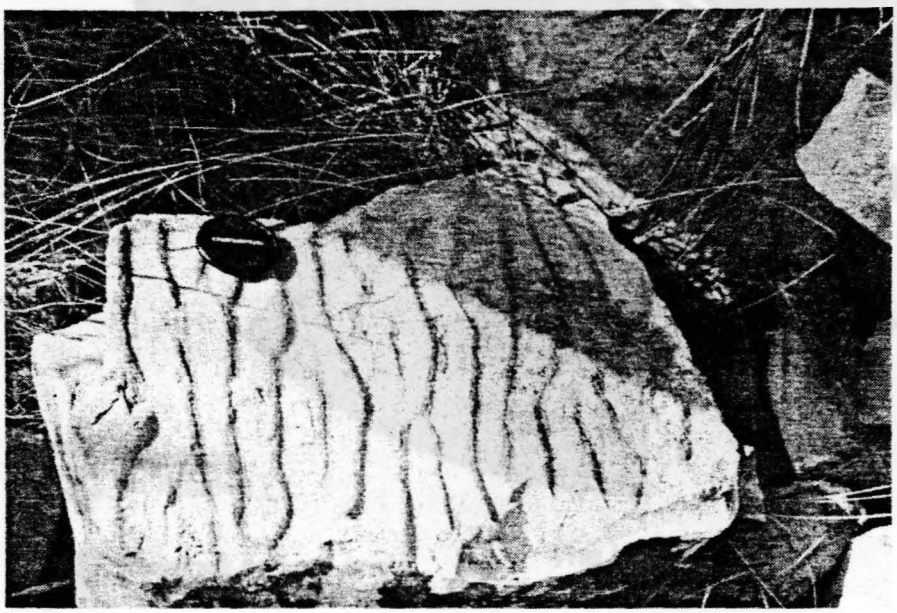


Figure 4.22. Planar bedded supermature quartz-arenite subfacies (f4b) with asymmetric bifurcating ripples. (Dunbar Farm).

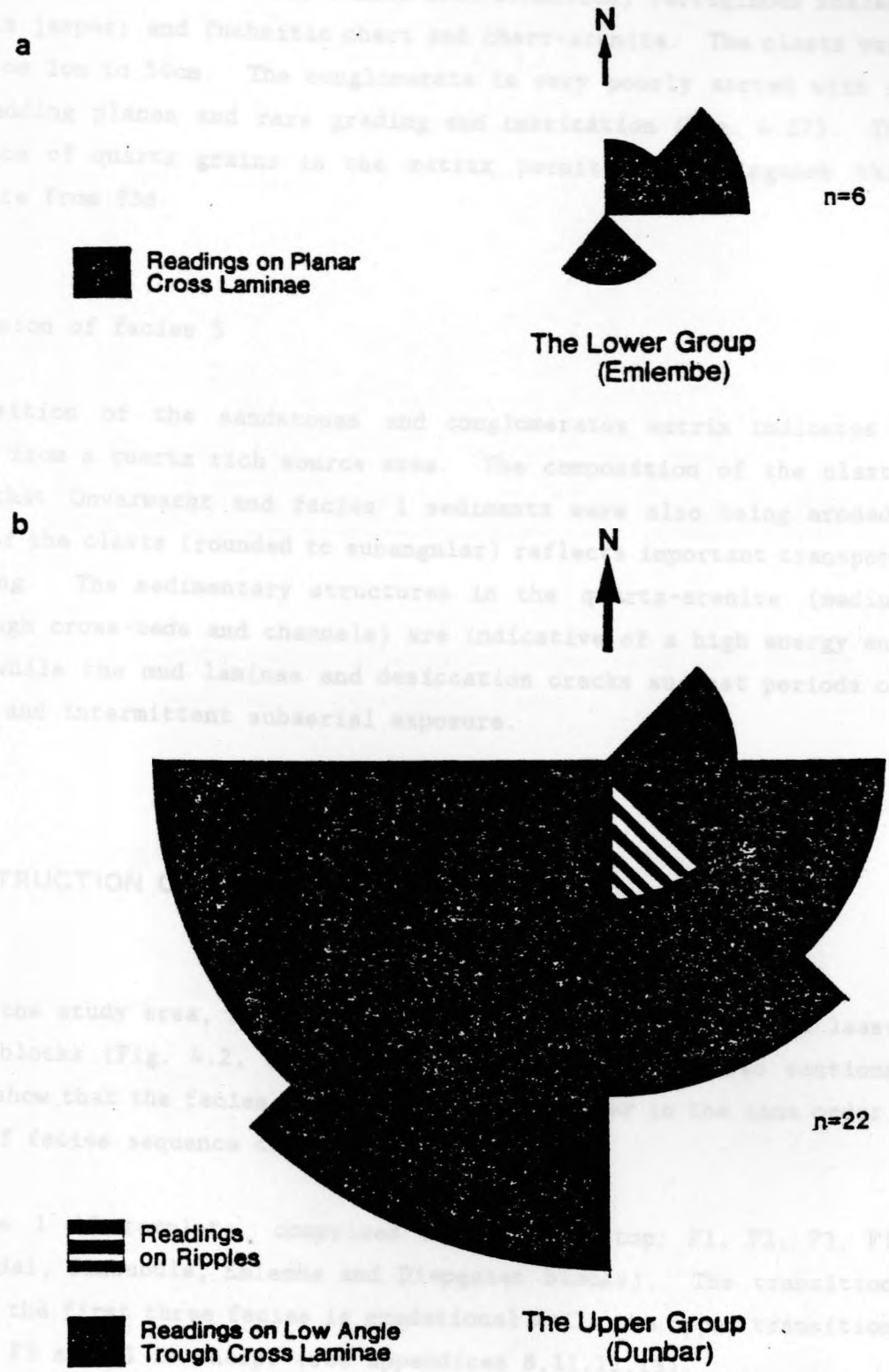


Figure 4.23. Paleocurrent directions rotated to the horizontal, following the method described by F. C. Phillips (1973). a = Lower Group, b = Upper Group.

The conglomerate is mostly clast supported with a sand size matrix. The clasts are well rounded to subangular and include spheroid bearing chert; chert with "mud pool" structure; banded iron formation; ferruginous shales; vein quartz jasper; and fuchsitic chert and chert-arenite. The clasts vary in size from 2cm to 50cm. The conglomerate is very poorly sorted with no visible bedding planes and rare grading and imbrication (Fig. 4.27). The predominance of quartz grains in the matrix permit to distinguish this conglomerate from f3d.

Interpretation of facies 5

The composition of the sandstones and conglomerates matrix indicates a derivation from a quartz rich source area. The composition of the clasts suggests that Onverwacht and facies 1 sediments were also being eroded. The shape of the clasts (rounded to subangular) reflects important transport or reworking. The sedimentary structures in the quartz-arenite (medium scale through cross-beds and channels) are indicative of a high energy environment while the mud laminae and desiccation cracks suggest periods of quiescence and intermittent subaerial exposure.

4.4 CONSTRUCTION OF THE FACIES SEQUENCE

Throughout the study area, all the lithofacies are encountered in at least two of the blocks (Fig. 4.2, appendices 8 to 13). The measured sections (Fig. 4.2) show that the facies always succeed each other in the same order. Two types of facies sequence can be defined:

1. Sequence 1 if complete, comprises from base to top: F1, F2, F3, F1 (Josefsdal, Simbubule, Emlembe and Diepgezet blocks). The transition between the first three facies is gradational while the upper transition between F3 and F1 is sharp. (see appendices 8,11,12,13).

2. Sequence 2 if complete, comprises from base to top: F4 and F5 (Dunbar and Xecacatu blocks). The transition between the two lithofacies is also gradational.

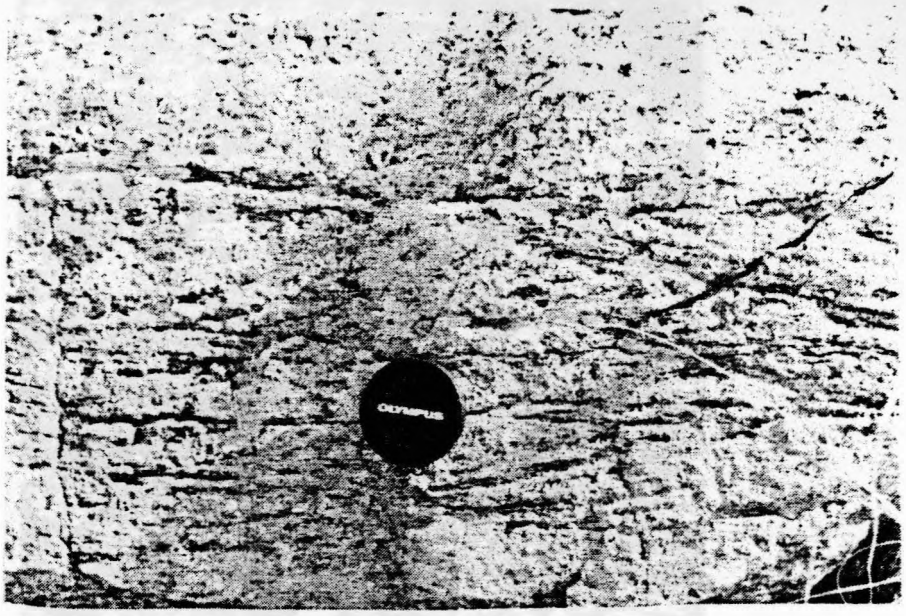


Figure 4.24. Immature quartz-arenite subfacies (f5a) with trough cross-bedding. (Diepgezet Farm).

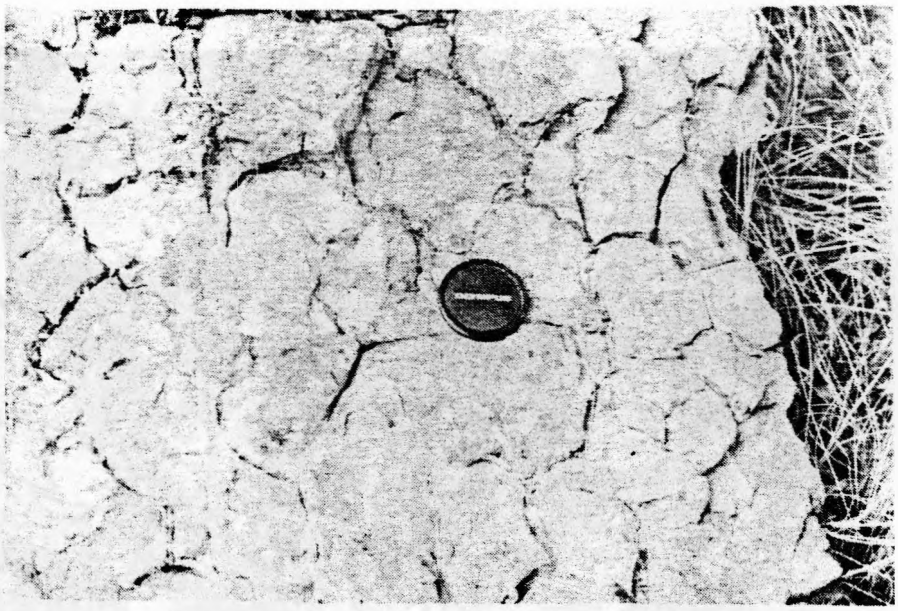


Figure 4.25. Desiccation cracks on the bedding plane in the immature quartz-arenite subfacies (f5a). (Diepgezet Farm).



Figure 4.26. Pebbly immature quartz-arenite subfacies (Dunbar Farm).

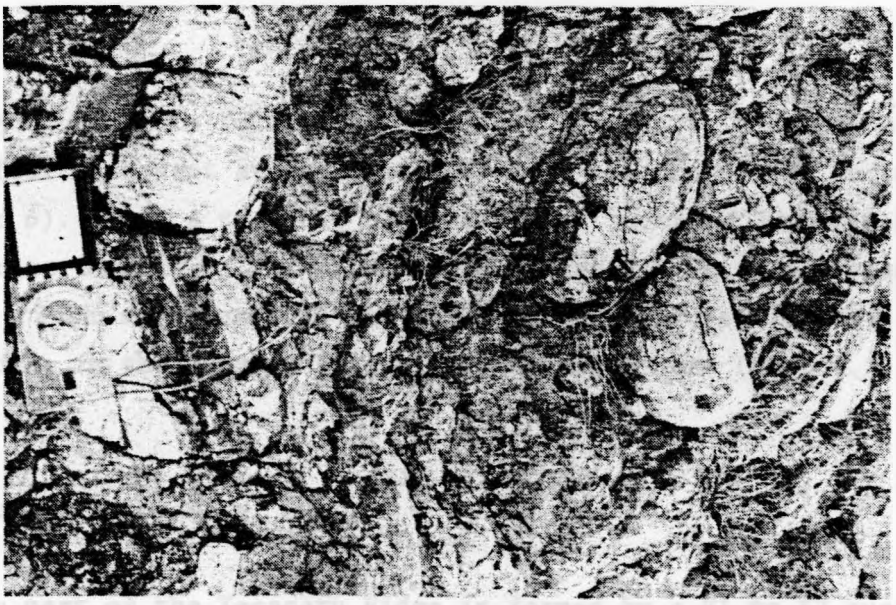


Figure 4.27. Clast supported Q-conglomerate subfacies (f5c) (Josefdal Farm)(Compass is 10cm long).

Sequence 1 is characterised by the dominance of chert grains over quartz grains in facies F2 and F3. Sequence 2 is characterised by the dominance of quartz grains in facies F4 and F5 (section 4.2). The chert/quartz dominance is generally easily identified in the field. Two exceptions were noted, one in the Josefsdal block and one in the Xecacatu block. In the Josefsdal block, the last f3d unit becomes progressively richer in quartz grains upwards, but the rock retains f3d characteristics. In the northern part part of the Xecacatu Ridge, the immature quartz-arenite has f5a and f5b characteristics but the matrix contains both chert and quartz grains in variable proportions.

These two different facies sequences could represent either lateral correlatives or two different levels in the stratigraphy. This question can be resolved by examining the relationships between the two sequences: (i) Do they occur together in any of the tectonic blocks? (ii) If so, which sequence is overlying which and what is the nature of the contact? The study of such relationships leads to the construction of a probable stratigraphy.

4.5 DEVELOPMENT OF A PROPOSED STRATIGRAPHY

In the study area, both facies sequences are frequently incomplete due to the thrust faults present at the base and/or at the top of the successions (see Chapter 6). When a tectonic block contains parts of both facies sequences, facies sequence 1 is unconformably overlain by facies sequence 2 (Fig. 4.1). Such relationships can be seen at three localities; in the Xecacatu Ridge, in the Manzima Valley and on Mendon Farm (Fig. 4.1).

The Xecacatu Ridge locality

The southern part of the Xecacatu Ridge is formed by a F1 to F3 succession (sequence 1) folded into a syncline. Further north, the syncline is formed by the folding of rocks belonging to facies F4 and F5 (sequence 2) (Fig. 4.1). The contact between the two sequences is strongly overprinted by

silica and iron metasomatism and is thus difficult to trace. However, an angular relationship between the two sequences can be distinguished. Sedimentary rocks of subfacies f5b (sequence 2) cross-cut sedimentary rocks of subfacies f1b and f1c (sequence 1). The contact is sedimentary and marked by ferruginous conglomerate lenses with clasts up to 0.5 m in diameter. The clasts comprise lithologies characteristic of f1a, f1b, f1c, and f2b subfacies (Table 4.2).

The Manzima Valley locality

In the eastern part of the Manzima Valley, (Fig. 4.1), below the Xecacatu Ridge, a small hill is formed by a syncline comprising Onverwacht sedimentary rock and rocks of subfacies f1b, f1c, f3d, f3c (sequence 1) and f5c (sequence 2) (Table 4.2). The core of the syncline is formed by f5c sedimentary rocks which cross cut sequence 1 and Onverwacht sedimentary rocks (Fig. 4.22 a,b). The contact between the two sequences is irregular as well as angular, and the f5c conglomerate has cut channels into the underlying Onverwacht and sequence 1 sedimentary rocks. The f5c conglomerate contains chert boulders up to 1m in diameter and cobbles of f3a chert-arenite. The matrix of the conglomerate is ferruginous at the contact. As can be seen in figure 4.22b, the unconformity cross-cuts both limbs of the underlying syncline but is folded itself into a syncline. This indicates that the unconformity developed after folding of sequence 1 and was then folded together with sequence 1. Similar unconformities which can be shown to be synsedimentary or intraformational have been studied in detail by Lamb (1984, in press) in Swaziland. He demonstrated that such unconformities formed during one particular deformational events.

The Mendon Farm locality

On Mendon Farm (Fig. 4.1) the base of sequence 2 cross-cuts sedimentary rocks of the Onverwacht Group and of sequence 1 (De Wit, 1983). The unconformity is present all along the base of the Dunbar block (sequence 2) but has been obscured by later activation of the contact as a fault plane and strong silica metasomatism (De Wit, pers. comm., 1983).

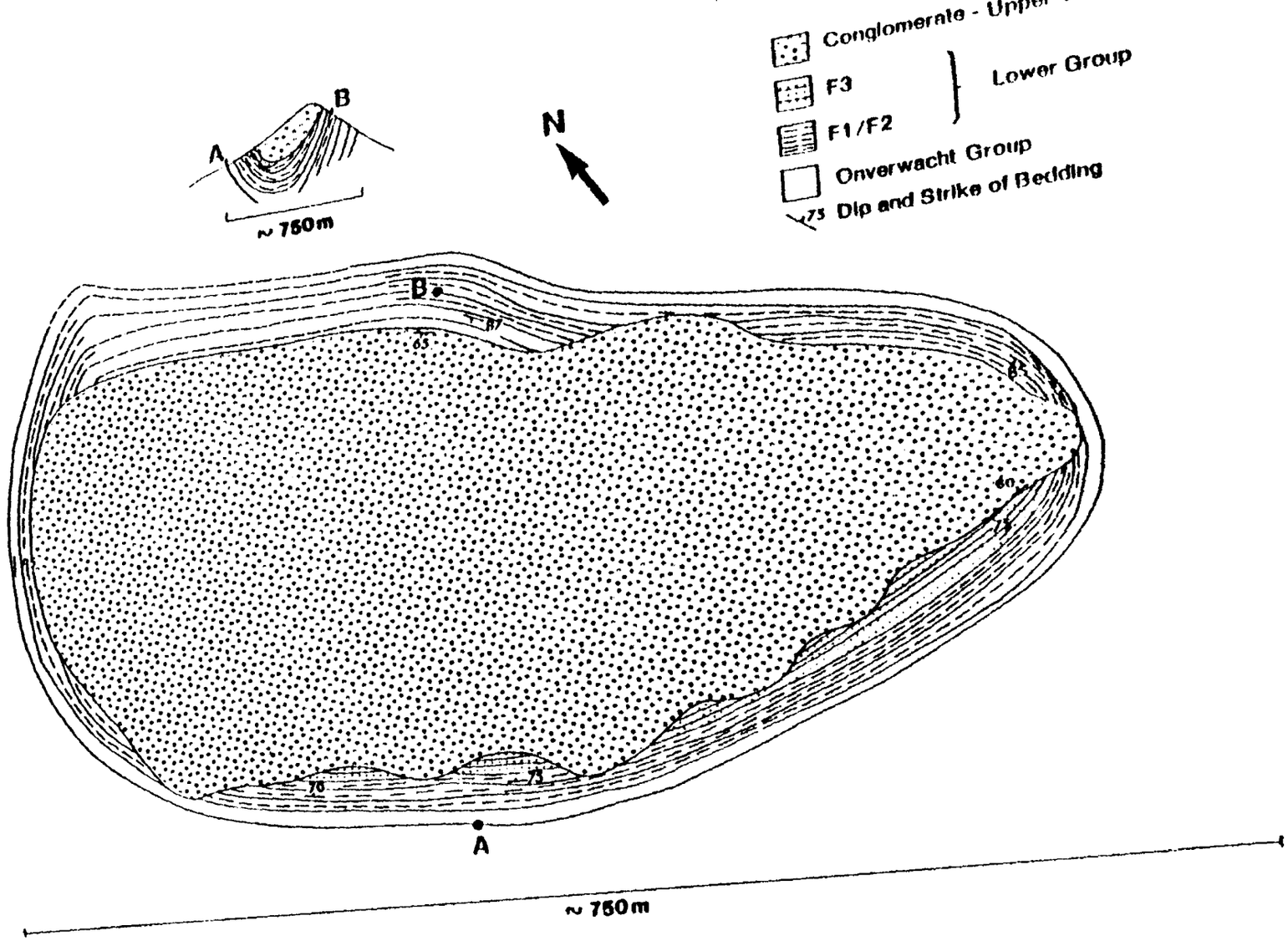


Figure 4.28. Diagram showing the Manzima Valley uncomformity.
a = plan view, b = cross section (see Fig. 4.1
for location, and Fig. 6.31).

As can be seen in figure 4.28, facies sequence 1 conformably overlies the Onverwacht Group. A similar relationship can also be observed in figure 4.1, above the T junction thrust (labelled i on Fig. 4.1) where jaspilite and ferruginous cherts conformably overlie spheroid bearing Onverwacht chert. The relationships described above together with the younging directions indicate that sequence 1 conformably overlies the Onverwacht Group and underlies stratigraphically sequence 2. An unconformity is present between the last two sequences. Thus, a stratigraphic column can be built as shown in table 4.2.

Table 4.2: Proposed stratigraphy of the sedimentary rocks in the study area.

Lithologies	Stratigraphy
Facies sequence 2	Upper Group
Facies sequence 1	Lower Group
Spheroid or lapilli bearing silicified sediments	Onverwacht Group

The Lower Group conformably overlies the Onverwacht Group and is unconformably overlain by the Upper Group. The Lower Group comprises successively facies F1, F2, and F3 in possibly several such cycles (cf Josefsdal block, Fig. 4.2). The Upper Group comprises rocks belonging to facies F4 and F5.

In thin fault bounded tectonic slices, the recognition of facies permits the allocation of the sedimentary rocks so either the Lower or the Upper Group. For example the fault bounded Elelegile Ridge (Fig. 4.1) is formed by sedimentary rocks of facies F5 and thus probably belongs to the Upper Group. The tectonic window of conglomerate in the Havelock Spruit Valley (Fig. 4.1, Chapter 6) is formed by clast supported conglomerates with a

matrix of chert grains (f3d) and is therefore probably part of the Lower Group (Table 4.2).

The variation in thickness of the Lower Group is interpreted as a result of the proximal or distal nature of the environment. In the Simbubule and Josefsdal blocks, the transition from F1 to F3 occurs over 300 and 160m respectively (Fig. 4.2) and would suggest a distal environment. In the Diepgezet block, the transition from F1 to F2 to F3 occurs over 800m while the F2 to F3 transition is 500m thick in the Emlembe block suggesting that these sequences were relatively more proximal.

In Swaziland, stratigraphic units equivalent to the Lower and Upper Groups were independently studied by Lamb (1984; in press). Correlations between the Swaziland stratigraphy and that described in this study have been established, taking the tectonic complexity into account, during a joint field investigation. The Lower Group described in this study probably corresponds to Lamb's Diepgezet Group while the Upper Group probably corresponds to his Malalotcha Group.

4.6 PALEOENVIRONMENTAL INTERPRETATION

Both groups contain sandstone and conglomerate with few intercalated thin shale units (section 4.2). The problems related to the interpretation of such Archaean sequences which can occur in deep water as well as in shallow water environments have been pointed out by Turner and Walker (1973). The approach they advocate in order to separate the different environments has been followed here: basically, three questions should be borne in mind when Archaean sandstone and conglomerate facies are being interpreted:"

1. Is the facies association with "basinal" rocks? These might be either normal turbidites, or the background sediment of the basin (pelagic shale) which would be metamorphosed in the Archaean to pyritic black or dark gray argillite.

2. Is the facies association with "shallow water" rocks? These would be identified with cross-bed sets thicker than 10-15cm, and absence of normal turbidites and argillites.

3. What is the position of the sands and conglomerates within the overall stratigraphic facies sequence? If the overall sequence can be broadly interpreted as representing transgression (deepening) or regression (shallowing), the position of the sands and conglomerates within the sequence could give an important clue as to their environment of deposition."

4.6.1 THE LOWER GROUP

The Lower Group comprises successively from bottom to top hemipelagic sedimentary rocks (F1, section 4.2.1) fine to medium grained turbidity current deposits (F2, section 4.2.4) and "coarse grained turbidites" including various types of gravity flow (F3, section 4.2.3). A gradational transition can be observed between those three facies.

Coarse turbiditic assemblages have been described in numerous submarine fans: in the Cambrian flysch of Canada (Rocheleau and Lajoie, 1974); in the Precambrian Longsford Formation of Norway (Pickering, 1983); in the Eocene Wagwater trough in Jamaica (Wescott and Ethridge, 1983); in the Drosgol formation, West Central Wales (James, 1983). The successions described in these submarine fans all bear strong similarities with the one described in the Lower Group, with a gradational transition from hemipelagic sediments to coarse grained turbidity current deposits. The Lower Group is thus interpreted as a prograding submarine fan on the following bases:

1. The "background" sedimentation is formed by iron rich sediment and mud indicative of an hemipelagic setting.

2. These fine grained sediments grade upwards into turbidity current deposits.

3. Within the jaspilites and the ferruginous cherts, the abundance of slab shaped clasts and slump folds, indicate deposition on a slope (see section 4.2.1). Brecciola deposits from submarine fans in the Troy and Hudson areas, (Friedman et al., 1982) are remarkably similar to the slab shaped clasts-bearing interbeds found in f1a and f1b subfacies (Table 4.1, Fig. 4.3). Such debris flow deposits are commonly found on both modern and ancient submarine slopes (McIlreath and James, 1979; Stanley and Kelling 1978).

4. The Lower Group forms an upward coarsening sequence similar to modern and ancient submarine fan sequences.

5. The cross-laminated sets found in the Lower Group are never thicker than 10 to 15cm which may suggest a deep water environment (Turner and Walker, 1973).

The sharp F4/F1 contact on the top of the sequence in the Josefsdal and Diepgezet blocks is interpreted as indicating the resumption of hemipelagic sedimentation due to a temporary lack of coarse sediment supply in the area. In Swaziland where the sequence of the Diepgezet block is more complete, F1 is further overlain by more coarse sediments of the F2 and F3 facies types (see also Lamb, 1984). Thus the Lower Group could have originally been composed of several stacked F1-F2-F3 cycles.

The coarse clastic sediments of the Lower Group are derived from Onverwacht and intraformationally from the sedimentary rocks.

4.6.2 THE UPPER GROUP

The Upper Group comprises sedimentary rocks of facies 4 and 5 (Table 4.1). As seen previously, facies 4 and 5 are interpreted as deposited in a high energy environment, above wave base, with intermittent subaerial exposure and quiescent periods. The palaeocurrent data is indicative of a fluvial environment while the the absence of overbank features argues against meandering rivers. A braided fluvial environment is therefore suggested

for the Upper Group. In terms of braided alluvial deposits, the following facies (Miall, 1977 a,b) are represented:

1. Gm: massive or crudely bedded gravel (subfacies f5c)

2. St: trough cross-bedded sandstone (subfacies f5 a,b)

3. Sp: planar laminated sandstone (F4)

4. Sr: ripple cross-laminated sandstone which contain a variety of asymmetric ripples with an amplitude less than 5cm (F4).

An alluvial fan environment is proposed on the following bases:

1. The Upper Group contains sedimentary structures which are common in alluvial environments.

2. Paleocurrent data from the Dunbar block (Fig. 4.28b) suggests transport directions to the south. The unimodal high variance nature of the palaeocurrent pattern, further suggests an alluvial fan environment (Miall, 1977 b).

3. The unconformity between the Lower and the Upper Group is marked by lenses of conglomerates which contain clasts of the Lower Group (see section 4.4). Basal alluvial fan deposits normally rest unconformably on bedrock and contain blocks and boulders of that bedrock, implying a local derivation. This type of basal contact is unknown in deep basin conglomerates, and is uncommon in most other fluvial conglomerates (Turner and Walker, 1973). Synsedimentary folds developed during the formation of the unconformity have been described in sedimentary rocks equivalent to the Upper Group in Swaziland (Lamb, 1984, in press). Such features are typical of alluvial fan deposits (Riba, 1976; Miall, 1977 b).

4. While the geometry of the Upper Group deposits is not known, comparison can be made with other well studied alluvial fans:

   The Van Horn sandstone alluvial fan, Texas (McGowen and Groat, 1975). This alluvial fan sequence comprises interbedded pebbly sandstones and

conglomeratic units 5 to 50m thick. The base of the sequence is formed by coarse to medium grained trough cross-bedded sandstones. Dewatering structures are typical of the braided distributary subfacies. The sequence is very similar to the Upper Group sequences (Fig. 4.2).

The Witwatersrand basin, South Africa. The upper Witwatersrand gold bearing sequences have been interpreted as braided alluvial fans (Vos, 1975; Minter, 1982). Similarities between the Witwatersrand alluvial deposits and the Upper Group sequences include: the broadly upward coarsening nature of the sequence; the presence of both mature and immature sandstones and the lack of mudstone beds (for the Upper Witwatersrand division).

5. Eriksson (1977; 1978) interpreted as alluvial fan deposits some of the Moodies Group sedimentary sequences in the northern part of the greenstone belt. Amongst the various sedimentary facies he described, lithologies characteristic of facies F4 and F5 (Table 4.1) can be recognised in his descriptions of impure sandstones, orthoquartzitic sandstones and clast supported conglomerates (Eriksson, 1978).

The Upper Group is thus interpreted as syn or post-orogenic alluvial fan deposits. Only two sequences of the upper group are present in the study areas and both are bounded by tectonic contact. Thus it is felt that detailed studies of other Upper Group successions could refine the proposed environmental interpretation by determining which sequences are more distal or proximal.

CHAPTER 5

5.0 METASOMATISM AND CHEMICAL REPLACEMENT

5.1 INTRODUCTION

Silica, iron and carbonate replacement has affected both the igneous and the sedimentary rocks in the study area. The Onverwacht igneous rocks may be replaced by silica, iron and carbonate while the Onverwacht sedimentary rocks have only been replaced by silica and carbonate (Chapters 2 and 3).

Iron and silica replacement occurs at the base of the Lower Group and some of the Lower Group conglomerates have been silicified (Chapter 4). The three types of replacement are described separately.

5.2 SILICA METASOMATISM

The following rock types have been observed in various stages of silicification: massive pillowed lavas, spinifex textured igneous rocks, pseudo pillowed igneous rocks (Chapter 2); lahars, conglomerates, sandstones, silt stones, mudstones and volcaniclastic rocks (Chapter 3,4).

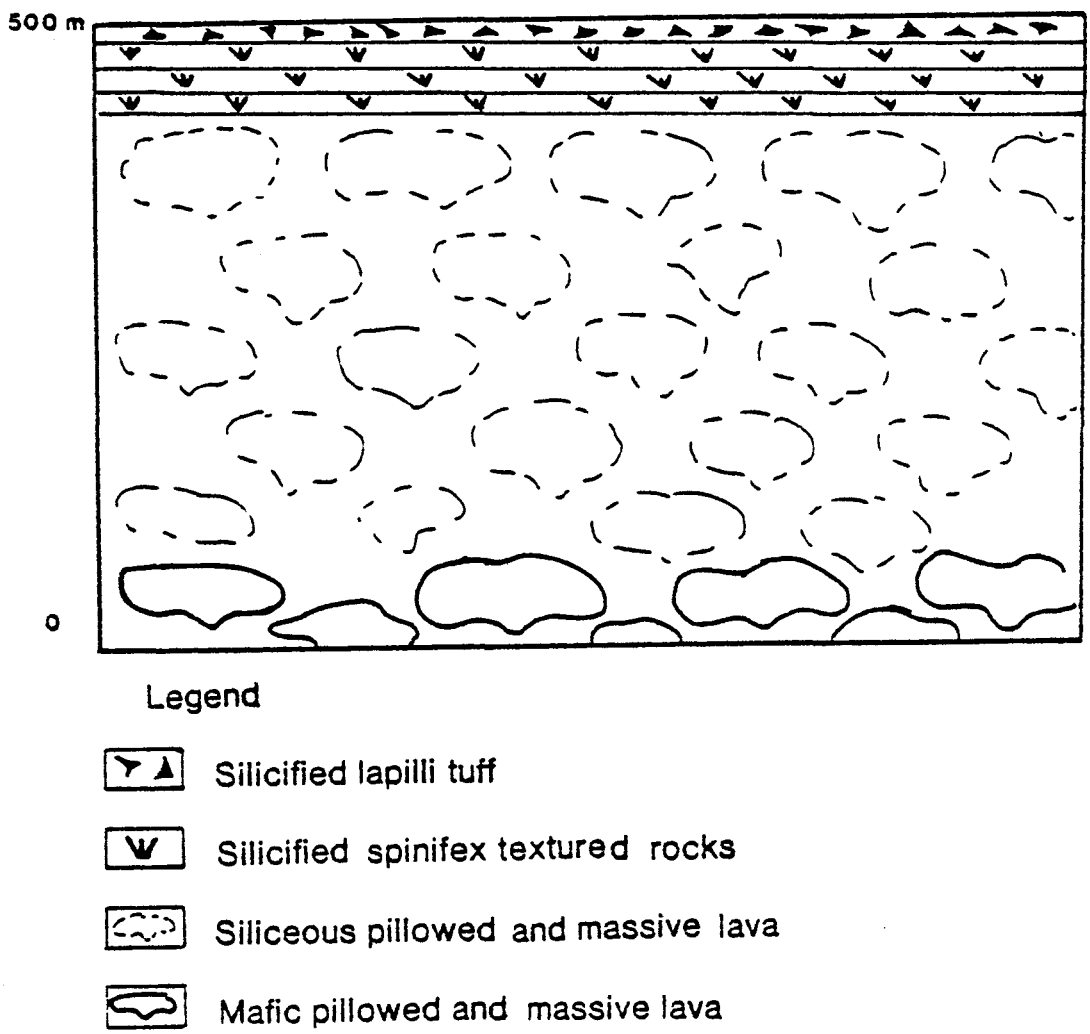


Figure 5.1. Schematic diagram showing the transition from mafic to silicified mafic lava. Josefsdal Farm.

In the igneous rocks, transitions can be seen from spinifex textured cherts to partially silicified lavas to mafic lavas. A good example of such a transition is exposed in the northern part of Josefsdal Farm (Fig. 5.1). At this locality, mafic pillow lavas grade upwards into partially silicified pillow lavas and spinifex textured fuchsitic cherts. The top of the sequence is formed by a unit of silicified lapilli tuff. Both the top and basal contacts of this sequence are truncated by thrusts. Across strike the transition from unaltered mafic to totally silicified mafic rock occurs over a distance of 500m.

The various silicified rock types occur as clasts in conglomerates of both the Upper and the Lower Group, indicating that silicification is not just a recent surface phenomenon. These observations are consistent with a silicification process which occurred early in the history of the greenstone belt. Moreover, no evidence for deformation, including compaction, is noticeable in the silicified igneous and sedimentary rocks. Approximately 80% of the Onverwacht Group is silicified, and about 30% of these rocks are now lithologically cherts (Chapter 2,3, see also Map). In the absence of clear evidence for large volume changes, such large scale silicification cannot be attributed solely to local silica remobilisation during compaction, dewatering or circulation of normal connate waters. The silica replacement is interpreted as resulting from the introduction of external silica bearing fluids into the sequence and is thus sensu stricto a metasomatic process.

5.2.1 SILICA REPLACEMENT

Two types of replacement can be distinguished in the field which hereafter will be referred to as type A and type B. In type A replacement, original structures are perfectly preserved. By contrast, such features are partially to totally obliterated in type B replacement.

(a) Type A silica replacement occurs predominantly in the Onverwacht Group and in the ferruginous shales and chert-arenites of the Lower Group. Locally, Lower Group conglomerates can also be affected by type A replacement.

The preservation of delicate primary textures such as spinifex textures and sedimentary structures and grains suggests that very fine intergranular silica replacement occurred on a molecular scale. This Archaean mode of replacement was probably analogous to Phanerozoic silicification of wood (Stein, 1982). In the silicified sedimentary rocks, microquartz replacement of a colloform silica cement, has been observed in all types of sand grade sedimentary rocks (Chapter 3,4). Therefore, silica emplacement also occurred on an inter granular scale. It is believed likely that both processes were synchronous. If such is the case, silicification took place during early diagenesis, as silica bearing fluids precipitated a colloform cement throughout the porous and permeable strata. Thus, type A replacement occurred prior to compaction and was pervasive. Spinifex textured crystals and olivine crystals are known to be rich in chrome. The fuchsitic (chrome rich) nature of the silicified spinifex textured rocks (De Wit et al., 1982) testifies that chrome was not entirely removed during this type A metasomatism. Similarly the preservation of structures such as cross-beds outlined mainly by sericite and carbon indicates that the original chemistry of the rock has been enriched in silica but that other chemical elements have not been entirely removed. Type A replacement could have been continuous throughout the stratigraphy or polyphase or inhomogeneous. The presence of silicified Lower Group shales below silicified conglomerates indicates that it was inhomogeneous while the presence of silicified clasts in conglomerates which are themselves silicified along strike suggest that it was polyphase. These observations are consistent with those described by De Wit et al. (1982 a). However, in the absence of isotope data, it is not possible to determine whether the silica bearing fluids were all derived from the same source or not.

(b) Type B silica replacement is found in the Onverwacht sedimentary rocks as well as in the fine grained ferruginous sedimentary rocks of the Lower Group; and along the unconformities between the Upper and Lower Groups (Chapter 4). This type of replacement has occurred in 50% - 60% of the cherts.

Type B replacement is best exposed along the southern part of the Xecacatu Ridge (Fig. 5.2a). At this locality, Lower Group ferruginous shales and cherts can be traced along strike into black and white banded cherts. The boundaries of this type B replacement zone are clearly visible in the landscape. This zone is 200m thick and 500m wide. Its original vertical

dimension is not known because the base is truncated by a thrust (Fig. 5.2.a,b). Three sections have been measured across the type B replaced zone and the data derived from these sections is summarised in figure 5.2.b.

The cherts in this type B replaced zone consist of alternating black and white silica bands, 1 to 10cm thick, in which no primary textures can be recognised. In thin section, the rock is entirely composed of microquartz after colloform silica.

Within these cherts, black and white silica fronts with botryoidal features are present both across and along the bedding planes (Fig. 5.3). As was first pointed out by De Wit et al. (1982 a), these silica fronts infiltrated the sediments both in an upward and downward direction. Areas up to 10cm by 20cm in which no banding can be recognised are abundant throughout the black and white chert.

On the margins of the replaced zone and within the black and white cherts, isolated patches which have only been affected by type A replacement are preserved. Such isolated areas range from 5 to 20cm wide, and have diffuse boundaries (Fig. 5.4). Colloform silica indentations clearly cross cut such preserved areas.
The presence of patches only affected by type A replacement in units affected by type B replacement and the passage along strike from type A to type B replaced zones suggest that the latter has been superimposed on type A replacement. Similar black and white banded cherts can be traced along strike into spheroid bearing cherts (locality B/7, main Map) and into lapilli bearing cherts of the Onverwacht Group (locality D-E/7-8, main Map) and into cherts with silicified spinifex textures.

When there is a lack of lateral outcrop continuity or a tectonic break, it is difficult to determine whether such B type cherts have replaced Onverwacht Group or Lower Group rocks. Such cherts have been mapped as undifferentiated (see main Map).

The more obliterative nature of type B replacement suggests that during this process, removal of original chemical elements from the sedimentary and igneous rock has reached near completion. Field data indicates that type B replacement represents a more advanced stage of silicification. This is interpreted to be due to a higher fluid/rock ratio (flux, cf Reed, 1983).



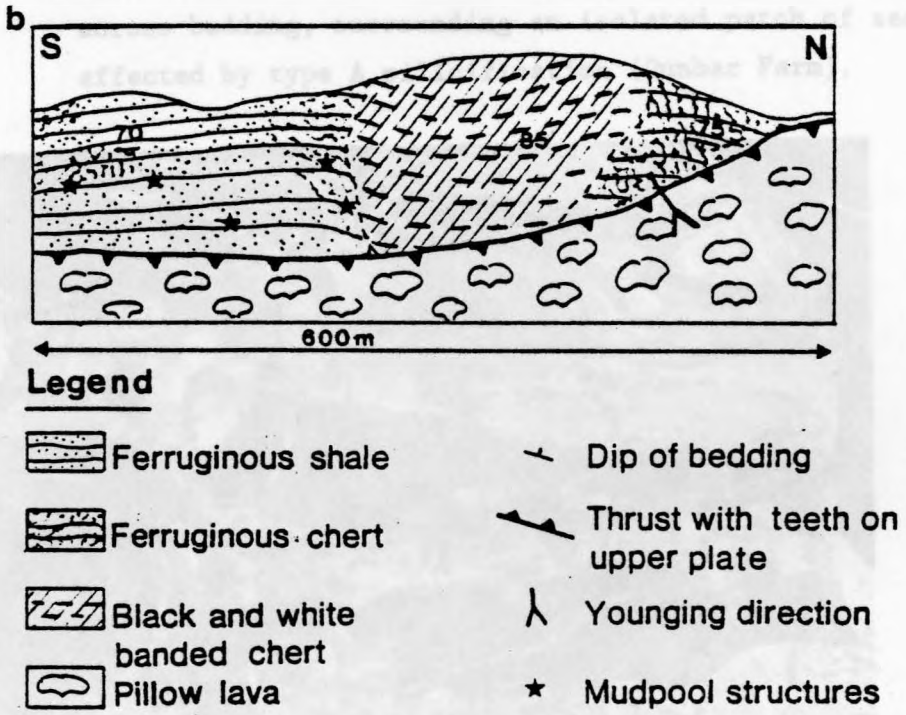


Figure 5.2.a. Large scale type B replacement visible in the landscape.
b. Panoramic sketch of the replacement zone, constructed from three measured sections.

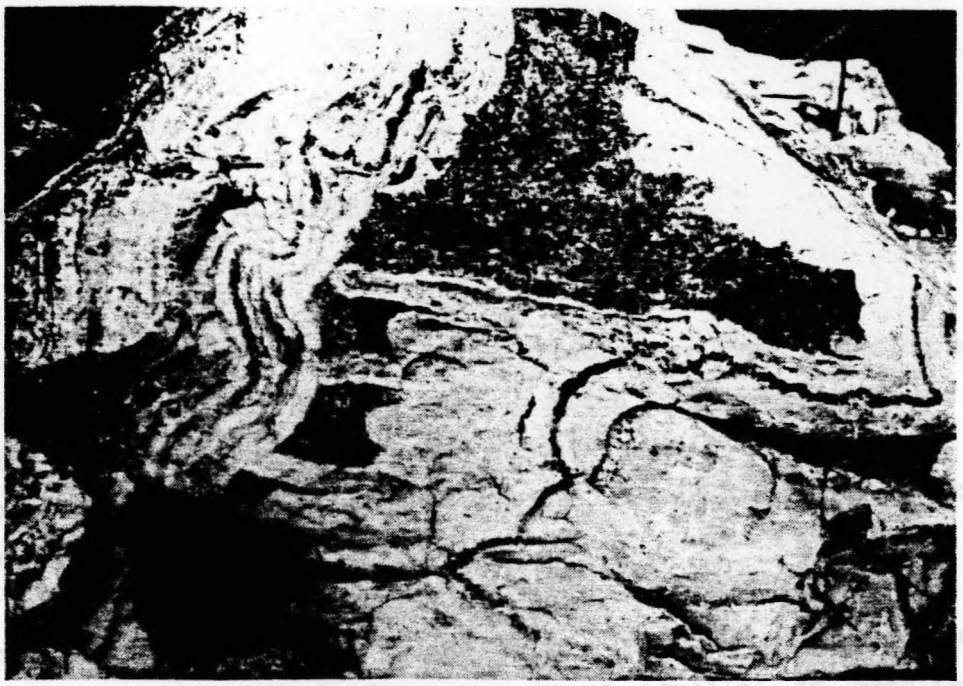


Figure 5.3. Banded black and white chert with silica front along and across bedding, surrounding an isolated patch of sediments affected by type A silicification (Dunbar Farm).



Figure 5.4. Type B silica replacement in which isolated areas affected by Type A replacement (A) are present. In the latter bedding planes can still be recognised. (Dunbar Farm).

If this interpretation is correct, these zones may indicate proximity of a fossil fluid discharge zone.

5.2.2 SILICA-FILLED FRACTURES

Silica filled fractures are found in rocks affected by type A and/or type B silica replacement. The fractures vary in width from 1mm to 10cm and can be traced for up to 1,5m both along and across strike. The fractures are filled by black or white silica and botryoidal features can be developed in the widest fractures.

The fractures occur both parallel to and at an angle to the bedding planes (Fig. 5.5, 5.6). Where such fractures occur parallel to bedding in silicified mudstones (type A replacement) they can be difficult to distinguish from sedimentary structures (Fig. 5.5).

The fractures are linked together in a complex network (Fig. 5.7). The fractured zones vary from 10cm to 100cm in width and may occupy the whole thickness of the chert unit which contain them. Original stratigraphy can generally still be reconstructed across the fractures. Similar networks also occur in the silicified igneous rocks. However, because exposure is rarely complete between silicified sediments and silicified lava, silica filled fractures have not been traced from one to the other.

Within the networks of fractures described above, the rocks become breccias. Within these breccias, the original stratigraphy cannot be reconstructed, due to rotation of the fragments (Fig. 5.7, 5.8). Brecciated zones can vary from a few centimetres to 1,5 m in size and are generally impersistent along strike. The lithology of the fragments is identical to that of the host rock (Fig. 5.7). The fragments are poorly sorted, very angular, and vary in size from 0,2 to 50cm. In the silicified sediments, the silica breccia commonly contains slab shaped fragments (long axis/short axis ratios ≥ 4). In both sedimentary and igneous rocks which have been affected by type A silicification, primary textures are preserved within the fragments.

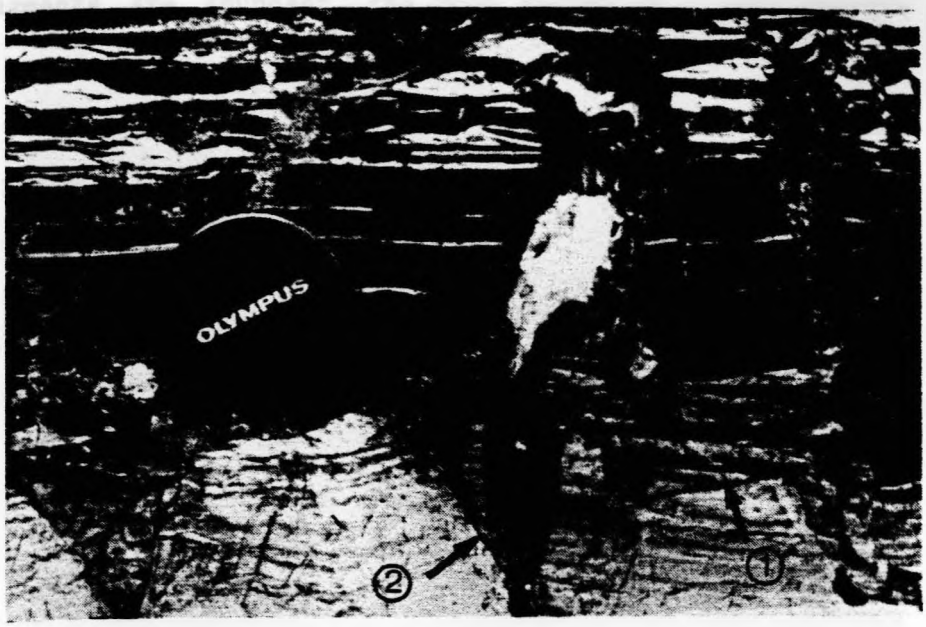


Figure 5.5. Black silica fractures, parallel (arrow 1) and perpendicular (arrow 2) to bedding in a silicified sediment. (Dunbar Farm).

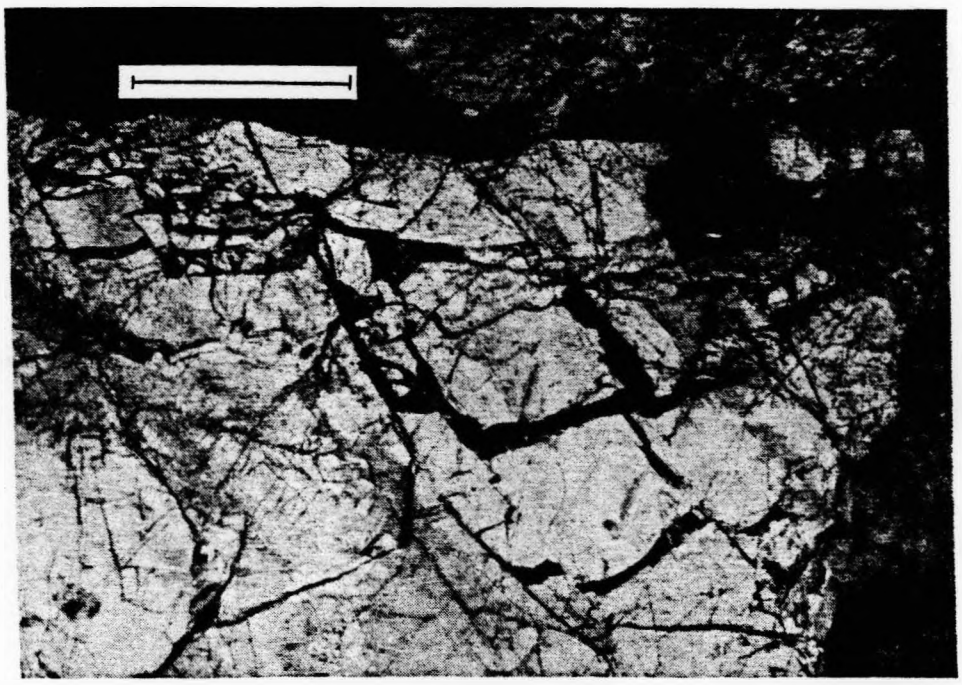


Figure 5.6. Network of silica filled veins in silicified sediments. Note the development of silica cemented breccia in the top left corner. (Josefsdal Farm). Scale bar = 10cm.

In the Onverwacht silicified sedimentary rocks, rounded fragments can be seen within the silica cemented breccias (Fig. 5.9 a,b,c,d). When the rounded fragments are abundant, the rock resembles a conglomerate (Fig. 5.10).



Figure 5.7. Silica cemented breccia in debris flow of the Hooggenoeg Formation (Diepgezet Farm). Width of field = 80 cm



Figure 5.8. Silica cemented breccia in spinifex texture bearing cherts (Diepgezet Farm).

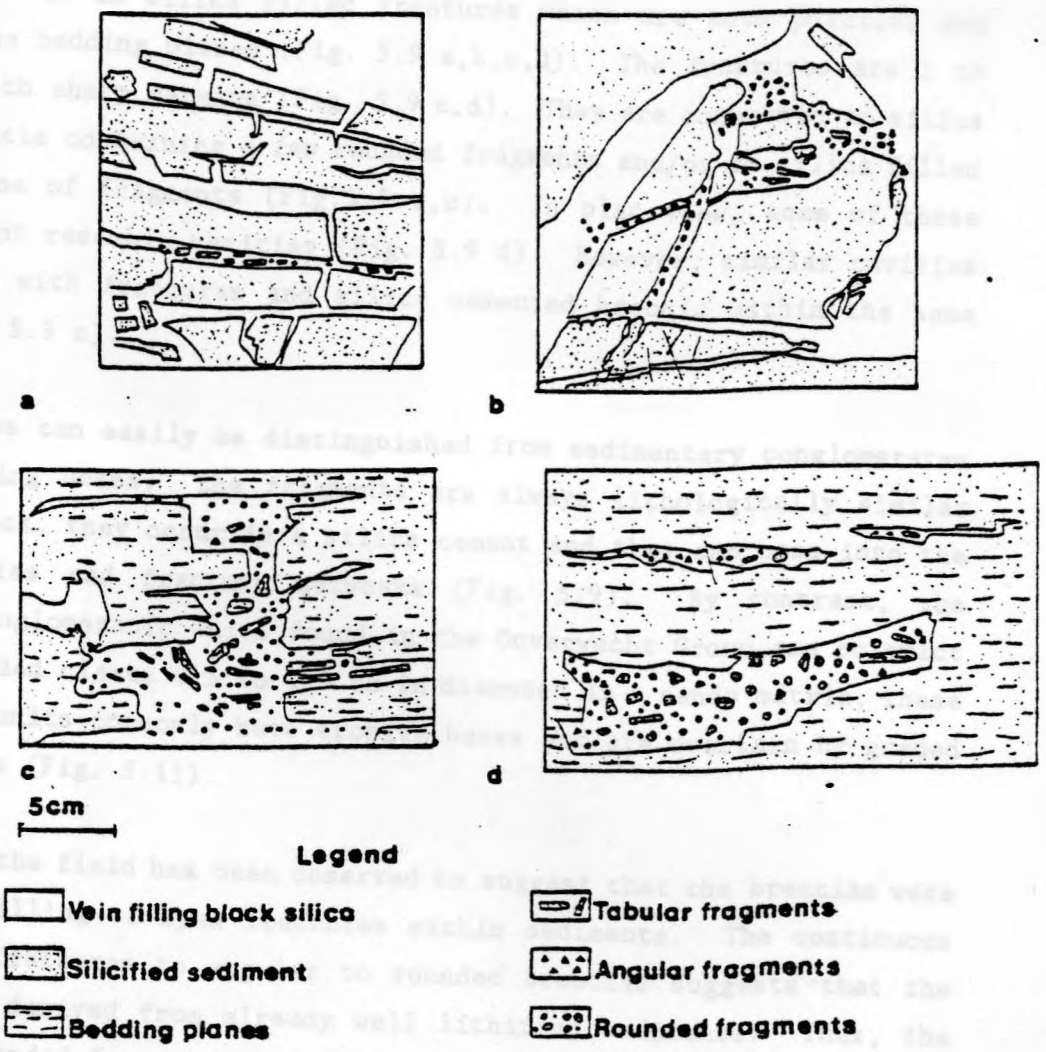


Figure 5.9. Silica cemented breccias showing the relationships between rounded and angular fragments within the silica veins. Traced from photographs. (Josefsdal Farm). a = silica filled fractures and angular fragments; b,c = development of rounded and angular fragments; d = in two dimensions, the fragments can appear to occur within lenses cross-cutting the bedding planes.

This rock type is poorly sorted and clast supported with a black silica cement, after colloform silica around the fragments. The lithology of the rounded fragments is the same as that of the host rock (Fig.5.10). These fragments are rounded to subrounded, commonly slab shaped and randomly oriented, they vary in size from 0,3 to 10cm.

Such rocks occur in silica filled fractures which are both parallel and oblique to the bedding planes (Fig. 5.9 a,b,c,d). The fractures are 2 to 50cm wide, with sharp margins (Fig. 5.9 c,d). They are connected to silica cemented breccia containing a few rounded fragments and/or to silica filled fractures free of fragments (Fig.5.9 a,b). In plan view, some of these fractures might resemble cavities (Fig. 5.9 d). However, similar cavities are connected with fractures and silica cemented breccia within the same outcrop (Fig. 5.9 c).

Such rock types can easily be distinguished from sedimentary conglomerates on the following bases: the fragments are always lithologically similar to the host rock, they occur in a silica cement and they can pass into the angular breccias and fracture networks (Fig. 5.9). By contrast, the sedimentary conglomeratic units found in the Onverwacht Group are polymict with well rounded clasts 0,5 to 1,5 cm in diameter in a sandy matrix, these conglomeratic units commonly have erosive bases and are overlain by graded sandstone units (Fig. 5.11).

No evidence in the field has been observed to suggest that the breccias were derived by infilling of open fractures within sediments. The continuous spectrum from fractures to angular to rounded breccias suggests that the fragments were derived from already well lithified sediments. Thus, the formation of rounded fragments is directly related to a fracturing mechanism and interaction with silica bearing fluids.

The features described above are similar to those believed to have formed by hydraulic fracturing (Phillips, 1972; Gibson and Watkinson, 1979; Nairn and Wiradiradja, 1980; Gibson et al., 1983) and the rock structures described above are similarly interpreted. Accordingly, the following chronology and mechanism is proposed to account for the formation of such breccia and fracture zones:

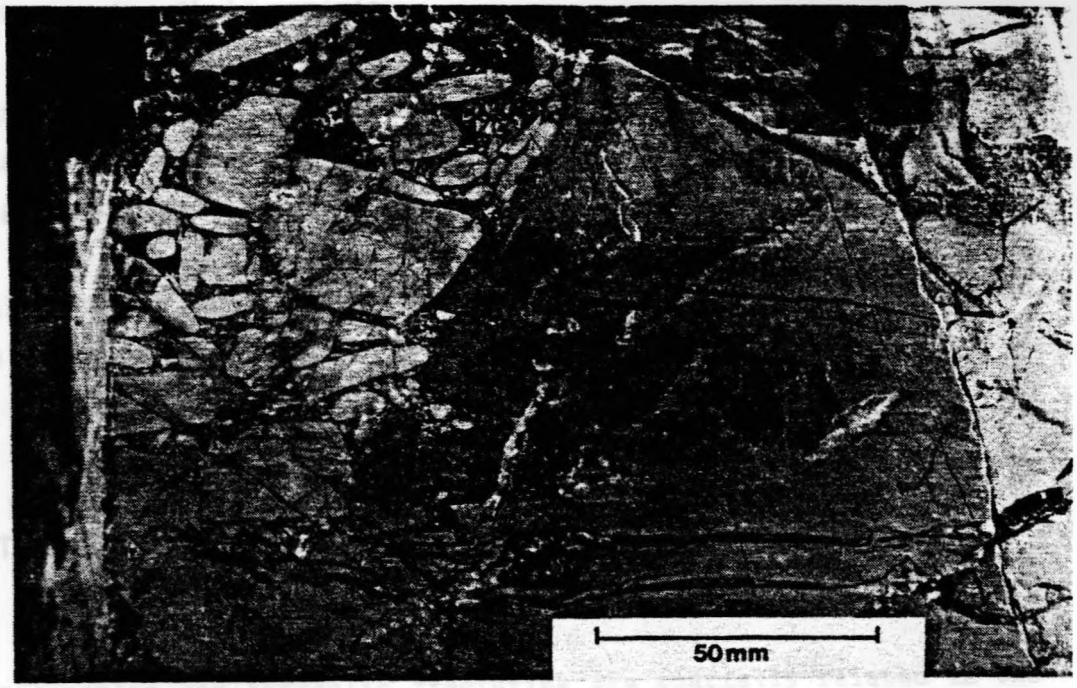


Figure 5.10. Silica cemented breccia with rounded clasts interpreted as hydraulic breccia. (Rosentuin Farm).



Figure 5.11. A sedimentary conglomerate unit in the Onverwacht sedimentary rocks (Granville Grove Farm).(contrast with fig. 5. 10)

1. Silicified igneous and sedimentary rocks fractured by brittle failure under increasing fluid activity.

2. Fracture propagation ahead of the advancing fluid caused the rock to burst apart and form angular breccias. On a large scale, collapse or stoping might have also occurred.

3. Initially, fluid flux passing through the brecciated zone would be high enough to cause the fragments to be rounded by fluid erosion.

5.2.3 INTERPRETATION

Silica metasomatism and hydraulic fracturing are spatially related in the map area. From the field observations described previously, in one outcrop the following chronology, shown in figure 5.12, can be envisaged.

1. Deposition of the sediments above an igneous pile.

2. Introduction of silica rich fluids into the unlithified sediments and the porous igneous rocks (Fig. 5.12a) caused differential silicification of the rocks and the formation of a silica cement in the sediments (type A replacement). Locally, in fluid discharge zones, fluid/rock ratios were very high (type B replacement).

3. The silicified sediments and lavas fractured by brittle failure under fluid pressures (fig. 5.12.b) Hydraulic breccias were developed (Fig. 5.12.c).

On a larger scale, it is believed that the above stages are part of an evolutionary process, as illustrated in figure 5.12. The fluids reached non-silicified porous and permeable areas through fractures developed in the silicified zones (Fig. 5.12.b).

Stage 2 probably occurred during early diagenesis. The hydraulic fracturing could be due to a later introduction of silica bearing fluids or be part of the same continuous process. Some observations suggest that all three

stages may have been in fact contemporaneous and part of the same event (Stanistreet et al., 1981, Fig. 4; De Wit et al., 1982 a, Fig. 5; this study, Fig. 5.13). As can be seen in these figures, individual spheroids have moved within silica filled fractures developed in lithified sedimentary rocks. Such features indicate that while cracks were developed in lithified, presumably silicified, sediments, the overlying unit was not yet lithified, thus allowing individual grains to move separately. Both units are now silicified.

These observations indicate that both fracturing and silicification occurred while the sediments were not totally lithified and perhaps while sedimentation was still taking place. Silica metasomatism continued in a polyphase and inhomogeneous manner throughout the stratigraphy.

5.3 THE IRON METASOMATISM

Iron oxides (hematite and magnetite) as well as iron hydroxides (geothite and limonite) are common in the following rock types: variolitic lavas; silicified lavas; jaspilite; ferruginous cherts; shale and tuff; and ferruginous chert-arenite (Chapter 2,4). Ferruginous breccias and iron enrichment is found along shear zones (Chapter 6) and along the unconformity between the Lower and Upper Groups (Chapter 4).

It is not known to what extent the iron content in the sedimentary rocks is due to (i) sedimentary deposition of iron (chemical or detrital) (ii) Archaean replacement or (iii) supergenic enrichment. However, the following observations can be made which suggest that metasomatic emplacement of iron, during silicification, has been of major importance.

1. Gradational contacts between jaspilite and all types of fine grained ferruginous sediments are ubiquitous (Chapter 4). In the field, it is difficult to determine exactly where the change from ferruginous shales or cherts to jaspilite is taking place.

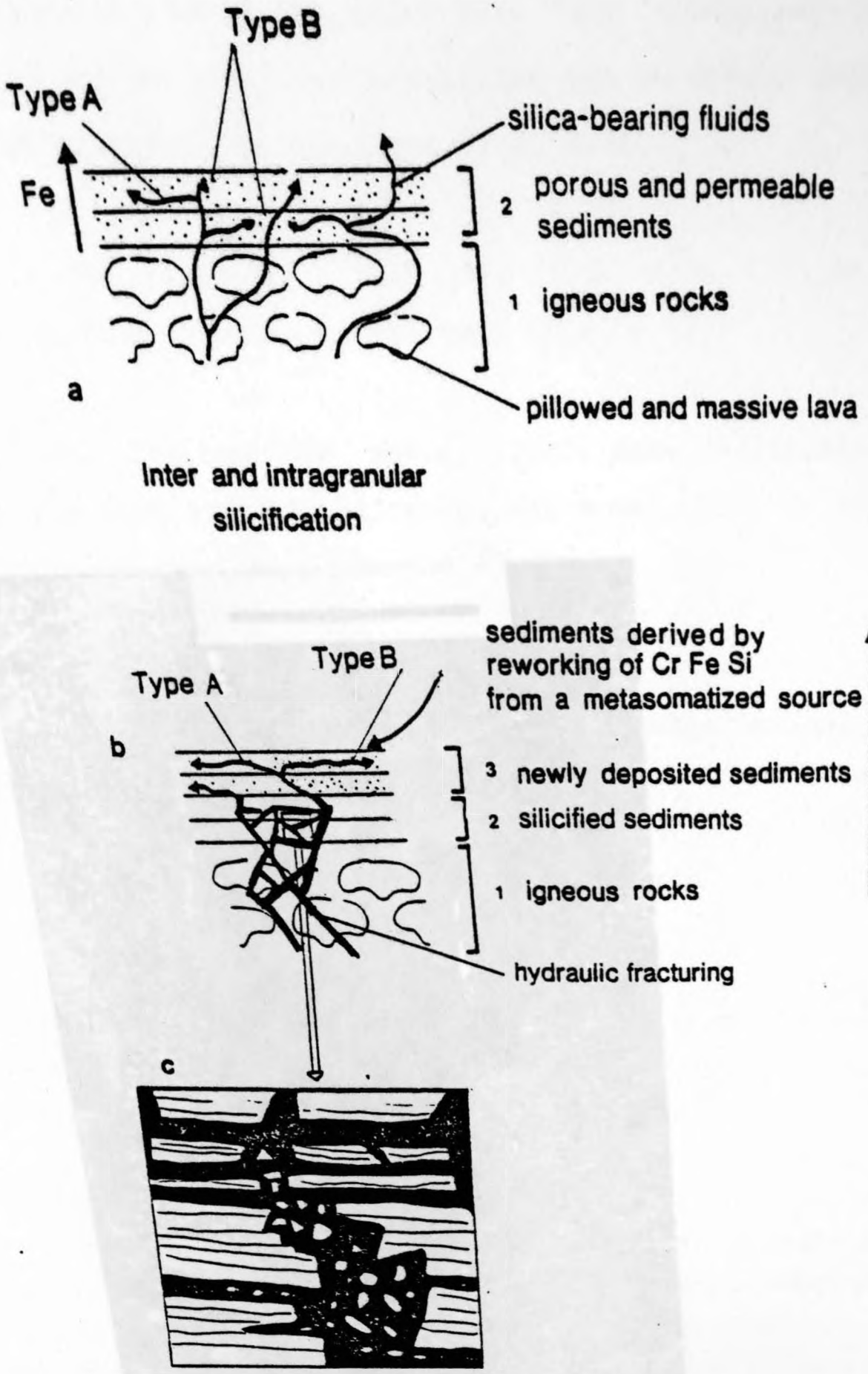


Figure 5.12. Proposed model for the silicification of the upper part of the Onverwacht Group. a = silicification of porous and permeable lavas and sediments; b = hydraulic fracturing of a silicified cap rock; c = development of hydraulic breccia. No scale is given because the features described can be observed at all scales from microscopic observation to outcrop scale.

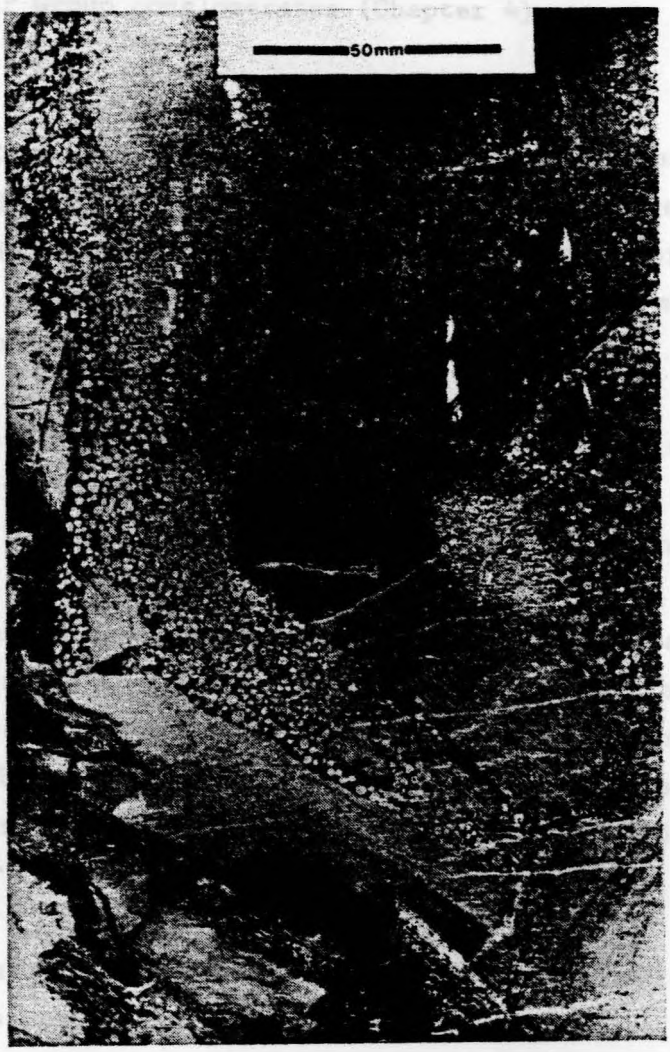


Figure 5.13. Individual spheroids within silica filled fractures developed in silicified sedimentary rocks. Specimen courtesy of M. de Wit (Hooggenoeg Farm).

2. Clastic textures and shard shaped fragments have been recognised in several jaspilite units and an irregular transition can be traced from ferruginous tuffaceous siltstone to jaspilite (Fig. 5.14).

3. Graded units can still be recognised within jaspilitic units with angular jasper clasts forming the base of the unit (Fig. 4.4).

4. Clasts of jaspilite, ferruginous shale, tuffaceous siltstone, ferruginous chert and iron enriched siltstone are common both in the Lower and Upper Group conglomerates (Chapter 4).

These features suggest that such rocks were originally clastic sediments which have been replaced by iron and silica and that supergene replacement is not a dominant process in the study area. The presence of jasper clasts within jaspilitic graded units suggest that some jasper must have been formed during or prior to the deposition of the Lower Group.

In silicified Lower Group conglomerates, clasts of jaspilite can be partially destroyed by type B silica replacement, indicating that iron and silica replacement locally predated type B silica replacement.

The presence of hemipelagic ferruginous sedimentary rocks at the base of the Lower Group (Chapter 4) suggest that exhalative fluids precipitated iron at the sea water/sediment interface (Fig. 5.12.b). The replacement of clastic sediments by iron and silica could be due to further fluid circulation through the sediments which were derived from the exhalative chemical deposits.

The absence of iron in the Onverwacht sedimentary rocks indicates that the iron bearing fluids post dated or were ahead of early silica bearing fluids (see also De Wit et al., 1982 a). Field data do not permit to distinguish between the two possibilities and both probably occurred.

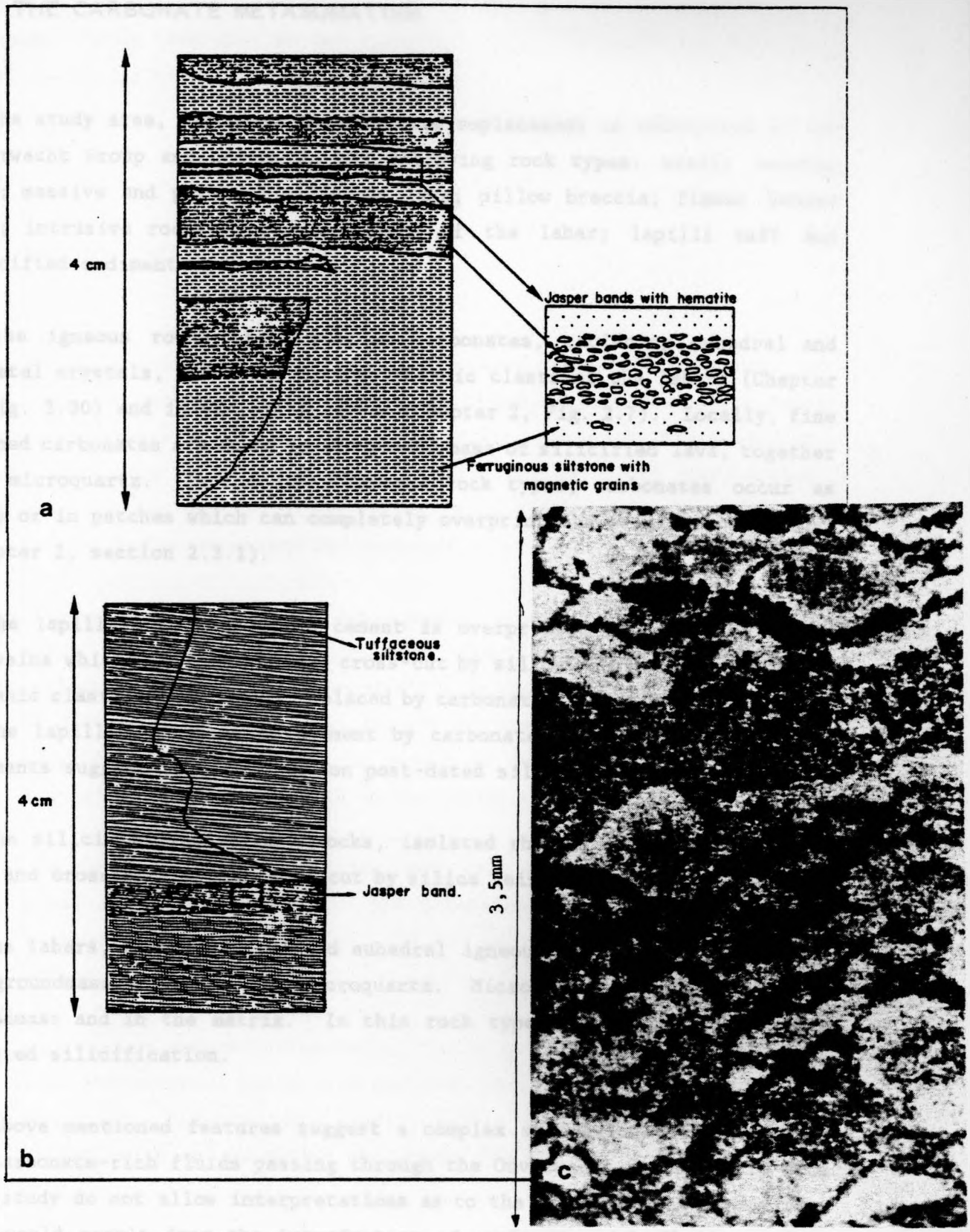


Figure 5.14. a,b Diagrams drawn from thin sections showing the transition from jasper beds to tuffaceous silstone. c = Photomicrograph of a jasper unit. (Josefsdal Farm).

5.4 THE CARBONATE METASOMATISM

In the study area, carbonate metasomatism replacement is restricted to the Onverwacht Group and occurs in the following rock types: ocelli bearing lava; massive and pillowed siliceous lava; pillow breccia; flaser banded rock; intrusive rocks; volcanic clasts of the lahar; lapilli tuff and silicified sedimentary rocks.

In the igneous rocks, fine grained carbonates, replacing euhedral and skeletal crystals, are found in the volcanic clasts of the lahars (Chapter 3, Fig. 3.30) and in variolitic lavas (Chapter 2, Fig. 2.7). Locally, fine grained carbonates are found in the ground mass of silicified lava, together with microquartz. In the other igneous rock types, carbonates occur as veins or in patches which can completely overprint the original mineralogy (Chapter 2, section 2.3.1).

In the lapilli tuff the silica cement is overprinted by carbonate rhombs and veins which cross-cut or are cross-cut by silica veins. The silicified volcanic clasts are partially replaced by carbonates (Chapter 3, Fig. 3.15). In the lapilli tuff the replacement by carbonates of silicified volcanic fragments suggest that carbonation post-dated silicification.

In the silicified sedimentary rocks, isolated rhombs occur throughout the rock and cross-cut or are cross-cut by silica veins (Chapter 3. Fig. 3.23).

In the lahars, carbonate replaced euhedral igneous crystals and occurs in the groundmass together with microquartz. Microquartz only occurs in the groundmass and in the matrix. In this rock type, carbonation could have predated silicification.

The above mentioned features suggest a complex succession of silica-rich and carbonate-rich fluids passing through the Onverwacht Group. Data from this study do not allow interpretations as to the origin of the carbonates. They could result from the introduction of carbonate-rich fluids or from remobilisation of primary carbonates.

Preliminary oxygen isotope studies studies indicate that carbonates of the Onverwacht Group are not of an igneous origin and were derived from exhalative fluids (Hughes, 1983).

5.5 SUMMARY AND DISCUSSION

The metasomatic features described above suggest important ingresses of silica, iron and carbonate by circulation of fluids through the stratigraphy recognised in the field area. Intra and inter-granular diffusion and hydraulic fracturing were the dominant mechanisms of fluid penetration. Silica metasomatism was initiated during early diagenesis. Zones of high fluid/rock ratio are recognised and interpreted as areas of fluid discharge.

The abundance of volcaniclastic and igneous products in the Onverwacht Group, which is generally interpreted as oceanic crust, (Anhaeusser, 1973 and others) suggest that mafic igneous activity could have provided the heat necessary for such fluid movements (De Wit and Stern, 1980). These workers interpreted the metasomatism as the result of hydrothermalism. This is compatible with field observations in the study area.

Several authors have also pointed out the similarities between the hydrothermal alteration present in the greenstone belt and that found around present day spreading ridges (De Wit et al., 1979; 1982 b; Barton 1982; Büttner, in prep).

It is known that in modern environments, fluids in the discharge zones along MOR's (e.g. hydrothermal vents) are enriched in silica (Hutchinson et al., 1980; Hart et al., 1974; Hart and De Wit, 1984). Below this zone, is a zone of silica depletion and magnesium enrichment (De Wit et al., 1982 b; Mottl, 1983).

If such a model is correct, silica was partially derived from the mafic and ultramafic Onverwacht rocks, during the hydrothermal circulation of sea water through the hot igneous pile (De Wit et al., 1979; 1982 b; Reed, 1983; Hart and De Wit, 1984).

The iron bearing fluids could have been derived from the iron-rich sediments of the Lower Group (section 5.3) as well as from the underlying volcanic pile (Bonatti et al., 1972 a,b; Bonatti, 1975). As was pointed out by Corliss et al. (1979) for sea floor hemipelagic sediments, it is difficult to establish the respective contribution of each possible source.

The abundance of Cr rich fuchsite in the silicified Onverwacht sedimentary rocks and its absence in the discharge zone (section 5.2.1) suggests that even chrome was mobile during extreme hydrothermal activity. As no detrital chromite has been observed in the Onverwacht sedimentary rocks, the chrome must also have been derived from the underlying ultramafic rocks by fluid activity. Similarly, Mg has also been totally removed in these discharge zones.

Serpentinite lenses below the silicified igneous rocks at Dunbar and Msauli indicated an Mg rich zone, possibly supporting the model for Mg enrichment beneath the discharge zone (see main Map).

In the study area, carbonate and silica replacement affected both relatively deep and shallow water sediments (Chapter 3,4). The evidence of subaerial volcanism during deposition of the Onverwacht sedimentary rocks (Chapter 3) and the alteration of both deep water and shallow sediments suggest that both subaqueous and subaerial hydrothermal systems were operative. In the Barberton greenstone belt, the presence of subaerial hydrothermal systems has been suggested by De Wit et al. (1982). If hydrothermal alteration was related to an oceanic spreading centre (De Wit et al., 1979; 1982 b; Barton, 1982; Büttner, 1983), then a situation must be envisaged in which volcanic islands are located along the spreading centre in order to account for the sedimentological evidence. Although a spreading ridge type of hydrothermal system seems to be most likely, the absence of geochemical and O^{18} isotopic data related to the alteration events in the study area does not allow further speculation.

CHAPTER 6

6.0 STRUCTURAL GEOLOGY

6.1 INTRODUCTION

The dominant topographic features of the map area are NE/SW trending ridges formed by Upper and Lower Group material (Fig. 6.1). Within these ridges, NE/SW oriented folds are developed which have been refolded in places (Fig. 6.2). From west to east, the following structural units have been distinguished amongst these ridges: the Sigadeni Tectonic Complex (Unit 1); the Waterfall Synclinorium (Unit 3); the Xecacatu Syncline (Unit 5); the Emlembe Syncline (Unit 7); the Simbubule Syncline (Unit 9); and the Makonjwa Tectonic Complex (Unit 12) (Fig. 6.2). These units are separated by Onverwacht Group material in which NE/SW and E/W oriented folds are developed.

Field evidence suggests that four periods of deformation have affected the rocks in the study area. The principal characteristics of each phase of deformation are summarised in table 6.2 while the symbols and abbreviations used in this chapter are listed on table 6.1. Figure 6.1 indicates the location of the various maps presented in this chapter.

The earliest phase of deformation recognised in the area (D1) only affected the Onverwacht Group and the base of the Lower Group (Table 6.1) and resulted in tectonic repetition of cherts and lavas.

The second phase of deformation (D2) led to the development of the dominant structural trend in this part of the belt. It is marked by NE/SW trending tight to isoclinal folds and by thrusts (Fig. 6.2) and is accompanied by the formation of a week axial planar cleavage in ferruginous shales of the Lower Group.

The third phase of deformation (D3) is manifested by open folds and the local development of an axial planar cleavage in Lower Group ferruginous sedimentary rocks and Onverwacht mafic lavas. D3 folds have a broad E/W orientation and E/W trending faults are commonly developed on the limbs of the folds.

NNW/SSE and N/S oriented normal faults (D4) represent the last phase of deformation recognised in the study area.

Each period of deformation will be discussed separately, and in chronological order. Small scale structures are described from restricted and well exposed regions, and then the structures are related to structures mapped over the entire study area. A kinematic interpretation is discussed at the end of this chapter and finally, restoration of a pre-D2 section is attempted which allows an estimate of the minimum amount of shortening across the area to be calculated.

6.2 THE FIRST PHASE OF DEFORMATION: D1

D1 is a phase of thrusting and folding during which the Onverwacht rocks and the basal 5 to 50m of the Lower Group, have been tectonically repeated forming <ONV> tectonic units (Table 6.1). In the field, D1 can be identified by the development of flaser banded rocks, by the repetition of lithological units and by the presence of overturned units of Onverwacht and basal Lower Group material.

As discussed in Chapter 2, the flaser banded rocks represent tectonites which can vary from a cataclasite to a mylonite (Fig. 2. 19,20,21). The

Table 6.1. List of abbreviations and symbols

Upper Group	UG
Lower Group	LG
Onverwacht Group + base of Lower Group (5 to 50m)	ONV
Tectonic unit (numbered from 1 to 12)	< >
Phase of deformation	Dn
folding related to Dn	fn
low angle reverse fault and listric reverse fault or thrust (Ramsay, 1967; McClay, 1981) related to Dn	tn
high angle normal fault related to Dn	ftn
schistosity developed during Dn	Sn

Table 6.2. Résumé of the deformational events in the study area

		Stratigraphy	Tectonic	Tectonic
	Structures	Involved	Trend	Transport
D1	Thrusts (t1)	ONV + LG	E - W	N? S?
	recumbent folds (f1)	ONV + LG	E - W	
D2	Thrusts (t2)	ONV + LG + UG	ENE - WSW	NW
	isoclimal folds (f2)	ONV + LG + UG	N - S to ENE - WSW	
D3	open folds (f3)	ONV + LG + UG	E - W to ENE - WNW	
	faults (ft3)	ONV + LG + UG	E - W	
D4	faults (ft4)	ONV + LG + UG	NNW - SSW to N - S	

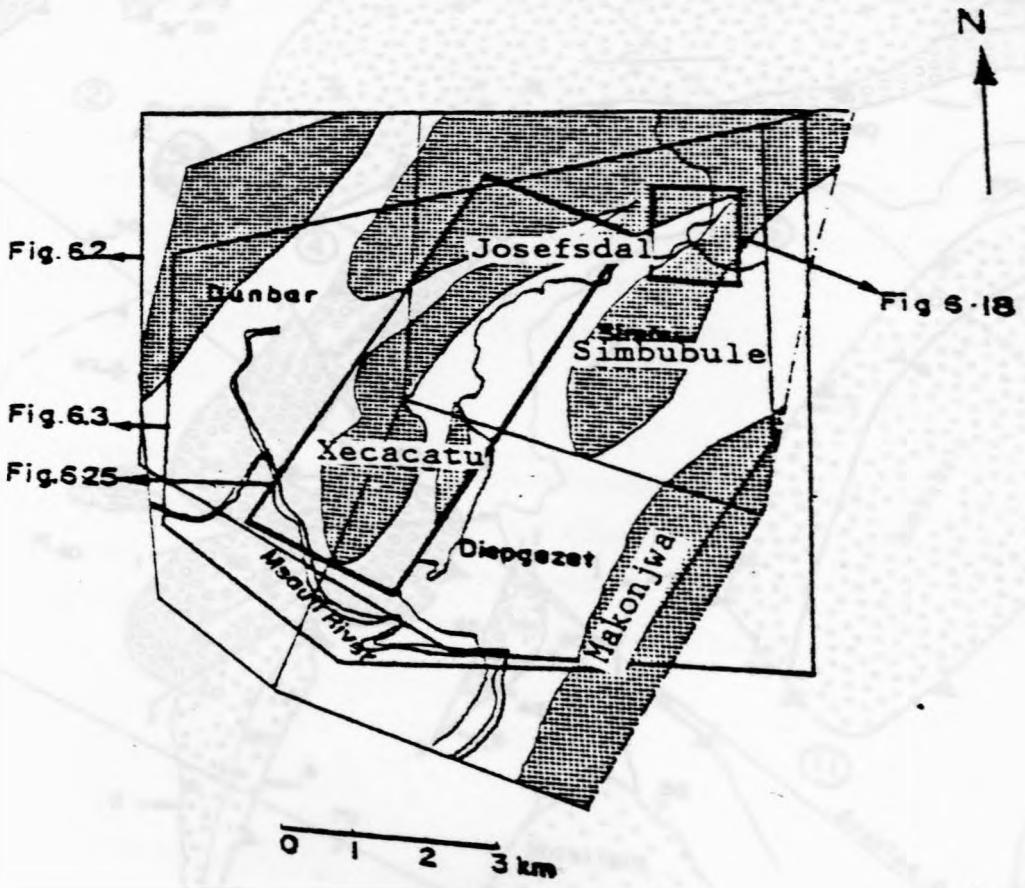


Figure 6.1. Locality map showing the location of the geological maps presented in Chapter 6 .

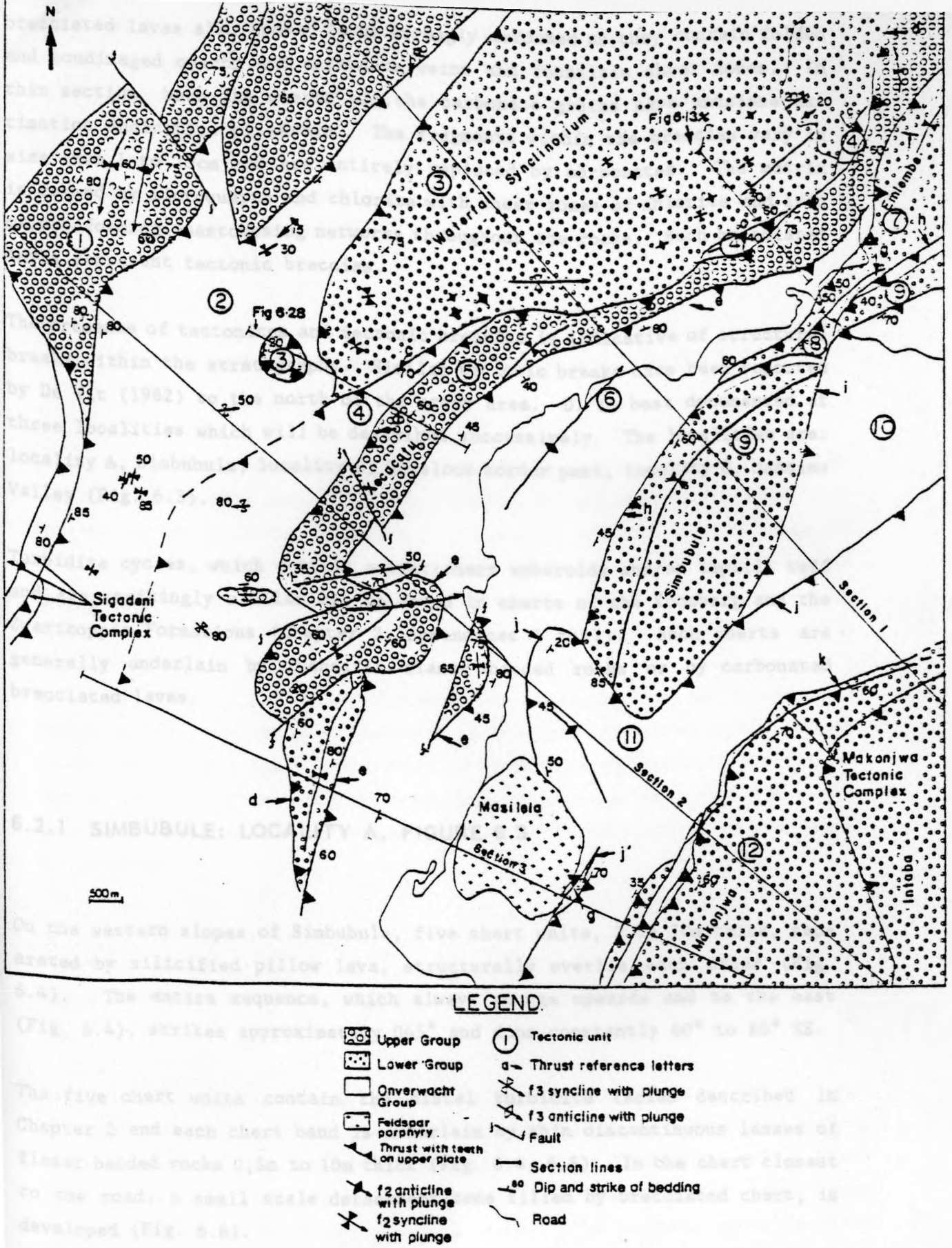


Figure 6.2. Simplified geological map of the study area showing the D2 tectonic units. The tectonic units are numbered and the thrusts are given letters. See figure 6.1 for location.

brecciated lavas also appear to be strongly deformed as they contain folded and boudinaged quartz and carbonate veins and fuchsitic shear zones. In thin section, both the quartz and the carbonate grains have undulose extinction indicative of strain. The fragments within the breccias vary in size from 1 to 15cm and are entirely replaced by carbonates. The matrix is formed by microquartz and chlorite with shear zones of chlorite and iron oxides forming anastomosing networks throughout the rocks. Such brecciated lavas represent tectonic breccias.

The presence of tectonites and tectonic breccias is indicative of structural breaks within the stratigraphy. Similar tectonic breaks have been reported by De Wit (1982) to the north of the study area. D1 is best documented at three localities which will be described successively. The localities are: locality A, Simbubule; locality B, Havelock border post; locality C, Manzima Valley (Fig. 6.3).

Turbidite cycles, which contain accretionary spheroids and/or lapilli tuff and are strikingly similar can be found in cherts of the Kromberg and the Zwartkoppie Formations (Chapter 2, Appendices 1 to 7). Such cherts are generally underlain by fuchsitic flaser banded rocks or by carbonated brecciated lavas.

6.2.1 SIMBUBULE: LOCALITY A, FIGURE 6.3

On the western slopes of Simbubule, five chert units, 2 to 50m thick, separated by silicified pillow lava, structurally overlie each other (Fig. 6.4). The entire sequence, which always youngs upwards and to the east (Fig. 6.4), strikes approximately 045° and dips constantly 60° to 80° SE.

The five chert units contain the distal turbidite facies described in Chapter 2 and each chert band is underlain by thin discontinuous lenses of flaser banded rocks 0,5m to 10m thick (Fig. 6.4, 6.5). In the chert closest to the road, a small scale detachment zone filled by brecciated chert, is developed (Fig. 6.6).

As discussed previously, the presence of flaser banded rocks below each of the cherts implies the existence of structural contacts between the various units. This fact, coupled with the sedimentological and lithological repetitions, suggest that the succession is the result of tectonic repetition. The D1 tectono-stratigraphy is further folded into a D2 neutral anticlinal fold and it is therefore not possible to determine whether it was upward or downward facing prior to D2.

6.2.2 THE BORDER POST AREA: LOCALITY B IN FIGURE 6.3

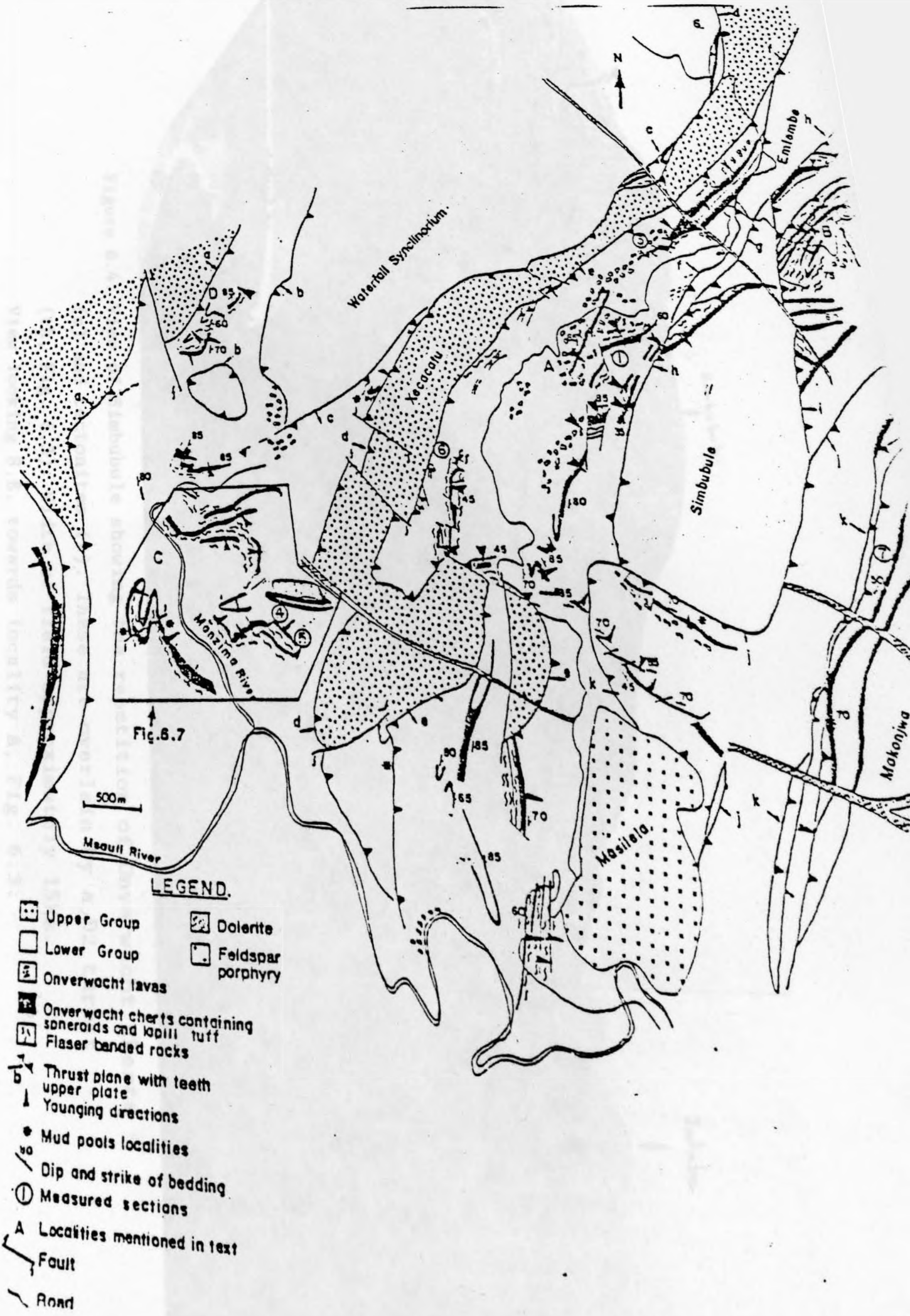
In the hills above the road leading from Barberton to Havelock, 1km from the Swaziland border post, four chert units, separated by silicified lavas and varying in thickness from 5 to 15 m, overlie each other. The units are overturned, facing to the west, while steeply dipping to the east. All four cherts contain proximal facies Bouma sequences (Chapter 3) and are structurally overlain by 10m to 20 m thick units of flaser banded rocks.

As at locality A (Fig. 6.3), the presence of tectonites in between the cherts and the occurrence of identical sedimentary structures in the various chert layer is similarly interpreted as indicative of tectonic repetition. Due to the lack of outcrop in Swaziland, it has not been possible to determine if the overturning is due to D1 or to the presence of an overturned D2 antiform.

6.2.3 THE MANZIMA VALLEY: LOCALITY C IN FIGURE 6.3

In the Southern part of the Manzima Valley, eight separate chert units contain proximal turbidite sequences and are underlain and/or overlain by flaser banded rocks or brecciated lavas 10 to 100 m thick (Fig. 6.7). These are all folded, indicating the presence of a structurally complicated stratigraphy prior to D2 folding (Fig. 6.4a). The tectonic units can vary from 50 to 150 m in thickness.

Figure 6.3. Simplified geological map showing the repetition of the Onverwacht silicified sedimentary rocks in the study area. (Location on Fig.6.1.)



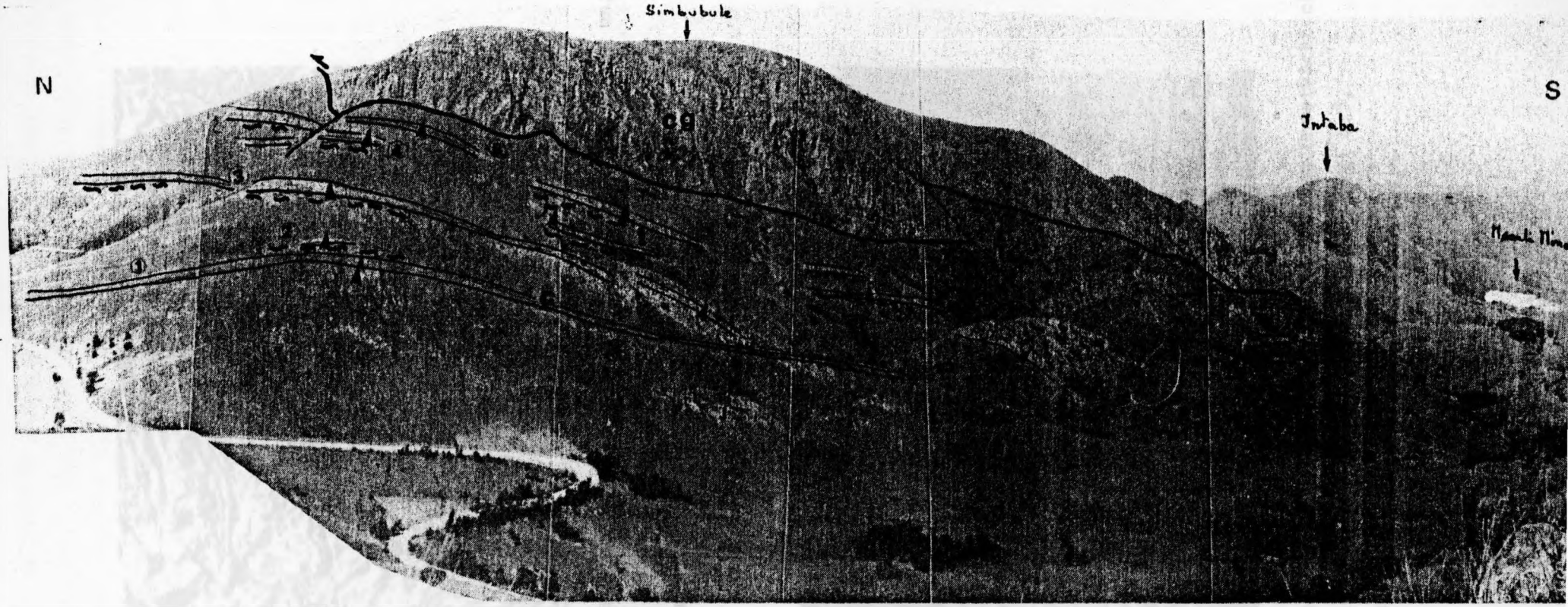


Figure 6.4. View of Simbubule showing the repetition of Onverwacht cherts (c) and tectonites (t). These are overlain by a D2 thrust (th, Fig. 6.3). Width of field approximately 15km. View looking S.E. towards locality A, Fig. 6.3.

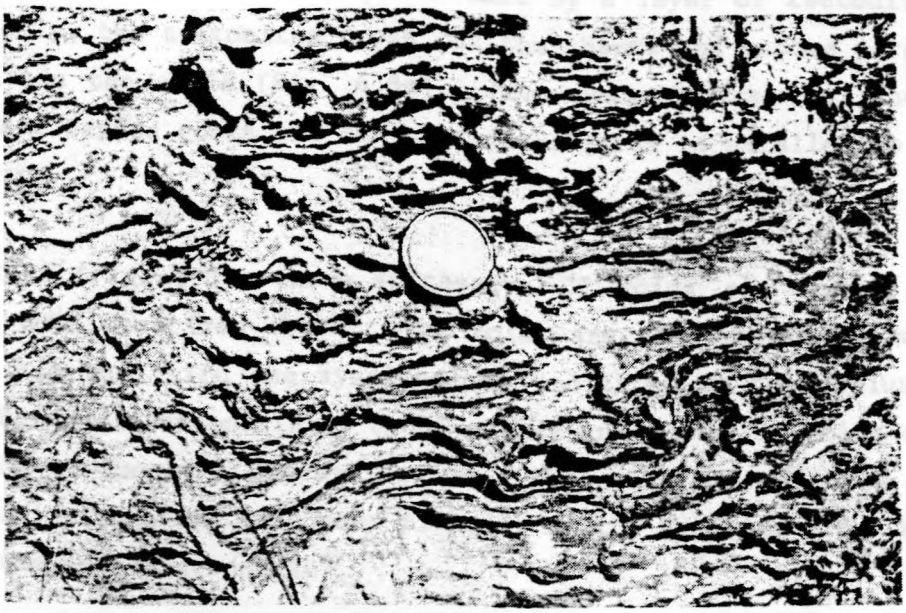


Figure 6.5. Flaser banded rock underlying an Onverwacht chert unit and showing folded and cross cutting quartz veins (Simbubule - Josefsdal Farm).

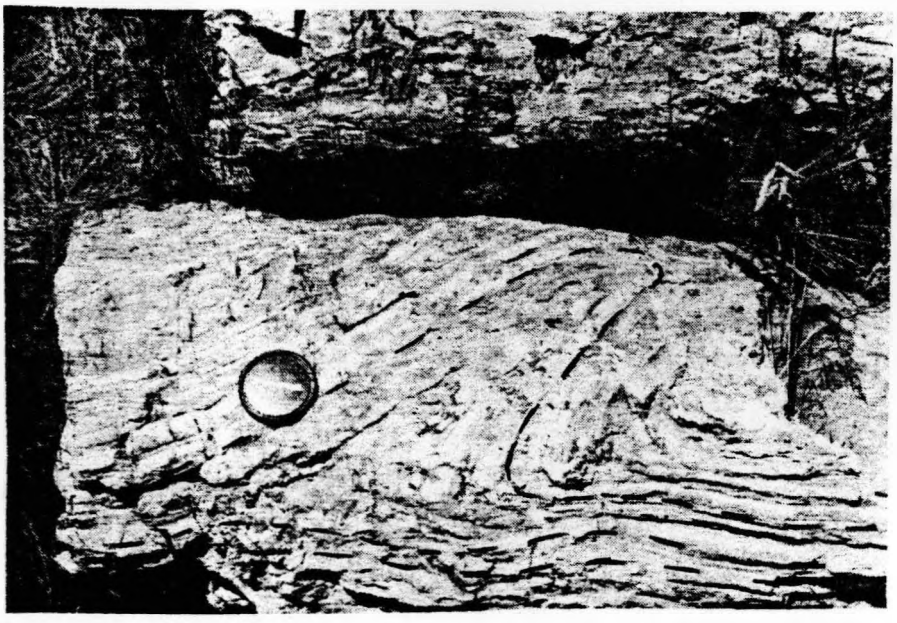


Figure 6.6. Small scale décollement structure in an Onverwacht chert unit (Simbubule, unit 1 locality A, Fig. 6.3, Josefsdal Farm).

The folded units comprise successively from bottom to top (Fig. 6.8a): flaser banded rocks or brecciated lavas, a chert layer with accretionary spheroids and a unit of silicified ferruginous shale which may contain mud pool structures (Chapter 4). The shale unit is frequently absent and the chert is then separated from the next unit by a layer of tectonite (Fig. 6.7). Locally, the tectonites cross cut the cherts and become parallel to bedding within the shale (Fig. 6.8a). Most commonly however, the fabric in the flaser banded rocks and the brecciated lavas is parallel to bedding in the cherts.

At locality A (Fig. 6.3), three successive D2 folds are formed in the structural unit described above. The folds are all synformal, two being anticlinal and the third one synclinal as indicated by their plunges and by the younging directions (Fig. 6.8b). They are symmetric folds of class 1c according to Ramsay's classification (1967) with N/S oriented steeply dipping axial planes and fold axes plunging to the SW (Fig. 6.9 a,b). The interlimb angles are around 20°.

The symmetric shapes of these f2 folds about N/S axes suggest that the unit was subjected to a broad E/W compression during D2. Therefore the geometry of the folds, i.e. three successive synforms with steep plunges and steep limbs, indicates that D2 folded an already steeply dipping to overturned E/W unit (Fig. 6.8b).

Similarly, at locality D (Fig. 6.3), the presence of an f2 synclinal antiform also demonstrates the overturning of the tectonic unit, prior to D2 (Fig. 6.8c, 6.9c). Such structures, showing large scale inversion of strata, are called fold nappes and were possibly initiated as recumbent folds (McClay, 1981).

6.2.4 D1 AND METASOMATISM

a) Silica Metasomatism

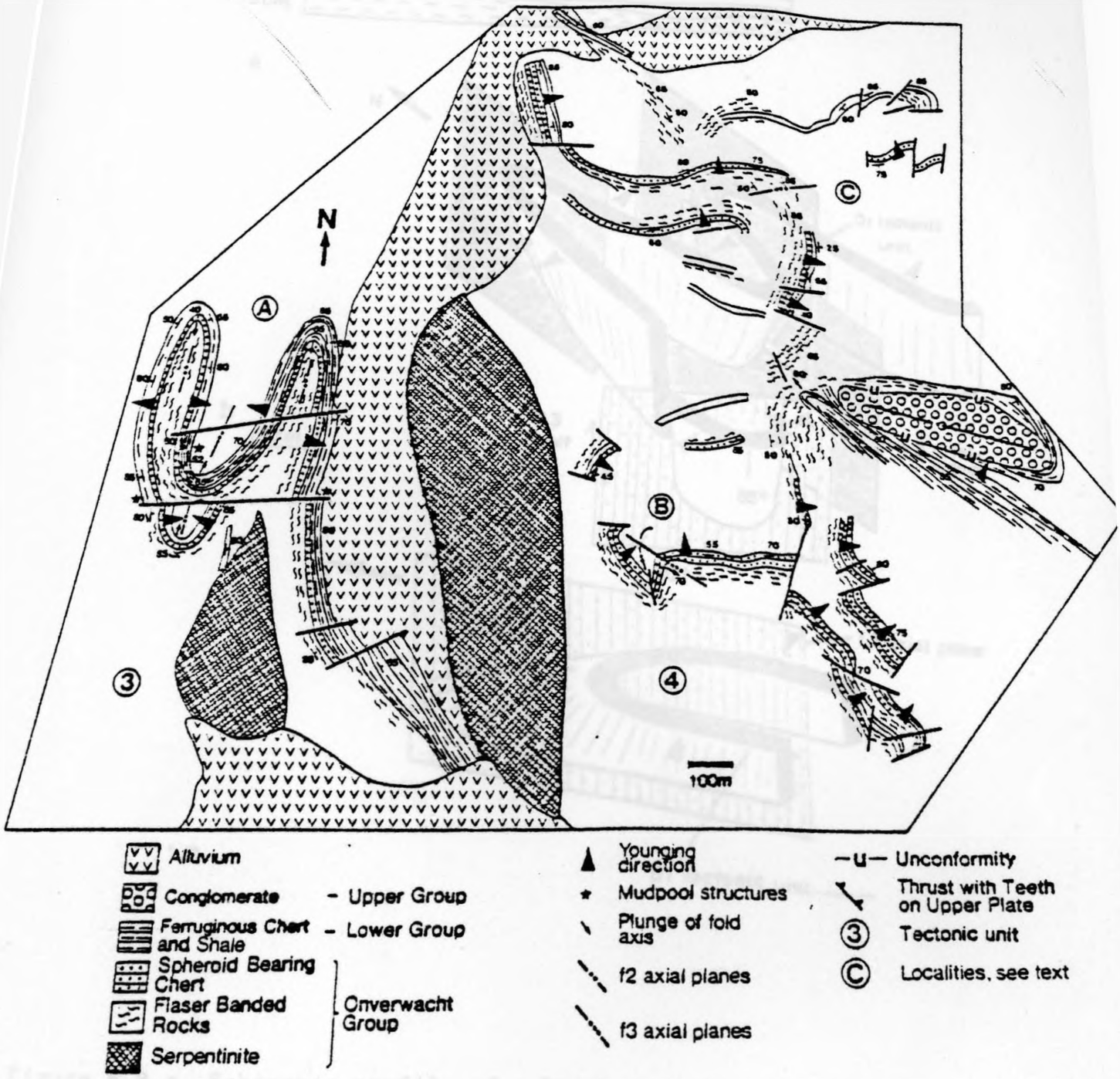


Figure 6.7. Geological map of the Onverwacht cherts in the Manzima Valley showing the refolding of D1 tectono-stratigraphy by D2 and D3 (see Fig. 6.1 for location).

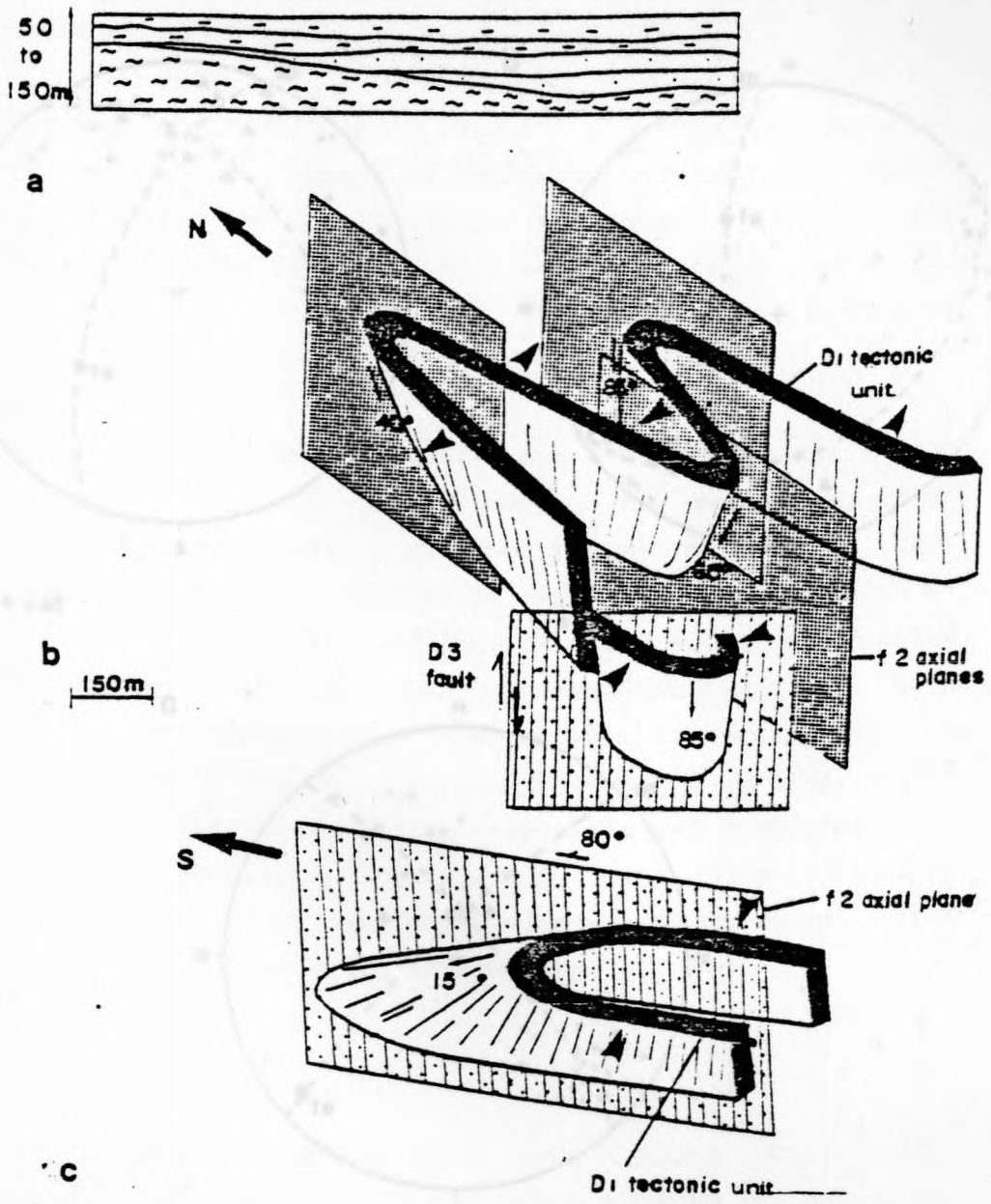


Figure 6.8.a Schematic profile of a D1 thrust slice (symbols as in Fig. 6.3).

b D2 folding of a D1 thrust slice. The symmetry of D2 folds and the younging directions( ) indicate that the unit was steeply dipping to overturned prior to D2. (loc. D. Fig. 6.7)

c Block diagram showing a D2 antiformal syncline. (loc. D. Fig. 6.3)

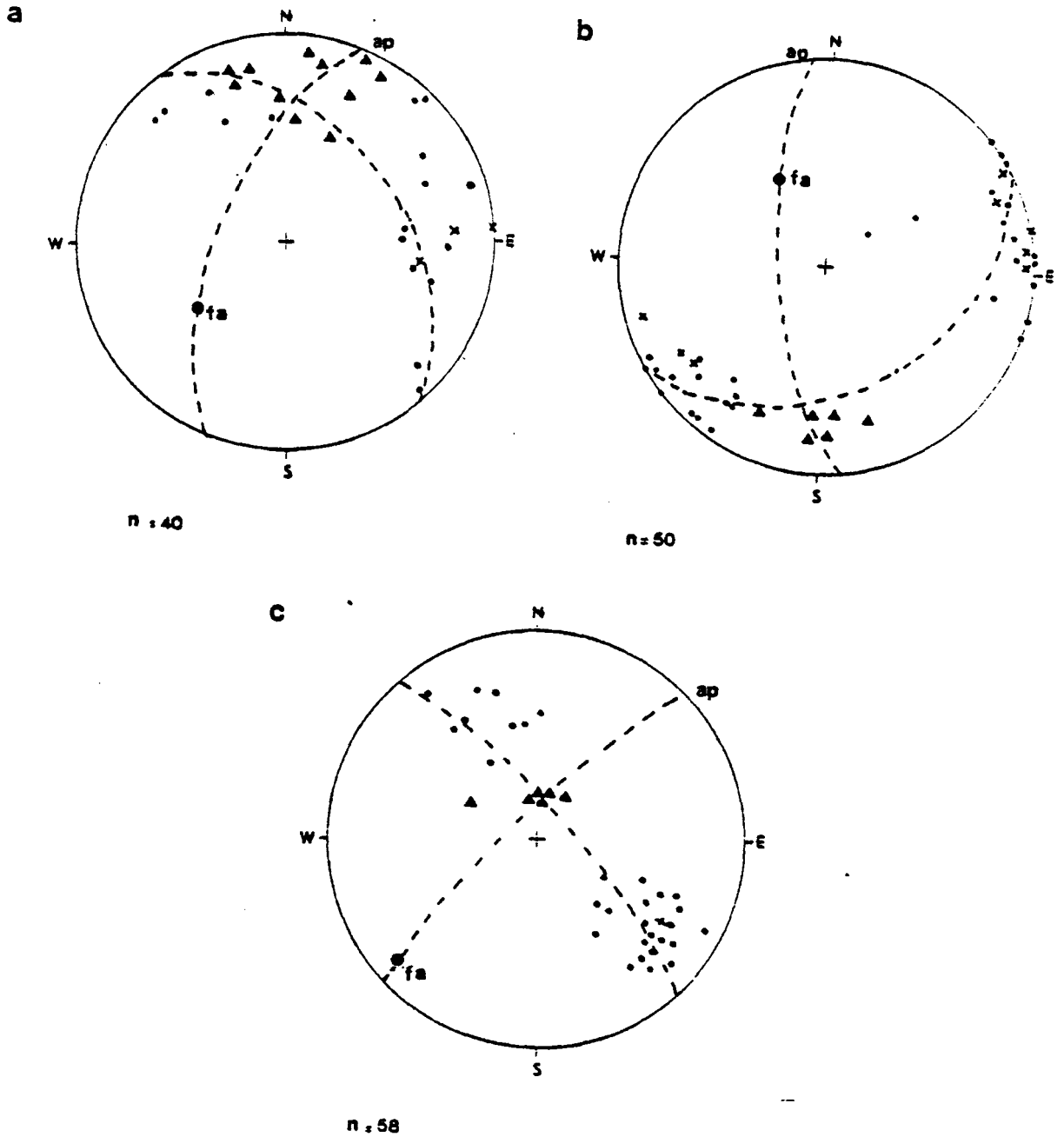


Figure 6.9 equal area projection of f2 folds, a: left synform represented in figure 6.8.b; b: right synform represented in figure 6.8.b; c: antiform represented in figure 6.8.c. fa = calculated fold axis; ap = calculated axial plane; • = pole to bedding in the limb; ▲= pole to bedding in the hinge zone; X = pole to the fabric present in the flaser banded rocks; n = number of measurements; dotted lines = best fit great circles, visually estimated.

The volcano sedimentary pile which has been tectonically repeated by D1 corresponds to that part the stratigraphy which has been strongly affected by silica metasomatism (Chapter 5).

In the flaser banded rocks underlying the thrust slices, folded silica veins contain features indicative of hydraulic fracturing and continuous shearing. In thin section, drusy growth fabrics are common. Crystals with undulose extinction and drusy crystals are deformed to a sigmoidal shape. Such features are formed under conditions of high fluid pressures (Beach, 1977).

As discussed previously, hydraulic fractures are a common feature in the Onverwacht Group and have been interpreted as the manifestation of syndepositional hydrothermal activity (Chapter 5, section 5.2.4). That movement was related to hydraulic fracturing can often be demonstrated on the outcrop scale. As can be seen in figures 6.6 and 6.10 small diapirs and décollement zones were developed within the sedimentary sequence. Such structures were initiated along silica veins parallel to bedding and were filled with silica cemented breccia. Evidence of movement can also be seen along single fractures where cross cutting veins have been displaced by up to 10cm along a bedding parallel silica vein (Fig. 6.11). Thus D1 tectonic stacks were initiated in zones of high fluid presence probably formed during hydrothermal activity, possibly during deposition.

b) Carbonate Metasomatism

The widespread occurrence of carbonates in D1 fuchsitic shear zones suggests that either shearing was more easily induced by the presence of carbonates, or that carbonate bearing fluid, found more permeable pathways in the shear zones. The importance of carbonates in the pillow breccia and pillow lavas in which the shear zones were developed (Chapter 2) indicates that the first explanation is more likely. The association of fuchsite and carbonates in Archaean shear zones which developed in volcanic rock has also been described in Kirkland Lake - Larder Lake area (Canada) by Tihor and Crocket (1977).

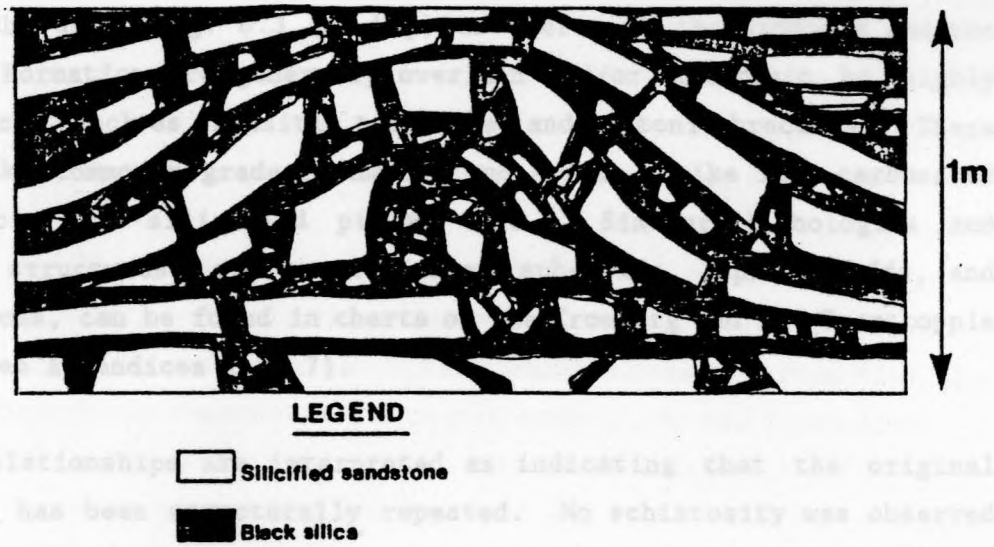


Figure 6.10. A small diapir filled with silica cemented breccia within a chert unit (Dunbar Farm).



Figure 6.11. Lateral displacement along a silica vein (arrowed) in Onverwacht silicified sediments (Dunbar Farm). Scale bar = 10cm.

6.2.5 D1 IN THE REST OF THE STUDY AREA AND SUMMARY

A tectono-stratigraphy similar to that described above can be found throughout the area (Fig. 6.3 and Map) as cherts of the Kromberg and the Zwartkoppie Formation are generally overlain and/or underlain by highly contorted rocks (such as fuchsitic tectonites and tectonic breccias). These deformed rocks commonly grade downwards and across strike into carbonated pillow breccia and silicified pillow lava. Similar lithologies and sedimentary structures, e.g. accretionary spheroids, lapilli tuffs, and Bouma sequences, can be found in cherts of the Kromberg and the Zwartkoppie Formation (see Appendices 1 to 7).

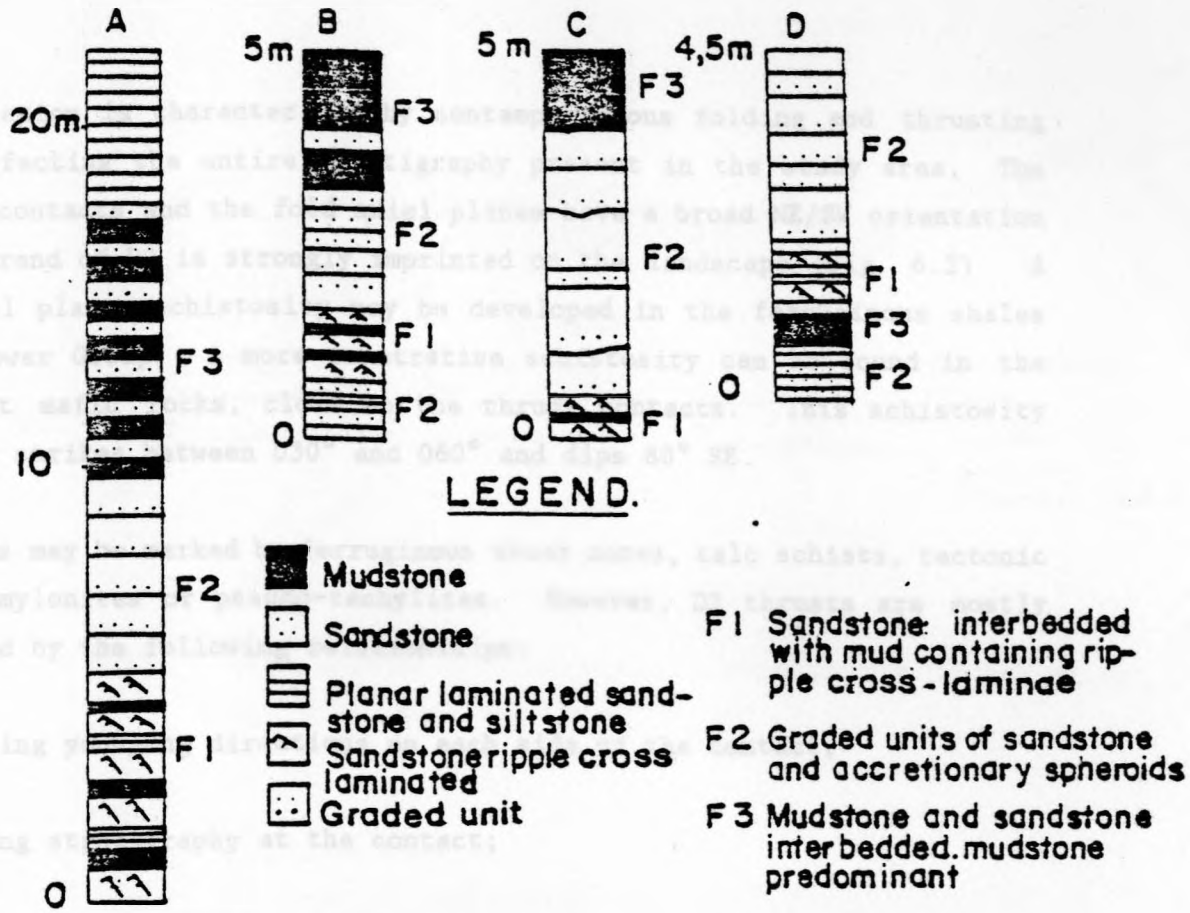
The above relationships are interpreted as indicating that the original stratigraphy has been structurally repeated. No schistosity was observed within the cherts, however, they are frequently brecciated (Chapter 5).

Thus in the study area, an early thrusting phase is manifested by the formation of fuchsitic flaser banded rocks and tectonic breccia and by repetition of similar lithological units without reversal in younging direction from one unit to the next. The tectonites generally parallel the bedding planes of the overlying sediments and locally cut up stratigraphy (Fig. 6.8a). Normal faulting cannot lead to the repetition of sedimentary units described above, and the tectonites are thus interpreted as indicative of listric faults or low angle thrusts similar to those described by De Wit (1982). In addition, the pre-D2 vertical to overturned disposition of the D1 tectono-stratigraphy in places, suggests that D1 also involved overturning to recumbent folding or the rotation of blocks (f1). Although no f1 fold closures have been preserved in the study area, f1 recumbent folds are clearly visible in Mendon Farm, 9km to the N (De Wit, 1982). These recumbent folds are underlain by fuchsitic tectonites similar to those described here.

From the above descriptions, it appears that D1 caused the deformation by thrusting of a sequence which comprised originally from bottom to top: pillowed and massive lava; a spheroid and lapilli tuff bearing sedimentary unit; and a unit of ferruginous shales which can contain mud pool structures. The presence of inverted thrust sheets containing D1 tectonic stacks together with the presence of D1 recumbent folds to the NW of the study area

(De Wit, 1983) suggest that the D1 stack were further affected by recumbent folding. Folding probably occurred around E/W oriented axes in the study area and tectonic transport could have been in a northern or southern direction (section 5.2.3).

Measured sections in cherts throughout the Onverwacht Group (Fig. 6.11), within and outside the study area, show that cherts containing similar spheroids and Bouma sequences can be found in the following "stratigraphic" units: the Theespruit Formation, (De Wit et al., 1983); the Middle Marker, (Stanistreet et al., 1982); the Kromberg Formation and the Zwartkoppie Formation; this study). In all these formations, cherts are underlain by tectonites or by mafic schist zones. This would further confirm that the entire Onverwacht Group represents a tectonic complex, as was first proposed by De Wit (1982) and De Wit et al. (1983) instead of a normal stratigraphic succession of volcanic cycles (Viljoen and Viljoen, 1970). The serpentinite lenses found within the Onverwacht Group are not repeated by D1 and occur below the D1 tectonic stacks (see Map). Thus, in the study area the original Onverwacht Group probably comprised successively: a layer of serpentinite; pillowed and massive lava; and sedimentary rocks. D1 tectonic repetition only affected the upper part of this Onverwacht sequence, and the base of the Lower Group. The D1 thrusting was probably initiated in zones of high fluid pressure developed during early hydrothermal activity (section 6.2.4).



Onverwacht Group

- Zwartkoppie Formation
- Kromberg Formation
- Hooggenoeg Formation
- Middle Marker
- Komati Formation
- Theespruit Formation
- Sandspruit Formation

Figure 6.12. Measured section in cherts of the Onverwacht Group showing the similarites between cherts belonging to different formations. (F1,F2,F3 after De Wit et al.,1983)
A = Theespruit chert (After De Wit et al., 1983)
B = Middle Marker chert (Rosentuin Farm)
C = Kromberg chert (Dunbar Farm)
D = Zwartkoppie chert (Diepgezet Farm)

6.3 SECOND PHASE OF DEFORMATION: D2

D2 deformation is characterised by contemporaneous folding and thrusting events affecting the entire stratigraphy present in the study area. The tectonic contacts and the fold axial planes have a broad NE/SW orientation and the trend of D2 is strongly imprinted on the landscape (Fig. 6.2). A weak axial planar schistosity may be developed in the ferruginous shales of the Lower Group. A more penetrative schistosity can be found in the Onverwacht mafic rocks, close to the thrust contacts. This schistosity generally strikes between 030° and 060° and dips 80° SE.

D2 thrusts may be marked by ferruginous shear zones, talc schists, tectonic breccia, mylonites or pseudo-tachylites. However, D2 thrusts are mostly identified by the following relationships:

1. Opposing younging directions on each side of the contact;

2. Missing stratigraphy at the contact;

3. Older rocks emplaced over younger rocks.

Although the contacts can be as steep as 80°, normal faulting cannot lead to such relationships. These relationships are interpreted here as indicative of low angle thrusts; which have been steepened by later deformation.

D2 folds are generally single hinge type folds, varying from class 1 b to 1 c (Ramsay, 1967) with interlimb angles varying from 15° to 50° (Fig. 6.13, 6.14, 6.15, 6.16, 6.17). One multiple hinge type fold (or box fold) was formed in the Waterfall Synclinorium (Fig. 6.13, 6.14). Strikes of axial planes for these f2 folds vary from 030° to 070° and the folds plunge 20° to 30° to the SE or 20° to 60° to the NE.

Within the <ONV> units, where f2 folds are superimposed on D1 structures, f2 axial planes vary in strike from 020° to 173° and dip steeply west-east (Fig. 6.9). The fold axes plunge steeply to the north or to the south, the two plunging directions could be due to the superposition of D3 which will be discussed later.

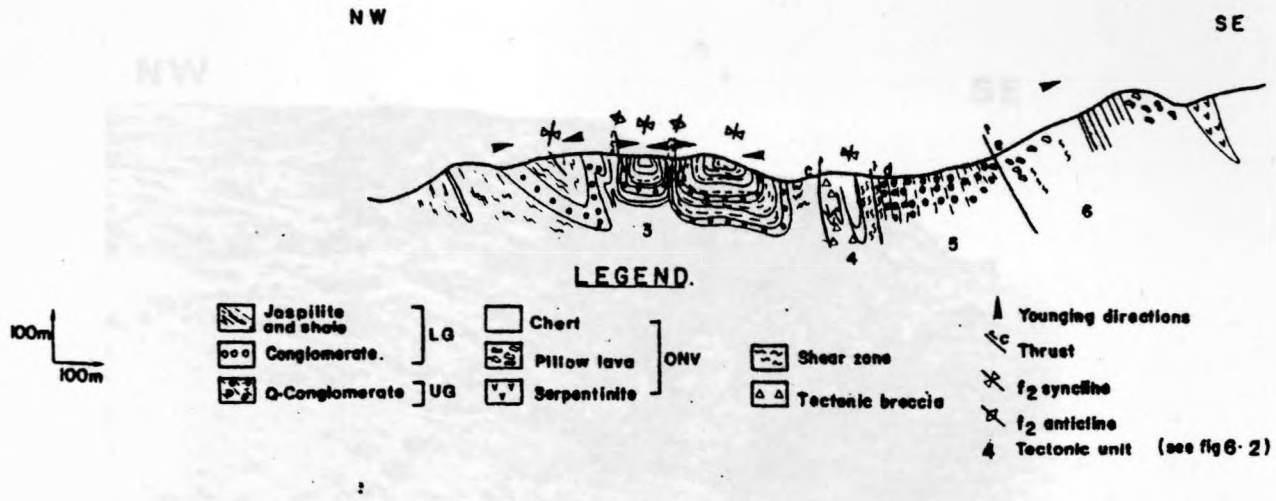


Figure 6.13. = Cross section in the Waterfall Synclinorium (location on Fig. 6.2). Note box fold.



Figure 6.14. = F2 folds in the Waterfall Synclinorium and adjacent structural units. c,d = Thrust contacts (see Fig. 6.2). View looking SW.

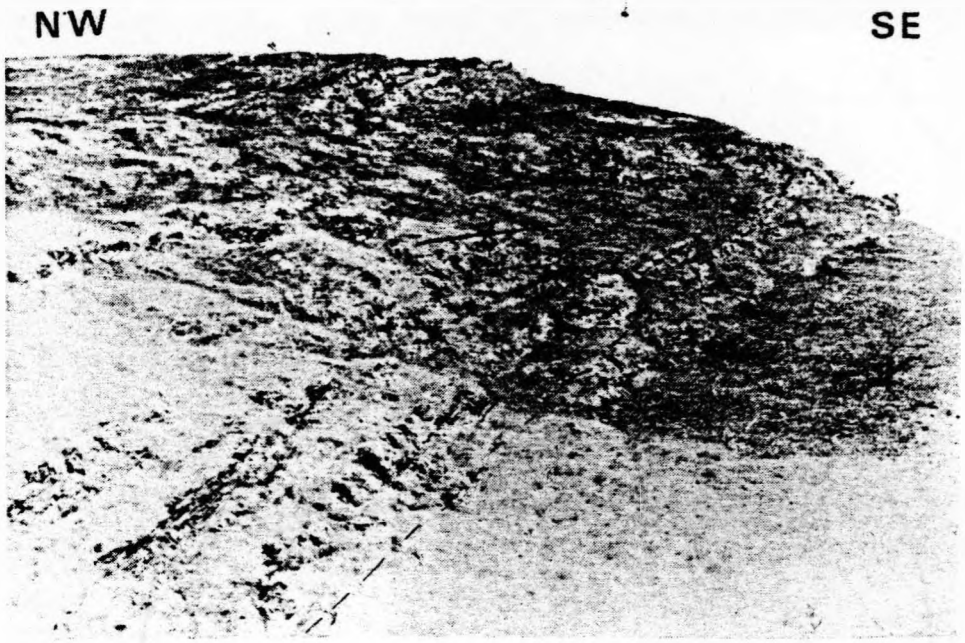


Figure 6.15. f2 S fold in the Waterfall Synclinorium. View looking NE. (Josefsdal Farm).

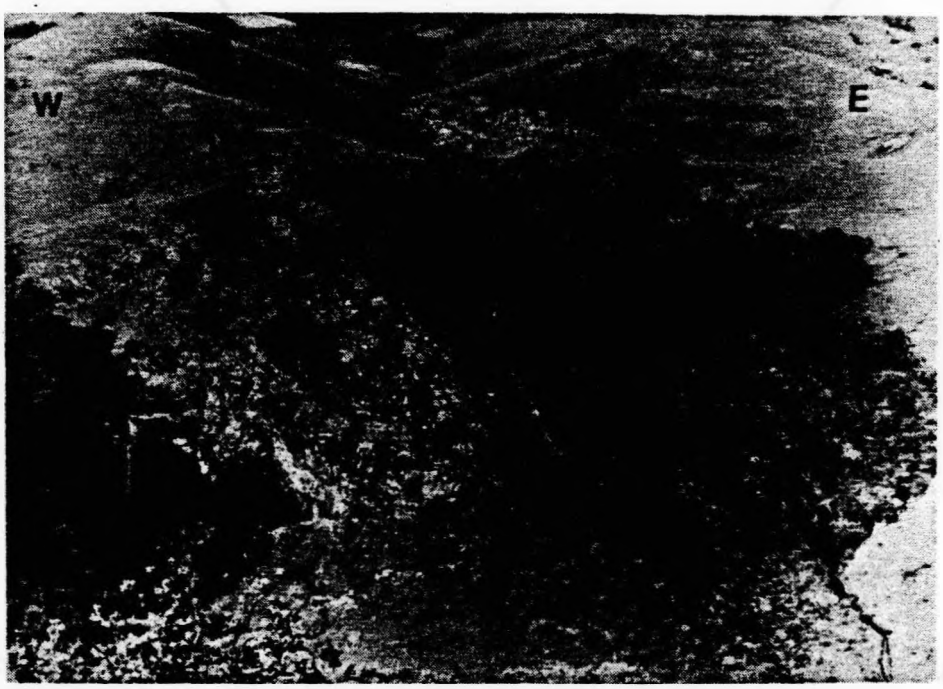


Figure 6.16. Tight, isoclinal f2 syncline in the Waterfall Synclinorium (unit 3, Fig. 6.2). View looking NE (Josefdal Farm)

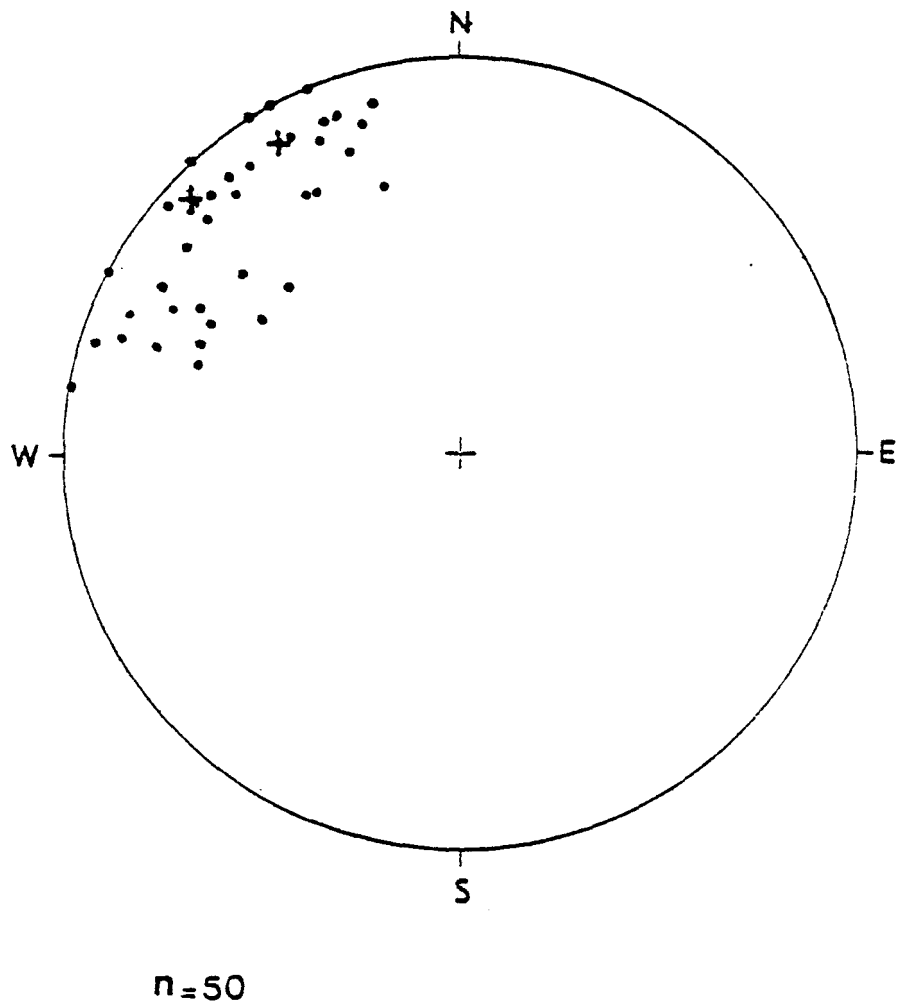


Figure 6.17. Equal area projection of f2 folds axial planes in the Waterfall Synclinorium (Unit 3, Fig. 6.2); • = pole to axial planes; x = pole to schistosity; n = number of measurements.

Measured sections indicate that there has been little or no thinning of the limbs. Thus, folding was probably predominantly by flexural slip (Ramsay, 1967). D2 structures are best exposed in two different areas which will be described successively, using detailed traverses and field relationships.

6.3.1 THE T-JUNCTION AREA

A simplified geological map of this area is presented in figure 6.18. The most striking feature in this area is the presence of an angular discordance between Lower Group sedimentary rocks (Unit 8) and Onverwacht cherts (Unit 9) (Fig. 6.19).

From west to east, the following structural contacts can be distinguished (Fig. 6.18, 6.19):

1. Unit 4 <ONV> is overlain by conglomerates of the Upper Group (Unit 5).

2. Unit 5, <UG>, is in turn overlain by Onverwacht Group material (Fig, 6.18).

3. This Onverwacht unit, Unit 6, is truncated by Unit 7, <LG>, which contains the Emlembe Syncline. This contact is marked by talc schists, schistose sandstones and shear zones.

4. The Emlembe Syncline is cross-cut by a unit of ferruginous sediments, Unit 8, <LG>, and the contact is marked by a ferruginous shear zone (Fig. 6.18).

5. Unit 8 is truncated by Unit 9 <ONV,LG>, forming a structural discordance clearly visible in the landscape (Fig. 6.20) along which pseudo-tachylite is developed in places (Fig. 6.21).

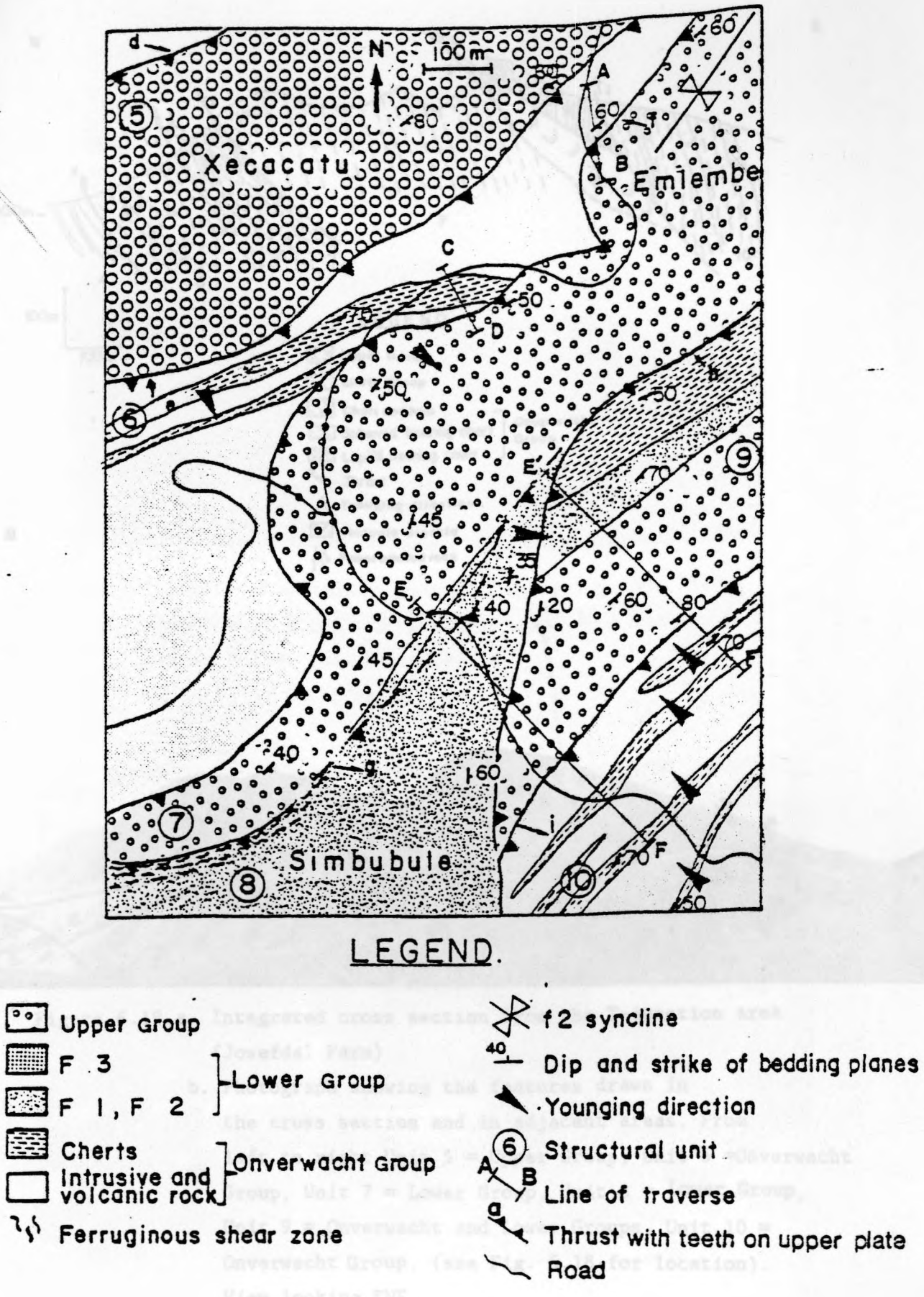


Figure 6.18. Simplified geological map of the T_ junction area (see Fig. 6.1 for location).

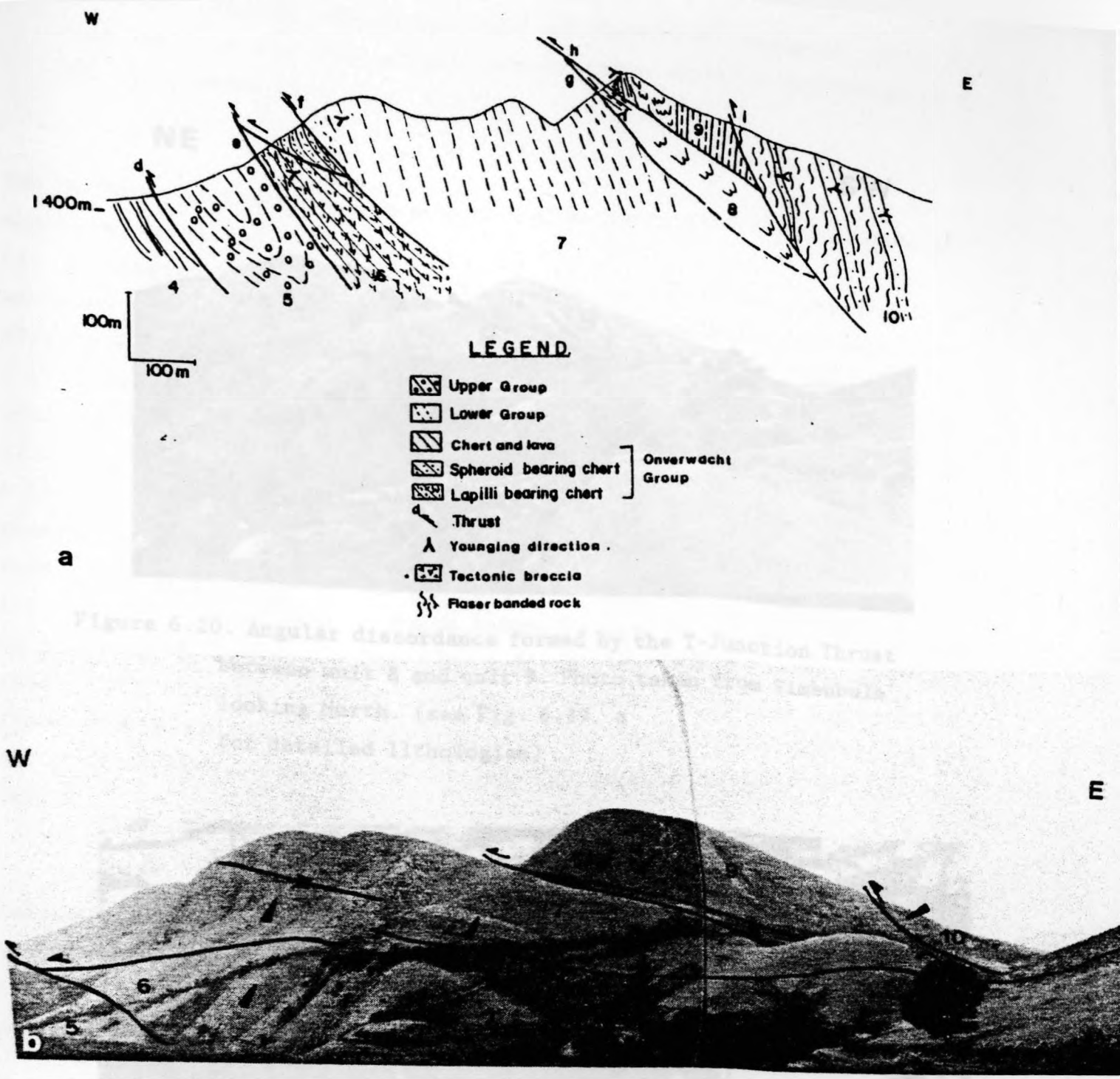


Figure 6.19.a. Integrated cross section from the T-junction area (Josefdal Farm)

b. Photograph showing the features drawn in the cross section and in adjacent areas. From left to right Unit 5 = Upper Group, Unit 6 =Onverwacht Group, Unit 7 = Lower Group, Unit 8 = Lower Group, Unit 9 = Onverwacht and Lower Groups, Unit 10 = Onverwacht Group. (see Fig. 6.18 for location). View looking ENE.

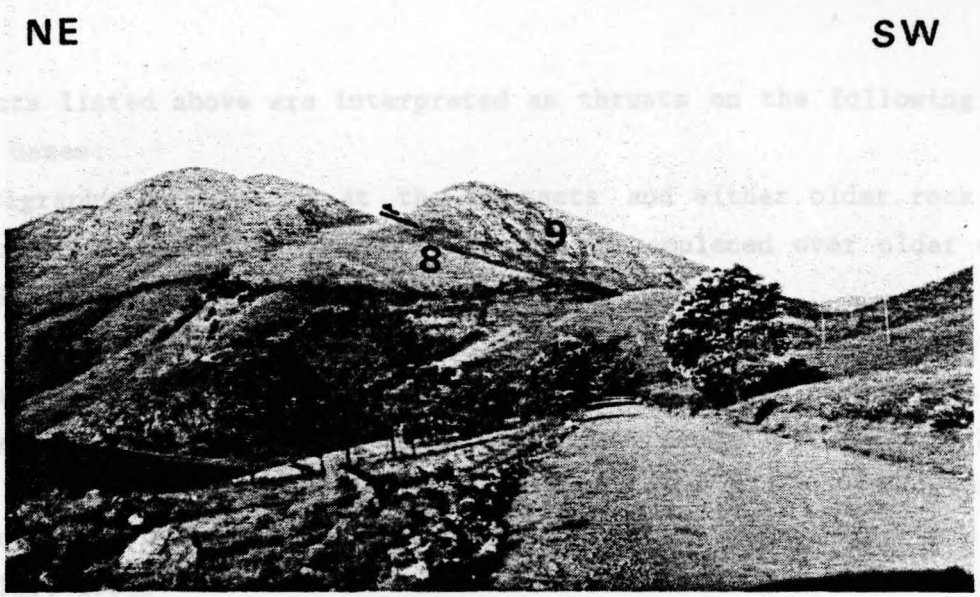


Figure 6.20. Angular discordance formed by the T-Junction Thrust between unit 8 and unit 9. Photo taken from Simbubule looking North. (see Fig. 6.19. a for detailed lithologies)

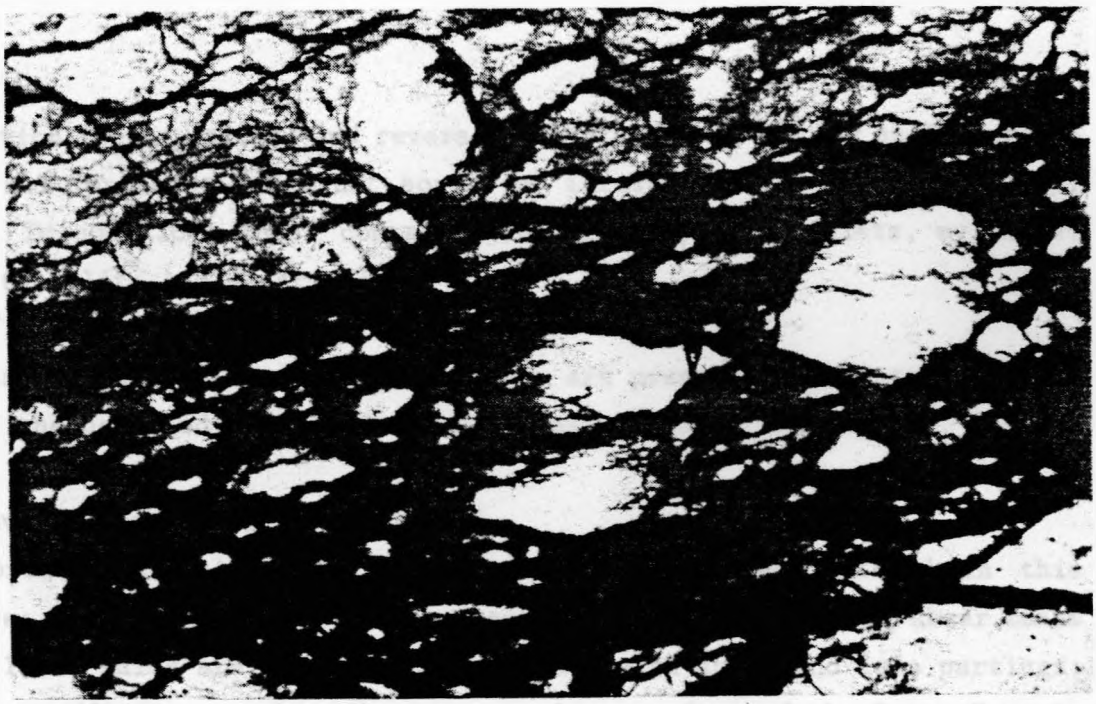


Figure 6.21. Photomicrograph of pseudo tachylite from the T-Junction thrust width of field = 3,5mm (see Fig. 6.19.c for location)

6. A steeply dipping overturned unit of Onverwacht material, Unit 9, overlies Unit 8. The contact between these units is manifested by a 30m thick shear zone (Fig. 6.22).

The contacts listed above are interpreted as thrusts on the following geometrical bases:

(i) Stratigraphy is missing at the contacts and either older rock are emplaced over younger rocks or younger rocks are emplaced over older ones (Fig. 6.19).

(ii) Some of the contacts dip between 15° and 45°, with older rocks overlying younger rocks (Fig. 6.24), thus representing low angle reverse faults.

(iii) Steeper contacts can bee seen to shallow at depth (tf, tg, ti, Fig. 6.19a). They represent reverse listric faults when older rocks overlie younger rocks and normal listric faults when younger rocks overlie older rock (McClay, 1981).

(iv) Some of the steeper contacts cannot be seen to shallow at depths due to the lack of exposure. They also emplace older rocks over younger rock (i.e. <ONV> over <UG> or <ONV> over <LG>). Such relationships indicate that these faults are contraction faults (McClay, 1981). They either shallow at depth or have been steepened by later deformation (Price, 1981; Coward, 1983).

Contraction faults, normal and reversed listric faults and low angle reverse faults all represent different sorts of thrusts (Ramsay, 1967; McClay, 1981). In addition, these contacts are marked by talc schists, mylonite, pseudo-tachylite and shear zones.

Three traverses from the T-Junction area, are presented below to emphasise some of the detailed aspect of the D2 thrust contacts (Fig. 6.18).

(a) Traverse A - B (Fig. 6.22a)

From north to south, the following rock types are encountered in this traverse: talc schists (Onverwacht Group) in which anastomosing shear zones 0,5 to 1,5cm thick are developed; sandstones with shale and talc partings; schistose siltstones and sandstones; sandstones (top of the Lower Group). All the units dip 60° to 75° SE while the schistosity strikes between 050° and 060° and dips 60° to 70° SE. At the southern end of the traverse, the

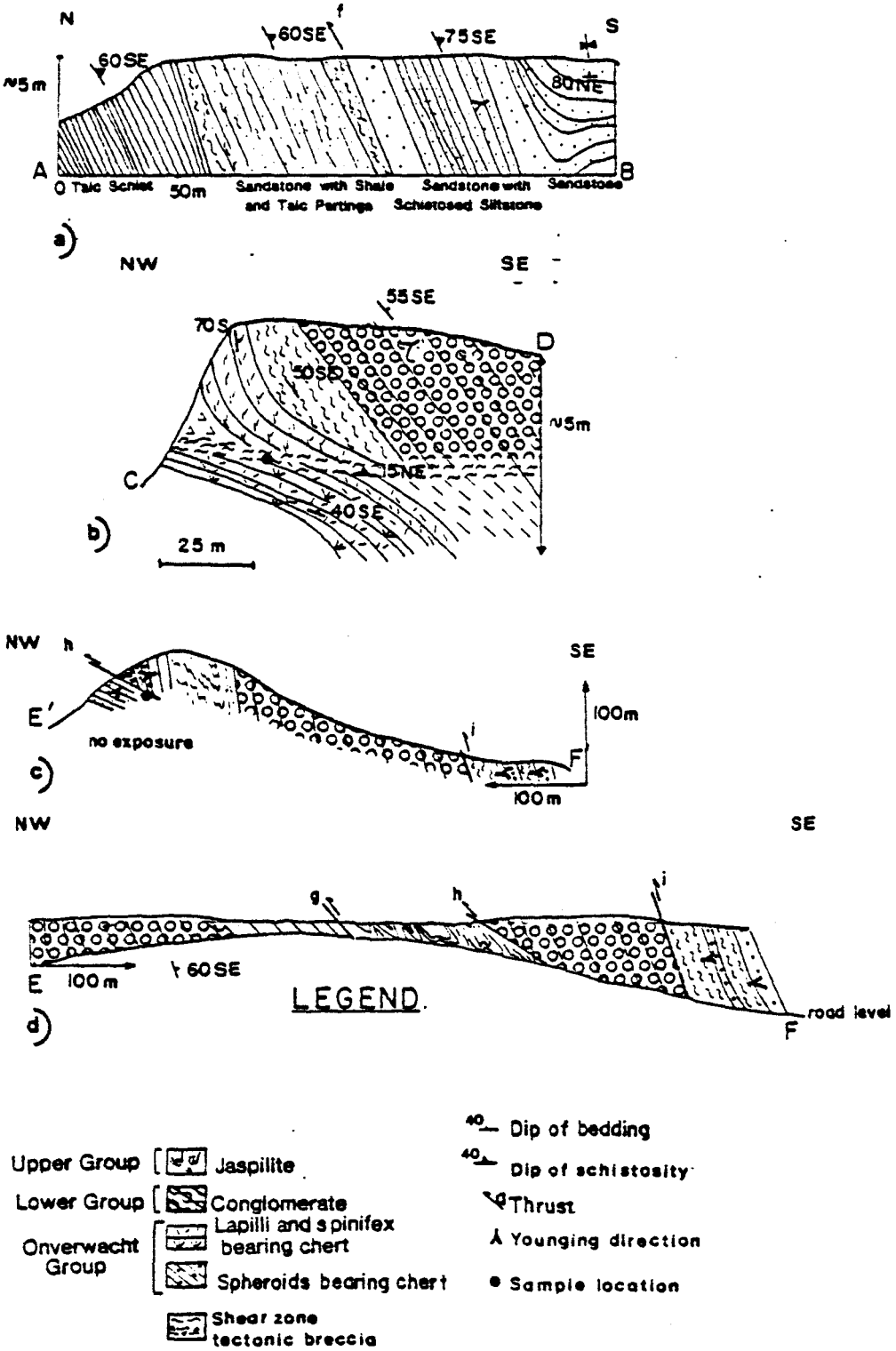


Figure 6.22.a,b,c,d Traverses in the T-Junction area (see Fig. 6.18 for location).

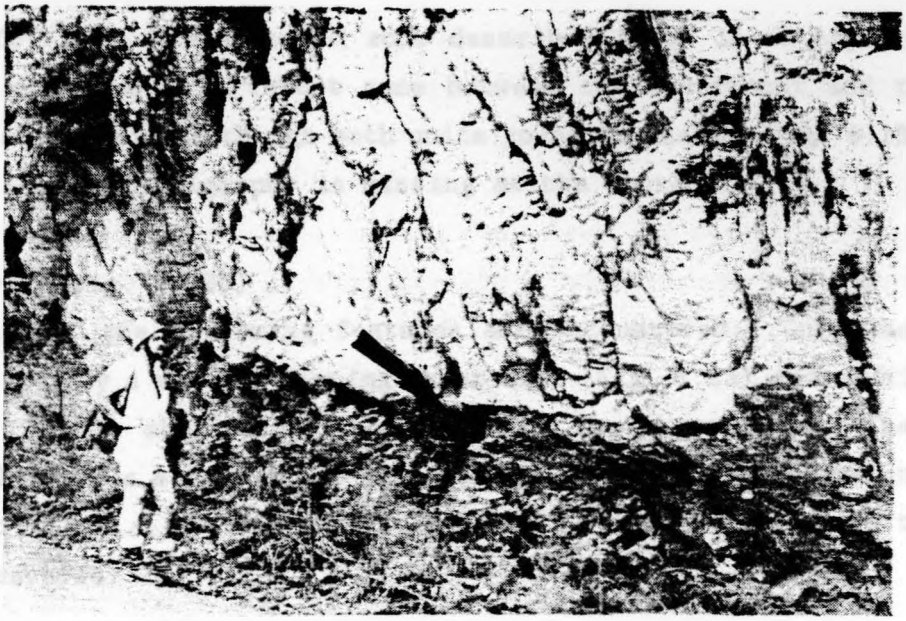


Figure 6.23. Traverse C-D in the T-junction area showing shallow dipping shear zone (arrow) within unit 6. Lapilli bearing cherts occur both above and below the shear zone (see Fig. 6.18 for location).

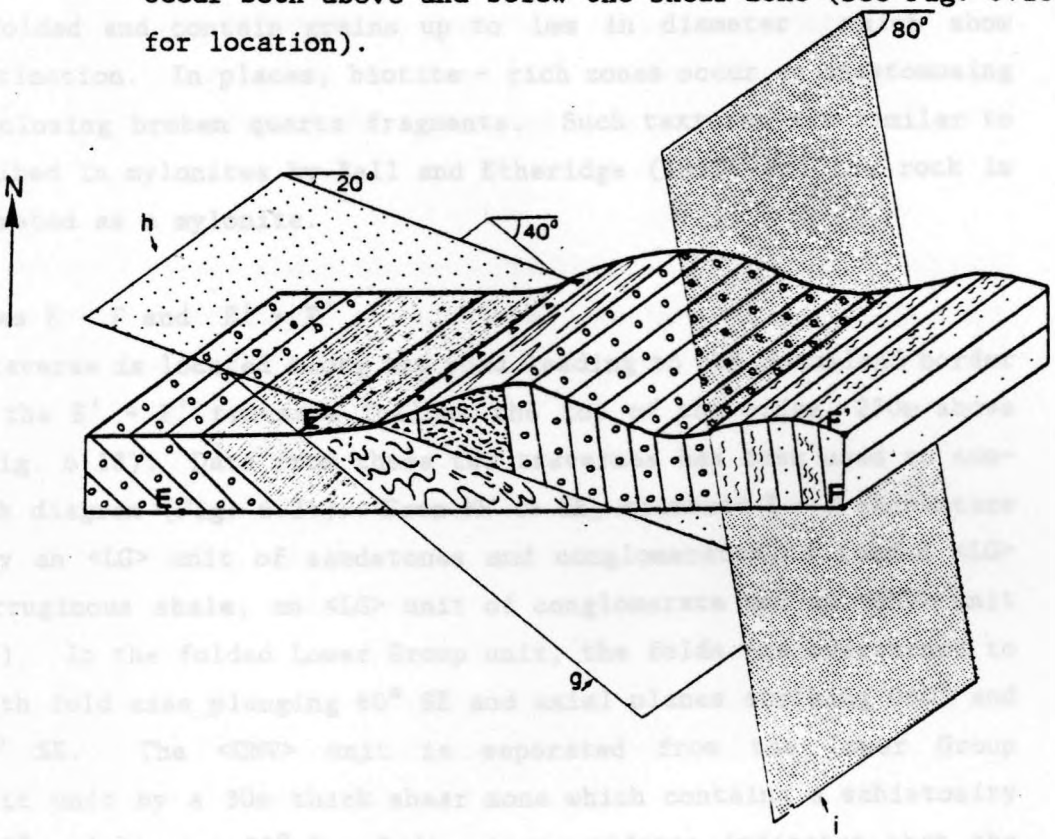


Figure 6.24. Block diagram showing traverses E - F and E' - F'. (see Fig. 6.18 for location, and Fig. 6.22 for the geological symbols.

dipping 50° to 80° SE. The deformed zone described above is interpreted as marking the presence of a thrust zone between the Onverwacht and the Lower Groups. In addition, although both units young to the SE (Fig. 6.18), the basal Lower Group stratigraphy is missing at the contact.

(b) Traverse C - D (Fig. 6.22b)

From north to south, the following features are encountered: Onverwacht cherts are cross-cut by a shallow dipping shear zone (Fig. 6.23) above which the cherts dip 70° S, shallowing downwards into the shear zone. These cherts are overlain by a second shear zone and by Lower Group conglomerates which dip 50° to 55° SE. The two shear zones can be seen to merge at the bottom of the traverse.

In thin section, a sample taken from the subhorizontal shear zone located with the Onverwacht Unit (Fig. 6.22b) shows the following characteristics: strained quartz aggregates are surrounded either by strained quartz grains formed by comminution or by recrystallised very fine grained quartz. Quartz veins are folded and contain grains up to 1mm in diameter which show undulose extinction. In places, biotite - rich zones occur as anastomosing networks enclosing broken quartz fragments. Such textures are similar to those described in mylonites by Bell and Etheridge (1973) and the rock is thus interpreted as a mylonite.

(c) Traverses E - F and E' - F'

The E - F traverse is located along the road leading to the Swaziland border post while the E' - F' traverse follows the top of the ridge, 250m above the road (Fig. 6.18). Data from these two traverses has been used to compile a block diagram (Fig. 6.24). From NW to SE, traverse E - F encounters successively an <LG> unit of sandstones and conglomerates, a folded <LG> unit of ferruginous shale, an <LG> unit of conglomerate and an <ONV> unit (Fig. 6.22d). In the folded Lower Group unit, the folds are overturned to the west with fold axes plunging 60° SE and axial planes striking 060° and dipping 60° SE. The <ONV> unit is separated from the Lower Group conglomeratic unit by a 30m thick shear zone which contains a schistosity striking 085° and dipping 80° S. Sedimentary evidence indicates that the <ONV> unit is downward facing and represents a D1 tectonic pile (section 6.2.2).

Along the E' - F' traverse (Fig. 6.22c), the second Lower Group unit is overlain by chert breccia and spheroid bearing chert of the Onverwacht Group with an angular discordance between the two units (Fig. 6.20). The cherts are overlain by folded ferruginous shales and jaspilites and by conglomerates. As in traverse E - F, the conglomerates are overlain by an overturned unit of Onverwacht material. In thin section a sample from the angular discordance (Fig. 6.22c) contains brecciated quartz grains and clasts surrounded by a network of devitrified grains and is typical of a pseudo-tachylite (Fig. 6.21). In places, open fractures are filled by fibrous chlorite.

6.3.2 THE XECACATU RIDGE

A simplified geological map of the Xecacatu Ridge is presented in figure 6.25. The ridge itself is formed by Upper and Lower Groups material, the latter being only exposed in the southern part of the ridge where an unconformity is developed between the two groups (Fig. 6.25, loc. A, Chapter 4).

Three cross sections spaced along the Xecacatu Ridge are presented in figure 6.27 to illustrate the structure of this area. As the geology of the ridge is further complicated by f3 folds, the cross-sections are taken from areas away from these folds (Fig. 6.25).

The ridge is formed by the Xecacatu Syncline whose axial plane varies in strike from 015° to 060° and dips to the southeast. The fold axis plunges 20° to 40° to the northeast (Fig. 6.26).

For the larger part of the strike length, the western limb of the syncline structurally overlies an <ONV> (unit 4) composed of silicified igneous rocks and cherts of the thick bedded spheroid facies (loc. B, Fig. 6.26). However, to the north east, unit 4 appears to wedge out so that north of locality C (Fig. 6.26), the Xecacatu Syncline directly overlies Lower Group sedimentary rocks, unit 3. Unit 4 reappears as a lens at locality I (Fig. 6.25). The contact between unit 4, <ONV>, and unit 5 <UG> is marked by a fuchsitic brecciated shear zone (loc. H, I on Fig. 6.25, 6.27). This <ONV>

unit is folded by steeply plunging to neutral f2 folds with axial planes striking 040° to 060° (loc. B, I, Fig. 6.13). The D1 fabric present in the flaser banded rocks is also folded by f2. The Xecacatu Syncline is interpreted as a detached unit, emplaced by a thrust onto unit 3 and unit 4. The fold axis of the Xecacatu Syncline is parallel to the thrust contact (td Fig. 6.23) and the fold is thought to have formed during the overthrusting (Fig. 6.27a).

The eastern limb of the Xecacatu Syncline, unit 5, is structurally overlain by an Onverwacht sequence, unit 6 (Fig. 6.27a). This unit contains cherts of the thin bedded spheroid facies and silicified lava (loc. D, Fig. 6.25). At locality E and F (Fig. 6.25), structural discordances are clearly evident between the Onverwacht cherts, unit 6, and the Upper Group conglomerates, unit 5. At locality G (Fig. 6.25). The Onverwacht unit (unit 6) cross-cuts the Xecacatu Syncline fold axis (Fig. 6.27b).
The contact between unit 5 <UG> and unit 6 <ONV> is marked by a crush breccia which contains clasts of conglomerate (Upper Group) and clasts which contain silicified spinifex texture (Onverwacht Group), and by ferruginous shear zones (loc. E, Fig. 6.25).

South of locality G (Fig. 6.25) Unit 5, <UG>, youngs to the east while unit 6 <ONV> youngs to the west (Fig. 6.27 b,c). The Xecacatu Syncline axial plane reappears one kilometre south of locality D (Fig. 6.25, 6.27c).

The contact between unit 5 and unit 6 is also interpreted as a thrust, emplacing Onverwacht material over the Xecacatu Syncline and cross- cutting the stratigraphy of unit 5 in a north-westerly direction (Fig. 6.25, loc.A). The anticline present in unit 6 has an axial plane parallel to the thrust contact (thrust e, Fig. 6.25).

In the two areas discussed above, D2 folds are broadly parallel to the basal thrust contacts and can be cross-cut by the overlying thrust sheet. Such folds are seen as contemporaneous with the emplacement of the thrust sheet which contains them.

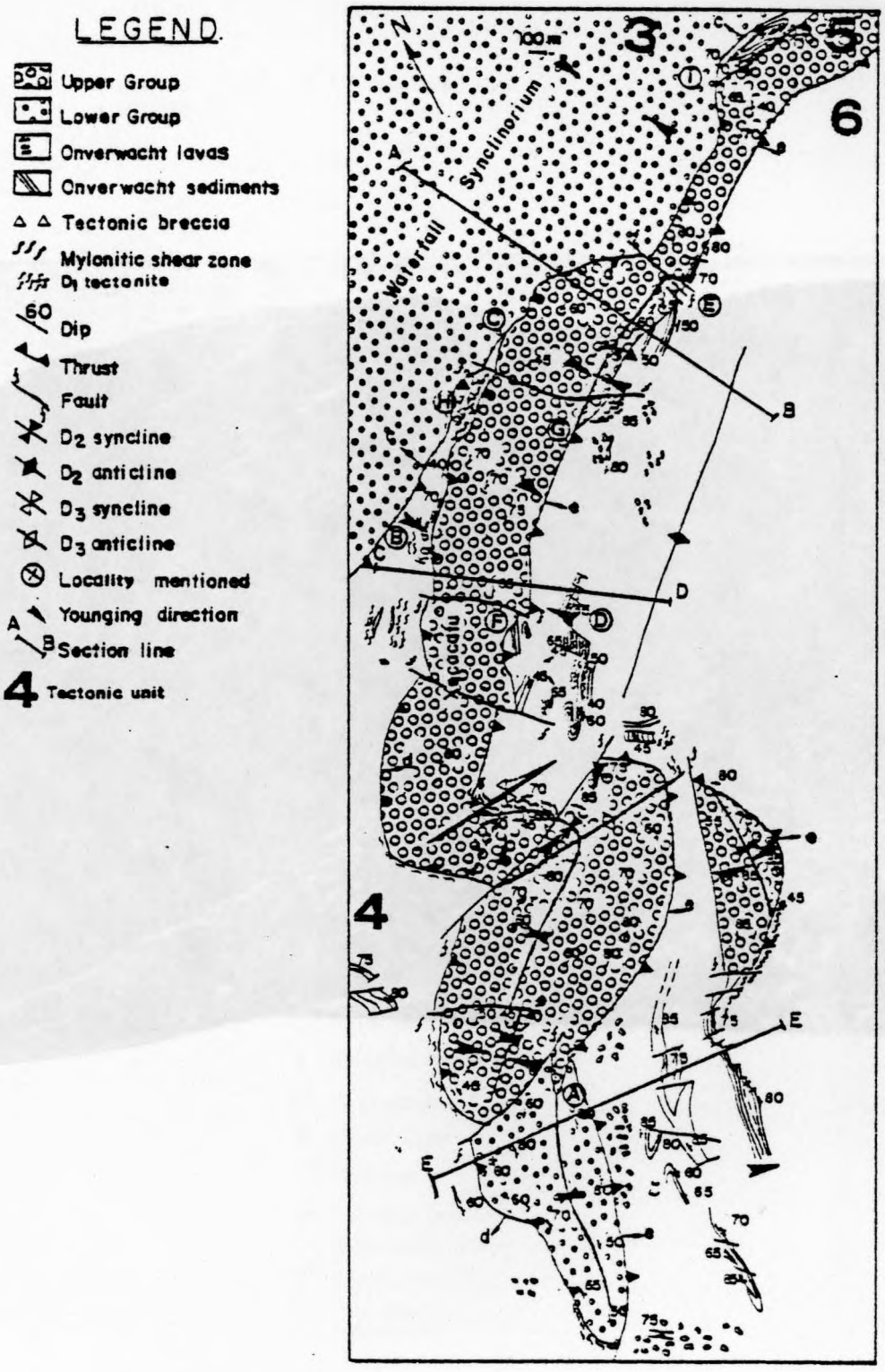


Figure 6.25. Simplified geological map of the Xecacatu Ridge (see Fig. 6.1 for location)



Figure 6.26. Upper Group quartz-arenite folded by the Xecacatu Syncline plunging 20° to the NE (unit 5, Fig 6.25).
View looking NE (Dunbar Farm)

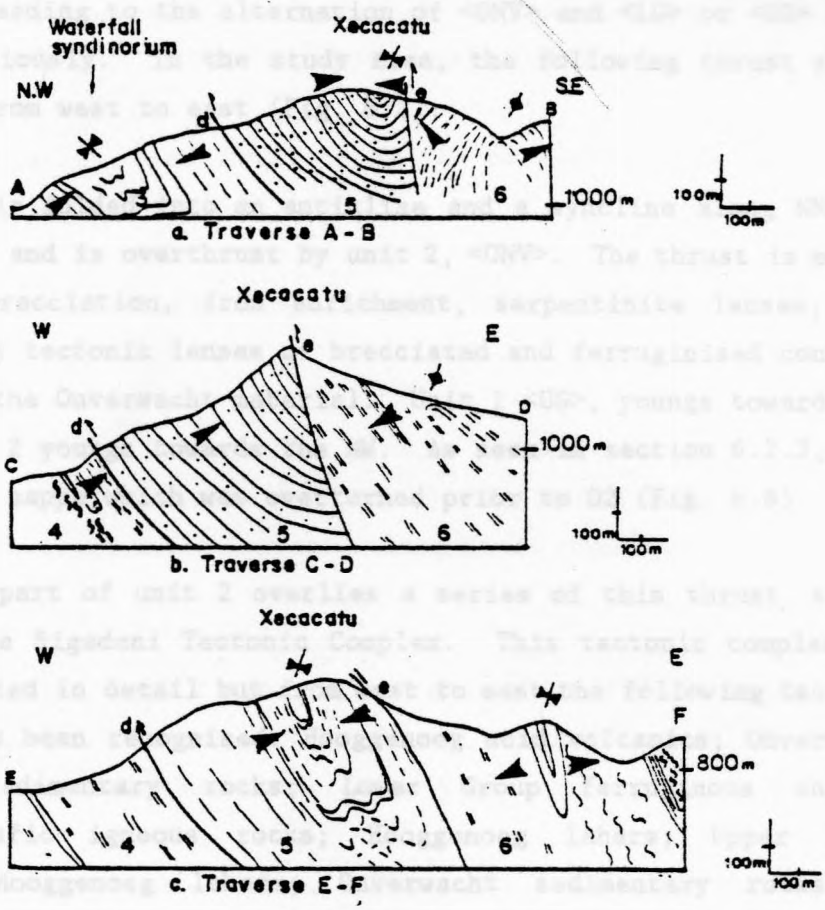


Figure 6.27. a - c Cross sections along the Xecacatu Ridge (see Fig. 6.25 for location)

6.3.3 D2 ELSEWHERE IN THE STUDY AREA AND SUMMARY

As can be seen in figure 6.2, D2 thrust slices and folds occur throughout the study area, leading to the alternation of <ONV> and <LG> or <UG> units as discussed previously. In the study area, the following thrust sheets are encountered from west to east (Fig. 6.2):

1. Unit 1, <UG> is folded into an anticline and a syncline along NNE/SSW oriented axes and is overthrust by unit 2, <ONV>. The thrust is marked by intense brecciation, iron enrichment, serpentinite lenses, talc schists and by tectonic lenses of brecciated and ferruginised conglomerate within the Onverwacht material. Unit 1 <UG>, youngs towards the SE while unit 2 youngs towards the NW. As seen in section 6.2.3, unit 2 represent a nappe which was overturned prior to D2 (Fig. 6.8).

   The southern part of unit 2 overlies a series of thin thrust slices which form the Sigadeni Tectonic Complex. This tectonic complex has not been studied in detail but from west to east the following tectonic succession has been recognised: Hooggenoeg acid volcanics; Onverwacht silicified sedimentary rocks; Lower Group ferruginous shales; Onverwacht mafic igneous rocks; Hooggenoeg lahars; Upper Group sandstones; Hooggenoeg lahars; Onverwacht sedimentary rocks and serpentinite (unit 2). The Sigadeni Complex is being studied and mapped together with the region located south of the study area, by De Wit (pers. comm., 1984), and will not be elaborated on any further in this study.

2. A tectonic contact is inferred between unit 2 <ONV> and unit 3 <LG>. Both units comprise D2 folds but young in the opposite direction while the contacts runs along a NE/SW direction and is thus not folded (Fig. 6.2). Unit 3 forms the Waterfall Synclinorium (Fig. 6.2). The contact, tb, is interpreted as a thrust but is mainly obscured by alluvium and thick forests. Unit 2 <LG> is thought to have been overthrust on unit 2 for the following reasons: both units are steeply dipping to the east, unit 2; <ONV> being structurally overlain by unit 3; <LG>. In addition, there is a klippe of Lower Group material which overlies talc shist, <ONV>, of unit 2 (Fig. 6.2). The dip of the schistosity in this klippe is 20°. These features are shown in figure 6.28.

3. The Waterfall Synclinorium (unit 3) is structurally overlain by unit 4. Younging directions in spheroid bearing cherts of unit 4 indicate that younging is to the east. This contrasts with younging directions in the Waterfall Synclinorium. To the south, unit 4 is separated from unit 2 by sheared serpentinite lenses and talc schists, and only unit 2 was overturned prior to D2 (Fig. 6.7, section 6.2).

4. Unit 4 <ONV> is in turn overlain by the Xecacatu Syncline, unit 5 (section 6.3.2, Fig. 6.25).

5. The Xecacatu unit is overlain by unit 6, <ONV> (section 6.3.2, Fig. 6.25).

6. Unit 6, <ONV>, is overlain by the Emlembe Syncline to the north (tf) (unit 7) and by the Simbubule Syncline to the south (unit 9). Both synclines are overturned to the west, along NE/SW trending axes (section 6.3.1, Fig. 6.18).

7. The Emlembe Syncline (unit 7) is overlain by unit 9 <ONV,LG> which forms the Simbubule Ridge. The contact, th, is dipping 30° to 65° SE and is marked by a ferruginous shear zone (Fig. 6.18).

8. Unit 9 <ONV,LG> truncates unit 6, <ONV>, unit 7 <LG> and unit 8 <LG>. North of the T-Junction, the Simbubule unit (unit 9) forms a distinct angular discordance with unit 8 <LG>: the T-Junction Thrust; (Fig. 6.20, section 6.3.1),th. The contact between unit 9 and unit 6 dips between 30° to 60° SE. While unit 6 only contain thin bedded turbidites, unit 9 contain thick bedded turbidites (Fig. 6.36)

9. Unit 9 (Simbubule) is in turn cross-cut by unit 10 (ONV), (Fig. 6.2). The later unit contains an overturned D1 tectono-stratigraphy (section 6.2.1; Fig. 6.3, loc. B).

10. Unit 10, <ONV> and unit 9, <ONV,LG>, are cross cut by unit 11, <ONV> (Fig. 6.36). The contact (tj) is marked by serpentinite lenses schists and talc schists, mafic (ferruginous shear zones). It corresponds to the Manhaar Fault (Viljoen and Viljoen, 1969 d; Büttner, 1983).

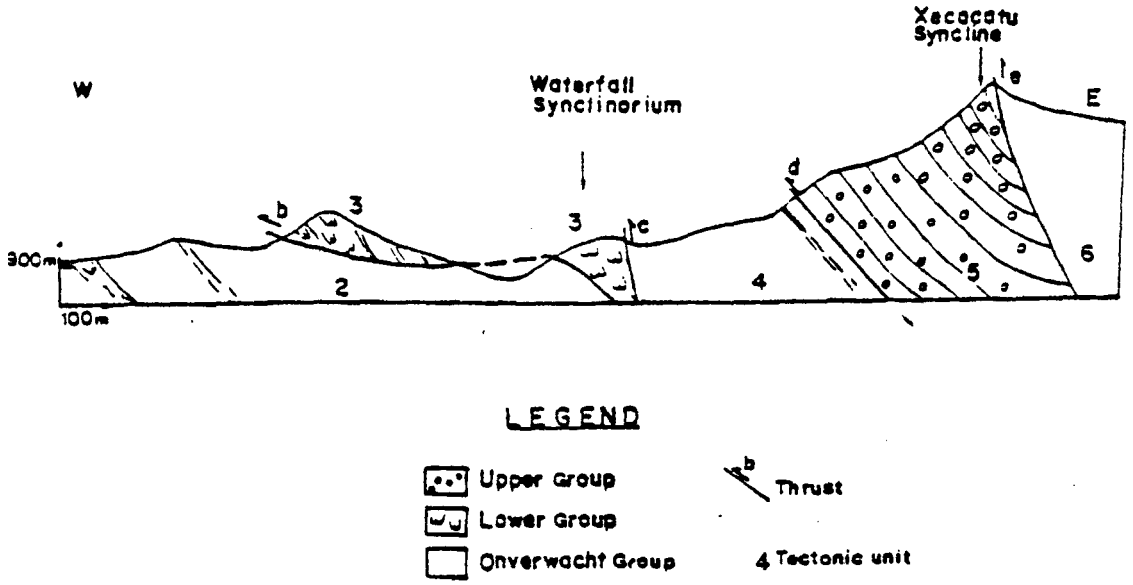


Figure 6.28 Cross section showing a klippe of Lower Group material over unit 2, <ONV>.

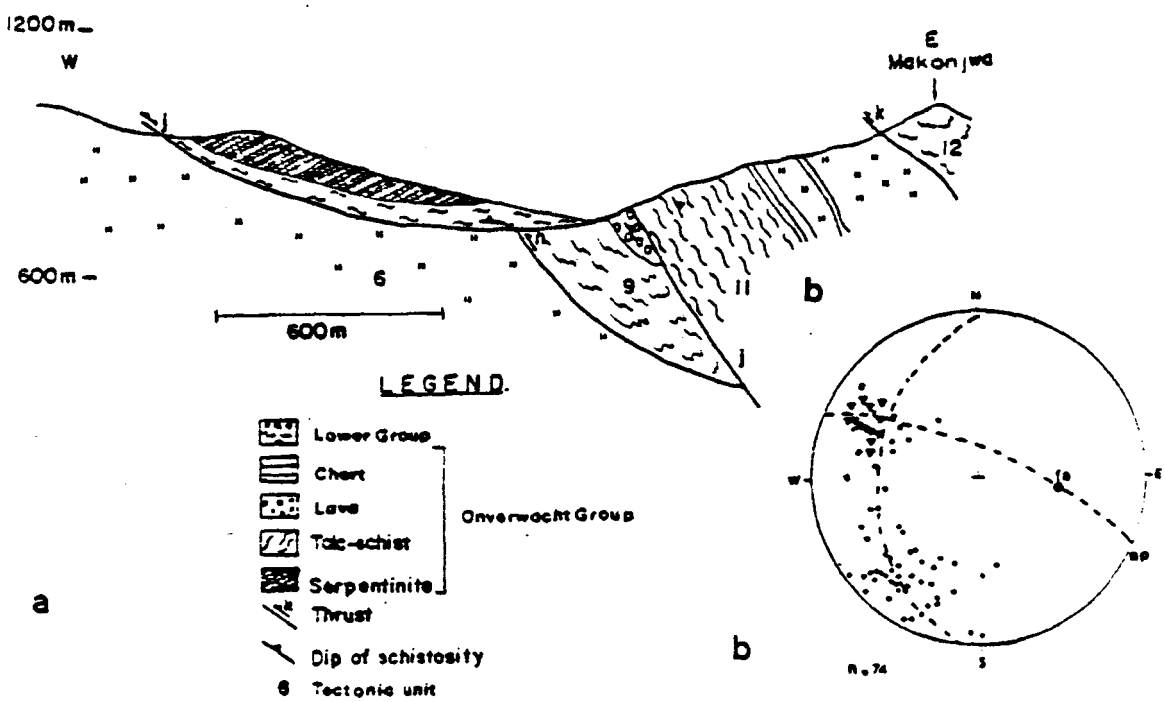


Figure 6.29.a = Interpretative cross sections in the ramp of unit 1 Diepgezet Farm (see Fig. 6.2).

b = Equal area projection of the f2 folds in the ramp; • = pole to bedding; ▲ = pole to D1 fabric; fa = fold axes; ap = axial plane; n = number of measurements; dotted line = best fit great circle, visually estimated.

The presence of serpentinite lenses and talc schists along the Manhaar Fault, both on surface and underground in the Msauli Mine (Büttner, 1983), evidence of opposite younging direction on each side of the fault (Büttner, 1983) suggests that the Manhaar Fault represents a thrust fault. Barton (1982) also suggested that the Havelock serpentinite body, located along strike from the Manhaar Fault, in Swaziland, had been emplaced on the cool leading edge of a major thrust. In this study, the Manhaar Fault will thus be referred to as the Manhaar Thrust (tj).

In the southern part of the Havelock Spruit, the trace of the Manhaar Thrust is arcuate and cuts across units 9 and 6 (tj, Fig. 6.36). A small lens of Lower Group conglomerate is exposed within this flexure which is interpreted as a ramp or an out of sequence thrust. It could have formed through contractional or extensional faulting. The lens of conglomerate is believed to represent a tectonic window into unit 9 <LG>. A section across the ramp is shown in figure 6.29a. Within the ramp, lapilli bearing cherts are folded over sheared serpentinites. The folds are plunging 50° SW and their axial planes strike 110° dipping 76° NE, broadly parallel to the orientation of the ramp. Due to late faulting, poor exposure and the lack of good younging directions, the pre-D2 orientation of the cherts could not be determined.

The Manhaar Thrust is cross-cut by the Masilela Porphyry (Fig. 6.2) which has been dated at 2.7 Ga (Büttner et al., 1983); this relationship gives a minimum age of 2.7 Ga for D2.

The Manhaar Thrust (tj) is overlain by a series of secondary thrust slices which form the Makonjwa Tectonic Complex (unit 12). This tectonic Complex has been studied in detail in Swaziland by Lamb (in prep.). In the study area, several thin structural units have been identified within the complex (Fig. 6.33c, Map). The thrusts are marked by ferruginous shear zones, mafic schists, serpentinite lenses and schistose spheroid bearing units. Because of the lack of well exposed contacts, stratigraphic markers, and younging directions, and due to the intense iron and silica metasomatism, it is often difficult to attribute the chert bands to either the Onverwacht or the Lower Group (Chapter 5). Thus, it has not been possible to determine if the tectonic slices were emplaced during D2 only or if an early D1 phase of thrusting has been reactivated by D2. In the Makonjwa Tectonic Complex,

the thrust slices have a NNE-SSW orientation and and dip 35° to 85° to the east.

As seen in the above descriptions, the axial planes of most F2 folds are broadly parallel to the thrust contacts. However, in the Xecacatu and Simbubule Synclines, the fold axes are cross-cut by the overlying <ONV> units (Fig. 6.25, loc. G, section 6.3.2, main Map). Such relationships indicate that folding was contemporaneous with the emplacement of the thrusts. In unit 11, <ONV>, the axial planes of the folds in the ramp are nearly perpendicular to the Manhaar Thrust (Fig. 6.29 a,b) and thus folding could have predated the thrusting in this area.

The various relationships discussed above indicate that D2 represents an extended phase of horizontal shortening perpendicular to a NE/SW trending axis.

6.4 THIRD PHASE OF DEFORMATION: D3

D3 is manifested by E/W oriented large scale open to tight folds (f3). Faulting (ft3) along ENE/WSW to ESE/WNW trends has frequently accompanied the formation of D3 folds. An S3 schistosity which ranges from 090,75°N to 130,80°N is locally developed in the Lower Group ferruginous shales. In unit 4, a S3 spaced cleavage striking 110° and dipping 80° S is found within mafic pillows. F3 folds have been recognised in unit 4, unit 5 and unit 9, and are described below.

(a) f3 folds in unit 4

In this unit of Onverwacht material, superposition of f3 folds on both D1 and D2 structures in clearly evident (Fig. 6.7, 6.30). F3 axial planes vary in strike from 080°to 130°and dip steeply to the north or to the south. The F3 folds have steep plunges to the SW (Fig. 6.7, loc. C) and to the SE (Fig. 6.7, loc. B, Fig. 6.30). The unconformity between the Lower and Upper Groups in the Manzima Valley appears to be refolded by f3 (Fig. 6.31, Chapter 4). The structure is not easily analysed due to lack of bedding in the Upper Group conglomerates and vegetation cover. However, two superposed phases of folding (f2 + f3) can be inferred from the following features: First, the syncline developed at this locality has a double closure and forms a basin pattern (Fig. 6.31). Both closures are near to vertical and the long axis of the basin strikes 120° An f3 isoclinal antiform, with an axial plane striking 130° and dipping 80°SW, is adjacent to the syncline. The antiform is underlain by a brecciated and sheared zone in which various types of fragments occur: ferruginous shale, broken pillow lava; carbonated lapilli; D1 tectonite; and black chert. It has the aspect of a tectonic mélange (Hsü, 1973).

(b) f3 in the Waterfall Synclinorium (unit 3, fig 6.2).

Within the synclinorium, a large-scale D3 folds which plunges steeply to the west is clearly defined by ferruginous tuffs with an axial plane striking 104°and dipping 60° SW. (Fig. 6.32 a,b).

(c) f3 in the Xecacatu Syncline (unit 5, Fig. 6.25).
In the southern part of the Xecacatu Ridge, the Xecacatu Syncline is refolded by large scale f3 folds along 080°, 70° N oriented axes. A cross-section illustrating the refolding is presented in figure 6.33b. As can be seen in this figure, the western part of the ridge contains only one limb of the D2 syncline and is folded into a D3 syncline together with the overlaying <ONV> unit (unit 6). The eastern part of the ridge contains both limbs of the D2 syncline and is refolded by a D3 anticline. ENE/WSW trending faults (ft3) are developed between the two D3 folds and appear to represent accommodation features.

(d) f3 in the Simbubule Syncline (unit 9, Fig. 6.2). The f2 fold axis of the Simbubule Syncline is refolded into a large scale f3 open fold. Although this fold can be seen on the outcrop pattern of the conglomerate, it is difficult to trace due to the lack of bedding and younging directions. However, small scale f3 folds in ferruginous shales, on the eastern limb of the Simbubule Syncline, indicate that f3 fold axes are steeply plunging to the north and that the axial planes vary in strike from 090° to 130°.

6.5 THE LAST PHASE OF DEFORMATION: D4

Throughout the study area, faults with a SE/NW to N-S orientation cut through the stratigraphy, forming deep and narrow valleys. These faults cross-cut D1, D2 and D3 structures and dolerite dykes are commonly found along the fault planes. F4 faults are generally clearly visible on aerial photograph but are frequently inaccessible in the field because of dense, impenetrable vegetation.

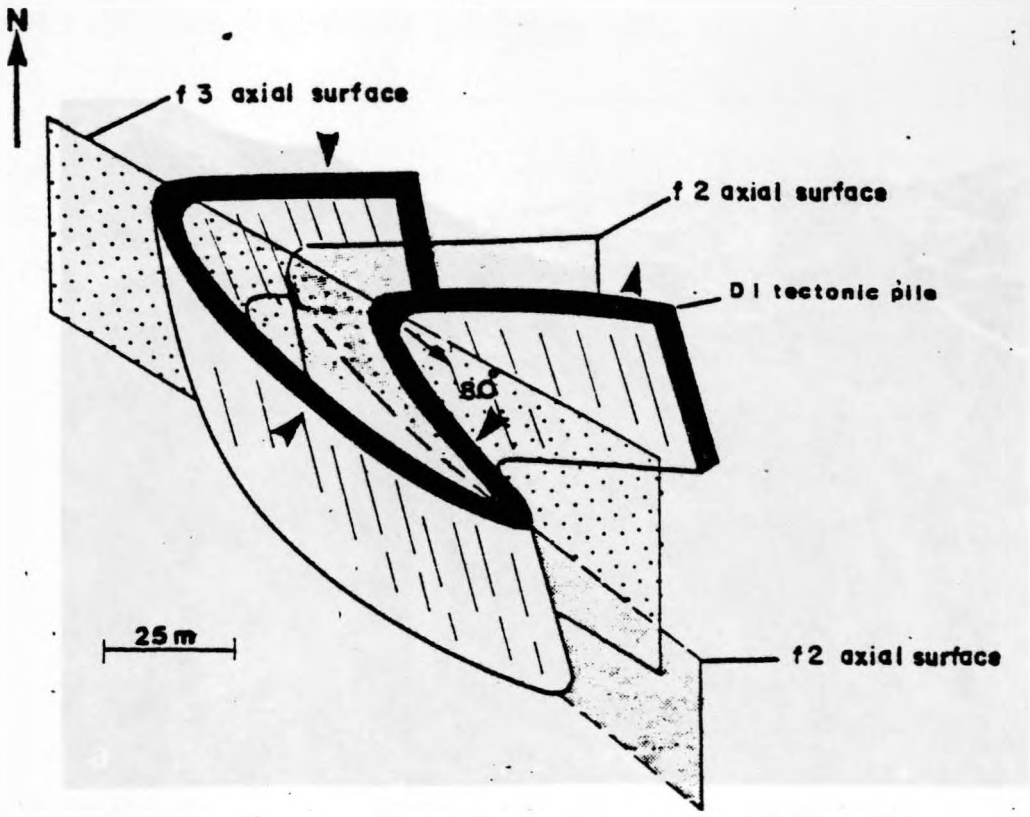


Figure 6.30. = Diagram showing the refolding of f2 folds by f3 in the Dunbar Valley

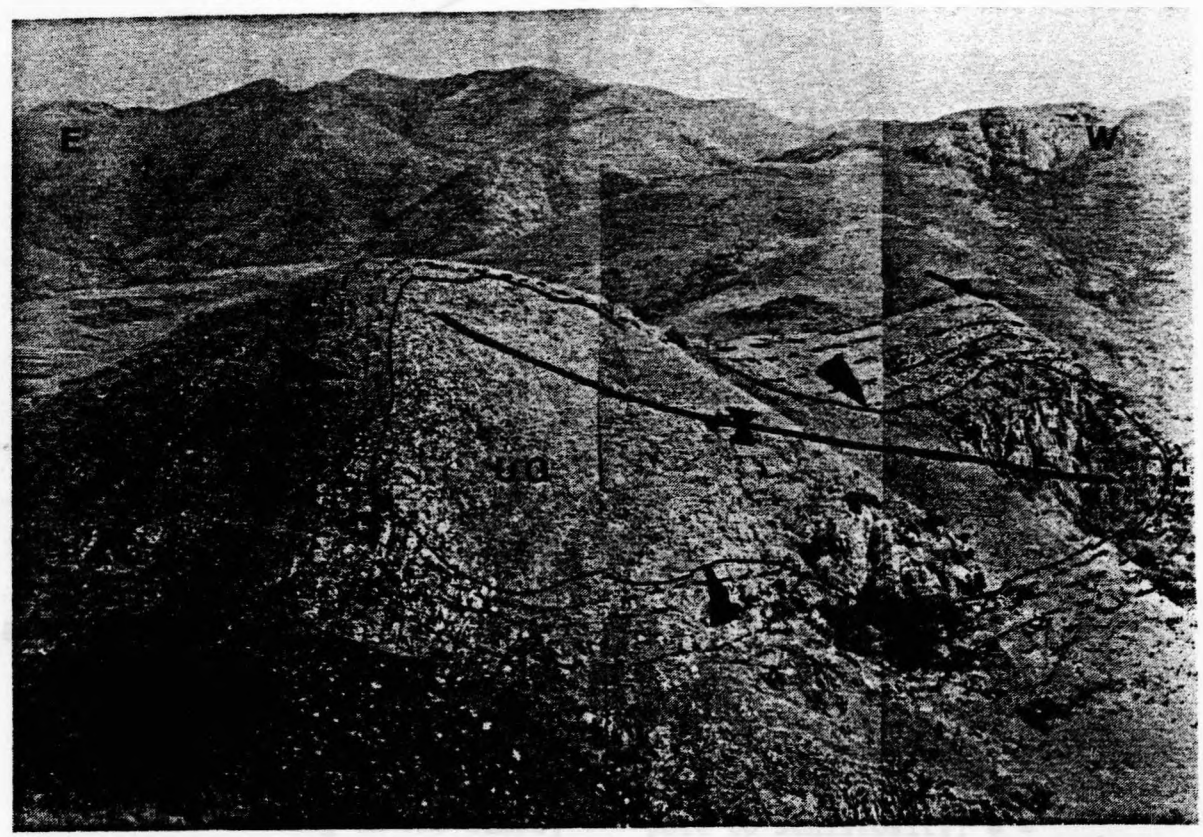
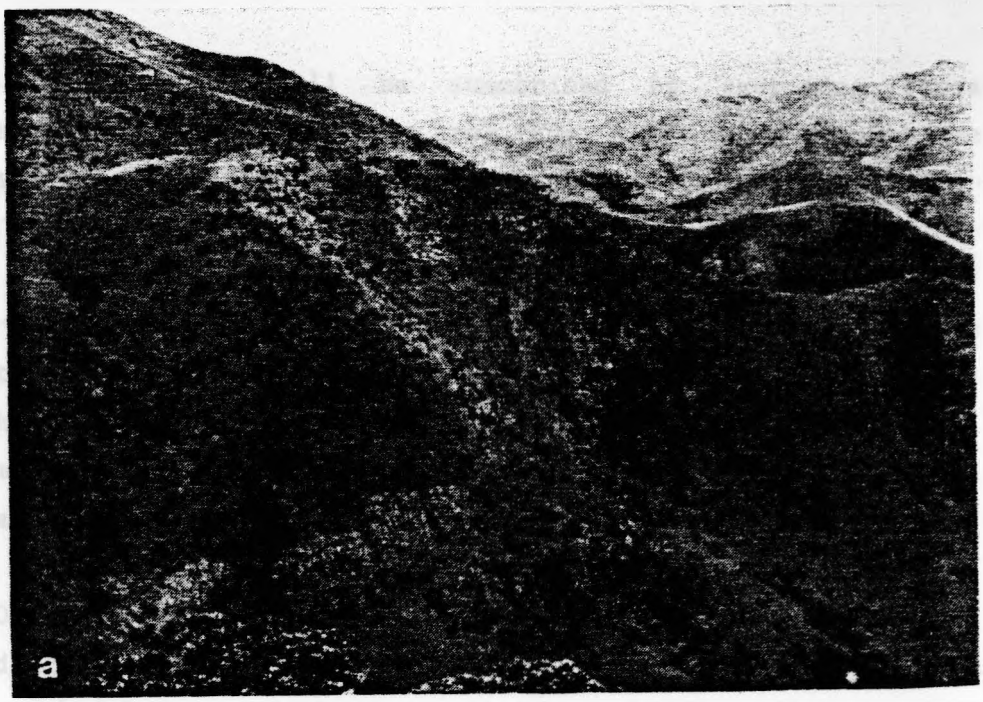


Figure 6.31. = Photograph of the basin pattern of the folded uncomformity in Manzima Valley. UG = Upper Group, d = dolerite. View looking East - Dunbar Farm.



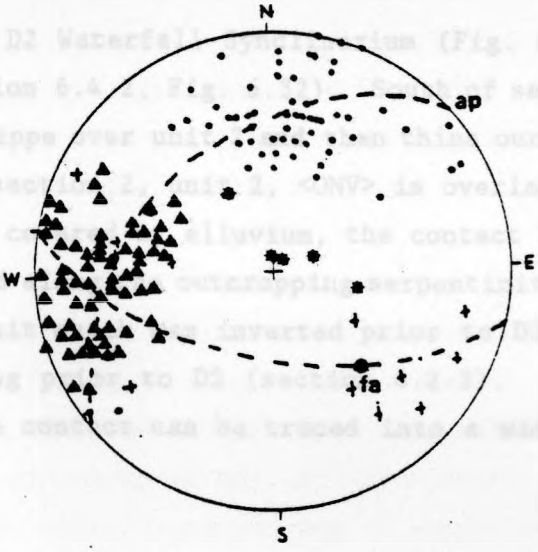


Figure 6.32.a = f3 fold in ferruginous tuff, unit 3 Fig. 6.15. View looking South Josefdal Farm

b = equal area projection of the f3 fold shown in Fig. 6.32.a ▲ = pole to bedding in the hinge zone; • = pole to bedding in the limbs; + = pole to schistosity; ✱ = pole to lineations, fa = fold axis; ap = axial plane; n = number of measurements; dotted lines = best fit great circle, visually estimated.

6.6 SUMMARY OF THE POLYPHASE DEFORMATION

The polyphase deformation will be summarised by examining three cross-sections through the entire study area (Fig. 6.33) together with the Map. From west to east, the following structural units are encountered:

1. Unit 1, <UG>. the base of this unit rests unconformably on the Onverwacht Group and Lower Group material (A.2 Map) (see also De Wit, 1983). This structural unit can be traced southward into the Sigadeni Thrust Complex (A. 5.8 Map, section 6.3.3) but reappears south of the study area (De Wit, pers. comm.).

2. Unit 2, <ONV>, is overthrust on unit 1 and folded by D2. This unit was overturned during D1 (section 6.2.3). The contact between unit 1 and unit 2 is marked by tectonic breccia and lenses of serpentinite.

3. Unit 3, <LG>, forms the D2 Waterfall Synclinorium (Fig. 6.33a), which is refolded by f3 (section 6.4.2, Fig. 6.32). South of section 1 (Fig. 6.33a) unit 3 forms a klippe over unit 2 and then thins out (Fig. 6.28). Thus, at the level of section 2, unit 2, <ONV> is overlain by unit 4, <ONV>. Although mainly covered by alluvium, the contact between these two units has been placed along the outcropping serpentinite lenses (E.6 Map) which separate a unit which was inverted prior to D2 from a unit which was normal facing prior to D2 (section 6.2.3). South of the Dunbar Valley (A.8), the contact can be traced into a wide shear zone (De Wit, pers. comm.).

4. Unit 4, <ONV>, is present on surface north of section 1 in two lenses (G.3, H.2 Map) and south of section 1 where it overlies unit 2. Similarly to unit 2, it comprises D1 stacks which have been folded by D2 and D3. South of section 2, f3 folds deform the unconformity between Upper and Lower Groups (section 6.4.1, Fig. 6.31).

5. Unit 5, <UG> contains the Xecacatu Syncline (section 6.3.2, Fig. 6.25, 6.26, 6.27). North of section 1 (I.1 Map), the axis of the syncline changes orientation from NE/SW to NW/SE. This change probably indicates the presence of a ramp structure. However, due to the lack of exposure,

the contact between unit 3 and 5 is difficult to trace. The Xecacatu Syncline is refolded by D3 in the south (Fig. 6.33b, section 6.4.3).

6. Unit 6, <ONV> cross-cuts the eastern limb of the Xecacatu Syncline (E.4,Fig. 5.25, section 6.4.3). This unit comprises a D1 stack, folded into an anticlinal neutral by D2. South of section 2 (D.8 Map) it forms a ramp which partially overlies the unconformity between the Upper and Lower Groups. North of the road leading to Barberton (I.2 Map) unit 6 thins out and unit 7 directly overlies unit 5. On the northern side of the cableway, exposure is very poor and unit 6 might be present as thin lenses of mafic schists.

7. Unit 7, <LG> is only present north of section 1 and contains the Emlembe Syncline (section 6.2.1).

8. Unit 8 <LG>, which is only present north of section 1 (H.4 Map), has already been discussed in section 6.3.1 (Fig. 6.18, 6.19 c,d).

9. Unit 9, <ONV,LG> contains the Simbubule Syncline (D2) which is refolded by D3 (section 6.4.4). North of section 1, it overlies unit 8 (H.4 Map) and unit 7 (I.3 Map). South of section 3, unit 9, <LG>, also outcrops as a tectonic window below unit 11 <ONV> (H.9 Map) (section 6.3.2, Fig. 6.33c).

10. Unit 10, <ONV> is an overturned unit which contains several D1 thrust slices (section 6.2.2, I.3 Map). North of section 1 (I.4/5 Map), a vertical fault has been observed in this unit, separating a NW/SE oriented D1 stack from a near vertical unit of black chert. This area has not been investigated in detail because, due to dense vegetation, outcrop is poor and access is difficult. Moreover, it has not been possible to determine if the black chert belongs to the Onverwacht or to the Lower Group. Thus, it is not known to which phase of deformation (D2, D3, or D4) this fault is related. For the reasons outlined above, the contact between unit 9 <LG> and unit 10 <ONV> is also difficult to follow on the eastern slopes of Simbubule. However, the contact is clearly visible in the landscape when viewed from the Makonjwa Ridge and from Swaziland. It has been refolded and faulted by D3.

11. Unit 11, <ONV>, is overlain by the Manhaar Thrust (section 6.3.3). A NW/SW oriented ramp is developed at the level of section 3 which contains f2 folds and is intruded by the Masilela Porphyry (Fig. 6.9, 6.7, H.7 Map, section 6.33c, Fig. 6.33c).

12. Unit 12, <ONV,LG> represents the Makonjwa Tectonic Complex (section 6.33c, Fig. 6.33 b,c).

6.7 THRUST EMPLACEMENT: A KINEMATIC DISCUSSION

The formation of mountain belts in general is currently explained by two main schools of thought. Van Bemmelen (1960; 1972; 1975), Aubouin (1965) and Ramberg (1981), amongst others, all maintain that mountain building and plate tectonics are mainly the result of vertical movements such as a diapiric rise of plutons, and upwelling movements in the mantle. On the other hand, Dewey and Bird (1970), Le Pichon (1968), Tapponier and Molnar (1976), and others, believe that tangential forces are principally responsible for the formation of orogenic belts. However, both theories agree that, on a smaller scale, thrust emplacement is due to movements, up or down slope, caused by gravitational forces. Down slope movements can be ascribed to gravity instability or gravity sliding. Up slope movements can be caused by gravity sliding (push from the rear) and by gravity spreading due to overburden pressures.

The secondary role of gravity in the formation of thrusts is now well established (Price, 1977; De Jong and Scholten, 1973; Ramberg 1981; McClay and Price, 1981). Various mechanisms have been developed for the formation and the emplacement of thrust sheets and nappes in a number of different tectonic settings, predominantly from Phanerozoic examples.

The mechanisms proposed can be divided into three main types, which are briefly summarised below.

(1) Diverticulation:

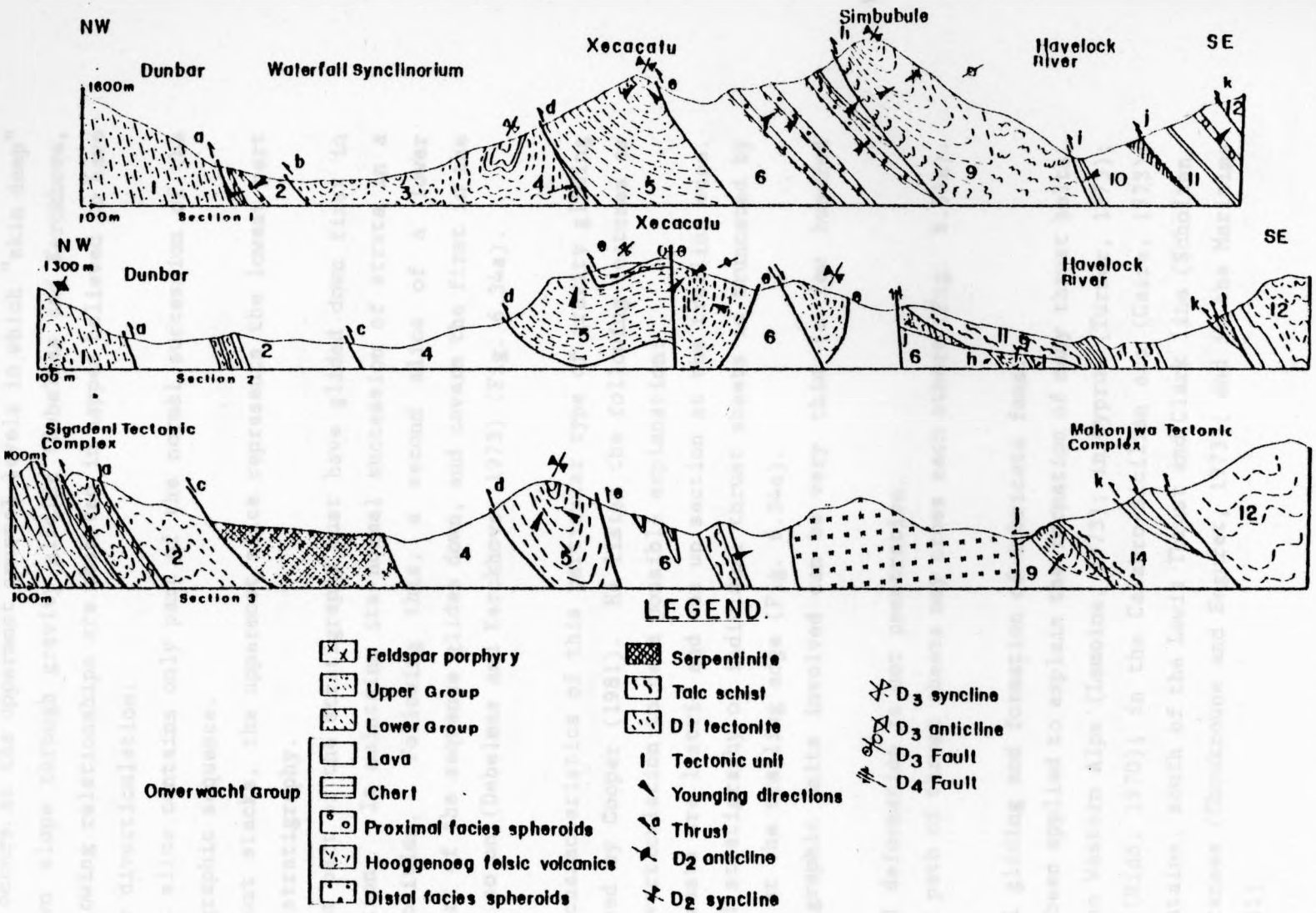


Figure 6.33.a,b,c. Cross-sections showing the superposition of the four phase of deformation (location on Fig. 6.2).

This process was first described by Lugeon (1943) for the Ultrahelvetic nappes at the base of the Pre-alpine nappes, and revised by Debelmas and Kerckhove (1973).

Diverticulation occurs at the uppermost crustal levels in which "skin deep" nappes move down slope through gravity gliding (Debelmas and Kerckhove, 1973). The following relationships are observed in nappes believed to have been emplaced by diverticulation:
(i) Every thrust slice contains only part of the normal succession of the original stratigraphic sequence.
(ii) In the thrust stacks, the uppermost slice represents the lowest part of the original stratigraphy.
Thus, the highest part of the stratigraphy must have glided down first in its final position. It maintains its normal succession of strata in a right-way up position. Following this, a second slice of a lower stratigraphic part of the sequence glides down, and covers the first in the same manner, and so on (Debelmas and Kerckhove, 1973) (Fig. 6.34a).

The geometrical characteristics of this particular type of gravity gliding have been reviewed by Cooper (1981). He listed the following features as essential for diverticulation to be a possible explanation:
(i) The basal thrusts are listric and cut up section at the trailing edge.
(ii) The internal stratigraphy of individual thrust sheets is truncated by the basal thrust at the trailing edge (Fig. 6.34a).
(iii) The stratigraphic units involved can be very thin (a few hundred metres).
(iv) The internal deformation is not penetrative.
(v) The transport path of thrust sheets may cross each others (Fig. 6.34a).

(2) Gravitational gliding and formation of imbricate fans:
This process has been applied to explain the formation of many thrust belts, for example in the Western Alps (Lemoine, 1973); in Cyprus (Turner, 1973); in New Zealand (Ridd, 1970); in the Calabro-Sicilian arc (Caire, 1973); in the Rocky Mountains, south of the Lewis Thrust and Clark line (Scholten, 1973); in the Pyrenees (Choukroune and Seguret, 1973); and in the Maritime Alps (Graham, 1981).

In this process, thin slabs detach themselves from a basement to glide down the palaeoslope. The resulting thrust stack forms a tectonic succession

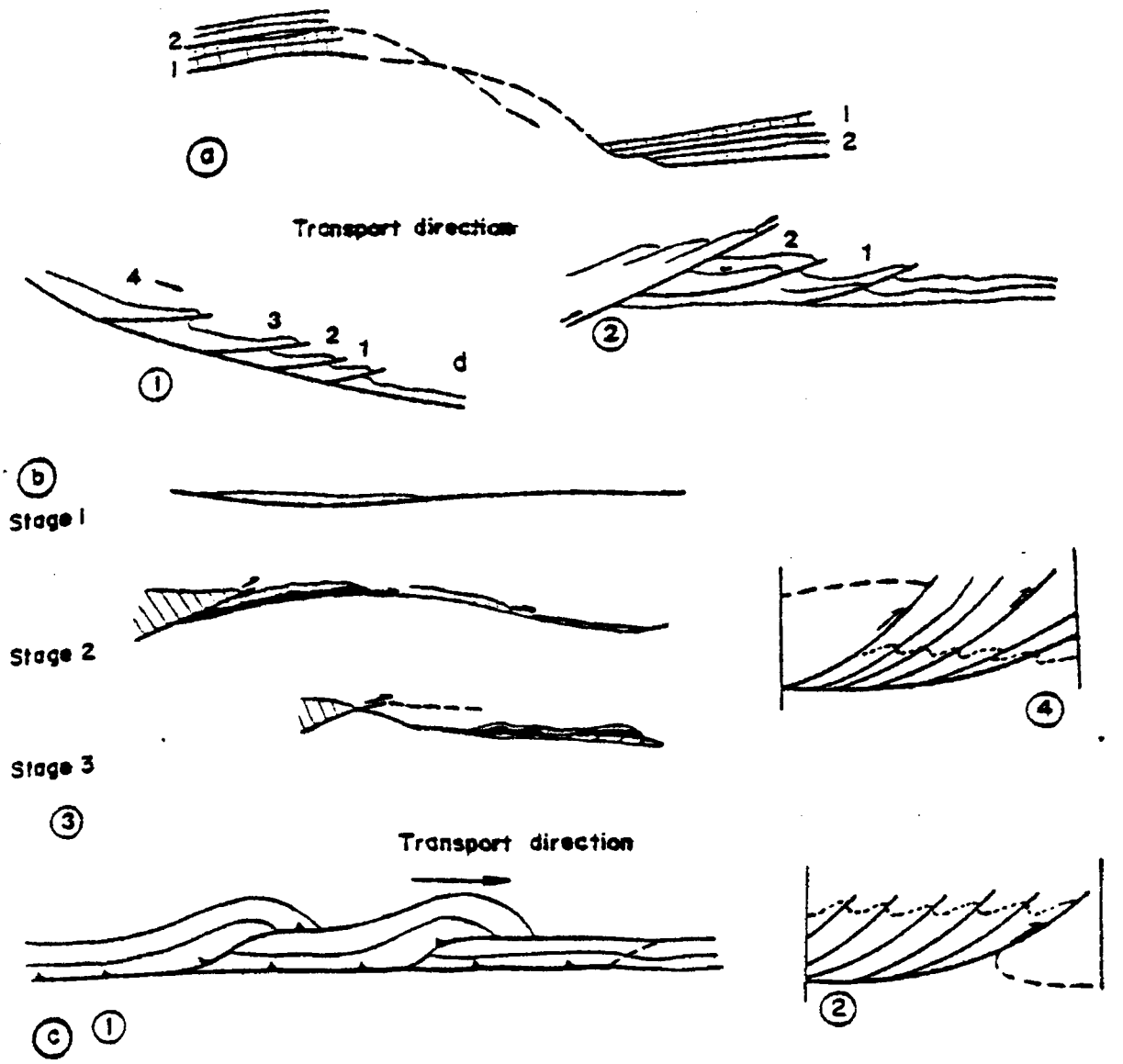


Figure 6.34 a) diverticulation mechanism (modified after Lemoine, 1973).

b) formation of an imbricate fan by gravity sliding (1) free gravity sliding , (2) sliding induced by a push at the rear (after Lemoine, 1973), (3) imbricate fan (after Sholten, 1973), (4) resulting trailing imbricate fan

c) gravity spreading (1) mechanism (2) imbricate fan resulting from gravity sliding (after Cooper, 1981)

which can be markedly different from the original one (Fig. 6.34b). The geometric characteristics of such a stack is that of a trailing imbricate fan. Up slope movement can also occur during the formation of a trailing fan (Lemoine, 1973, Fig. 6.34b). Trailing edge imbricate fans are marked by the following features (Boyer and Elliott, 1982):

(i) The basal thrust surfaces are listric and cut up section in the direction of transport at the leading edge.

(ii) At the trailing edge of each individual thrust, the internal stratigraphy is truncated by the overlying thrust sheet and not by the basal thrust surface (Fig. 6.34b).

(iii) In trailing imbricate fans, the highest sheet is the one formed last.

(iv) There is not necessarily any lateral stratigraphic continuity between successive thrust sheets.

(v) The potential amount of displacement between thrust sheets can greatly exceed the section length of individual thrust sheets (Cooper, 1981).

(3) Gravitational spreading:

This concept was first introduced by Bucher (1956) to explain thrusting in the foreland of the Canadian Rocky Mountains (Dahlstrom, 1969; Price, 1973; Ramberg, 1981).

In this mechanism, the initial thrust sheet moves up slope toward the foreland margin to overlie younger or older rocks. As the emplacement continues, the underlying rocks eventually attain their critical shear stress for failure due to the overburden. Thus, new thrusts cut under and ahead of older ones. Thrust slices are derived from the footwall and accreted onto the hanging wall. As a new thrust slice is initiated, it carries the older thrusts along in a piggy-back fashion (Elliott, 1976). Such a mechanism may lead to the formation of leading imbricate fans (Boyer and Elliott, 1982).

The geometrical characteristics of leading imbricate fans formed by gravitational spreading up slope are similar to trailing imbricate fans (Fig. 6.34c). In addition, there is lateral stratigraphic continuity between successive thrust sheets (Elliott, 1976). The amount of relative displacement between thrust sheets rarely exceeds the cross-strike length of the underlying thrust sheet (Cooper, 1981). Piggy back stacks always have a systematic order to the tectonic superposition (Elliott, 1976). The flat ramp trajectory causes the development of an anticlinal bulge over the

ramp due to the displacement of the hanging wall over the foot wall (Coward, 1983) (Fig. 6.34c).

In both leading and trailing imbricate fans, the thrust planes shallow at depth to meet a basal décollement surface (Boyer and Elliott, 1982; Coward, 1983). At surface level thrusts with dips steeper than 45° are due to later deformation according to Price (1973; 1981). However, Boyer and Elliott (1982) feel that both leading and trailing imbricate fans can meet the ground surface with a dip of 60°.

In this study, the two phases of thrusting are treated separately. Possible kinematics are discussed from the field evidence and the geometry of the thrust sheets.

6.7.1 THE FIRST PERIOD OF THRUSTING (D1)

The first deformation event (D1), is manifested in the field by the tectonic repetition of very thin stratigraphic units (5 to 150m thick) without any change in younging direction. Each tectonic unit is separated from its neighbours by fuchsitic tectonites (section 6.2.4). In some cases (Fig. 6.8) the D1 tectonics stacks, were overturned (downward facing) prior to D2 (section 6.2.3, Fig. 6.34).

Flaser banded rocks and brecciated lavas can be traced along and across strike into undeformed mafic igneous rocks. Thus, detachment was probably initiated within igneous rocks. These were located both below and within Onverwacht sedimentary rocks as indicated by the presence of 1 to 3m thick chert layers with silicified spinifex textures within the silicified sedimentary rocks of the Onverwacht Group. It is suggested that décollement within igneous rocks occurred both below and within the sediments. This would lead to the formation of very thin (5m minimum) structural units such as those found in the study area (Appendix 1, Fig. 6.3).

D1 décollement occurred through hydraulic fracturing and shearing at the interface between sedimentary and igneous rocks, where zones of high pore

pressure developed probably as a result of hydrothermal activity (section 6.2.4).

Hydraulic fracturing, indicative of high fluid pressure, has often been described within thrust slides (Price, 1977; Beach, 1979; 1981; 1982). It is perhaps the most important single mechanism of deformation operative in the crust (Fyfe et al., 1978). The importance and the role of high fluid pressure in gravity sliding has been well studied (Hubbert and Rubey, 1959; Platt, 1962; Chapman, 1974; and Price, 1977; amongst others). D1 thrusting only involved a thin (several hundred metres thick at the maximum) column of rocks. Thus, the development of high fluid pressure leading to décollement cannot be the result of overburden pressure. It is interpreted as the result of hydrothermal fluids which become trapped below a silicified cap rock (De Wit, 1982). Despite the lack of data on the pre-D1 palaeogeography the presence of a shallow water facies and of a distal and proximal deep water facies in the Onverwacht sedimentary rocks suggests the presence of a palaeoslope in pre-D1 times (see Chapter 3). The following sequence of events is thought to have led to the formation of the D1 imbricates.

(i) Silicification led to the lithification of the sediments and to the formation of a cap rock.
(ii) The fractures developed through this cap rock were eventually sealed by silica precipitation.
(iii) A zone of high fluid pressure was formed under the sealed cap rock and gliding of the imbricate was initiated.
(iv) The gliding may have stopped when fluid pressure dropped due to leakages of fluid at the break away gap (Chapman, 1974; Price, 1977; De Wit, 1982).

D1 is thus interpreted as a syn-sedimentary phase of gravity sliding triggered by hydrothermal activity (section 6.2.4). Several décollement zones were probably present at different levels of the original stratigraphic sequence. Thus, the D1 mechanism might have been similar to diverticulation in the sense that unit originally on top of the sequence are now located at the bottom of the tectonic stack (Fig. 6.34a). De Wit (1982) proposed a similar mechanism for D1 and Hughes (1970) described a similar type of gravity gliding triggered by heat and fluids in the Heart Mountain (U.S.A).

De Wit (1982) suggested that the mud pool structures, indicative of mud volcanism, could represent the remnants of the pull apart gaps where sliding was initiated. An association between mud volcanism and décollement zones has been reported from New Zealand (Ridd, 1970) and in Barbados (Chapman, 1974; Westbrook and Smith, 1973; Stride et al., 1983). However, the mud structures described by these authors are kilometre wide mud diapirs where mud extrusion is accompanied by the expulsion of clasts and large mud flow sheets. Such large structures have not been observed in the Barberton greenstone belt. Smaller structures (centimetre wide), similar to those found in Barberton, have been described in New Zealand (Ridd, 1970). These structures resemble mud pool structures seen by the present author at Geyser (Iceland), Yellowstone (USA) and at the Napoli Solfatares (Italy) (cf. De Wit et al., 1982 a). These structures occur in plastic mud with a firm consistency and are always associated with abnormally high pore pressure, indicated by hydrothermal activity, and gas release (Ridd, 1970).

In the study area, mud pool structures occur in silicified ferruginous shales overlying brecciated silicified sediment. They are widely and apparently randomly distributed amongst the silicified sedimentary rocks. Therefore, it is believed that they do not represent traces of fossil pull apart gaps but are part of the early hydrothermal activity. It is proposed that silica bearing fluids and gas reached the ferruginous mud overlying the silicified sediments and led to the formation of mud pools at the water/sediment interface. The porous mud was eventually silicified by the processes described in chapter 5 and integrated into the cap rock while mud pool structures were formed in the overlying porous mud unit (Fig. 6.35).

6.7.2 THE SECOND PERIOD OF DEFORMATION (D2)

The second phase of deformation (D2) resulted in contemporaneous folding and thrusting of the entire stratigraphy present in the study area. The field data clearly indicates that D2 led to the formation of an imbricate fan which extended throughout the whole of the study area (section 6.3, Fig. 6.7, 6.14, 6.16, 6.20).

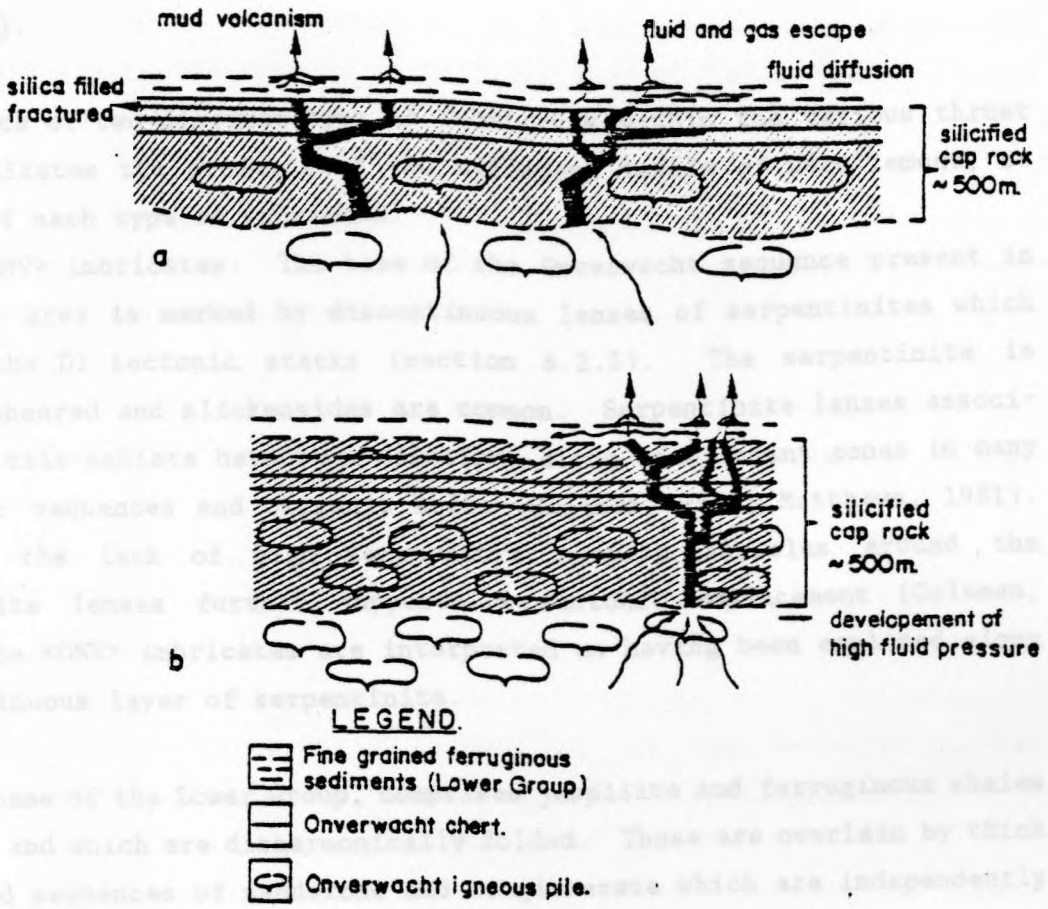


Figure 6.35. Model for the formation of mud pool structures. a) release of gas of fluids in a mud unit and development of mud pools. b) The mud unit is now silicified and mud pools form higher up in the stratigraphy.

The study of ramps and thrust contacts (Fig. 6.36) indicate that they cut up stratigraphy in a north westerly direction. Thus a NW transport direction, perpendicular to the broad regional tectonic trend is suggested for D2. Within the D2 fan, two types of imbricates can be distinguished. The first type only contains D1 tectonic units and is generally underlain by serpentinite lenses, talc schists and mafic schists (unit 2,4,6,10,11, section 6.3.3). The second type of imbricate only contains Upper Group and/or Lower Group material and the base is generally formed by folded jaspilites and ferruginous shales (units 3,5,8,12). An exception to the above occurs in unit 9 where spheroid bearing cherts, lavas and flaser banded rocks are present below the folded ferruginous shales and jaspilites (Fig. 6.36).

The presence of two distinct type of imbricates within the various thrust sheets indicates the presence of two different levels of décollement, at the base of each type of imbricate.

(i) The <ONV> imbricates: The base of the Onverwacht sequence present in the study area is marked by discontinuous lenses of serpentinites which underlie the D1 tectonic stacks (section 6.2.5). The serpentinite is strongly sheared and slickensides are common. Serpentinite lenses associated with talc schists have been described along décollement zones in many ophiolitic sequences and orogenic belts (Coleman, 1971; Matthews, 1981). Moreover, the lack of high temperature contact aureoles around the serpentinite lenses further supports a tectonic emplacement (Coleman, 1971). The <ONV> imbricates are interpreted as having been emplaced along a discontinuous layer of serpentinite.

(ii) The base of the Lower Group, comprises jaspilite and ferruginous shales and chert and which are disharmonically folded. These are overlain by thick undeformed sequences of sandstone and conglomerate which are independently folded into large scale folds. The overburden pressure of the overlying, coarse clastic sequence could have led to décollement along the ductile finely laminated basal layer. A similar mechanism has been described in detail by Kehle (1970) and has been applied in the Appalachians and in the Alps (Chapple, 1978). Several such décollement levels could have been present as jaspilites and ferruginous shales and cherts are found at different levels in the Lower Group, always overlain by thick clastic sequences (Chapter 4). As no time markers are available, it is not possible to de-

termine whether the shales and jaspilites underlying units 3,5,8,9 and 12 represent the same stratigraphic level or not.

Thus, the presence of at least two décollement zones has led to the formation of the D2 imbricate fan in the study area. To the north-west of the study area, a third décollement level appears to have existed along the unconformity between the Upper and the Lower Groups (De Wit, pers. comm.; Lamb, 1984). It is difficult to determine whether the D2 thrust sheets were moving predominantly up or down slope. Several factors must be borne in hind when attempting to decipher the mechanism operative during D2:

1. The effect of D3 on the geometry of the thrust planes cannot be assessed quantitatively, although it is believed that D3 led to the steepening of the thrust contacts.

2. Little time control is available on the emplacement of the various sheets. Thus it is not known whether the two décollement levels were acting simultaneously or not.

3. The lack of definite and well established data on the palaeolcope and palaeotopography prevent detailed palinspastic reconstruction for the time being.

Furthermore, the following relationships must also be accounted for:

1. The thrusts appear to be cutting up stratigraphy in the direction of the transport (Fig. 6.36). In unit 11, the ramp described earlier could, however, represent a contractional fault (section 6.3.3).

2. Stratigraphy is frequently missing at the contact between two thrust sheets when younger units, <LG> or <VG>, are emplaced over older units, <ONV>, which are further overlain by higher part of the stratigraphy units, <LG> (e.g.: units 1,2,3,5,6,7; Fig. 6.36). Such successions are difficult to explain with a simple thrust mechanism. This suggests the presence of both contractional and extensional faults. As no definite extensional faults have been observed in the field, pre- or syn-thrusting extensional faults are postulated. However, although such faults have been described within surge zones (Coward, 1982), the

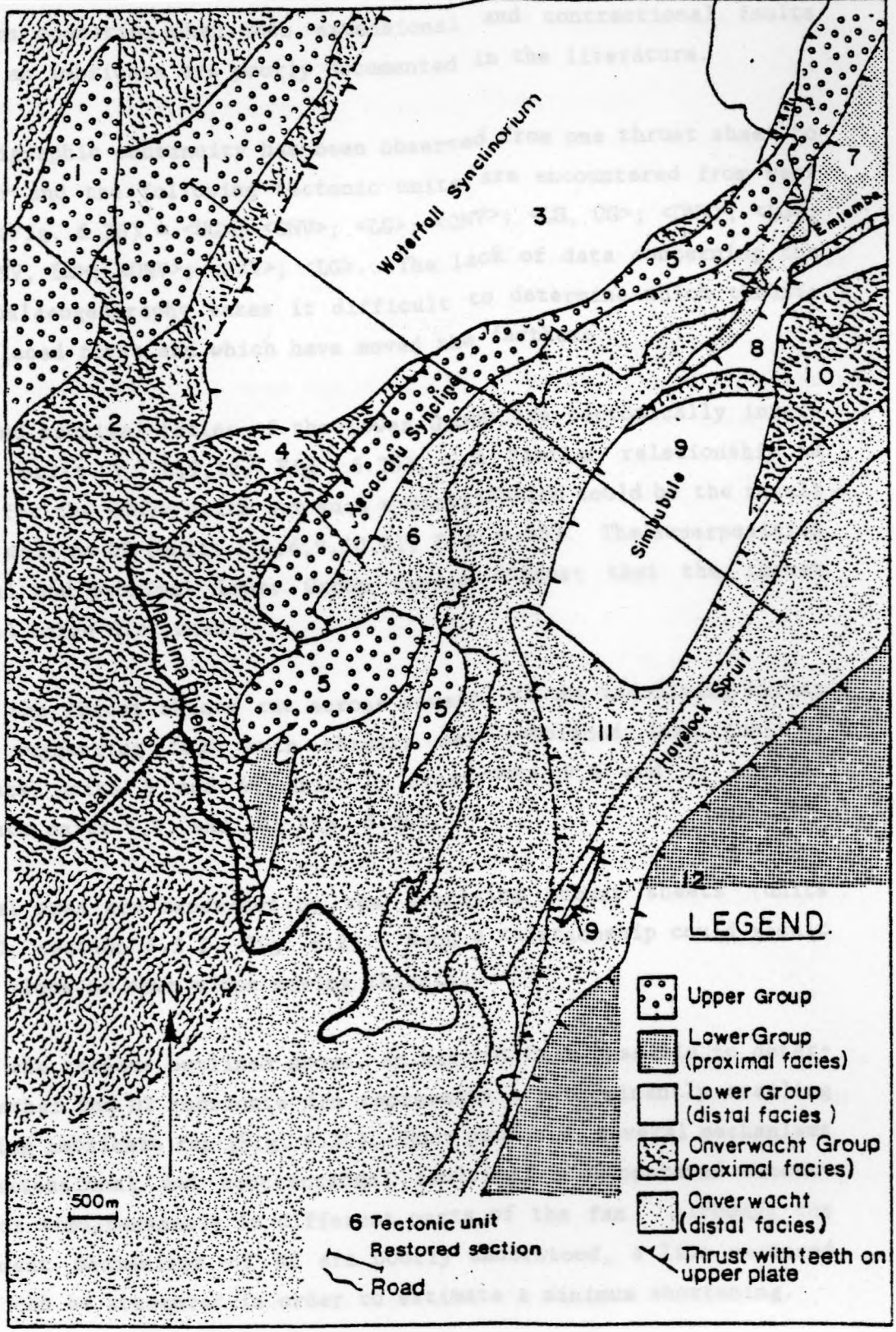


Figure 6.36 Simplified geological map showing the interstacking of distal and proximal facies. The section line indicates the location of the restored section presented in figure 6.37.

mechanisms operating when both extensional and contractional faults occur in an imbricate are poorly documented in the literature.

3. No stratigraphic continuity has been observed from one thrust sheet to the other and the following tectonic units are encountered from west to east (Fig. 6.36) = <UG>; <ONV>; <LG>; <ONV>; <LG, UG>; <ONV>; <LG>; <LG>; <ONV, LG>; <ONV>; <ONV>; <LG>. The lack of data concerning the pre-D2 palaeogeography makes it difficult to determine which thrusts were emplaced first and which have moved the farthest.

4. Distal and proximal facies of the Lower Group are tectonically inter-stacked (units 3,7,8,9,12, Fig. 6.36). A similar relationship is present for the <ONV> units but such a distribution could be the result of D1 as well as D2 (units 2,4,6,9,10,11, Fig. 6.36). The superposition of distal and proximal Lower Group facies suggest that the thrust travelled large distances.

5. Some of the thrust sheets cut across several of the underlying thrust sheets, suggesting that such thrusts were emplaced last (unit 5 cross-cuts units 3 and 4; unit 10 cross-cuts 9,8 and 7; unit 11 cross-cuts units 6,9, and 10; Fig. 6.36).

6. Synclinal axes are cross-cut by the overlying thrust sheets (units 5,6,9,10; section 6.3.2. Fig. 6.2). Such a relationship could result from up slope or down slope moving thrusts.

For all the reasons outlined above, it has not been possible to determine whether the D2 imbricate fan represents a predominantly trailing or leading imbricate fan (Fig. 6.34). Most probably, several mechanisms (e.g. extensional and contractional faulting) have operated successively or simultaneously in different parts of the fan. Although the emplacement mechanisms of D2 are poorly understood, a line restored section can be attempted in order to estimate a minimum shortening.

The following set of rules to which balanced cross-sections must comply has been complied from Dahlstrom (1969), Elliott (1983) and Hossack (1979):
i) Thrusts must always cut up section in the direction of transport.
ii) Data away from the section line should be projected down plunge on to the section.

iii) The line of section should be parallel to the slip or movement direction.
iv) A section is balanced simply by assuming plane strain.
v) If the section contains flexural slip folds, with their axes normal to the section, plane strain can be assumed as the beds will suffer no shortening or elongation along the axes.
vi) An acceptable depth to décollement must be inferred from other available data.

The section which has been used for a pre-D2 restoration does not appear to violate these rules (Fig. 6.36). The depth of the lower basal décollement has been fixed at 3km on following bases: Measured sections throughout the study area indicate a maximum thickness of 500m for the <ONV> units (upper Onverwacht and base of the Lower Group); 1060m and 1200m respectively for the proximal and distal facies of the Lower Group (see Chapter 4); and 1240m for the Upper Group (see Chapter 4). Thus, allowing for erosion, a minimum original thickness of 3km is inferred for the pre-D1 sequence present in the study area. This minimum is consistent with geophysical data which indicate that the belt has a maximum depth of 4 to 6km (Darracot, 1973).

On the assumption that the various thrust sheets were derived from originally lateral segments of the same basin, the line restored section across the entire area shows a minimum shortening of 75% (Fig. 6.37) which represents a minimum length for the following reasons:

1. The depth to the sole thrust is a minimum depth. Any increase in the depth to sole thrust on the balanced section will be accommodated in length of the flat of the thrust rather than in the length of the ramp (Butler, 1983). The height of the ramp is controlled by the thickness of the stratigraphy which is cross cut.

2. The amount of shortening due to D3 is not taken into account.

3. Only the base of the Onverwacht Group (the serpentinites) has been used for the restoration.

If a 75% shortening is accepted, it implies that prior to D2, the width of the study area has been reduced from at least 45km to 10km. Although such

an amount of shortening is high, it is close to the 80% minimum shortening calculated, with different methods, in the Swaziland part of the greenstone belt (Lamb, in press). The pre-D2 restored section still contains D1 structural units. D1 shortening cannot be unravelled from the data available in the study area. However, in view of the importance of D1 in terms of tectonic repetition, it can be safely assumed that the pre-D1 width of the basin was considerably greater.

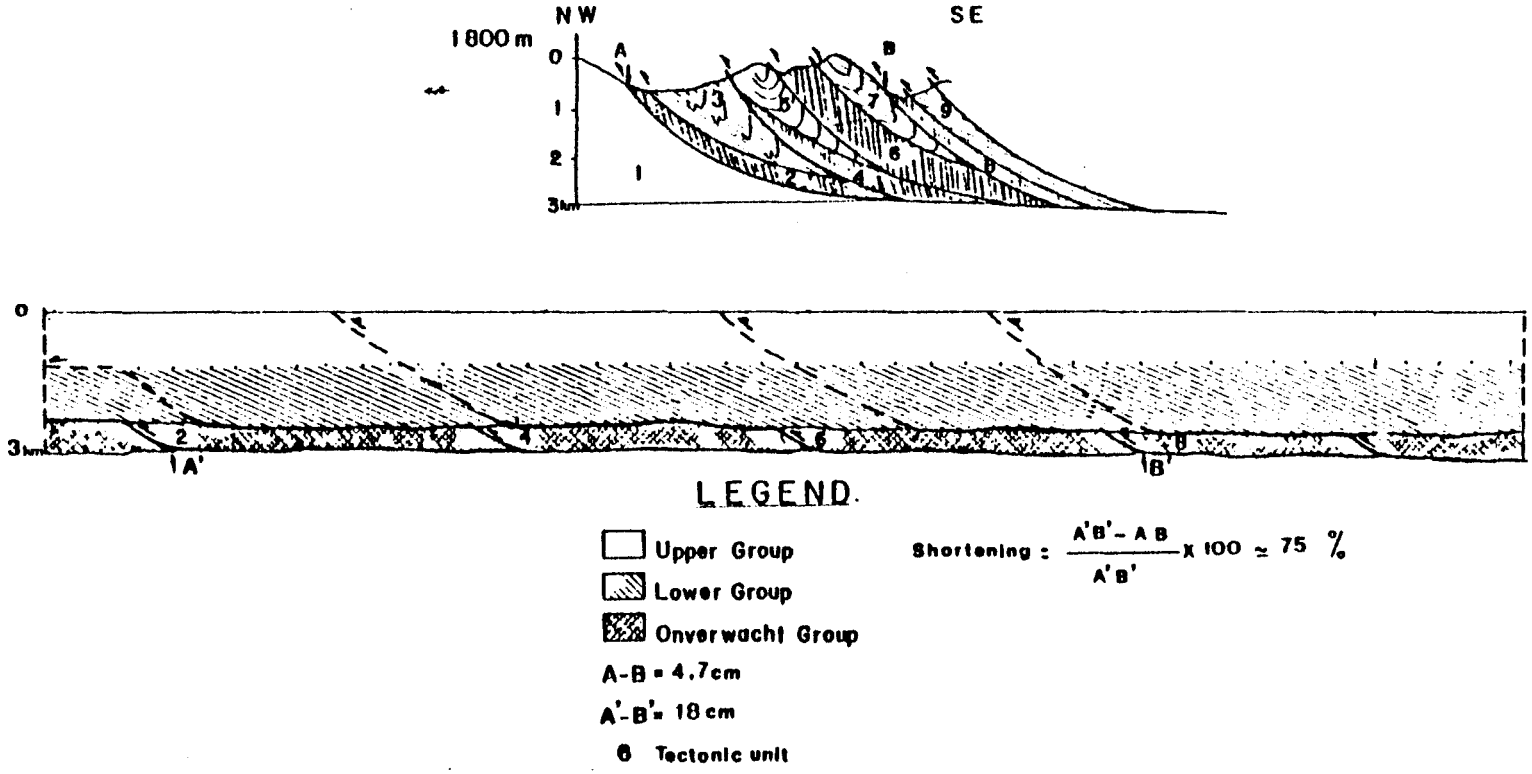


Figure 6.37 Line restored sections (see Fig. 6.36 for location)

CHAPTER 7

7.0 SUMMARY, CORRELATIONS AND TECTONIC IMPLICATIONS

7.1 INTRODUCTION

Mapping in the study area as well as the result of recent field work carried out elsewhere in the Barberton greenstone belt (Philpot, 1979; De wit et al., 1983; De Wit, 1982; 1983; Lamb, 1984; and in press) indicate that there are several severe shortcomings in the presently accepted stratigraphy of the Barberton greenstone belt (SACS, 1980). There are at least four observations which render the SACS stratigraphy impractical and outmoded:

1. Within the Onverwacht Group, tectonic repetition has been recognised to be a dominant feature and as presently defined, the Onverwacht Group represents a tectonic complex. For example, throughout the southern part of the belt, similar spheroid bearing cherts in the Theespruit, Hooggenoeg, Kromberg and Zwartkoppie Formations may have been part of the same original sedimentary unit.

2. Silicification of the upper part of the Onverwacht Group has obscured many of the original petrographical features within the stratigraphy, and has resulted in the formation of a series of cherts which have distinctly different origins. Metasomatic processes have been combined with tectonic processes to produce an apparently simple stratigraphy in which repetition of silicified units has been previously interpreted

as due to volcanic cyclicity (Viljoen and Viljoen, 1969 a-d; 1970). In the light of this work, the present stratigraphic subdivision of the Onverwacht Group into subgroups and formations must be reconsidered.

3. Evidence of syn- tectonic sedimentation have been recorded and must be accounted for in the stratigraphic column.

4. In the study area, a second phase of tectonic repetition has affected the entire stratigraphic column. Tectonic contacts have been observed within sequences previously interpreted as stratigraphic. As a result, tectono-stratigraphic units have been previously "lumped" together, without consistency, into either the Moodies or the Fig Tree Groups which were originally defined in the northern part of the belt.

7.2 PROPOSED MODIFIED STRATIGRAPHY FOR THE SOUTHERN PART OF THE BARBERTON GREENSTONE BELT

A proposed modified stratigraphy is presented in table 7.1. It is thought that this this stratigraphy can provide a useful working tool in the southern part of the belt. The bases on which this stratigraphy has been devised are outlined below:

The Onverwacht Group

The present study has shown that the previous distinction between Lower ultramafic to mafic and Upper mafic to felsic subgroups, appears to be largely the result of metasomatic and tectonic processes. Thus, the Onverwacht Group, as defined by SACS (1980), represents a tectonic complex whose igneous stratigraphy is not yet fully understood (De Wit and Stern, 1980).

In the study area, only the upper part of this complex is exposed. The Onverwacht Group originally comprised:
a unit of serpentinite;
pillowed and massive mafic to ultramafic units;
and a sedimentary unit (Table 7.1).

Table 7.1. Proposed stratigraphy

Lamb (1984)	Stratigraphy in study area		Present stratigraphic position according to the Barberton geological map (Anhaeusser et al., 1981)
Malalotcha Group (Group A) 1650m	Upper Group (1100m min.)		Moodies Group, Fig Tree Group
Group A / B	undifferentiated		
Diepgezet Group (Group B) 1850m	Lower Group (1880m min.)		Fig Tree Group
undifferentiated black & white banded cherts			
Onverwacht Group	Onverwacht Group	Sedimentary unit (100-200m?)	Zwartkoppie, Kromberg, Hooggenoeg, Theespruit Formations, Middle Marker
		Pillowed lavas	Kromberg, Hooggenoeg, Komati, Theespruit Formation
		Serpentinite	Zwartkoppie, Kromberg Formation
		mafic and ultramafic igneous rocks	Kromberg, Hooggenoeg, Komati, Theespruit, Sandspruit Formations

= unconformity

This sequence is at maximum 500m thick. Although the original thickness of the serpentinite unit is not known, it is believed that the whole of the Onverwacht Group may not have exceeded several kilometres, as suggested by De Wit and Stern (1980). This contrasts with a 14km thickness originally proposed by Viljoen and Viljoen (1969 a-d).

The Lower Group

The Lower Group conformably overlies the Onverwacht Group and comprises the lithofacies (F1, ferruginous shale, chert and tuff; and jaspilite; F2, ferruginous and tuffaceous siltstone and chert-arenite; F3, chert-arenite and conglomerate). In the study area, the maximum thickness of the Lower Group is 1880m. However, due to the presence of tectonic contacts (see Chapter 5) no complete Lower Group successions have been observed.

The base of the Lower Group may contain further unrecognised dislocation, now overprinted by the effects of metasomatism. Such would be the case if the mud pool structures are indicative of a subaerial environment (De Wit et al., 1982 a), as these structures overlie and are underlain by sediments interpreted here as deep water sediments.

The Upper Group

The Upper Group unconformably overlies the Lower Group in the study area. To the east in Swaziland, equivalent unconformable successions can be traced into conformable successions (Lamb, 1984, in press). The Upper Group is formed by supermature quartz-arenites (F4) and immature quartz-arenites and conglomerates (F5). The maximum thickness of the Upper Group is 1100m but, as for the Lower Group, complete successions have not been observed in the field area due to the presence of tectonic contacts.

7.2.1 PROBLEMS OF DEFINING THE BOUNDARIES BETWEEN THE GROUPS

a) The Onverwacht Group / Lower Group boundary

In the present study, the boundary between the Onverwacht Group and the Lower Group has been placed between the lapilli bearing cherts and the ferruginous fine grained sediments. It is proposed that the boundary be placed at this level for the following reasons:

1. Different volcaniclastic sediments occur above and below the boundary: lapilli in the Onverwacht Group, fine grained ferruginous tuff and tuffaceous and ferruginous siltstones in the Lower Group.

2. No ferruginous sediments have been noticed in the lapilli bearing cherts of the Onverwacht Group while the sediments which form the base of the Lower Group are ferruginous .

3. Evidence of current activity is abundant within the Onverwacht sedimentary rocks and rare in the overlying fine grained ferruginous sedimentary rocks of the Lower Group (Chapter 4).

Rock types of both groups frequently grade along and across strike into black and white banded cherts. Such cherts been mapped as undifferentiated. In these cherts the boundary between the two groups is obscured (see Table 7.1).

b) The Lower Group / Upper Group boundary

At three localities in the study area, the Upper Group can be observed to overlie unconformably the Lower Group. Additionally, in Swaziland, up to three separate intraformational unconformities can be distinguished within the Upper Group. The latter unconformable sequences may pass along strike into conformable sequences where a gradation can be observed from rocks which have been assigned to the Lower Group to rocks which have been assigned to the Upper Group (Lamb, 1984 and in press).

The recognition of conformable and unconformable sequences between the two groups and within the Upper Group means that the unconformities cannot be used as chronostratigraphic boundaries. Thus, in the Barberton terrane, where no time markers are available, the boundary between two groups cannot be precisely located where the contact is conformable and gradational. Additionally, some isolated tectonic units of sedimentary rocks have lithological affinities with both groups. The sandstones and conglomerates

in such units have an equal amount of cherts and quartz as well as sedimentary structures which cannot be ascribed with certainty to any of the lithofacies defined for each group. Such units occur to the north east of the study area and to the east in Swaziland (see also Lamb, 1984).

In order to prevent ambiguous stratigraphic division of conformable sequences or within tectonic units a new classification used by Lamb (1984) is adopted here. The following criteria used in this system divide post-Onverwacht sedimentary sequences into groups :

1. If two sequences are separated by an unconformity, then the upper sequence belongs to the Upper Group.

2. Sequences located below unconformities belong to the group they lithologically resemble.

3. Sedimentary rocks within tectonic units with distinct lithofacies assemblages belong to the group which is characterised by such assemblages.

4. Conformable sequences or tectonic units with ambiguous characteristics are undifferentiated.

The allocation of rocks to various groups using the above criteria is unambiguous and should prevent the confusion which has arisen from the use of the existing stratigraphy (see Table 7.1).

7.3 POSSIBLE CORRELATION OF THE DEFORMATION PHASE WITH OTHER PARTS OF THE BELT

Polyphase deformation has been reported both in the northern and in the southern part of the Barberton greenstone belt (Table 7.2). The tectonic history of the belt can only be fully reconstructed once precise correlations have been established throughout the belt. Table 7.2. presents several possible correlations, which are discussed below.

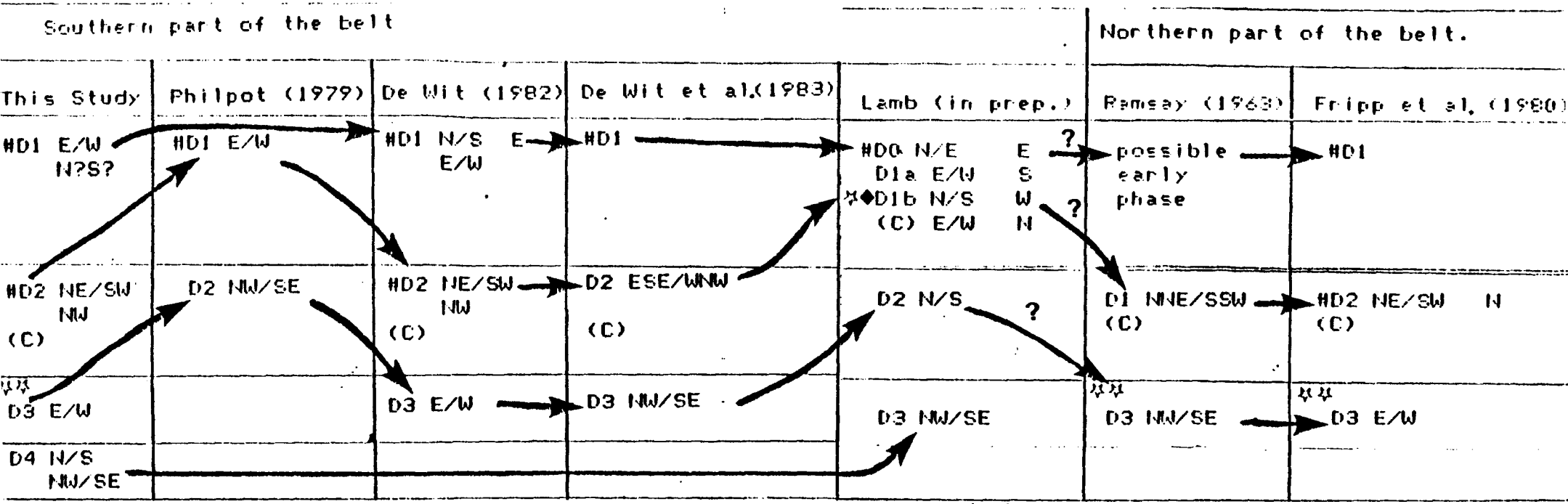
D1, in the study area, affected only the Onverwacht Group and the base of the Lower Group. It can be correlated with the early phase of deformation described by De Wit (1983) and De Wit et al. (1982 a), based on similarities in the style of the deformation and recognition of thrusts which affect similar stratigraphic units. In Swaziland, an early deformation, D2, (Lamb, 1984; in press) has also been correlated with this early phase of deformation. It is not known if the early phase of deformation present in the northern part of the belt as recognised by Ramsay (1963) and Fripp et al. (1980) also corresponds to D1 (Table 7.2).

D2 is the first cleavage forming event noticed in the study area. It has led to a minimum of 75% shortening and to the formation of an imbricate fan in which movement was to the NW. This phase of deformation can be correlated along strike with the D2 phase of De Wit (1982) and De Wit et al. (1983) and with the D1 phase of Philpot (1979) (see De Wit, 1983). In the northern part of the belt, the second phase of deformation also comprises a cleavage forming phase of contemporaneous thrusting and folding along NE/SW orientated axes. This phase is probably related to the D2 phase present in the southern part of the belt. If this is so, D2 occurred along NE/SW trends in the northern part of the belt, and within the study area, along N/S and E/W trends in Swaziland and along NW/SW to E/W trends to the west of the study area (Table 7.2).

The third event described in this study (D3) can be correlated along strike with Philpot's D2, De Wit (1982) and De Wit et al. (1983)'s D3. D3 can also be correlated with Lambs D3 (Table 7.2).

The D4 event can be correlated to Lamb's D3 which is a late phase of heterogeneous buckling (Table 7.2).

Table 7.2 Summary of the polyphase deformation as recognised in different parts of the belt (see Fig. 1.1) and possible correlations.



E/W : Structural trend; -> N : tectonic transport direction;
thrusting and folding; = synsedimentary folding;
* possibly caused by movement in the Ancient Gneiss Complex;
** possibly caused by late granitic intrusion;
C = well developed cleavage

7.4 GEOTECTONIC IMPLICATIONS FOR THE BARBERTON GREENSTONE BELT

7.4.1 SUMMARY OF EXISTING MODELS FOR THE FORMATION OF ARCHAEAN GREENSTONE BELTS

Several models which call for processes unique to the Archaean, have been proposed for the formation of the Barberton greenstone belt, (Viljoen and Viljoen, 1969 e; 1970; Anhaeusser, 1971 b; 1975; 1983; Condie, 1981; amongst others). All these models dispute the existence of plate tectonic mechanisms in the Archaean and propose distinctive Archaean geotectonic environments subsequently never developed throughout earth history.

Such models are based on the following assumptions:
i) A 24km thick conformable stratigraphic sequence (Fig. 1.2)
ii) Abundance of volcanic and sedimentological cyclicity
iii) Absence of horizontal shortening and of any tectonic repetitions.

As seen in this study, and as demonstrated by Williams and Furnell (1979), Philpot (1979), De Wit (1982; 1983) and De Wit et al. (1983), none of these assumptions appear to be valid. Therefore, other models warrant examination. Several models advocating a variably modified plate tectonic processes, have been applied to Archaean greenstone belts throughout the world:

1. Talbot (1973) proposed that the greenstone belts represented shreds of Archaean crust "skimmed off" and accreted in subduction complexes, the granodiorites being remobilised pre-greenstone sialic basement.

2. Burke et al. (1976) and Tarney et al. (1976) compared greenstone belts to marginal basins formed in a back-arc environment: Like the greenstone belt, the marginal basin rocks occur as megaxenoliths or elongate discontinuous strips within "granitic" rocks. They both typically contain early ultramafic and mafic volcanic successions followed by calk-alkaline successions and volcaniclastic and clastic sediments. Fossil marginal basin rocks have been commonly involved in interthrusting with basement rocks in a manner similar to that found in the

greenstone belt (Windley, 1976). In this model, the granodioritic rocks intruding and separating the supracrustal rocks would represent the roots of island arcs, either intruded into or tectonically juxtaposed with the greenstone sequences.

3. Sleep and Windley (1982) proposed that greenstone belts were formed in intra-arc environments. Although they agree that no direct evidence yet suggests that Archaean plate thicknesses were different from those of today; they argued that the Archaean oceanic crust was much thicker (> 20 km) than modern crust (&eqv. 5 km) from calculations based on the melting temperatures of peridotic komatiite. They found that Archaean igneous rocks could have been emplaced by a variant of modern plate tectonic mechanisms accounting for:
   i) possible differences in the accretion and subduction rates;
   ii) higher rates of breakdown of radioactive material;
   iii) higher mantle temperatures;
   iv) greater thickness of oceanic crust;
   v) the angle of dip of the subducting slab;
   vi) possible transition from polygonal to linear tectonics (Smith, 1981).
   They interpreted the Archaean metatonalites as the result of melting of the subducted slabs, favoured by the high mantle temperature. The gneissic belts were interpreted as the result of Cordilleran type compression.

In summary, there is still no consensus as to whether Archaean geotectonic processes were essentially different from those operative today. Furthermore, there does not appear to be any clear understanding to what extent Archaean processes might have been different from these observed in the Phanerozoic.

7.4.2 POSSIBLE EVOLUTIONARY MODEL FOR THE BARBERTON GREENSTONE BELT

From the present work, there is no reason to assume that Archaean processes were fundamentally different from those observed in the Phanerozoic. However, due to the very complex tectonic evolution of the belt (section 7.2) it is believed that only a tentative model is justified at this stage. Such a possible model is discussed below.

a) Formation of the Onverwacht Group

The similarities between the Onverwacht Group and a typical ophiolite were pointed out as early as 1968 (Anhaeusser et al., 1968). However, these authors later argued that the Barberton Greenstone belt could only have formed by processes unique to the Archaean (Viljoen and Viljoen, 1969 e; 1970; Anhaeusser et al., 1969; Anhaeusser, 1975; 1978; 1983) and that the Onverwacht Group represented the remnants of a primitive ensimatic lithosphere.

De Wit and Stern (1980) revived the comparison with phanerozoic ophiolites by suggesting
(i) that the Komati Formation represented an intrusive unit which might contain sheeted feeder dyke complex similar to those found in Phanerozoic ophiolite.
(ii) that mafic sections of the Hooggenoeg and Theespruit Formations could represent deformed, originally horizontal, overlying extrusive units fed by the dykes and
(iii) that ultramafic plutonic units could represent the associated magnetic cumulates and/or residual mantle material.

De Wit et al. (1983) mentioned the presence of a previously undescribed diamitite which contain gneissic pebbles in the lower part of the Onverwacht Group. They suggested that the Onverwacht Group was originally locally overlying and/or intruding a sialic crust. Hunter (1974) considered the Ancient Gneiss Complex to represent remnants of such a basement.

In the study area the Onverwacht sequence comprises serpentinite layers, massive and pillowed lavas and silicified sediments. The serpentinite is

allochthonous (see Chapter 5) with an original dunitic composition (Büttner, 1983). Such a sequence is also strikingly similar to Phanerozoic ophiolite sequence (Steinmann, 1926; Dewey and Bird, 1970; 1971). Thus, following De Wit and Stern (1980), the Onverwacht Group is seen as an ophiolite sequence, as defined by Moores and Vine (1971): "A sequence from variably serpentinised dunite and peridotite through gabbro to lava, capped by sediments".

It is now widely accepted that such a sequence represents oceanic lithosphere and crust probably originally formed at spreading centres and emplaced within an orogenic belt (Coleman, 1971; Le Pichon, 1968; Spray, 1983). The hydrothermal systems present during the formation of the Onverwacht Group have characteristics similar to those found along present day spreading centres suggesting that the Onverwacht Group could have been originally formed along a spreading centre (Fig. 7.1.a).

b) Formation of the Onverwacht tectonic complex

Ophiolitic sequences are emplaced by obduction either during island arc/Cordilleran type of orogenesis or during collision (Dewey and Bird, 1970; 1971). A combination of both processes can also occur (Dewey and Bird, op. cit.).

The D1 thrusts have been interpreted as having developed along zones of high pore pressure which formed as a result of hydrothermal activity (see Chapter 6). Such an interpretation implies that D1 took place close to the spreading centre while the igneous pile was still hot and hydrothermal systems were still active. Thus, D1 is an intra-oceanic event. Overthrusting of hot thin lithosphere, around a spreading centre, has been advocated as a mechanism to initiate ophiolite obduction (Spray and Roddick, 1980; Spray, 1983). These authors suggested that ophiolites are initially deformed within the oceanic realm prior to their final continental emplacement. However, the mechanisms they envisage involves the formation of deep seated décollement zones and differs from the one postulated for the D1 event. Some of basal Lower Group hemipelagic sediments are also tectonically repeated together with the Onverwacht Group, and form part of the Onverwacht Tectonic Complex.

c) Deposition of the Lower Group

As seen in Chapter 4, the Lower Group is interpreted as having formed by the deposition of hemipelagic sediments which were overlain by a prograding submarine fan (Fig. 7.1b). The lithologies of the clasts and the abundance of chert grains in the sandstones and conglomerates indicate that the fan was derived from the reworking of the D1 tectonic pile. Quartz (granitic ?) detritus were only provided to the upper part of the distal fan (Chapter 4). No unconformities have been observed between the Onverwacht and the Lower Groups (Table 7.1). However, planar disconformities and tectonic contacts could have been overlooked. The base of the Lower Group (Facies 1) has been repeated together with the Onverwacht sedimentary rocks by D1. Thus, the base of the Lower Group is pre- to syn-D1. From base to top, the Lower Group forms a gradational sequence interpreted as a prograding submarine fan. Thus, the upper part of the Lower Group is interpreted as a syn and post-D1 sequence.

In the northern part of the belt, the Fig Tree Group has been interpreted as a submarine fan in which sediments were derived from the Onverwacht Group, granitic components only appearing in the upper part of the sequence (Condie et al., 1970).

Paleocurrent data derived from the study area suggests both a S and a NE transport direction. Similar results have been obtained from the corresponding sequences in Swaziland (Lamb, in prep.). Eriksson (1980 a) suggested that sediment transport direction throughout the belt was to the north, during deposition of the Fig Tree Group, although his palaeocurrent data are mainly derived from the northern part of the belt.

These apparently contradictory results can only be reconciled once detailed structural and sedimentological correlations have been established between the northern and southern part of the Belt.

d) Deposition of the Upper Group

The Upper Group is interpreted as a fluvial sequence. In the study area, the Lower and Upper Groups are separated by an unconformity (Chapter 4, Table 7.1). The Upper Group sediments were probably derived from a granitic terrane as well as from the underlying Lower and Onverwacht Groups.

In Swaziland, stratigraphic sequences equivalent to the Lower and Upper Groups are separated by by unconformities which can be traced into conformable sequences (Lamb, in press). In the northern part of the belt, granitic detritus is predominant in the Moodies Group (Condie et al., 1970). Part of the Moodies Group has been interpreted as a fluvial sequence but no unconformities have been recognised between the Fig Tree Group and the Moodies Group (Eriksson, 1977; 1978; 1980 a-b). In the study area, palaeocurrent data suggest that current flow was to the south. In Swaziland, current directions were to the south and to the north with a smaller ESE component in the upper Malalotcha Group (Table 7.1), while NW and NE and southern trends have been found in the basal Malalotcha Group (Lamb, in press). In the northern part of the belt, Eriksson (1977) interpreted the Moodies Group as representing a fan delta prograding into marine sediments in which currents flowed to the north. The various sediment transport directions could be due to the presence of various separate sedimentary basins.

Eriksson (1980 b) proposed that the Fig Tree and Moodies Groups represented an evolving Atlantic type margin rather than a trench type margin. However, in an Atlantic type margin, the sediments are mainly derived from the continent (Dewey and Bird, 1971). In a trench type margin, the sediments are derived from the oceanic crust or from the volcanic arc, if present (Dewey and Bird, 1970; Karig, 1974).

The Moodies, the Malalotcha and the Upper Groups were probably derived from combined sources of granitic terranes and from the underlying sequences (Fig. 7.1). The granitic terrane could have represented a continent or the roots of a volcanic arc, as is the case in the Andes (Dalziel et al., 1974). Hunter (1974) suggested that the tonalite diapirs of the Ancient Gneiss complex resulted from partial melting of early sialic crust mixed with mantle material. Thus, the mechanism he proposed is similar to that the formation of an island arc above a subduction zone. Furthermore, although evidence is rarely directly preserved, subduction is a necessary consequence of oceanic spreading on a constant radius Archaean crust (Sleep and Windley, 1982) Thus it is thought that a trench type margin may have been developed during syntectonic deposition of the Lower Group and part of the Upper Group.

e) The D2 event

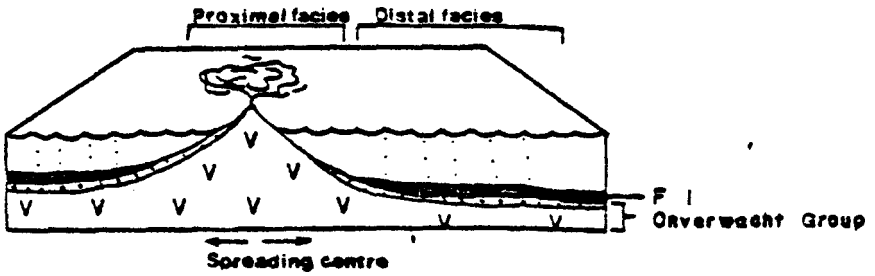
The Upper Group and the underlying sequences have been deformed into a imbricate fan during D2 and the following remarks can be made on the D2 event:

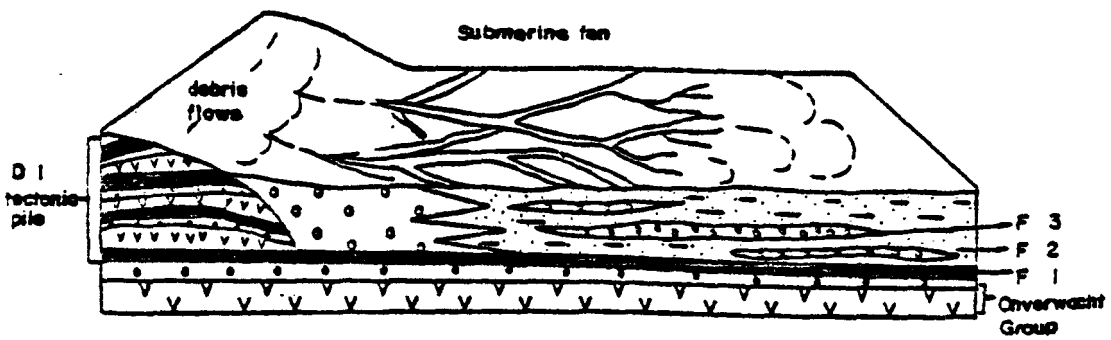
1. The tectonic interstacking of distal and proximal facies within the tectono-stratigraphy (Fig. 6.36), is characteristic of convergent margins and collision induced orogenic belt (Dewey and Bird, 1970).

2. In contrast to D1, D2 sense of thrusting seems to have been more restricted, movement varying throughout the belt from N to NW to W, (Table 7.2). A collision mountain belt is characterised by a single dominant sense of thrusting (Dewey and Bird, 1970).

3. In the study area the Lower Group is interpreted as a syn and post-orogenic sequence deposited on oceanic crust. It is unconformably overlain by a fluvial sequence, the Upper Group. In addition, in Swaziland, stratigraphic sequences equivalent to the Upper Group have been deposited during nappe emplacement (Lamb, in prep.). Such relationships are typical of collision belts (Dewey and Bird, 1970).

Thus, D2 is interpreted as representing a phase of deformation related to the obduction of an ophiolite sequence in a north westerly direction. It could be part of a collision event.





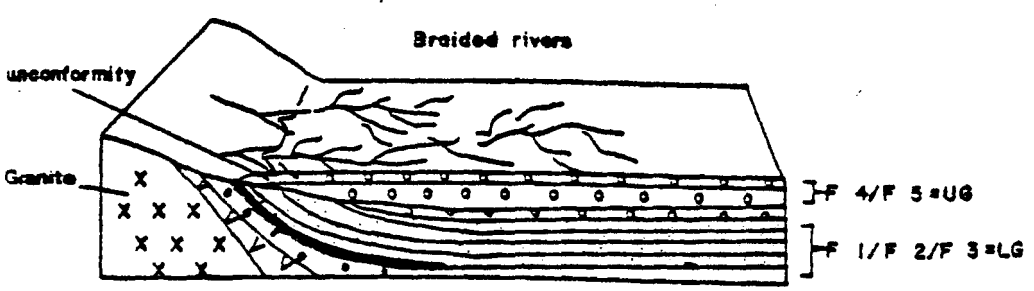
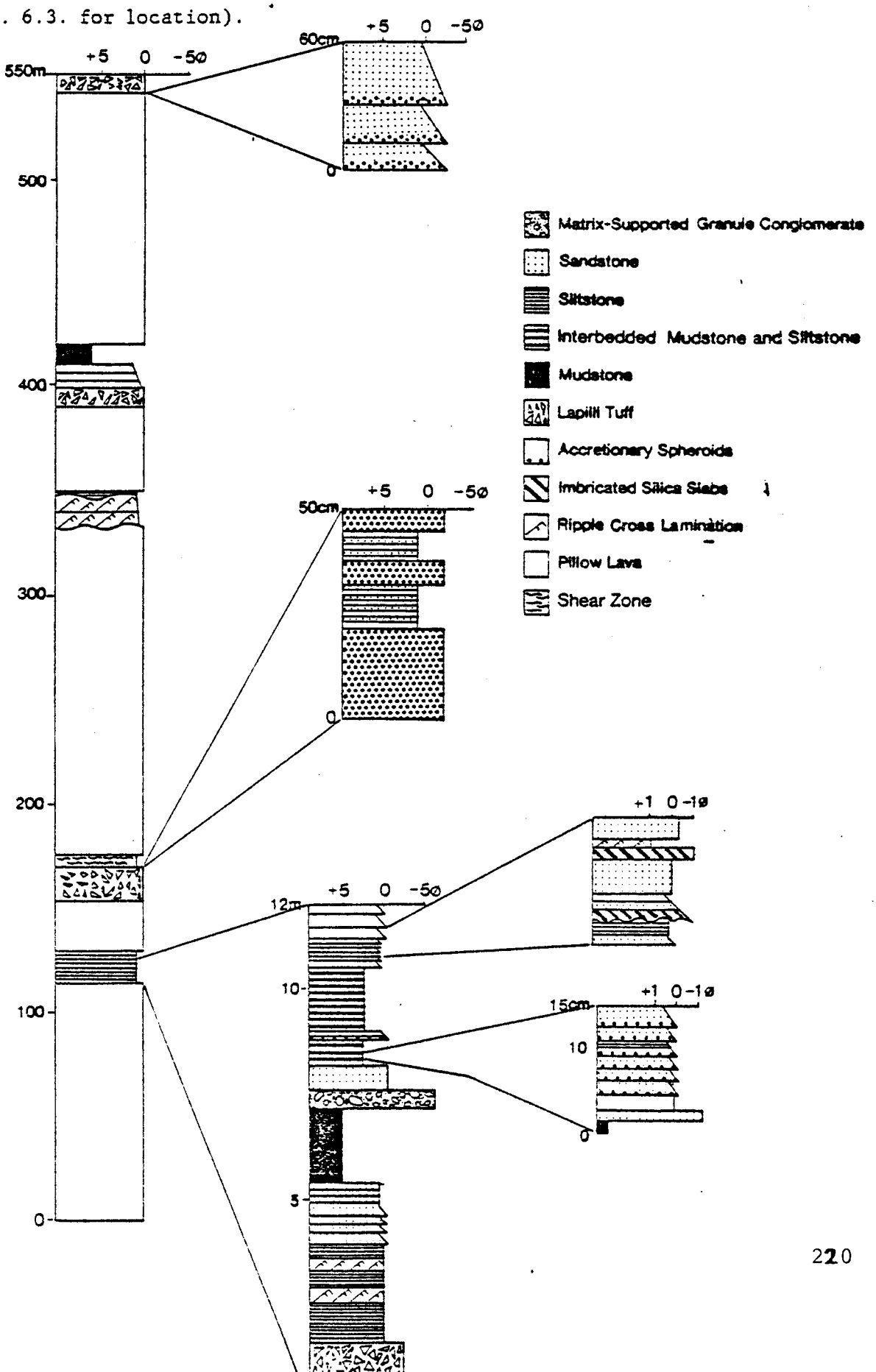
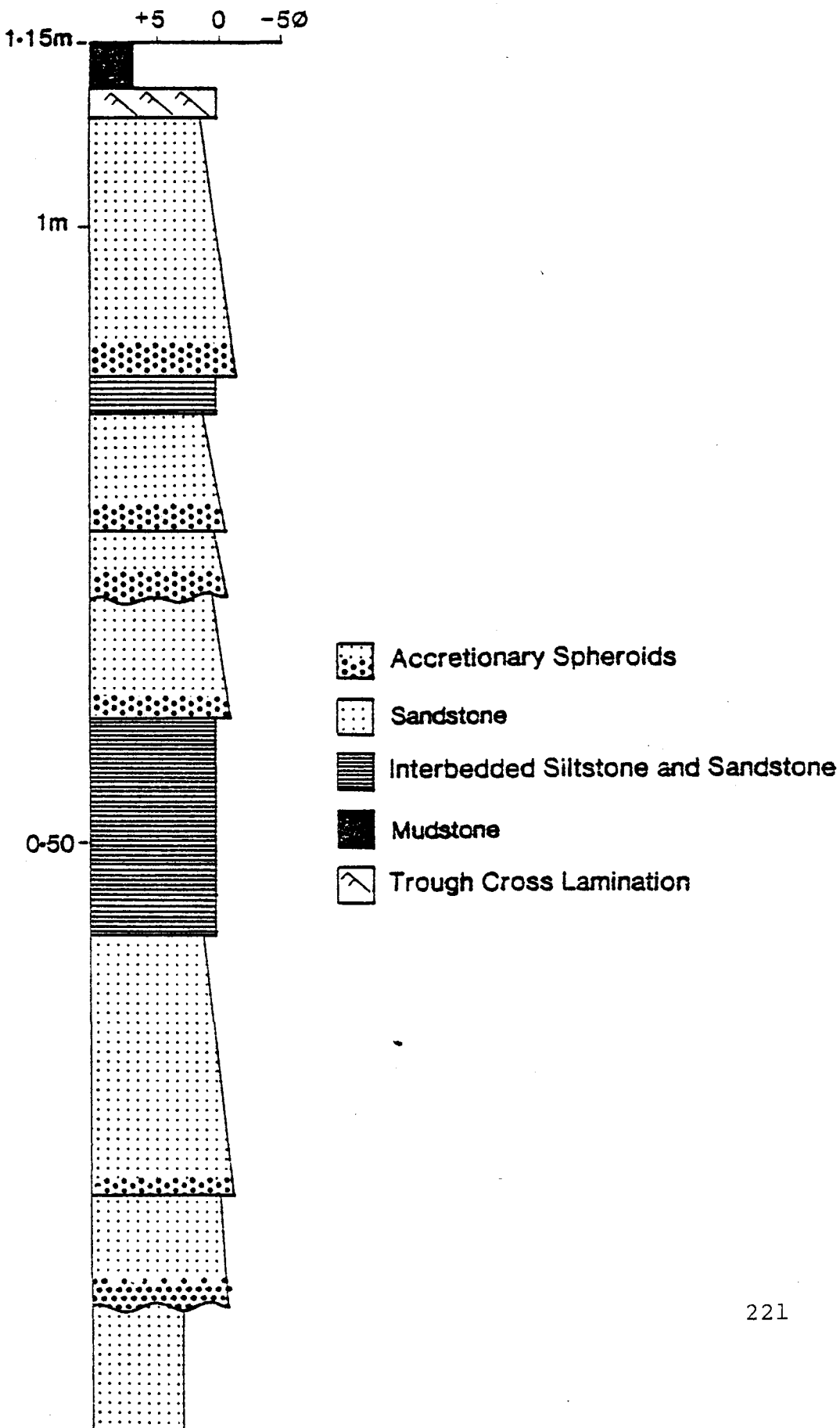


Figure 7.1. Simple cartoon showing the proposed paleoenvironmental evolution of the southern Barberton greenstone belt The tectonic events are not indicated on the diagram.

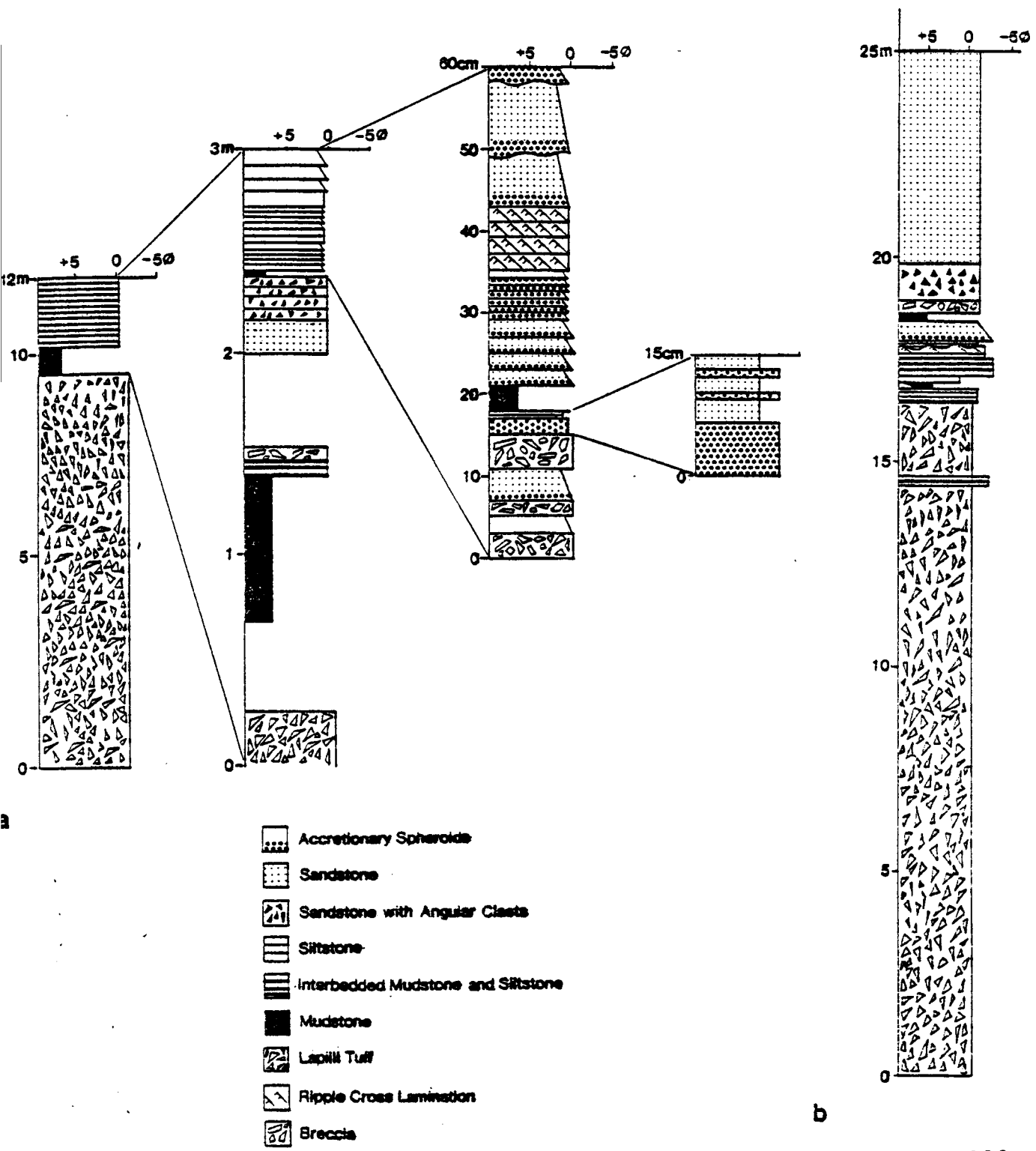
Measured section on the western slope of Simbubule showing the repetition of chert units of the Kromberg Formation which contain similar lithofacies (see Fig. 6.3. for location).



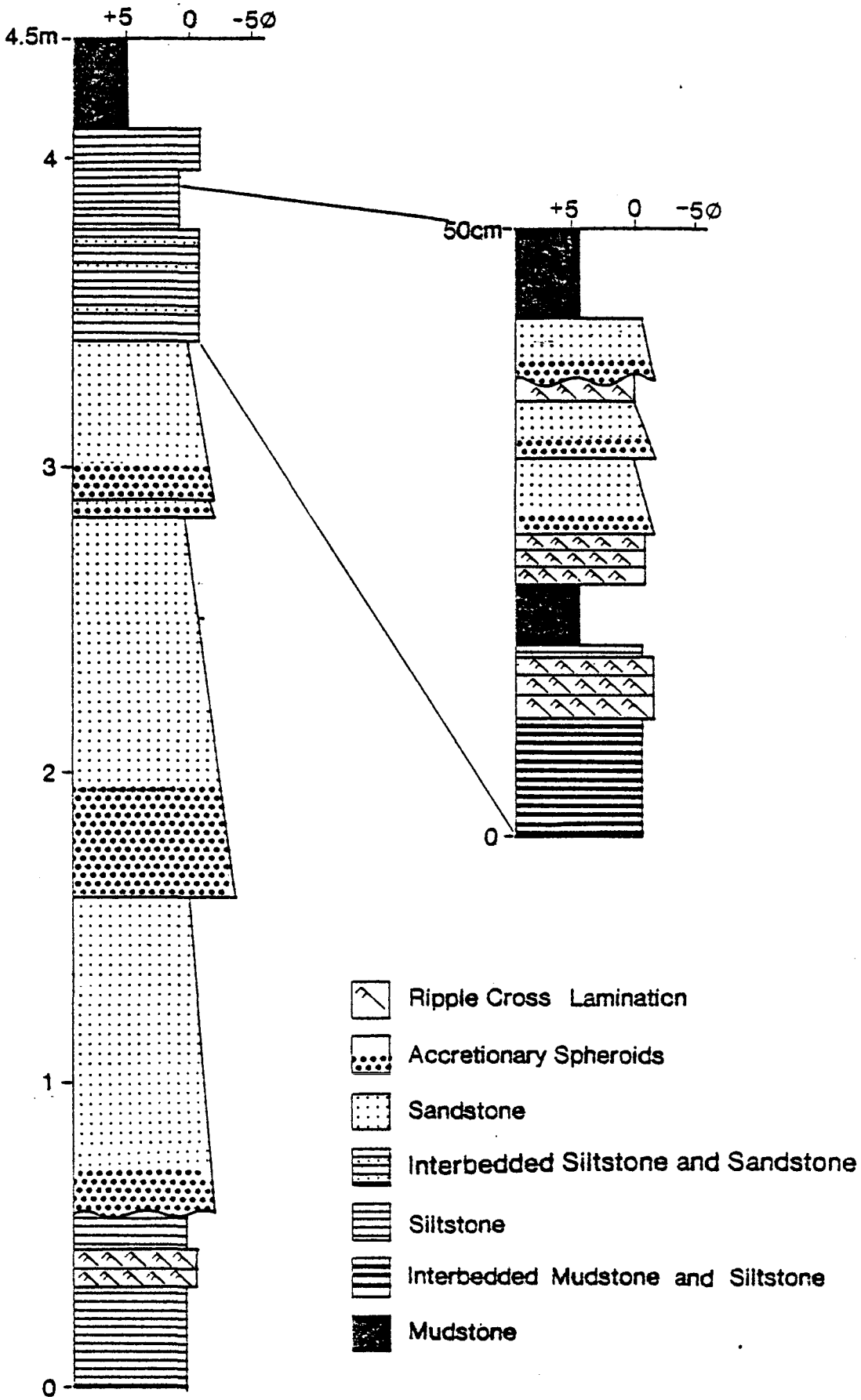
Measured section of a chert unit of the Kromberg Formation 1 km from the Havelock border post which contain thick bedded sedimentary cycles (see Fig. 6.3. for location).



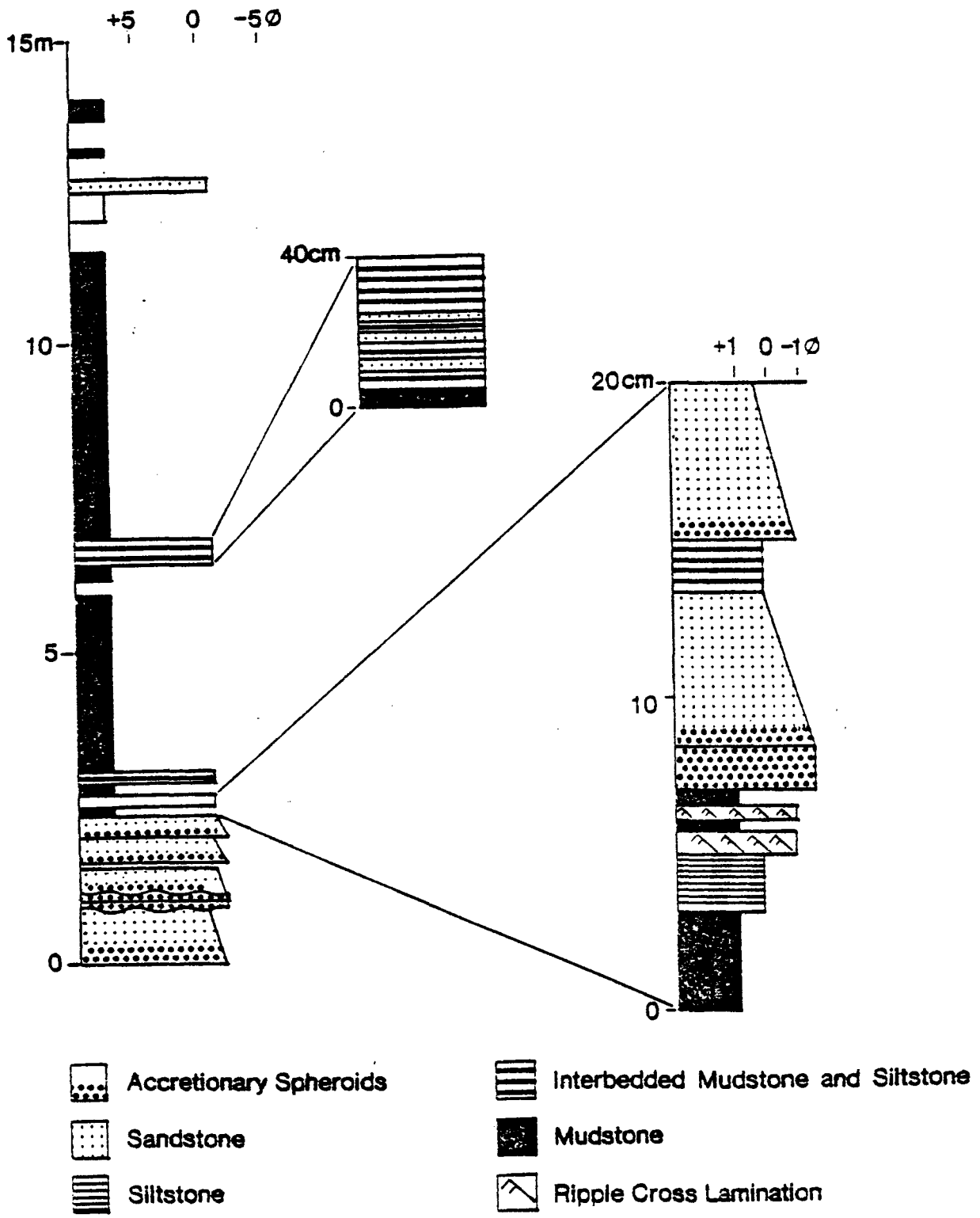
Measured section of chert units of the Kromberg Formation which contain thin bedded sedimentary cycles and the lapilli tuff facies (Josefdal Farm, see Fig. 6.3. for location).



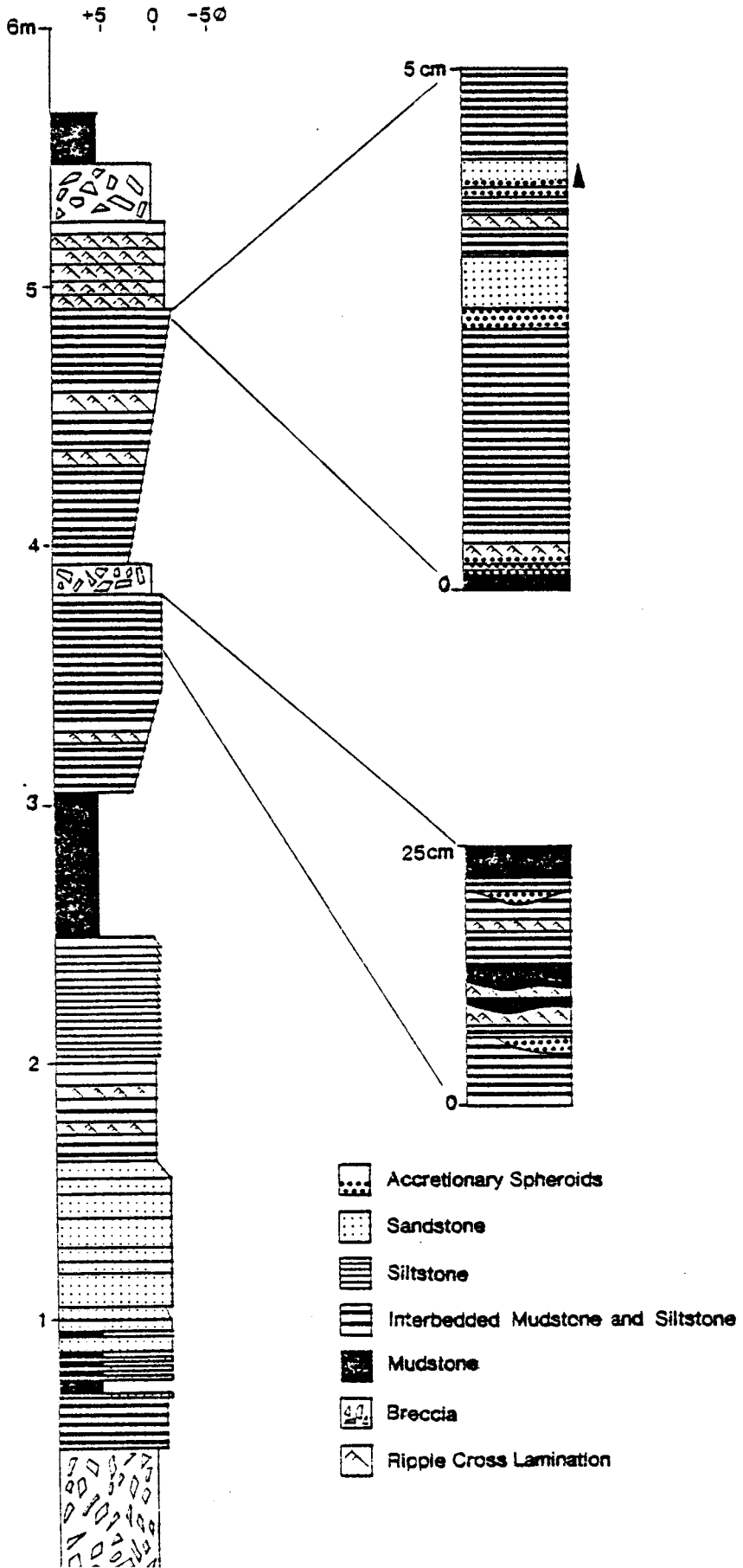
Measured section of a chert unit of the Kromberg Formation which contain thick bedded sedimentary cycles (Dunbar Farm, see Fig. 6.3. for location).



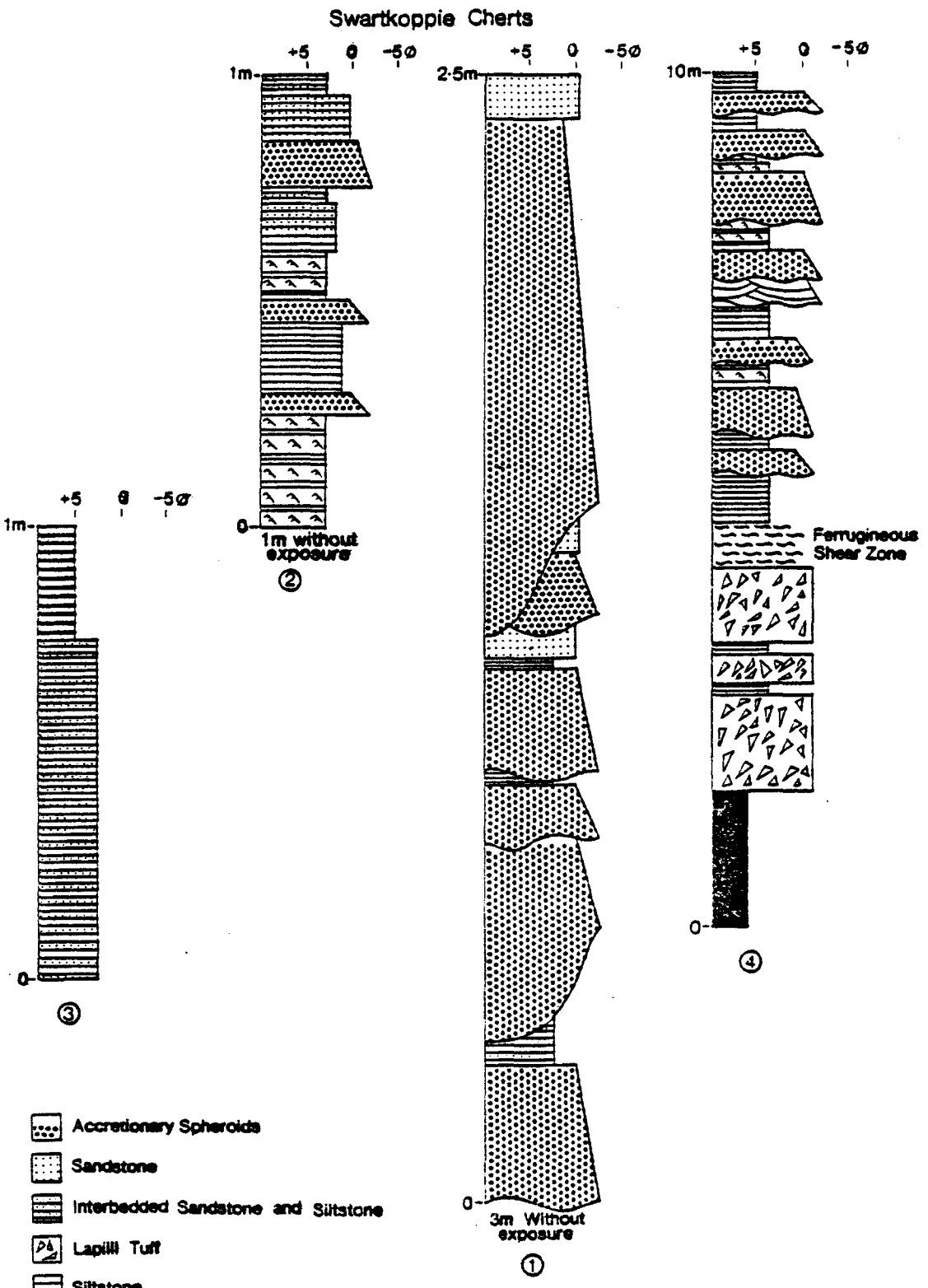
Measured section of a chert unit of the Kromberg Formation which contain thick sedimentary cycles (Dunbar Farm, see Fig. 6.3. for location).



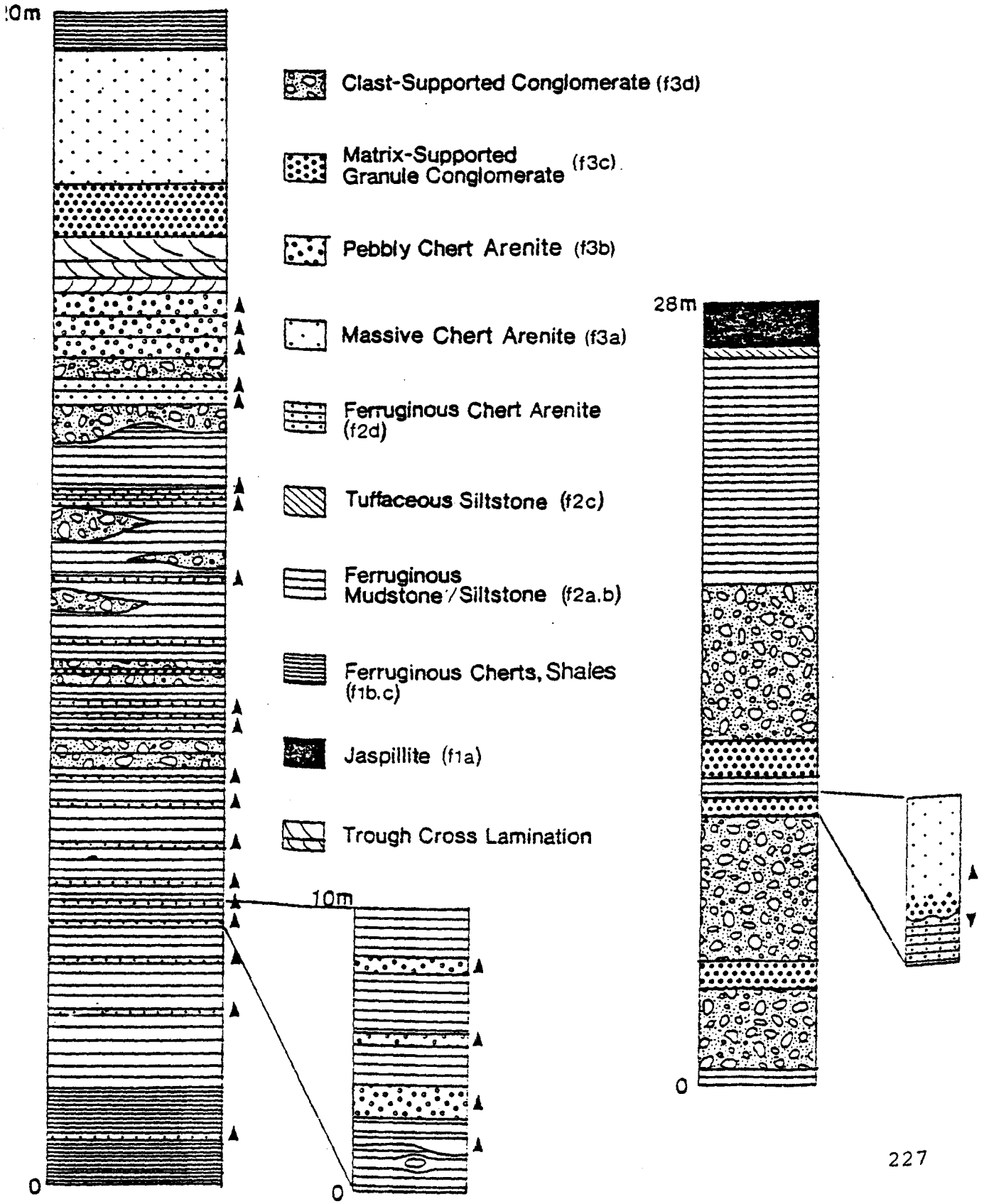
Measured section in a chert unit of the Kromberg Formation showing thin bedded sedimentary cycles (Josefsdal Farm, see Fig. 6.3. for location).



Measured section in a chert of the Swartkoppie Formation showing thick bedded sedimentary cycles (Diepgezet Farm, see Fig. 6.3. for location).

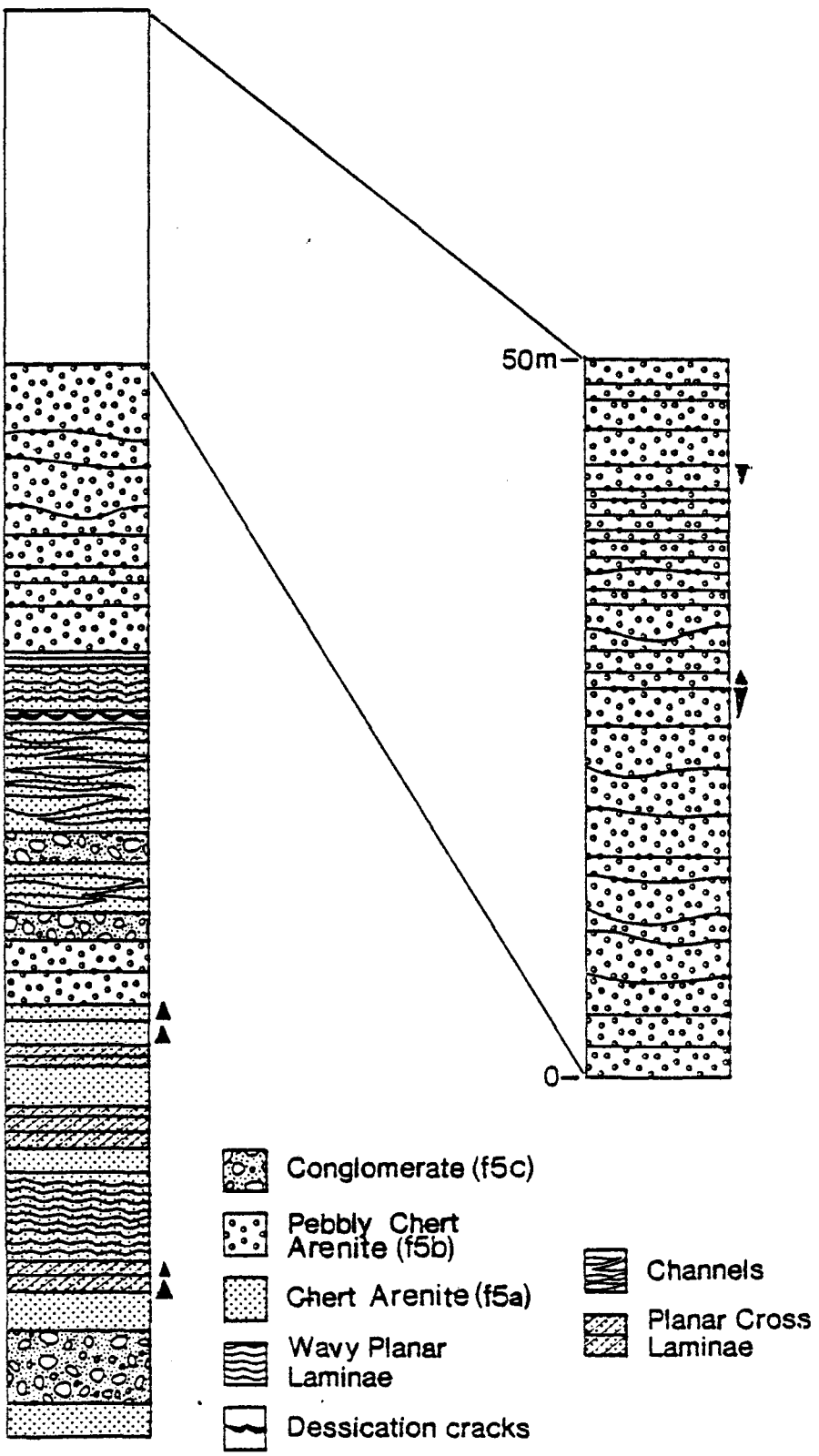


Measured section in the Josefsdal block (Josefsdal Farm, see Fig. 4.1. for location).

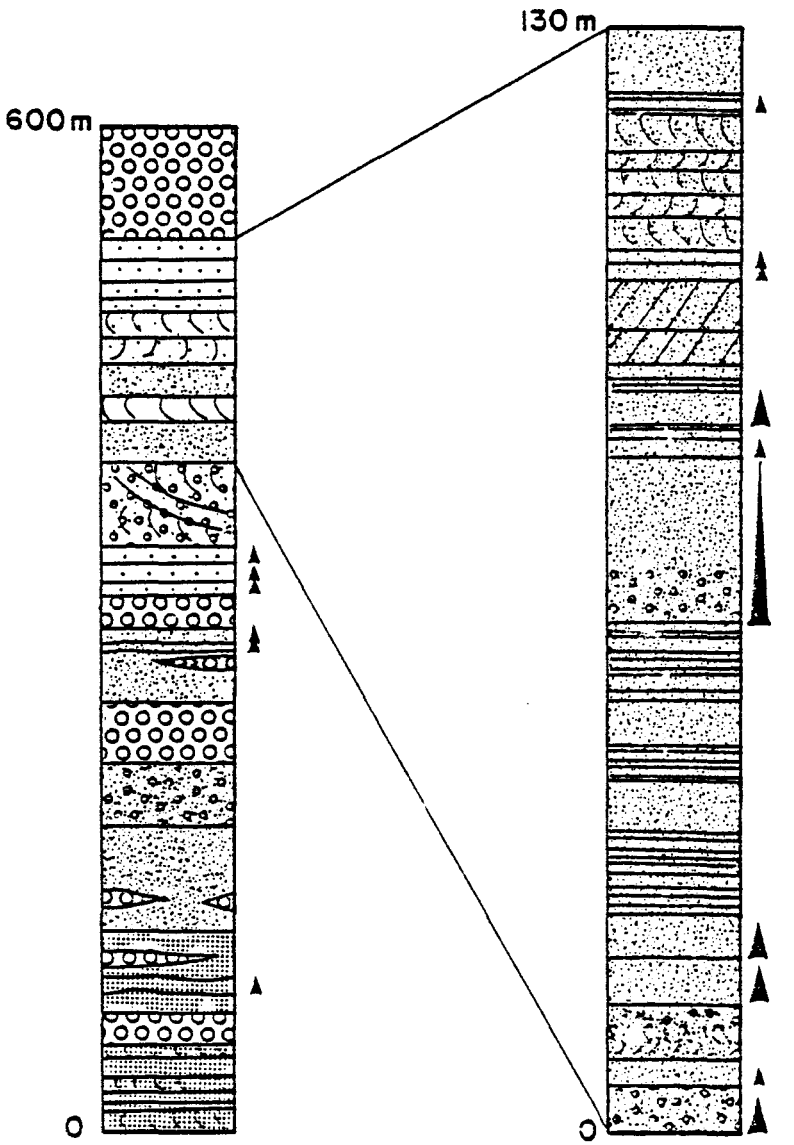


b

Measured section in the Xecacatu block (Diepgezet Farm, see Fig. 4.1. for location). file



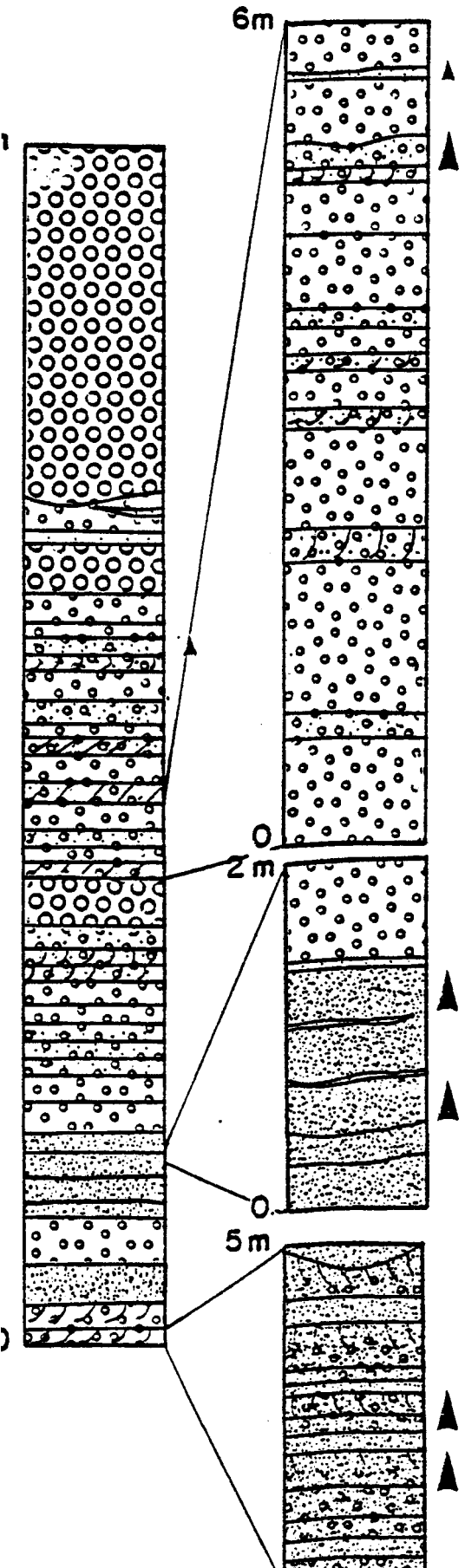
Measured section in the Xecacatu block (Josefsdal Farm, see Fig. 4.1. for location).



LEGEND.

- Clast supported conglomerate (f5c)
- Pebbly immature quartz arenite (f5b)
- Immature quartz arenite (f5a)
- Planar bedded mature quartz arenite
- Cross bedded mature quartz arenite
- F4
- Trough cross bedding
- Planar cross bedding
- Planar bedding
- Graded unit

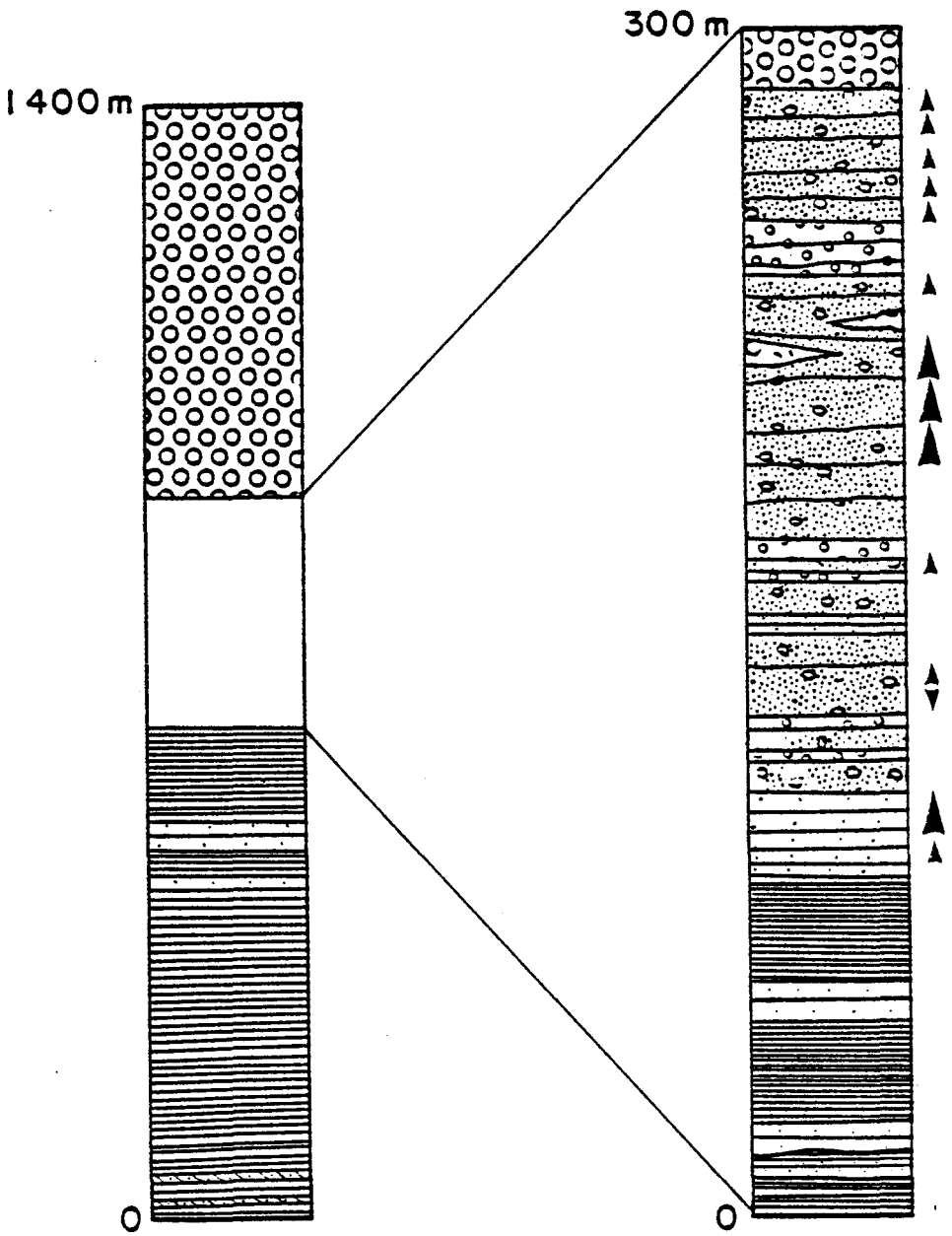
Measured section in the Emlembe block (Josefsdal Farm, see Fig. 4.1. for location).



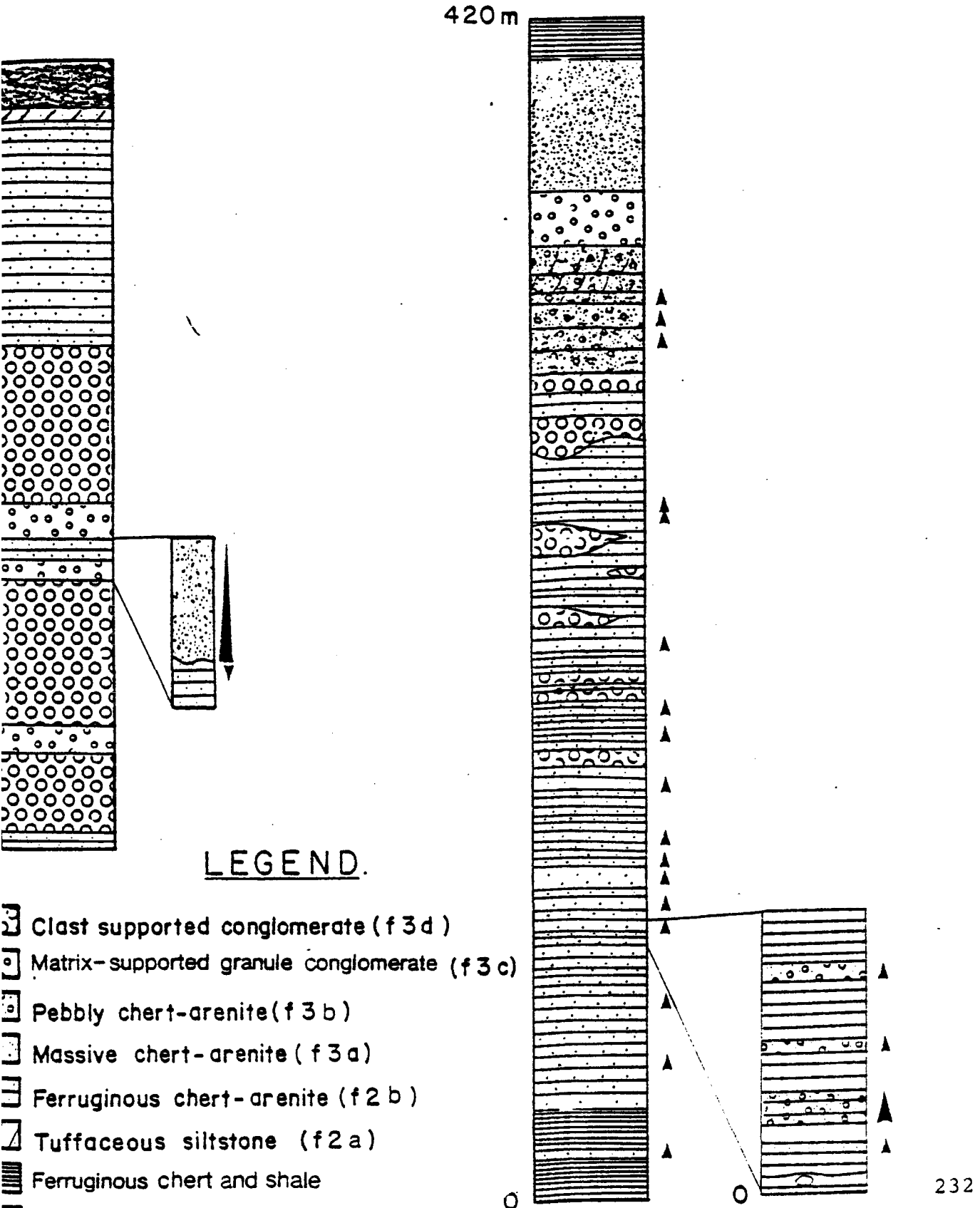
LEGEND

- Clast supported conglomerate (f 3 d)
- Matrix supported granule conglomerate (f3c)
- Pebbly chert arenite with cross laminated sandy top (f 3 b)
- Pebbly chert arenite (f 3 b)
- Massive chert arenite (f3a)
- Planar cross beds
- Trough cross beds

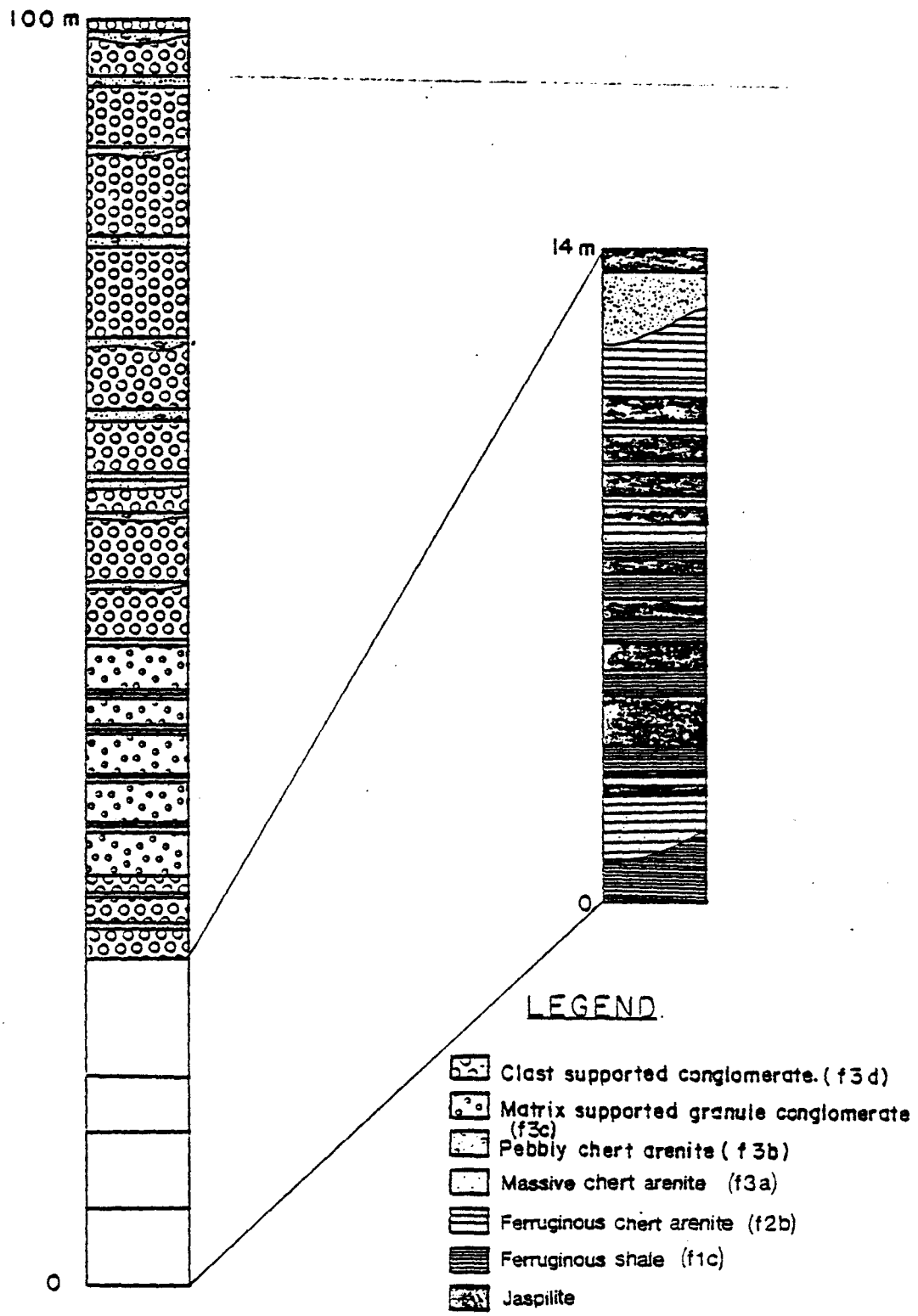
Measured section in the Diepgezet block (Diepgezet Farm, see Fig. 4.1. for location).



Measured section in the Josefsdal block (Josefsdal Farm, see Fig. 4.1. for location).



Measured section in the Simbubule block (Josefsdal Farm, see Fig. 4.1. for location).



8.0 LIST OF REFERENCES

Anhaeusser, C.R., 1969 a,

The stratigraphy, structure and gold mineralisation of the Jamestown and Sheba Hills areas of the Barberton greenstone belt. Ph.D thesis., Univ. Witwatersrand, (unpubl.), 332 pp.

Anhaeusser, C.R., 1969 b,

A comparison of pebble and fold deformation in the Nelspruit granite aureole, Barberton greenstone belt. Trans. geol. Soc. S. Afr., vol. 72, p. 49 - 60.

Anhaeusser, C.R., 1971 a,

The Barberton Mountain Land, South Africa. A guide to the understanding of the Archaean geology of Western Australia. Spec. Publ. geol. Soc. Aust., vol. 3, p. 103 - 119.

Anhaeusser, C.R., 1971 b,

Cyclic volcanicity and sedimentation in the evolutionary development of Archaean greenstone belts of shield areas. Spec. Publ. geol. Soc. Aust., vol. 3, p. 57 - 70.

Anhaeusser, C.R., 1973,

The evolution of the early Precambrian crust of southern Africa. Phil. Trans. R. Soc. Lond., vol. A. 273, p. 359 - 388.

Anhaeusser, C.R., 1975,

Precambrian tectonic environments. Ann. Rev. Earth Planet Sci., vol. 3, p. 31 - 53.

Anhaeusser, C.R., 1976,
The geology of the Sheba Hills area of the Barberton greenstone belt, South Africa, with particular reference to the Eureka Syncline. Trans. geol. Soc. S. Afr., vol. 79, p. 253 - 280.

Anhaeusser, C.R., 1978,
The geological evolution of the primitive earth: evidence from the Barberton Mountain Land. In: Evolution of the earth's crust. Tarling, D.H., (ed.), Academic Press, London, p. 71 - 106.

Anhaeusser, C.R., 1983,
Structural elements of Archaean granite greenstone terranes as exemplified by the Barberton greenstone belt, southern Africa. Econ. Geol. Res. Unit, Univ. Witwatersrand, Johannesburg, Inf. circ. no. 162, 22 pp.

Anhaeusser, C.R., Mason, R., Viljoen, M.J. and Viljoen, R.P., 1969,
A reappraisal of some aspects of Precambrian shield geology. Bull. geol. Soc. Am., vol. 80, p. 2175 - 2200.

Anhaeusser, C.R., Roering, C., Viljoen, M.J. and Viljoen, R.P., 1968,
The Barberton greenstone belt: a model of the elements and evolution of an Archaean fold belt. Annex. Trans. geol. Soc. S. Afr., vol. 71, p. 225 - 253.

Anhaeusser, C.R., Robb, L. J. and Viljoen. M.J., 1981,
Provisional geological map of the Barberton greenstone belt and surrounding granitic terrane, Eastern Transvaal and Swaziland. In: Contributions to the geology of the Barberton Mountain Land. Anhaeusser, C.R., (ed), accompanying Spec. Publ. geol. Soc. S. Afr. no. 9.

Aubouin, J., 1965,
"Geosynclines", Elsevier, Amsterdam, 335 pp.

Barton, C.M., 1982,
Geology and mineral resources of Northwest Swaziland (Barberton greenstone belt). Bull. geol. Surv. Mines Dept. Swaziland, no. 10, 97 pp.

Barton, J.M. Jr., 1981 a,

The pattern of Archaean crustal evolution in southern Africa as deduced from the evolution of the Limpopo Mobile Belt and the Barberton granite-greenstone terrane. Spec. Publ. geol. Soc. Aust., vol. 7, p. 21-31.

Barton, J.M. Jr., 1981 b,

A summary of geochronologic and Sr-isotopic data from the Barberton Mountain Land, Southern Africa. In: Archaean geology of the Barberton Mountain Land. Anhaeusser, C.R., (ed), Excursion guidebook: Geocongress 1981. Geol. Soc. S. Afr. p. 22-25.

Beach, A., 1977,

Vein arrays, hydraulic fractures and pressure-solution structures in a deformed flysch sequence, S.W. England. Tectonophysics, vol. 40, p. 201 - 225.

Beach, A., 1979,

Pressure solution as a metamorphic process in deformed terrigenous sedimentary rocks. Lithos, vol. 12, p. 51 - 58.

Beach, A., 1982,

Chemical processes in deformation at low metamorphic grades: Pressure solution and hydraulic fracturing. Episodes, vol. 4, p. 22 - 25.

Bell, T.H. and Etheridge, M.A, 1973,

Microstructure of mylonites and their descriptive terminology. Lithos, vol. 6, p. 337 - 348.

Bonatti, E., 1975,

Metallogenesis at oceanic spreading centers. Ann. Rev. Earth Planet. Sci., vol. 3, p. 401 - 431.

Bonatti, E., Fisher, D.E., Joensuu, O., Rydell, H.S. and Beyth, M., 1972 a,

Iron-manganese-barium deposit from the northern Afar Rift (Ethiopia). Econ. Geol., vol. 67, p. 717 - 730.

Bonatti, E., Kraemer, T. and Rydell, H., 1972 b,
Classification and genesis of submarine iron-manganese deposits. In: Ferromanganese deposits on the ocean floor. Horn, D., (ed.), Washington. DC., Nat. Sci. Found., p. 149 - 165.

Bouma, A.H., 1962,
Sedimentology of some flysch deposits. Elsevier, Amsterdam, 168 pp.

Boyer, S.E. and Elliott, D., 1982,
Thrust Systems. Bull. Am. Assoc. Petrol. Geol., vol. 66, p. 1196 - 1230.

Bucher, W.H., 1956,
Role of gravity in orogenesis. Bull. geol. Soc. Am., vol. 67, p. 1295 - 1318.

Burke, K., Dewey, J.F. and Kidd, W.S.F., 1976,
Dominance of horizontal movements, arc and microcontinental collisions during the later permobile regime. In: the early history of the earth. Windley, B.F., (ed.), Wiley, Chichester, U.K., p. 113 - 129.

Butler, W.H., 1983,
Balanced cross-sections and their implications for the deep structure of the northwest Alps. J. struct. Geol., vol. 5, p. 125 - 137.

Büttner, W., 1983,
Mineralogische, geologische und geochemische Untersuchungen zun genese der Msauli-Asbert-Lagerstätte, Barberton greenstone belt, Südafrika. Dissertation, Univ. Köln, (unpubl.).

Büttner, W., Barton, J.M., Jr. and Saager, R. 1983,
Geochemistry, age and origin of some porphyry intrusions in the Onverwacht Group, Barberton greenstone belt. Trans. geol. Soc. S. Afr., vol. 86, p. 1 - 10.

Caire, A., 1973,
The Calabro-Sicilian Arc. In: Gravity and tectonics. De Jong, K.A. and Scholten, R., (ed.), Wiley, New York, p. 157 - 174.

Chapman, R.E., 1974,

Clay diapirism and overthrust faulting. Bull. geol. Soc. Am., vol. 85, p. 1597 -1602.

Chapple, W.M., 1978,

Mechanics of thin-skinned fold and thrust belts. Bull. geol. Soc. Am., vol. 89, p. 1189 - 1198.

Choukroune, P. and Seguret, M., 1973,

Tectonics of the Pyrenees: Role of compression and gravity. In: Gravity and tectonics. De Jong, K.A. and Scholten, R (ed.), Wiley, New York, p. 141 - 156.

Coleman, R.G., 1971,

Plate tectonic emplacement of upper mantle periodotites along continental edges. J. Geophys. Res., vol. 76, p. 1212 - 1222.

Condie, K.C., 1981,

Archaean greenstone belts. Developments in Precambrian geology vol. 3, Elsevier, Amsterdam, 434 pp.

Condie, K.C., Macke, J.E. and Reimer, T.O., 1970,

Petrology and geochemistry of early Precambrian graywackes from the Fig Tree Group, South Africa. Bull. geol. Soc. Am., vol. 81, p. 2759 - 2775.

Cooper, M.A., 1981,

The internal geometry of nappes: criteria for models of emplacement. In: Thrust and nappe tectonics. McClay, K.A. and Price, N.J. (eds.), Spec. Publ. geol. Soc. Lond. no. 9, p. 225 - 234.

Corliss, J.B., Dymond, J., Gordon, L.I., Edmond, J.M., Von Herzen, R.P., Ballard, R.D., Green, K., Williams, D., Bainbridge, A., Crane, K. and Van Andel, T.H., 1979,

Submarine thermal springs on the Galapagos rift. Science, vol. 203, p. 1073 - 1082.

Coward, M.P., 1982,

Surge zones in the Moine thrust zone of NW Scotland. J. struct. Geol., vol. 4, p. 247 - 256.

Coward M.P., 1983,

Thrust tectonics, thin skinned or thick skinned and the continuation of thrusts to deep in the crust. J. struct. Geol., vol. 5, p. 113 - 123.

Criddle, A.J., 1974,

A preliminary description of micro-crystalline pyrite from the nannoplankton ooze at Site 251, Southwest Indian Ocean. In: Initial Reports of the Deep Sea Drilling Project, vol. 26, p. 603 - 607.

Dahlstrom, C.D.A., 1969,

Balanced sections. Can. J. Earth. Sci., vol. 6, p. 743 - 757.

Dalziel, I.W.D., de Wit, M.J. and Palmer, K.F., 1974,

A fossil marginal basin in the Southern Andes. Nature, vol. 250, p. 291 - 294.

Darracott, B.W., 1975,

The interpretation of the gravity anomaly over the Barberton Mountain Land, South Africa. Trans. geol. Soc. S. Afr., vol. 78, p. 123 - 128.

Debelmas J. and Kerckhove, C., 1973,

Large gravity in the French-Italian and French-Swiss Alps. In: Gravity and tectonics. De Jong, K.A. and Scholten, R., (eds.), Wiley, New York, p. 189 - 200.

De Jong, K.A. and Scholten, R., 1973,

Gravity and tectonics. Wiley, New York, 502 pp.

Dewey, J.F. and Bird, J.M. 1970,

Mountain belts and the new global tectonics. J. geophys. Res., vol. 75, p. 2625 - 2647.

Dewey, J. F. and Bird, J. M., 1971,
Origin and emplacement of the ophiolite suite: Appalachian ophiolites in Newfoundland. J. geophys. Res., vol. 76, p. 3179 - 3206.

De Wit, M.J., 1982,
Gliding and overthrust nappe tectonics in the Barberton Greenstone Belt. J. struct. Geol., vol. 4, p. 117 - 136.

De Wit, M.J., 1983,
Preliminary geologic map of part of the southern sector of the Barberton Greenstone Belt. Spec. Publ. geol. Soc. S. Afr., no. 9., p. 185 - 187.

De Wit, M.J. and Stern, C., 1978,
Pillow talk. J. Volcanol. Geotherm. Res., vol. 4, p. 55 - 80.

De Wit, M.J. and Stern, C., 1980,
A 3500 Ma ophiolite complex from the Barberton Greenstone Belt, South Africa: Archaean oceanic crust and its geotectonic implications. Extended Abstr. 2nd Internat. Archaean Symp. Perth, p. 83 - 85.

De Wit, M. J., Hart, R., Stern, C. R. and Barton, C.M., 1979,
Metallogenesis related to the seawater interaction with 3.5 b.y. oceanic crust. XVII General Assembly: International Ass. Physical Science of Oceans. Abstract, also published in EOS 1980, vol. 61, p. 386.

De Wit, M.J., Hart, R., Martin, A. and Abbott, P., 1982 a,
Archaean abiogenic and probable biogenic structures associated with hydrothermal vent systems and regional metasomatism, with implications for greenstone belt studies. Econ. Geol., vol. 77, p. 1783 - 1802.

De Wit, M.J., Hart, R. and Pyle, D., 1982 b,
Mg metasomatism of the oceanic crust; implications for the formation of ultramafic rock types. Abstract with programme., geol. Soc. Am.

De Wit, M.J., Fripp, R.E.P. and Stanistreet I.G., 1983,
On some field observations within the Barberton greenstone belt along parts of its southern margin. Spec. Publ. geol. Soc. S. Afr., no. 9, p. 21 - 29.

Dimroth E., 1979,
Diagenetic facies of iron formation. In: Facies Models. Walker, R., (ed.), Geoscience Can. Rept. Series 1, p. 175 - 182.

Donaldson, C. H., 1982,
Spinifex-textured komatiites: a review of textures, composition and layering. In: Komatiites. Arndt, N.T. and Nisbet, E.G., (eds.). Allen and Unwin, London, 526 pp.

Draper, D., 1914,
Notes on a section from Barberton to the Komati River. Trans. geol. Soc. S. Afr., vol. 6, p. 162 - 164.

Elliott, D., 1976,
The motion of thrust sheets. J. geophys. Res., vol. 81, p. 949 - 963

Elliott, D., 1983,
The construction of balanced sections. J. struct. Geol., vol. 5, p. 101.

Eriksson, K.A., 1977,
A palaeoenvironmental analysis of the Archaean Moodies Group, Barberton Mountain Land, South Africa. Ph.D. thesis, Univ. Witwatersrand, (unpubl.), 155 pp.

Eriksson, K.A., 1978,
Alluvial and destructive beach facies from the Archaean Moodies Group, Barberton greenstone belt, South Africa. In: Fluvial sedimentology. Miall, A.D., (ed.), Mem. can. Soc. Petrol Geol., no. 5, p. 287 - 311.

Eriksson, K.A., 1980 a,

Hydrodynamic and palaeogeographic interpretation from the Archaean Fig Tree Group of the Barberton Mountain Land, South Africa. Bull. geol. Soc. Am., vol. 91, p. 21 - 26.

Eriksson, K.A., 1980 b,

Transitional sedimentation styles in the Moodies and Fig Tree Groups, Barberton greenstone belt, South Africa: evidence favouring an Archaean continental margin. Precambrian Res., vol. 12, p. 141 - 160.

Folk, R.L., 1974,

Petrology of sedimentary rocks. Univ. of Texas, geol. 370 k, 383 l, 383 m, Hempill publishing Co., 170 pp.

Friedman, J.N., Sanders, G.E. and Martini, I.P., 1982,

Sedimentary facies, products of sedimentary environments in a cross section of the clastic Appalachian Mountains and adjoining Appalachian basins. In: IAS 11th International Congress. Field excursion guide, McMaster University, Hamilton, Ontario, Canada, 189 pp.

Fripp, R.E.P., Van Nierop, D.A., Callow, M.J., Lilly, P.A. and Du Plessis, L.U.,1980,

Deformation in part of the Archaean Kaapvaal Craton, South Africa. Precambrian. Res., vol. 13, p. 241 - 251.

Furnes, H, Fridleifsson, I.B and Atkins, F.B., 1980,

Subglacial volcanics. On the formation of acid hyaloclastites. J. Volcanol. Geotherm. Res., vol. 8, p. 85 - 110.

Fyfe, W.S., Price N.J. and Thompson, A.B., 1978,

Fluids in the earth crust. Elsevier, Amsterdam, 383 pp.

Gay, N.C., 1969,

The analysis of strain in the Barberton greenstone belt, eastern Transvaal, using deformed pebbles. J. Geol., vol. 77, p. 377 - 396.

Gibson, H.L. and Watkinson, D.H., 1979,
Silicification in the Amulet "Rhyolite" Formation, Turcotte Lake section, Noranda area, Quebec. Geol. Surv. Can. Pap. 79.1B, p. 111 - 120.

Gibson, H.L., Watkinson, D.H. and Comba, C.A.A., 1983,
Silicification: Hydrothermal alteration in the Archaean geothermal system within the Amulet Rhyolite Formation, Noranda, Quebec. Econ. Geol., vol. 78, p. 954 - 971.

Gill, W.D. and Kuenen, P.H., 1957,
Sand volcanoes on slumps in the carboniferous of County Clare, Ireland. Quart. J. geol. Soc. London, vol. 113, p. 441 - 460.

Graham, R.H., 1981,
Gravity sliding in the Maritime Alps. In: Thrust and nappe Tectonics. McClay, K.R. and Price, N.J., (eds.). Spec. Publ. geol. Soc. Lond. no. 9., p. 335 - 355.

Groves, D.I., Dunlop, J.S.R. and Buick, R., 1981,
An early habitat of life. Scientific American, Oct. 81, p. 58 - 65.

Hall, A.L., 1918,
The geology of the Barberton gold mining district. Mem. geol. Surv. S. Afr., vol 9, 324 pp.

Hamilton, P. J., Evensen, N. M., O'Nions, R. K., Smith, H.S. and Erlank, A. J., 1979,
Sm-Nd dating of Onverwacht Group volcanics, southern Africa. Nature, vol. 279, p. 298 - 300.

Harms, J. C., Southard, J. B. and Walker, R. G., 1982,
Structures and sequences in clastic rocks. Soc. Econ. Pal. Min., Short course no. 9.

Hart, R. and De Wit, M.J., 1984,
Hydrothermal alteration in the 3,5 by old Onverwacht Group of South Africa Abstract in: Workshop on Early Archaean. April 1984, Lunar and Planetary Institute, Houston.

Hart, S.R., Erlank, A.J. and Kable, E.J.D., 1974,
Sea floor basalt alteration: Some chemical and Sr isotopic effects. Contr. Mineral. Petrol., vol. 44, p 210 - 230.

Heinrichs, T., 1980,
Lithostratigraphische Untersuchungen in der Fig Tree Gruppe des Barberton belt zwishen Unsoli und Lomati (Südafrika). Gottinger Arb. Geol. Palaeont, vol. 22, p. 118.

Horne, J.C. and Ferm, J.C., 1978,
Carboniferous depositional environments in the Pocahontas basin, eastern Kentucky and southern West Virginia. A field guide. Dept. Geol. Univ. South Carolina.

Hossack, J.R., 1979,
The use of balanced sections in the calculation of orogenic contraction: A review. J. geol. Soc. Lond., vol. 13, p. 705 - 711.

Hsü, K.G., 1973,
Mesozoic evolution of the California Coast Ranges: a second look. In: Gravity and Tectonics. De Jong, K.A. and Scholten, R. (eds.), Wiley, New York, p. 373 - 396.

Hubbert, M.K. and Rubey, W.W., 1959,
Role of fluid pressure in mechanics of overthrust faulting. Bull. geol. Soc. Am., vol. 70, p. 115 - 166.

Hughes, C.J., 1970,

The Heart Mountain detachment fault, a volcanic phenomenon? J. Geol., vol. 78, p. 107 - 116.

Hunter, D.R., 1974,

Crustal development in the Kaapvaal Craton. Precambrian Res., vol. 1, p. 259 - 294.

Hurley, P.M., Pinson, W.J., Jr., Nagy, B. and Teska, T.M., 1972,

Ancient age of the Middle Marker Horizon, Onverwacht Group, Swaziland sequence, South Africa. Earth Planet. Sci. Letters., vol. 14., p. 360 - 366.

Hutchinson, R.W., Fyfe, W.S. and Kerrich, R., 1980,

Deep fluid penetration and ore deposition. Minerals Sci. Eng, vol. 12, p. 107 - 102.

Jackson, M.P.A. and Robertson, D.I, 1983,

Regional implications of Early Precambrian strains in the Onverwacht Group adjacent to the Lochiel Granite, north west Swaziland. In: Contributions to the geology of the Barberton greenstone belt. Anhaeusser C.R., (ed.). Spec. Publ. geol. Soc. S. Afr. no. 9, p. 45 - 63.

Jahn, B., Gruau, G. and Glikson, A.Y., 1982,

Komatiites of the Onverwacht group, S. Africa: REE geochemistry, Sm/Nd age and mantle evolution. Contr. Mineral. Petrol., vol. 80, p. 25 - 40.

James, D.M.D., 1983,

Sedimentation of deep-water slope-base and inner-fan deposits. The Drosgol Formation (Ashgill) West Central Wales. Sediment. Geol., vol. 34, p. 21 - 40.

Jopling, A.V. and Walker, R.G., 1968,

Morphology and origin of ripple drift cross-lamination with examples from the Pleistocene of Massachusetts. J. sediment. Petrol., vol. 38, p. 971 - 984.

Karig, D. E., 1974,
Evolution of arc systems in the western Pacific. Ann. Rev. Earth. Planet. Sci, vol. 2, p. 51 - 75.

Kehle, R.O., 1970,
Analysis of gravity sliding and orogenic translation. Bull. geol. Soc. Am., vol. 81, p. 1641 - 1664.

Kindle, C.H. and Whittington, H.B., 1958,
Stratigraphy of the Cow Head Region, Western Newfoundland. Bull. geol. Soc. Am., vol. 69, p. 315 - 342.

Kimberley, M.M., 1982,
Archaean sea floor weathering of Black river volcanics. Abstracts of the 11th Congress of the International Association of Sedimentologists, Hamilton, Canada.

Kynaston, H., 1906,
The geology of the Komatipoort Coalfield. Mem. geol. Surv. Transvaal, vol. 2, 55 pp.

Lamb, S.H., 1984,
Structures and sedimentology on the eastern margin of the Archaean Barberton greenstone belt, northwest Swaziland. Ph.D. thesis, Univ. Cambridge (unpubl.).

Lamb, S.H., 1984,
Structures on the eastern margin of the Archaean Barberton greenstone belt, northwest Swaziland. In: Precambrian Tectonics Illustrated. Kröner, A. and Greiling, R. (eds.). E. Schweizerbart'sche Verlagsbuchhandling, Germany, p. 19 - 39.

Lemoine, M., 1973,
About gravity gliding tectonics in the Western Alps. In: Gravity and tectonics. De Jong, K.A. and Scholten, R., (eds.). Wiley, New York, p. 201 - 216.

Le Pichon, X., 1968,
Sea floor spreading and continental drift. J. geophys. Res., vol. 73, p. 3661 - 3697.

Lowe, D.B., 1979,
Sediment gravity flows: Their classification and some problems of application to natural flows and deposits. In: Geology of continental slopes. Doyle, L.J. and Pilkey, O.H., (eds.). Spec. Publ. Soc. Econ. Pal. Min., no. 27, p. 75 - 82.

Lowe, D.R., 1983,
Restricted shallow-water sedimentation of Early Archaean stromatolitic and evaporitic strata of the Strelley Pool Chert, Pilbara Block, Western Australia. Precambrian Res., vol. 19, p. 239 - 283.

Lowe, D.R. and Knauth, L.P., 1977
Sedimentology of the Onverwacht group (3.4 billion years), Transvaal, South Africa and its bearing on the characteristics and evolution of the early earth. J. Geol., vol. 85, p. 699 - 723.

Lowe, D.R. and Knauth, L.P., 1978
The oldest marine carbonate ooids reinterpreted as volcanic accretionary lapilli. Onverwacht Group, South Africa. J. sediment. Pet., vol. 48, p. 709 - 722.

Lowe, D.R. and Lo Piccolo, R.D., 1974,
The characteristics and origins of dish and pillar structures. J. sediment. Pet., vol 44, p. 484 - 501.

Lowe, D.R., Nocita, B.W., Ransom, B.L. and Byerly, G.R., 1983,
Tectonic sheets in the Archaean Onverwacht and Fig Tree Groups, Barberton Mountain Land, South Africa. EOS, vol. 64, p. 318.

Lucchi, F.B., 1970,
Sedimentografia. Atlas fotographico delle structure primarie dei sedimenti Zanichelli, Bologna, 152 pp.

Lugeon, M., 1943,
Une nouvelle hypothese tectonique: la diverticulation. Bull. Soc. Vaud. Sci. Nat., vol. 62, p. 301 - 303.

Maldonado, A. and Stanley, D.J., 1978,
Nile Cone depositional processes and patterns in the Late Quaternary. In: Sedimentation in submarine canyons, fans and trenches. Stanley, P.J. and Kelling, G. (eds.). Dowden, Hutchinson and Ross, Stroudsburg, p. 239 - 257.

McClay, K.R., 1981,
What is a Thrust? What is a Nappe? In: Thrust and Nappe tectonics. McClay, K.R. and Price, N. J. (eds.). Spec. Publ. geol. Soc. London. no. 9, p. 7 - 9.

McClay, K.R. and Price, N.J., 1981,
Thrust and nappe tectonics. McClay, K.R. and Price, N.J. (eds.). Spec. Publ. geol. Soc. Lond. no. 9, 539 pp.

Macdonald, G. A., 1972,
Volcanoes. Prentice-Hall, Englewood Clipps, New Jersey, 510 pp.

McGowen, J.H. and Groat, C.G., 1975,
Van Horn Sandstone, West Texas: an alluvial fan model for mineral exploration. Bureau. econ. geol. Univ. Texas. Report of investigation no. 72, 57 pp.

McIlreath, I.A. and James, N., 1979,
Carbonate slopes. In: Facies Model. Walker R.G., (ed.). Geoscience Can. Rept. Series no. 1, p. 133 - 144.

McKee, E.D. and Weir G.W., 1963,
Terminology for stratification and cross stratification in sedimentary rocks. Bull. geol. Soc. Am., vol. 64, p. 381 - 390.

Matthews, P. E., 1981,

Eastern or Natal section of the Namaqua-Natal mobile belt in Southern Africa. In: Precambrian of the Southern Hemisphere. Hunter, D.R., (ed.). Elsevier, Amsterdam, 882 pp.

Miall, A.D., 1977 a,

A review of the braided river depositional environment. Earth. Sci. Rev., vol. 13, p. 1 - 62.

Miall, A.D., 1977 b,

Fluvial sedimentology. Notes to accompany a lecture series on fluvial sedimentology. Can. Soc. Pet. geol.

Minter, W.E.L., 1982,

Sedimentology of the Witwatersrand basin. Optima, vol. 30, p. 263 - 272.

Moore, R.C., 1949,

Meaning of facies. Mem. geol. Soc. Am., no. 39, p. 1 - 34.

Moore, J.G. and Peck, D.L., 1962,

Accretionary lapilli in volcanic rocks of the western continental United States. J. Geol., vol. 70, p. 182 -193.

Moores, E. M. and Vine, F. J., 1971,

The Troodos Massif, Cyprus and other ophiolites as oceanic crust, evaluation and implications. Phil. Trans. Roy. Soc. Lond. A268, p. 443 - 466.

Mottl, M.J., 1983,

Metabasalts, axial hot springs and the structure of hydrothermal systems at mid-oceanic ridges. Bull. geol. Soc. Am., vol. 94, p. 161 - 180.

Nairn, L.A. and Wiradiradja, S., 1980,

Late quaternary hydrothermal explosion breccia at Kawerau geothermal field, New Zealand. Bull. Volcanol., vol. 43, p 1 - 13.

Phillips, F.C., 1973,
The use of stereographic projection in structural geology. Edward Arnold, London, Third edition, 90 pp.

Phillips, W.J., 1972,
Hydraulic fracturing and mineralisation. J. geol. Soc. Lond., vol. 128, p. 337 - 359.

Philpot, H.G., 1979,
The geology of a portion of the Stolzburg Schist belt, Barberton Mountain Land, Eastern Transvaal. BSc (Hons) Rept., Univ. Witwatersrand, (unpubl.).

Pickering, K.T., 1983,
Transitional submarine fan deposits from the late Precambrian Kongsfjord Formation submarine fan, N.E. Finmark, N. Norway. Sedimentology, vol. 30, p. 181 - 199.

Platt, L.B., 1962,
Fluid pressure in thrust faulting, a corollary. Am. J. Sci., vol. 260, p. 107 - 114.

Price, N.J., 1977,
Aspects of gravity tectonics and the development of listric faults. J. geol. Soc. Lond., vol. 133, p. 311 - 327.

Price, R.A., 1973,
Large-scale gravitational flow of supracrustal rocks, southern Canadian Rockies. In: Gravity and tectonics. De Jong, K.A. and Scholten, R., (eds.). Wiley, New York, p. 491 - 502.

Price, R.A., 1981,
The Cordilleran foreland thrust and fold belt in the southern Canadian Rocky Mountains. In: Thrust and Nappe tectonics. McClay K.R. and Price N.J., (eds.). Spec. Publ. geol. Soc. Lond. no. 9, p. 427 - 448.

Ramberg, H., 1981,
Gravity, deformation and the earth's crust. Academic Press, London, 452 pp.

Ramsay, J.G., 1963,
Structural investigations in the Barberton greenstone belt, Eastern Transvaal. Trans. geol. Soc. S. Afr., vol. 66, p. 353 - 401.

Ramsay, J.G., 1967,
Folding and fracturing of rocks. McGraw-Hill, New York, 568 pp.

Reading, H.G., 1978,
Sedimentary environment and facies. Reading, H.G., (ed.). Blackwell, Oxford, 557 pp.

Reed, M.H., 1983,
Seawater-basalt reaction and the origin of greenstone and related ore deposits. Econ. Geol., vol. 78, p. 466 - 485.

Reimer, T.O., 1967,
Die Geologie der Stolzburg Synklinale im Barberton Bergland (Transvaal, Südafrika). Unveroff. Unveiopp. Dipl. Arb, Goeth Univ. Frankfurt-am-Main.

Reimer, T.O., 1975a,
Untersuchungen uber Abragung, Sedimentation und Diagenese im frühen Prakambrium am Beispiel der Sheba Formation (Südafrika). Geol. Jb. Reihe B., vol. 17.

Reimer, T.O., 1975b,
Palaeogeographic significance of the oldest known oolite pebbles in the Barberton Mountain land. Sediment. Geol.,vol. 14, p. 123 - 133.

Reineck, H.E. and Singh, I.B., 1980,
Depositional sedimentary environments. Springer-Verlag, Berlin, 439 pp.

Riba, O., 1976,
Syntectonic unconformities of the Alto Cardener, Spanish Pyrenees: a genetic interpretation. Sediment. Geol., vol. 15, p. 213 - 233.

Ridd, M.F., 1970,
Mud volcanoes in New Zealand. Bull. Am. Assoc. Petrol. geol., vol. 54, p. 601 - 614.

Rocheleau, M. and Lajoie, J., 1974,
Sedimentary structures in resedimented conglomerate of the Cambrian flysch, L'Islet, Quebec Appalachians. J. sediment. Petrol., vol. 44, p. 826 - 836.

South African Committee for Stratigraphy (SACS), 1980,
Stratigraphy of South Africa Part I (Comp. L.E. Kent). Lithostratigraphy of the Republic of South Africa, South West Africa/Namibia and the Republics of Bophuthatswana, Transkei and Venda. Handb. geol. Surv. S. Afr., vol. 8, 690 pp.

Scholten, R., 1973,
Gravitational mechanism in the Northern Rocky Mountains of the United States. In: Gravity and tectonics. De Jong, K.A. and Scholten, R. (eds.). Wiley, New York, p. 473 - 430.

Self, S. and Sparks, R.S.J., 1978,
Characteristics of widespread pyroclastic deposits formed by the interaction of silicic magma and water. Bull. Volcanol., vol. 41, p. 196 - 216.

Self, S. and Sparks, R.S., 1979,
Discussion: the oldest marine carbonate ooids reinterpreted as volcanic accretionary lapilli, Onverwacht Group, South Africa. J. Sediment. Petrol., vol. 49, p. 661 - 678.

Selley, R.C., 1982,
An introduction to sedimentology (2nd Edition). Academic Press, London, 408 pp.

Sibson, 1977,

Fault rocks and fault mechanisms. J. geol. Soc. Lond., vol. 133, p. 191 - 213.

Siesser, W.G. and Rogers, J., 1976,

Authigenic pyrite and gypsum in South West African continental slope. Sedimentology, vol. 23, p. 567 - 577.

Sleep, N.H. and Windley, B.F., 1982,

Archaean plate tectonics: constraints and inferences. J. Geol., vol. 90, p. 363 - 379.

Smith, J.V., 1981,

The first 800 million years of earth's history. Phil. Trans. Royal. Soc. London, vol. 301, p. 401 - 422.

Spray, J. G., 1983,

Lithosphere asthenosphere decoupling at spreading centres and initiation of obduction. Nature, vol. 304, p. 253 - 255.

Spray, J. G. and Roddick, J. C., 1980,

Petrology and 40Ar/30Ar geochronology of some hellenic sub-ophiolite metamorphic rocks. Contr. Miner. Petrol., vol. 72, p. 43 - 55.

Stanistreet, I.G., De Wit, M.J. and Fripp, R.E.P., 1981,

Do graded units of accretionary spheroids in the Barberton greenstone belt indicate an Archaean deep water environment? Nature, vol. 293, p. 280 - 284.

Stanistreet, I.G, De Wit, N.J. and Paris, I., 1982,

Cherts of the Barberton Greenstone Belt and their palaeoenvironmental and palaeotectonic significance. Abstracts of the 11th Congress of the International Association of Sedimentologists, Hamilton, Canada, p. 1.

Stanley, D.J. and Kelling G., 1978,

Sedimentation in submarine canyons, fans and trenches. Dowden, Hutchinson and Ross, Stroudsburg, 395 pp.

Stein, C.L., 1982,
Silica recrystallization in petrified wood. J. Sediment. Petrol., vol. 52, p. 1277 - 1282.

Steinmann, G., 1927,
Die ophiolithischen zonen in den Mediterranean Kettenbizgen. Proc. 15th Internat. Geol. Congr., Madrid, part 3, p. 637 - 667.

Steyn, M.V.R., 1965,
Basal rocks of the Swaziland system in the Steynsdorp valley and Fairview areas of the Barberton greenstone belt. In: Symposium on the geology of the Barberton greenstone belt. Geol. Soc. S. Afr., (unpubl.), 37 pp.

Stride, A.H., Belberson, R.H. and Kenyon, N.H., 1982,
Structural grain, mud volcanoes and other features on the Barbardos Ridge complex revealed by Gloria long-range side-scan sonar. Marine Geol., vol. 49, p. 187 - 196.

Talbot, C. J. 1973,
A plate tectonic model in the Archaean crust. Phil. Trans. R. Soc. Lond. A 273, p. 413 - 427.

Tankard, A.J., Jackson, M.P.A., Eriksson, K.A., Hobday, D.K., Hunter, D.R. and Winter, W.E.L., 1982,
Crustal evolution of Southern Africa. Springer-Verlag, New York, 523 pp.

Tapponnier, P. and Molnar, P., 1976,
Slip-line field theory and large scale continental tectonics. Nature, vol. 264, p. 319 - 324.

Tarney, J., Dalziel, I.W.D. and De Wit, M.J., 1976,
Marginal basin "Rocas Verdes" complex from S. Chile: a model for Archaean greenstone belt formation. In: The Early history of the Earth. Windley, B.F., (ed.). Wiley, Chichester, p. 131 - 146.

Tihor, L.A. and Crocket, J.H., 1977,
Gold distribution in the Kirkland Lake-Larder Lake area, with emphasis on Kerr Addison type ore deposits. A progress report. Geol. Surv. Can., Pap. 77-1A, p. 363 - 369.

Trendall, A.F., 1965,
Pisolitic tuffs in western Australia. Ann. geol. Surv. West. Aust. Rep. 1964, p. 51 - 54.

Turner, W.M., 1973,
The Cyprian gravity nappe and the autochthonous basement of Cyprus. In: Gravity and tectonics. De Jong, K.A. and Scholten, R., (ed.). Wiley, New York, p. 287 - 304.

Turner, C.T. and Walker, R.G., 1973,
Sedimentology, stratigraphy and crustal evolution of the Archaean greenstone belt near Sioux Lookout, Ontario, Canada. J. Earth. Sci., vol. 10, p. 817 - 845.

Van Bemmelen, R.W., 1960,
New view of east alpine orogenesis. Proc. 21st Internat. Geol. Congr., Copenhagen, part 18, p. 99 - 116.

Van Bemmelen, R.W., 1972,
Geodynamic models: an evaluation and a synthesis. Developments in Geotectonics, 2, Elsevier, Amsterdam.

Van Bemmelen, R, W., 1975,
Some basic problems in geonomy. Progress in geodynamics, p. 9 - 20. North Holland publ. Co., Amsterdam.

Van der Berg, M.L.J., 1969,
Report on the Geology of the Josefsdal Area (Barberton greenstone belt). Unpubl. Rep. E.T.C. Mines Ltd.

Van Eeden, O.R., 1941,
Die geologie van die Shebarante en omstreke, distrik Barberton. DSc thesis. Univ. Stellenbosch (unpubl.).

Viljoen, M.J. and Viljoen, R.P., 1969 a,
An introduction to the geology of the Barberton granite-greenstone terrain. In: Upper Mantle project. Spec. Publ. geol. Soc. S. Afr., vol. 2, p. 9 - 28.

Viljoen, M.J. and Viljoen, R.P., 1969 b,
The geology and geochemistry of the lower ultramafic unit of the Onverwacht Group and a proposed new class of igneous rocks. In: Upper Mantle Project. Haughton, S.H. (ed.). Spec. Publ. geol. Soc. S. Afr., vol. 2, p. 55 - 85.

Viljoen, M.J. and Viljoen, R.P. 1969 c,
Evidence for the existence of a mobile peridotitic magma from the Komati Formation of the Onverwacht Group. In: Upper Mantle project. Haughton, S.H. (ed.). Spec. Publ. geol. Soc. S. Afr., vol. 2., p. 87 - 112.

Viljoen, M.J. and Viljoen, R.P., 1969 d,
The geological and geochemical significance of the upper formations of the Onverwacht Group. In: Upper Mantle Project. Haughton, S.H. (ed.). Spec. Publ. geol. Soc. S. Afr., vol. 2, p. 113 - 151.

Viljoen, M.J. and Viljoen, R.P., 1969 e,
A reappraisal of granite-greenstone terrains of shield areas based on the Barberton model. In: Upper Mantle Project. Haughton, S.H. (ed.). Spec. Publ. geol. Soc. S. Afr., vol. 2, p. 245 - 274.

Viljoen, M.J. and Viljoen, R.P., 1970,
Archaean vulcanicity and continental evolution in the Barberton region, Transvaal. In: African magmatism and tectonics. Clifford, T.N. and Gass, I.G. (eds.). Oliver and Boyd, Edinburgh, p. 27 - 39.

Viljoen, M.J. and Viljoen, R.P., 1979,
Discussion. Reassessment of part of the Barberton type area, South Africa. A comment. Precambrian Res., vol. 9, p. 349 - 352.

Viljoen, M.J. Viljoen, R.P., Smith, H.S. and Erlank, A.J., 1983,
Geological, textural and geochemical features of komatiitic flows from the Komati Formation. In: Contributions to the geology of the Barberton Mountain Land. Anhaeusser, C.R., (ed.). Spec. Publ. geol. Soc. S. Afr. no. 9, p. 1 - 20.

Visser, D.J.L., (Compiler), Van Eeden, O.R., Joubert, G.K., Sohnge, A.P.G., Van Zyl, J.S., Rossow, P.J., Taljaard, J.J. and Visser, D.J.L., 1956,
The geology of the Barberton area. Spec. Publ. geol. Surv. S. Afr., vol. 15, 242 p.

Vos, R.G., 1975,
An alluvial plain and lacustrine model for the Precambrian Witwatersrand deposits of South Africa. J. Sediment. Petrol., vol. 45, p. 480 - 493.

Walker, G.P.L., 1971,
Grain size characteristics of pyroclastic deposits. J. Geol., vol. 79, p. 696 - 714.

Walker, R.G., 1975,
Generalized facies models for resedimented conglomerates of turbidite association. Bull. geol. Soc. Am., vol. 86, p. 737 - 748.

Walker, R.G., 1978,
Deep-water sandstone facies and ancient submarine fans: Models for exploration for stratigraphic traps. Am. Ass. Petrol. Geol., vol. 62, p. 932 - 966.

Walker, R.G. (ed.), 1979,
Facies Models. Walker. Geoscience Can. Rept. Series 1, p. 91 - 102.

Walker, R.G. and Mutti, E., 1973,
Turbidite facies and facies associations. In: Turbidites and deep water sedimentation. Middleton, G.V. and Bouma, A.H., (eds.). Pacific Section, Soc. Econ. Pal. Min., Short Course Notes (Los Angeles), p. 119 - 157.

Wescott, W.A. and Ethridge, F.E., 1983,
Eocene fan delta-submarine fan deposition in the Wagwater trough, east central Jamaica. Sedimentology, vol. 30, p. 235 - 247.

Westbrook, G.K. and Smith, M.J., 1983,
Long décollements and mud volcanoes: Evidence from the Barbados Ridge complex for the role of high pore-fluid pressure in the development of an accretionary complex. Geology, vol. 11, p. 279 - 283.

Williams, H. and McBirney, A.R., 1979,
Volcanology. Freeman, Cooper and Co, San Francisco.

Williams, D.A.C. and Furnell, R.G., 1979,
Reassessment of part of the Barberton type area. Precambrian Res., vol. 9, p. 325 - 347.

Windley, B.F., 1976,
New tectonic models for the evolution of Archaean continents and oceans. In: The early history of the earth. Windley, B. F. (ed.). Wiley, Chichester, U.K., p. 105 - 112.

York, D., Hall, C.M., Masliwec, A., Langridge, R.L. and Hale, C.J., 1981,
^{40}Ar - ^{39}Ar age measurements on the Onverwacht volcanics. EOS, vol. 62, p. 429.